Synthèse et formulation des nanoparticules polymère ciblant l'E-sélectine : évaluation in vitro dans un modèle d'endothélium activé

Emile Jubeli

UNIVERSITÉ PARIS-SUD 11

ECOLE DOCTORALE :

INNOVATION THÉRAPEUTIQUE : DU FONDAMENTAL A L'APPLIQUÉ

PÔLE : PHARMACOTECHNIE ET PHYSICO-CHIMIE PHARMACEUTIQUE

DISCIPLINE

PHARMACOTECHNIE ET BIOPHARMACIE

ANNÉE 2010 – 2011 SÉRIE DOCTORAT N° 1107

THÈSE DE DOCTORAT

Soutenue le 17/05/2011

par

M. Emile JUBELI

Synthèse et formulation des nanoparticules polymère ciblant l'E-sélectine

Évaluation *in vitro* dans un modèle d'endothélium activé

Composition du jury :

Rapporteurs :	Pr. Hatem FESSI	PU-UMR-CNRS 5007 Université Lyon 1
	Dr. Sandrine CAMMAS-MARION	CR-UMR-CNRS 6226 ENSCR
Examinateurs :	Pr. Elias FATTAL	PU-UMR-CNRS 8612 Université Paris-Sud
	Dr. Gilles CHIOCCHIA	DR-INSERM-U 1016 Institut Cochin
Directeur de la thèse :	Dr. Gillian BARRATT	DR-UMR-CNRS 8612Université Paris-Sud
Co-directeur de la thèse :	Dr. Laurence MOINE	CR-UMR-CNRS 8612Université Paris-Sud

A mes parents

ces deux professeurs qui ont dédié leur vie à l'enseignement, et qui ont réussi à me transmettre les valeurs de travail, de respect et de partage.
A ces deux chandelles qui ont fondu pour m'éclairer le chemin

et

à mon frère

celui qui a toujours su être à mes côtés même quand il était loin

A mon épouse Rime

la joie de ma vie, mon partenaire de combat, mon amie de tous les jours

Cette thèse a été réalisée à la faculté de pharmacie de l'Université Paris Sud 11 à Châtenay-Malabry, au sein de l'UMR CNRS 8612 Physio - Chimie - Pharmacotechnie – Biopharmacie dirigée par le Professeur Elias Fattal, et sous la direction scientifique des Dr. Gillan Barratt et Dr. Laurence Moine.

Je tiens à adresser mes plus sincères remerciements :

Au professeur Elias Fattal pour m'avoir accepté au master de biopharmacie et pharmacotechnie, pour ses conseils et pour son soutien tout au long de mon parcours à l'université Paris Sud, jusqu'au jour de ma soutenance en acceptant de faire partie du jury.

Au Professeur Patrick Couvreur pour m'avoir permis de travailler au sein de l'UMR 8612.

Au Dr. Gillian BARRATT mon directeur de thèse pour m'avoir accueilli au sein de l'équipe, m'avoir donné l'opportunité de réaliser cette thèse, et pour son soutien dans mes activités de recherche et d'enseignement, pour nos discussions professionnelles ainsi que pour sa disponibilité et la confiance qu'il m'a toujours accordée. Merci beaucoup Gillian pour ta patience, pour ton encadrement, et vraiment… merci pour tout!

Au Dr. Laurence Moine pour avoir codirigé cette thèse, et m'avoir suivi dans mes premiers pas dans le domaine des polymères, pour l'immense temps qu'elle m'a accordé, pour son grand soutien sur le plan scientifique et personnelle. Un grand merci à toi, chère Laurence pour ta confiance, ton aide, ta disponibilité, merci pour tout le savoir que tu m'as transmis, un savoir qui marquera mon parcours professionnel à vie.

Aux Professeur Hatem Fessi et Dr. Sandrine Cammas-Marion, pour avoir accepté de juger cette thèse.

Au Dr. Gilles CHIOCCHIA, pour sa collaboration, sa sympathie et ses encouragements pendant le peu de temps que nous avons travaillé ensemble. Cela m'a fait vraiment plaisir de travailler avec vous, Je tiens à vous remercier également d'avoir accepté de faire partie du jury.

Aux Dr. Christine Vauthier et Professeur Denis Labarre pour leur aide, leur grande gentillesse, les discussions scientifiques très enrichissantes au cours de ces années. Merci à vous deux pour tous les moments agréables passés au goûter de l'après- midi.

A tout les enseignants de laboratoire notamment, Amélie Bochot, Karine Anderieux, Vincent Faivre, Michel Deyme, Kawthar Bouchemal, Hervé Hillaireau, Sinda Lepetre pour leur sympathie et pour m'avoir beaucoup donné en tant qu' étudiant en master d'abord et en tant que moniteur par la suite.

Aux docteur Nicolas Tsapis et docteur Ruxendra Gref pour leur amitié, leurs conseils et leurs grandes gentillesses.

Au professeur Najet Yagoubi, sans son soutien et sa compréhension je n'aurais pu finir la rédaction de ma thèse à temps..

Au docteur Claire Gueutin pour son aide, sa disponibilité et pour les bons moments passés dans son bureau.

Au docteur Valérie Nicolas, pour son aide, ses conseils, son investissement dans les travaux avec la microscopie confocal.

Au docteur Didier Desmaele pour ses conseils et son aide lors de la deprotection chimique par hydrogénation.

A Mme. Danielle Jaillard pour sa disponibilité et son aide technique qui m'a permis de me familiariser avec le TEM.

Aux Dr. Helene Chacun et Dr. Jean Jaques Vachon pour leur aide et leur sympathie.

A Anne-Laure Ramon pour son aide, et sa disponibilité pour les manipulations in vivo effectué à l'institut Gustave Roussy.

A tous les étudiants des équipe IV et V, notamment Khelil, Christelle, Guillaume, Van, Marian, avec qui j'ai partagé le bureau, les très nombreuses discussions scientifiques, et les tables de midi et de 16h.

Je voudrais aussi remercier tous les statutaires, étudiants, post-doc de l'unité que j'ai rencontré au cours de cette thèse, avec une pensée particulière pour Khaire, Rym, Davidé, Eléonore, Ali, Olivier, Mounira Barbara, Perrine Nathalie, Simona, Amélie, Benjamin, avec qui j'ai eu le plaisir de passer des moment très agréables. Merci pour votre amitié.

Je tiens à remercier spécialement :

Mes parents Fadia et Isam, mes vrais guides, pour tout ce qu'ils m'ont donné au cours de toutes ces années, pour leur soutien continu, leur confiance et les valeurs qu'ils m'ont transmises.

Mon frère Basel pour son écoute, son soutien, son aide, notamment administratif, et pour les valeurs qu'il défend avec constance.

Ma chère épouse Rime, pour son soutien dans ce combat que nous menons ensemble depuis plus de six ans sans souffler, pour être à mon côté quotidiennement dans les bons et les moins bons moments. Merci pour m'avoir donné tant de force pour continuer mon chemin afin de réaliser ce rêve d'avoir le doctorat.

Mes beaux-parents qui ont réalisé leurs thèses de doctorat, également en France, il ya trente ans tout juste. Un grand merci pour la confiance, les conseils et le soutien.

Merci à tous ceux qui ont contribué directement ou indirectement à la réalisation de cette thèse et que j'aurais pu omettre.

Sommaire

Liste des abréviations

Terme	Anglais	Français
ATRP	Atom Transfer Radical Polymerization	Polymérisation radicalaire contrôlée par transfert d'atomes
BSA	Bovine Serum Albumin	Albumine sérique bovine
CH2Cl2	Dichloromethane	Dichlorométhane
DCC	N,N' Dicyclohexyl carbodiimide	N,N ' Dicyclohéxyle carbodiimide
Con A	Concanavalin A	Concanavaline A
DMAP	Dimethylaminopyridine	Diméthylaminopyridine
DMF	diméthylformamide	Dimethylformamide
EDTA	Ethylenediaminetetraacetic acid	Acide éthylènediaminetétraacétique
EPR	Enhanced permeability and retention effect	Effet de perméabilité et de la rétention
FCS	Fetal Calf Serum	Sérum de veau Fœtal
HEBIB	β-hydroxylethyl α-bromoisobutyrate	β-hydroxyle-éthyle α-bromoisobutyrate
HPLC	High-performance liquid chromatography	Chromatographie en phase liquide à haute performance
HUVEC	Human umbilical vein endothelial cells	Cellules endothéliales de veine ombilicale humaine
TNF-α	Tumor necrosis factor	Facteur de nécrose tumorale
Man-glu-Bz	Dibenzyl N – [(6-azido–6-deoxy–2,3,4–tri–O-benzyle-α-D-Mannopyranosyl)]-L-glutamic acid	Dibenzyl N – [(6-azido–6-deoxy–2,3,4–tri–O-benzyle-α-D-Mannopyranosyl)]-L- acide glutamique
Man-glu-OH	[(6-azido–6-deoxy–α-D-Mannopyranosyl)]-L-glutamic acid	[(6-azido–6-deoxy–α-D-Mannopyranosyl)]-L- acide glutamique
MTT	3-[4,5-dimethylthiazol-2-yl]-2,5-diphenyltetrazolium) bromide	3-[4,5-dimethylthiazol-2-yl]-2,5-diphenyltétrazolium) bromide
MTX	Methotrexate	Méthotrexate
MWCO	Molecular weight cut-off	
NMR	Nuclear magnetic resonance	Résonance magnétique nucléaire

term	Anglais	Français
NP	nanoparticles	Nanoparticules
PBS	Phosphate buffered saline	Tampon phosphate
PEGMA	Poly ethylene glycol methacrylate	Méthacrylate de poly éthylène glycol
PEGMMA	Polyethylene glycol methyl ether methacrylate	méthacrylate de poly éthylène glycol méthyle éther
PLA	Poly lactide	Poly lactide
PMEDTA	Pentamethyldiethylenetriamine	Pentamethylediethylenetriamine
RES	Reticular endothelial system	System reticulo endothelial
RT	Room temperature	Temperature ambiante
ROP	Ring opening polymerization	Polymérisation par l'ouverture de cycle
SD	Standard Deviation	Ecart type
SEC	Size exclusion chromatography	Chromatographie d'exclusion stérique
$Sn(OCt)_2$	Tin (II) 2ethyl hexanoate	Tin (II) 2éthyle héxanoate
TEM	Transmission electronic microscopy	Microscope electronique à transmission
TFA	Trifluoroacetic acid	Acide tri fluoroacétique
THF	Tetrahydrofuran	Tétrahydrofurane
UV	Ultraviolet	Ultraviolet

Introduction générale

A la suite de son introduction dans l'organisme, un principe actif est soumis à une multitude de phénomènes depuis son site d'administration jusqu'à son élimination. A une dose donnée, l'efficacité thérapeutique d'une molécule, ses éventuels effets indésirables et sa toxicité dépendent de sa distribution dans l'organisme, dans les organes, dans les cellules, voire même dans les compartiments subcellulaires. Cette distribution ne dépend que de la nature de la molécule.

La modification de la distribution d'une molécule active, afin de la rendre plus favorable qu'elle n'est naturellement, représente depuis pratiquement quarante ans une stratégie très stimulante dans le domaine de la recherche pharmaceutique. Cela nécessite d'associer le principe actif à un vecteur capable de l'adresser de façon spécifique et spatio-temporel vers son site d'action en la détournant de ses sites de toxicité [1].

Un tel vecteur doit avoir une taille suffisamment petite pour lui permettre de circuler dans le sang et d'arriver au niveau de sa cible sans avoir été retenu au niveau de certains organes et/ou sans emboliser accidentellement des vaisseaux sanguins de diamètres inférieurs. Ainsi, sa taille doit être submicronique de l'ordre de 1nm à plusieurs centaines de nanomètres. C'est du fait de cette exigence de taille que l'ensemble de ces stratégies de ciblage est regroupé sous le terme de « nanotéchnologie ».

Un paramètre également très important pour l'utilisation de nanovecteurs dans le domaine pharmaceutique est la biocompatibilité. Afin de respecter le milieu et les tissus environnants, ces composés doivent répondre à un certain nombre de critères de toxicité et d'immunogénécité. L'usage de ces matériaux étant temporaire, un critère supplémentaire s'additionne à ceux mentionnés précédemment qu'est la biodégradabilité. Autrement dit, ces matériaux et leurs produits de dégradation doivent être en mesure d'être excrétés (par exemple, par les reins) [2].

Les nombreux progrès réalisés dans le domaine des nanotechnologies ont permis le développement de systèmes de plus en plus perfectionnés capables à la fois d'encapsuler des PA hydrophobes, fragiles et/ou aux effets secondaires graves et de les guider vers leur cible biologique.

Les premiers vecteurs parus dans les années 60 sont des liposomes [3] composés de bicouches lipidiques complètement biocompatibles. Depuis, de nombreux systèmes ont été proposés, tels que les micelles, les nanoparticules polymériques [4], les nanoparticules lipidiques[5] , les nanoparticules squalénisées [6], les nanoparticules d'or [7] et les nanoparticules organométalliques [8]. Ces objets sont fabriqués par l'association à l'échelle

moléculaire de matériaux divers comme les lipides, les protéines, les polymères, des substances inorganiques ou minérales, au moyen de techniques variées.

Le choix des matériaux utilisés pour leur préparation doit permettre de conférer simultanément aux objets de nombreuses caractéristiques : la biocompatibilité, la flexibilité structurale, la possibilité de formulation sous formes pharmaceutiques convenables et la capacité à associer des principes actifs à des doses suffisantes pour avoir un effet thérapeutique. Dans ce contexte, les polymères synthétiques sont de plus en plus étudiés comme vecteurs de molécules biologiquement actives (protéine, enzyme, peptide, principe actif). Leur facilité de synthèse liée à une grande diversité architecturale font de ces polymères de bons candidats au regard des applications de plus en plus ciblées et de la nécessité d'ajuster structure et application.

Parmi les nanoparticules, nous pouvons distinguer les nanosphères et les nanocapsules. Les nanosphères sont des systèmes de type matriciel dans lesquelles le principe actif est dispersé au sein d'une matrice polymère, alors que les nanocapsules sont des systèmes vésiculaires constitués d'une cavité aqueuse ou huileuse dans laquelle le médicament est solubilisé ou suspendu entourée d'une membrane polymère (Fig. I).

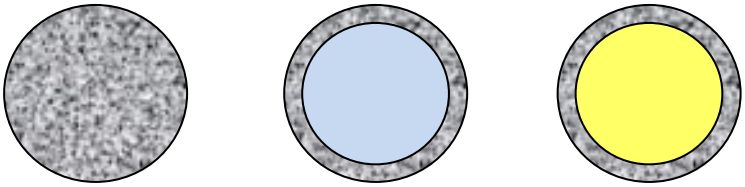

Fig. I Représentation Schématique des types de nanoparticules :
Nanosphère, nanocapsule à cœur aqueux et nanocapsule à cœur huileux

Le contact des nanoparticules avec les molécules biologiques, notamment au niveau sanguin après une administration intra-vasculaire, a des conséquences majeures sur leur distribution. En effet, selon la nature de leur surface ces particules colloïdales seront exposées à un phénomène d'opsonisation, ce qui consiste en l'adsorption sélective de certaines protéines plasmatiques sur leur surface. Ainsi, Il est admis que les propriétés de surface de ces systèmes ont un rôle primordiale dans le contrôle de leur biodistribution *in vivo* [9].

La première génération de nanoparticules composées essentiellement de polymère hydrophobe tel que le poly(acide lactique) PLA poly(acide lactique-co-glycoliques) (PLGA) ou poly(alkyle cyanoacrylates) (PACA) subit rapidement le phénomène d'opsonisation et donc une capture par les cellules du système réticulo-endothéliale (RES) et les macrophages [9]. Cela, en soit, pourrait être une méthode de ciblage de ces cellules [10, 11], mais quand ces

dernières ne constituent pas la cible visée au plan thérapeutique, il en résulte une distribution inadéquate.

Le greffage sur la surface de nanoparticules de longues chaînes de polymères hydrophiles comme le poly(éthylène glycol) (PEG) [12] ou de polysaccharides [13] rend cette surface hydrophile et permet aux nanoparticules d'éviter, ou au moins de limiter, leur contact avec les protéines plasmatiques. Cela diminue les phénomènes de reconnaissance rapide par le RES et augmente le temps de résidence dans le sang. Cette deuxième génération de nanoparticules dites « furtives » permet de cibler de manière passive les sites d'inflammation [14] ou les tumeurs[15, 16] en utilisant le phénomène d'augmentation de la perméabilité vasculaire et de la rétention (Enhanced Permeability and Rétention effet) (Fig. II).

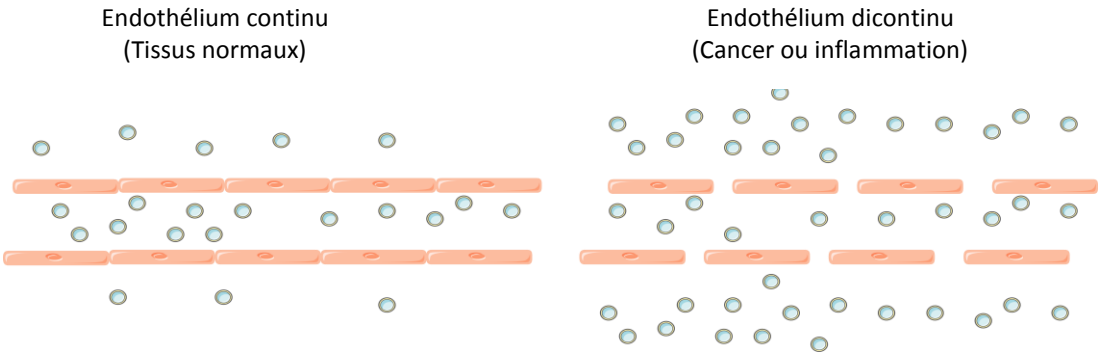

Fig. II schéma représentant le phénomène EPR (Enhanced Permeaility and Retention effect)

Les vecteurs de troisième génération sont ceux dotés sur leur surface, en plus du polymère hydrophile, d'un élément de reconnaissance spécifique d'une cible biologique comme par exemple, un récepteur situé à la surface des cellules à cibler (Fig. III). Ces éléments de reconnaissance pilotent les vecteurs dans l'organisme de façon précise, afin d'optimiser leurs distributions et par conséquent leurs efficacités.

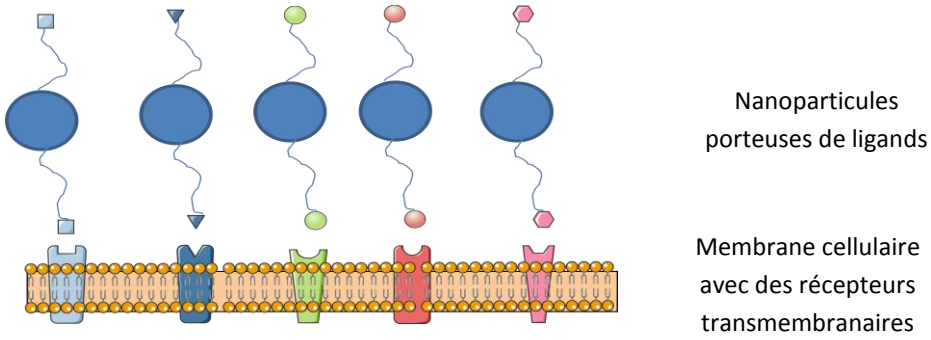

Fig. III Représentation schématique de l'interaction des nanoparticules de troisième génération avec les récepteurs cellulaires

L'objectif de cette thèse était de développer un nouveau système vecteur de troisième génération capable de mimer les interactions leucocytes / cellules endothéliales activées afin de l'exploiter dans une nouvelle stratégie d'administration ciblée de principes actifs pour le traitement de la polyarthrite rhumatoïde.

La polyarthrite rhumatoïde se caractérise par une inflammation chronique de la membrane synoviale des articulations. Cette inflammation est amplifiée par le recrutement de leucocytes circulants vers le liquide synovial par chimiotaxie [17]. L'extravasation des leucocytes dans les sites d'inflammation est facilitée par l'expression de molécules d'adhésion comme les sélectines sur les cellules endothéliales [18]. L'expression de l'E-sélectine à la surface des cellules endothéliales activées par les cytokines, permet l'immobilisation des leucocytes sur les cellules endothéliales [19] par l'intermédiaire de liaisons faibles entre ces dernières et leurs ligands portés par les leucocytes (motifs glucidiques comme le sialyl Lewis X) [20].

Notre stratégie de recherche s'appuie sur la conception de nanoparticules polymère porteuses de ligands glycosylés capables d'interagir de façon spécifique avec l'E-sélectine exprimée au niveau des articulations atteintes de polyarthrite rhumatoïde. Cela implique dans un premier temps de développer une méthodologie efficace pour la construction de macromolécules et d'objets macromoléculaires décorés de motifs glycosylés positionnés sur les chaînes de polymère de façon à les rendre accessible vis-à-vis de leur récepteur.

Les vecteurs envisagés pour cibler l'endothélium activé doivent répondre à un certain nombre d'exigences. Leur taille doit être inférieure à 200 nm, comme précédemment mentionné, afin qu'ils puissent être administrés par voie intraveineuse. Les produits de dégradation des polymères qui les constituent doivent être non toxiques et assimilables par le métabolisme pour s'assurer de leur biocompatibilité. En outre, leur structure doit limiter leur détection par le système immunitaire et enfin ils doivent être munis d'un élément de reconnaissance spécifique vis-à-vis de l'endothélium activé pour contrôler leur distribution *in-vivo*.

Les vecteurs nanoparticulaires que nous proposons sont de type cœur / couronne et décorés d'unités saccharidiques. Ils ont été formulés par nanoprécipitation à partir d'un copolymère amphiphile avec une architecture à blocs. La partie hydrophobe centrale est entourée d'une couronne hydrophile dont l'encombrement stérique et la mobilité doivent limiter l'opsonisation de la particule. Le ciblage actif a été assuré par la présence d'un mime du sialyl Lewis X aux extrémités des chaînes de polymères hydrophiles à la surface du vecteur permettant ainsi une bonne accessibilité vis à du récepteur E-sélectine

Dans le but d'utiliser ces vecteurs pour le traitement de la polyarthrite rhumatoïde, nous avons choisi d'encapsuler et véhiculer le méthotrexate comme principe actif pour cibler les articulations atteintes. Parmi les médicaments utilisés dans le traitement de fond de la polyarthrite rhumatoïde, le methotrexate (MTX) reste le plus utilisé, c'est un anti métabolite antifolique, inhibiteur compétitif de la dihydrofolate réductase nécessaire à la synthèse de l'ADN. Son utilisation sous forme orale ou injectable est cependant accompagnée d'effets indésirables importants comme des risques d'hémato toxicité (anémie, neutropénie), fibrose, et pneumopathie interstitielle, il est aussi hautement tératogène. Ce profil d'effets secondaires amène souvent à l'arrêt du traitement. Il est donc intéressant dans ce travail de trouver un moyen d'administration du MTX pour limiter ses effets secondaires.

Le plan selon lequel cette thèse s'articule est le suivant :

- La première partie consiste en une revue de la littérature portant sur les différentes stratégies ayant été développées pour le ciblage de l'E-sélectine. Ce chapitre fait l'objet d'un article de revue intitulé en préparation intitulé : « E-sélectine as a target for drug delivery and molecular imaging »
- La deuxième partie comprend l'ensemble des travaux expérimentaux réalisés. Ils sont divisés en trois chapitres :
    - Le premier chapitre concerne la mise au point d'une synthèse de copolymère amphiphile avec une architecture à bloc muni sur sa partie hydrophile d'un monosaccharide (glucopyranoside), comme modèle d'un ligand glucidique. La préparation et la caractérisation des nanoparticules à partir de ce copolymère sont également présentées. Ce chapitre fait l'objet d'un article scientifique intitulé « Synthesis, characterization and molecular recognition of sugar-sunctionalized nanoparticles prepared by a combination of ROP, ATRP and Click Chemistry » publié dans Journal of Polymer Science Part A: Polymer Chemistry.
    - Le deuxième chapitre a pour but d'évaluer l'encapsulation de méthotrexate dans ces nanoparticules modèles.
    - Le troisième chapitre traite de la préparation de nanoparticules fonctionnalisées avec un ligand de l'E-sélectine et l'évaluation *in vitro* de leurs interactions avec des cellules endothéliales humaines. Ce chapitre fait l'objet d'un article scientifique intitulé « Preparation of E-selectin targeting nanoparticles and preliminary *in vitro* evaluation » soumis dans Bioconjugate chemistry.

- Enfin nous terminerons cette thèse par une discussion générale de l'ensemble des résultats suivi d'une conclusion.

Références bibliographiques

1. Couvreur, P. and C. Vauthier, *Nanotechnology: intelligent design to treat complex disease.* Pharm Res, 2006. **23**(7): p. 1417-50.
2. Vauthier, C., et al., *Poly(alkylcyanoacrylates) as biodegradable materials for biomedical applications.* Adv Drug Deliv Rev, 2003. **55**(4): p. 519-48.
3. Gregoriadis, G., *Drug entrapment in liposomes.* FEBS Lett, 1973. **36**(3): p. 292-6.
4. Couvreur, P., et al., *Polycyanoacrylate nanocapsules as potential lysosomotropic carriers: preparation, morphological and sorptive properties.* J Pharm Pharmacol, 1979. **31**(5): p. 331-2.
5. Müller, R.H., M. Radtke, and S.A. Wissing, *Solid lipid nanoparticles (SLN) and nanostructured lipid carriers (NLC) in cosmetic and dermatological preparations.* Advanced Drug Delivery Reviews, 2002. **54**(Supplement 1): p. S131-S155.
6. Couvreur, P., et al., *Squalenoyl nanomedicines as potential therapeutics.* Nano Lett, 2006. **6**(11): p. 2544-8.
7. Hussain, N., et al., *Formulation and stability of surface-tethered DNA-gold-dendron nanoparticles.* International Journal of Pharmaceutics, 2003. **254**(1): p. 27-31.
8. Horcajada, P., et al., *Porous metal-organic-framework nanoscale carriers as a potential platform for drug delivery and imaging.* Nat Mater. **9**(2): p. 172-8.
9. F. Puisieux, G.B., S. Benita, G. Couarraze, P. Couvreur, J-Ph. Devissaguet, C. Dubernet, E. Fattal, H. Fessi and C. Vauthier.. Eds., S. Dumitru and M. Szycher, , *Polymeric micro- and nanoparticles as drug carriers. Polymeric Materials for Biomedical Applications*, ed. M.D. Inc. 1993, New York.
10. Chiannilkulchai, N., et al., *[Nanoparticles of doxorubicin: colloidal vectors in the treatment of hepatic metastases in animals].* Bull Cancer, 1989. **76**(8): p. 845-8.
11. Liance, M., et al., *Experience with doxorubicin-bound polyisohexylcyanoacrylate nanoparticles on murine alveolar echinococcosis of the liver.* International Journal for Parasitology, 1993. **23**(3): p. 427-429.
12. Gref, R., et al., *Poly(ethylene glycol)-coated nanospheres: potential carriers for intravenous drug administration.* Pharm Biotechnol, 1997. **10**: p. 167-98.
13. Passirani, C., et al., *Long-circulating nanoparticles bearing heparin or dextran covalently bound to poly(methyl methacrylate).* Pharm Res, 1998. **15**(7): p. 1046-50.
14. Ishihara, T., et al., *Preparation and characterization of a nanoparticulate formulation composed of PEG-PLA and PLA as anti-inflammatory agents.* International Journal of Pharmaceutics. **385**(1-2): p. 170-175.

15. Sasatsu, M., H. Onishi, and Y. Machida, *Preparation and biodisposition of methoxypolyethylene glycol amine-poly(dl-lactic acid) copolymer nanoparticles loaded with pyrene-ended poly(dl-lactic acid).* International Journal of Pharmaceutics, 2008. **358**(1-2): p. 271-277.
16. Yadav, A.K., et al., *Development and characterization of hyaluronic acid decorated PLGA nanoparticles for delivery of 5-fluorouracil.* Drug Deliv. **17**(8): p. 561-72.
17. Wikaningrum, R., et al., *Pathogenic mechanisms in the rheumatoid nodule: comparison of proinflammatory cytokine production and cell adhesion molecule expression in rheumatoid nodules and synovial membranes from the same patient.* Arthritis Rheum, 1998. **41**(10): p. 1783-97.
18. Kriegsmann, J., et al., *Expression of fibronectin splice variants and oncofetal glycosylated fibronectin in the synovial membranes of patients with rheumatoid arthritis and osteoarthritis.* Rheumatol Int, 2004. **24**(1): p. 25-33.
19. Garrood, T., L. Lee, and C. Pitzalis, *Molecular mechanisms of cell recruitment to inflammatory sites: general and tissue-specific pathways.* Rheumatology (Oxford), 2006. **45**(3): p. 250-60.
20. Phillips, M.L., et al., *ELAM-1 mediates cell adhesion by recognition of a carbohydrate ligand, sialyl-Lex.* Science, 1990. **250**(4984): p. 1130-2.
21. Miller, R.A., J.M. Brady, and D.E. Cutright, *Degradation rates of oral resorbable implants (polylactates and polyglycolates): rate modification with changes in PLA/PGA copolymer ratios.* J Biomed Mater Res, 1977. **11**(5): p. 711-9.
22. Yamaoka, T., Y. Tabata, and Y. Ikada, *Distribution and tissue uptake of poly(ethylene glycol) with different molecular weights after intravenous administration to mice.* J Pharm Sci, 1994. **83**(4): p. 601-6.
23. Banquy, X., et al., *Selectins Ligand Decorated Drug Carriers for Activated Endothelial Cell Targeting.* Bioconjugate Chemistry, 2008. **19**(10): p. 2030-2039.
24. Stella, B., et al., *Biological characterization of folic acid-conjugated poly(H2NPEGCA-co-HDCA) nanoparticles in cellular models.* J Drug Target, 2007. **15**(2): p. 146-53.
25. Gref, R., et al., *Surface-engineered nanoparticles for multiple ligand coupling.* Biomaterials, 2003. **24**(24): p. 4529-4537.
26. Huisgen, R., *Kinetics and Mechanism of 1,3-Dipolar Cycloadditions.* Angewandte Chemie International Edition in English, 1963. **2**(11): p. 633-645.
27. H. FESSI, J.P.D., F. PUISIEUX et C. THIES, *Procédé de préparation de systèmes colloïdaux dispersibles d'une substance sous forme de nanoparticules.* 1986: France.

Etude bibliographique

Ciblage de l'E-sélectine pour la deliverance des medicaments et l'imagerie médicale

E-selectin as a target for drug delivery and molecular imaging

Emile Jubeli, Laurence Moine and Gillian Barratt*

Université Paris-Sud11, Faculté de Pharmacie 5 rue J.B. Clément CHATENAY-MALABRY FR 92296 [1]UMR 8612 CNRS, IFR 141, France

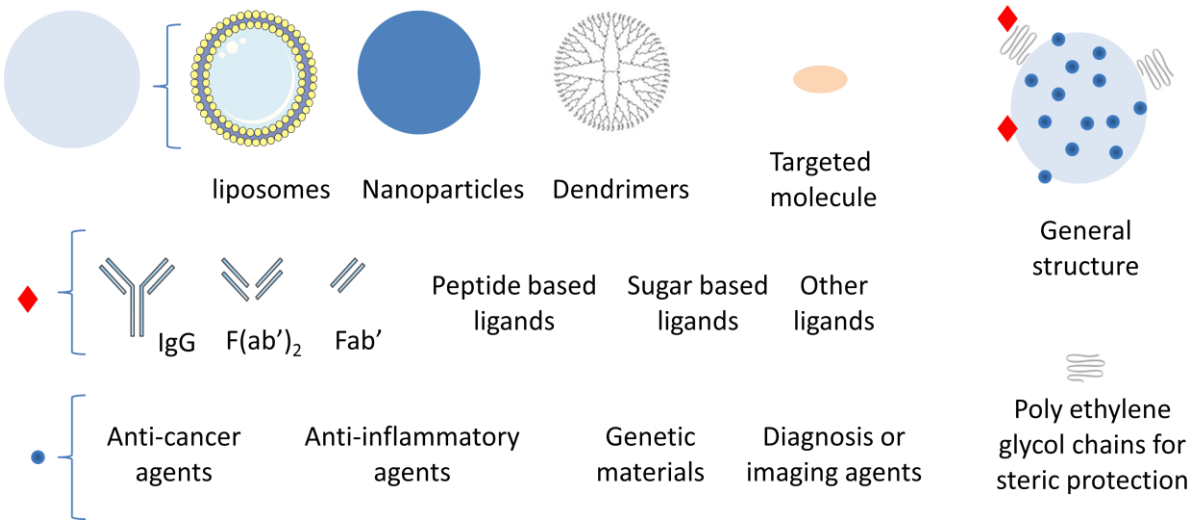

* To whom correspondence should be addressed: Tel: +33 1 46 83 56 27-; Fax: +33 1 46 83 53 12-; e-mail: Gillian.barratt@u-psud.fr

Keywords: E-selectin, Drug delivery, molecular imaging, HUVECs, receptor/ligand

Abstract

E-selectin, also known as CD62E, is a cell adhesion molecule expressed on endothelial cells activated by cytokines. Like other selectins, it plays an important part in inflammation and in the adhesion of metastatic cancer cells to the endothelium. E-selectin recognises and binds to sialylated carbohydrates present on the surface proteins of certain leukocytes.

E-selectin has been chosen as a target for several therapeutic and medical imaging applications, based on its expression in the vicinity of inflammation, infection or cancer. These systems for drug delivery and molecular imaging include immunocongugates, liposomes, nanoparticles, and microparticles prepared from a wide range of starting materials including lipids, synthetic polymers, polypeptides and organo-metallic structures.

After a brief introduction presenting the selectin family and their implication in physiology and pathology, this review focuses on the formulation of these new delivery systems targeting E-selectin at a molecular level.

1. Introduction

Selectins are a family of three receptors composed of calcium-dependent type I transmembrane glycoproteins with an extracellular lectin-like domain. They are classified by their site of expression into E-selectin (activated endothelium [1, 2]), P-selectin (platelets [3, 4] and endothelial cells [5, 6]), and L-selectin (lymphocytes [7]). Selectins allow adhesion between leukocytes and platelets in contact with the vascular endothelium during inflammation or tissue damage [8]. At a molecular level they are able to recognize sialylated, fucosylated and sulfated glycans found on glycoproteins, glycolipids or proteoglycans [9] to mediate the initial attachment or “tethering” of free-flowing leukocytes to the vessel wall through reversible adhesion that permits the cells to roll in the direction of flow [10, 11]. The physiological expression of selectins is strictly controlled in order to limit inflammatory reactions, and is modified in inflammation and cancer metastasis to allow adherence of leukocytes or cancer cells, respectively, on endothelial cells.

Advances in molecular and cellular biology have elucidated the role played by each of these receptors in a range of pathological disorders involving aberrant trafficking of immune cells. P-selectin is involved in inflammatory disorders such as acute lung injury [12], psoriasis [13], and rheumatoid arthritis [14]. It plays a role in hemostasis [15, 16] and hematogenous spread of tumor cells [17, 18]. For detailed information about the pathological rôles and therapeutic targeting of P-selectin, the reader is directed to the review published by Ludwig and co-workers [19]. It is also well documented today that E-selectin is deeply implicated in many disorders including inflammatory diseases, cardiovascular disorders, cancer and metastasis. On the other hand, there is little evidence for the direct involvement of L-selectin in pathology, although some studies have reported variations in levels of the receptor and/or its soluble form (sL-selectin) in serum in some patients with HIV-infection [20], insulin-dependent diabetes mellitus [21], meningeal leukemia [22], multiple sclerosis [23] and sepsis [20]. However, its soluble form, sL-selectin, was found to be decreased in patients with Kawasaki Syndrome and in patients with risk factors for acute ischemic stroke even in the absence of disease [24].

In the light of these observations, interest in this family of receptors has been growing during the last two decades; in particular in the possibility of using them as a pharmacological target for the treatment of the diseases mentioned above. In fact, different selectin-based therapeutic strategies have been proposed, including the inhibition of their expression in pathological situations, targeting their ligands, or using them as molecular targets for delivery of therapeutic and diagnostic agents.

In this present review, a summary of physiological and pathological role of E-selectin will be given, followed by a detailed presentation of systems which have been proposed to target it in inflammation, cancer, cardiovascular disorders, for drug delivery, gene transfer and medical molecular imaging. A general discussion summarizes the key points in the development of such systems.

2. E-selectin: an interesting target for drug delivery

2.1 Physiology of E-selectin

E-selectin (64 kDa) also known as CD62E, ELAM-1 and LECAM-2, is expressed specifically by endothelial cells. Relative molecular weight values of 100 and 115 kDa have been detected for different glycosylated forms [25]. The primary structure of E-selectin contains several domains: an amino terminal lectin-like domain, followed by an epidermal growth factor (EGF)-like domain and six repeated motifs (about 60 amino acids each) similar to those found in some complement-binding proteins [2]. The lectin-like domain, and (EGF)-like domain mediate interaction with leukocytes, while the role of the complement binding-like regions is not yet well defined, but they probably serve, at least in part, as spacers to hold the other domains away from the cell surface [26].

E-selectin is not constitutively expressed by endothelial cells [1, 2]; its expression is stimulated by inflammatory molecules such as tumor necrosis factor (TNF-α), interleukin-1 (IL-1) and bacterial lipopolysaccharide (LPS) [2, 27, 28]. However, some recent studies have detected its expression in non stimulated endothelial cells *in vitro* [29]. Its expression is maximal four hours after cytokine stimulation and decreases rapidly thereafter. E-selectin expressed on the surface of the cell is gradually internalized by endocytosis [30] and degraded in lysosomes [31] so that it is no longer detectable after 24 hours [2]. It was recently demonstrated that E-selectin clusters in both clathrin-coated pits and lipid rafts of endothelial cells but is internalized only by clathrin-coated pits. The distribution of E-selectin into two different domains on the cell membrane markedly enhances its ability to mediate leukocyte rolling in flow conditions [32].

A soluble form of E-selectin (sE-selectin) is generated by enzymatic cleavage or when activated endothelial cells shed damaged parts of their surface. It seems that the concentration of sE-selectin is directly correlated with cell surface expression [33]. The exact role of SE-selectin is not known; however, as some studies have found that it exerts a chemotactic signal towards neutrophils, it may trigger the migration of these cells [34]. Other reports suggest that it may limit E-selectin-mediated rolling of activated leukocytes by competing for binding sites on the cell surface, thus “downregulating” the inflammatory

response [35]. Whatever the case, the circulating concentration of circulatory E-selectin can be used as a marker of activation of the endothelium and is therefore useful as a clinical tool for diagnosis of tumors and acute inflammatory processes.

2.2 E-selectin ligands

E-selectin, recognizes several structures carried by glycoproteins. Among the ligands that have attracted the most attention are: E-selectin ligand-1 (ESL-1) [36] which binds specifically to E-selectin but not to P- and L-selectin, P-selectin glycoprotein ligand-1 (PSGL-1) [37], L-selectin [38], CD43 [39], CD44 [40], β2 integrins [41] and death receptor-3 (DR3) [42].

Selectins have been found to recognize particular carbohydrate motifs: Sialyl lewis x (SLE^x) and Sialyl lewis a (SLE^a) found at the terminus of the structure of glycoproteins and glycolipids on the surface of leukocytes and tumor cells [43, 44]. The molecular bases of E-selectin-SLE^x interaction are well documented [45, 46]. Many groups have reported the synthesis of SLE^x analogs able to recognize and bind to E-selectin [47, 48].

Interaction of E-selectin with its ligand leads to the rolling of leukocytes on inflamed endothelial cells [49] which is the first step of the firm adhesion and transmigration to the surrounding tissue. More information about selectins, their ligands, role in physiology and pathology as well as their targeting are available in several published reviews [8, 19, 50-52].

2.3 Pathological implication of E-selectin

As mentioned above, although E-selectin has an important role in the physiological mechanisms regulating inflammation reactions, it is well documented today that it is also involved in many diseases. Since the pathological implications of E-selectin have also been previously reviewed only a brief summary will be provided here.

2.3.1 E-selectin and inflammation

The expression of E-selectin on endothelium during acute or chronic inflammatory reactions has been extensively studied, focusing on its involvement in the recruitment of immune cells [9, 50] through interaction with its ligands located on their surface.

E-selectin has been detected on vascular endothelium in liver sections from patients with primary biliary cirrhosis, acute allograft rejection, alcoholic liver disease, but not on normal liver endothelium [53]. Bronchial biopsies in chronic bronchitics had an increased number of E-selectin-positive vessels when compared with both asymptomatic smokers and normal subjects [54]. Vascular endothelium in retroocular connective tissues of patients with

Graves' ophthalmopathy is strongly positive for E-selectin [58]. E-selectin has been found to be expressed at low level in non inflamed tissue, including the synovium [33], but its expression is up-regulated during rheumatoid arthritis (RA) in the inflamed synovial endothelium [59-61]. It is also expressed in the rheumatoid nodules in patients with PA [59] and is implicated in the recruitment of inflammatory cells into the tissue [62]. This expression is reduced after TNF-α blocking therapy [63].

High levels of the soluble form (sE-selectin) have also been reported in patients with inflammatory diseases: bronchial asthma [64], eczema [65], Graves's disease [66] Guillain-Barre syndrome [67] Kawasaki disease [68] atopic dermatitis [69], psoriasis [70] and inflammatory bowel disease [71].

These observations in patients have been complemented by some information from animals models. In a murine model of anti-glomerular basement membrane glomerulonephritis, 2 h after disease induction 75% of the glomeruli were positive for E-selectin while it was undetectable in untreated mice [55]. In mice with experimental autoimmune uveoretinitis, the vessels of the inner retina showed strong staining for E-selectin, in contrast to the eyes of normal mice [56]. Still in mice, coronary vascular expression of E-selectin is involved in the pathogenesis of ischemic-reperfused zones [57].

2.3.2 E-selectin and cancer cells

The pathological role of E-selectin is not restricted to inflammatory disorders. It has also been detected in some cancer tissues, indicating a potential involvement in the pathogenesis of this disease [72].

E-selectin has been detected on the endothelial cells of small vessels adjacent to cancer nests in patients of human colorectal cancer. This expression appears to be induced by some stimuli originating from the cancer cells, since the degree of expression is inversely correlated to the distance of the blood vessels from the cancer nests [73]. In primary gastric cancer, *de novo* expression of E-selectin on blood vessels was observed, particularly in highly vascularized tumor areas [74]. Furthermore, the expression of E-selectin was found to be significantly higher in malignancies than in benign tumors in head and neck [75] and breast tumors [76].

In vitro, it was observed that conditioned medium from Ehrlich Ascites tumor (EAT) cells was able to induce expression of E-selectin in human umbilical vein endothelial cells (HUVECs) suggesting that tumor cells secrete cytokines or other factors stimulating expression of this receptor [77].

2.3.3 E-selectin and metastasis

Adhesion of tumor cells on vascular endothelium of the target organ is a key step in the cascade of metastasis. It is now well established that the couple SLE^x/E-selectin is an important mediator in the adhesion of cancer cells on the endothelium in metastasis formation [78] by a mechanism similar to that of the adhesion of immune cells (scheme 1).

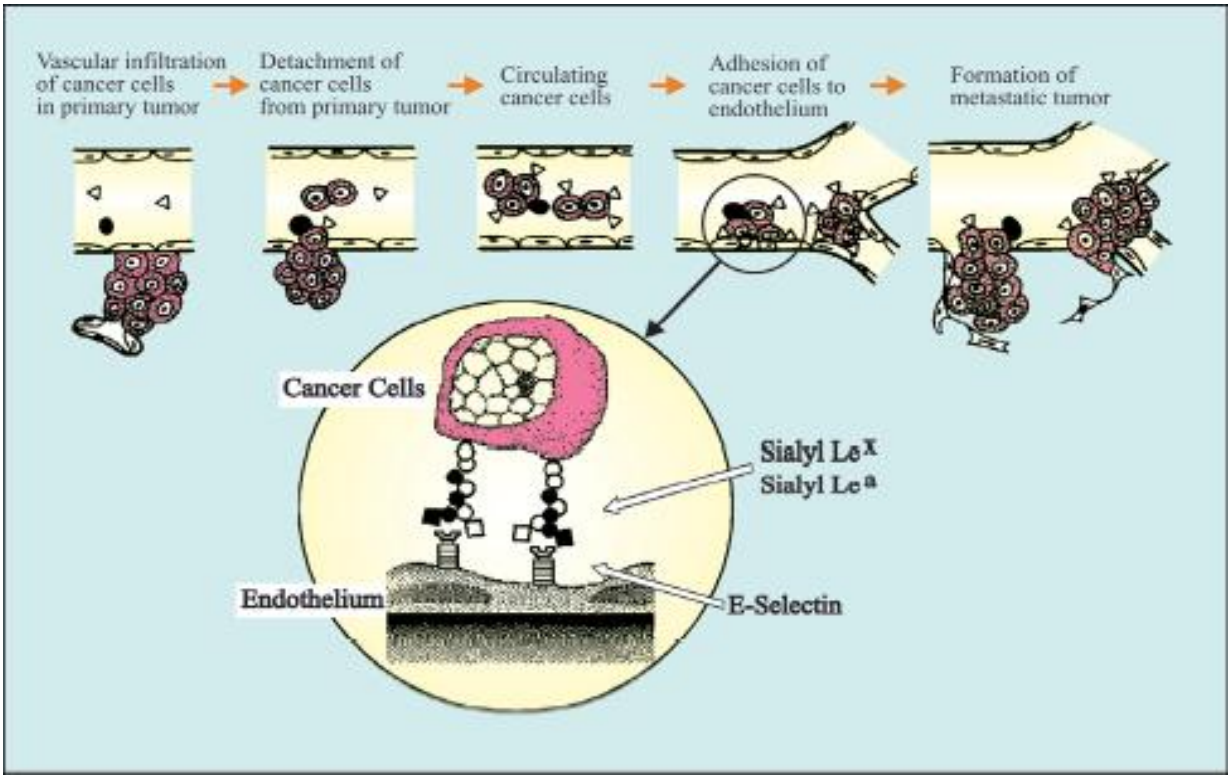

Scheme 1: Schematic representation of the different steps involved in cancer metastasis (Reproduced with permission from [83]. Copyright J. Wiley and Sons, UK)

Takada et al have determined that the adhesion of 12 cultured human epithelial cancer cell lines of colon, pancreas lung and liver origin on the endothelium was achieved in an E-selectin-dependent way [79]. Other studies have demonstrated that E-selectin is an intermediary in the adhesion of H-59 murine carcinoma and two highly metastatic human colorectal carcinoma lines to the liver endothelium [80] and of breast cancer cells to endothelial cell monolayers [81, 82].

E-selectin is involved in hepatic metastases of breast cancer [83] and colorectal cancer [73]. Other data indicate a role for the SLE^x/E-selectin interaction in bone metastases of prostate cancer [84] and liver metastases of gastric cancer [85].

When injected into the spleens of nude mice, human colon carcinoma cell lines with high levels of surface SLE^x colonized to the liver more efficiently than low SLE^x cells. This adhesion was partially inhibited by blocking antibodies specific for E-selectin [86].

3 E-selectin as a target

As a result of this demonstrated expression of E-selectin in the vicinity of inflammation, infection or cancer it has become a natural target for therapeutic intervention.Different strategies to exploit and modulate E-selectin-mediated binding include blocking its interaction with its ligands, blocking its ligands and inhibiting the glycosyltransferases associated with biosynthesis of selectin carbohydrate binding determinants [51]. These strategies could inhibit immune and cancer cell adhesion in inflammation and metastasis, respectively.

Another targeting strategy is the use of E-selectin as a receptor for the delivery of anti-inflammatory or anti-cancer drugs and for medical imaging systems containing an imaging agent (scheme 2). This last approach will be described in this review.

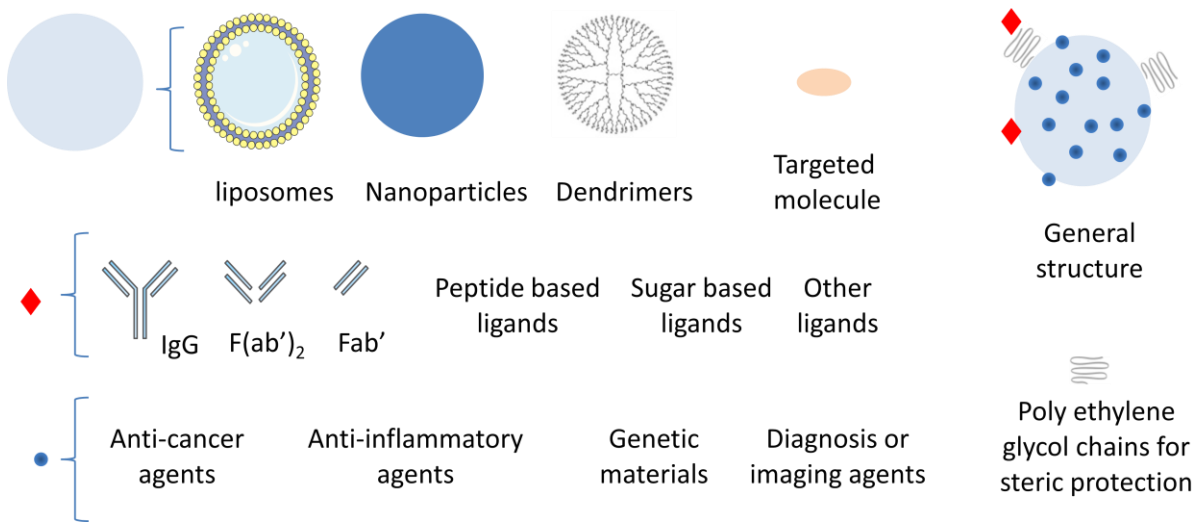

Scheme 2. Schematic representation of the different concepts used to target E-selectin

3.1 General targeting – Proof of concept

The different studies that have demonstrated the efficiency of targeting E-selectin with a view to developing drug delivery systems are listed in Table 1. They are classified by the recognition element employed; i.e antibody-based systems and small molecular ligands and analogs.

3.1.1 Antibody-based targeting

Both liposomes and microspheres have been used as supports to couple anti-selectin antibodies.

3.1.1.1 Liposomes

The group of Dr. Bendas has targeted E-selectin by means of liposomes decorated with monoclonal anti-E-selectin antibodies (mAb) coupled directly to the surface. It could be shown that these immunoliposomes selectively bound to selectin-expressing HUVECs under either static or simulated blood flow conditions. The lipid/antibody ratio was found to be an essential factor determining the efficacy of the system [87].

In a second study, they chose to use polyethylene glycol stabilized liposomes which would have a longer circulation time in the organism. When anti E-selectin mAb was directly connected to the surface of the liposomes (inserted among PEG chains), a higher PEG concentration reduced the E-selectin-mediated binding with E-selectin-transfected Chinese Hamster Ovarian cells, as a result of either reduced antibody accessibility or reduced efficiency of antibody coupling or both. When the mAb was attached to the distal ends of PEG, higher concentrations of PEG led to higher cell binding [88]. A proportion of the liposomes bound to the cells were subsequently internalized, mainly by an endocytotic mechanism involving, E-selectin-mediated endocytosis to accumulate in the endosomes [89].

Spragg et al prepared liposomes of various types conjugated with the anti-E-selectin H18/7 mAb. The best binding to activated HUVECs was obtained when the mAb was attached to the surface without sterically stabilization, while PEG-stabilized liposomes showed lower cell association because the PEG reduced the amount of antibody that could be coupled to the surface and also limited the accessibility of the antibody to the receptor. Among the different formulations tested, cationic immunoliposomes showed a relatively high level of nonspecific binding due to interactions with the anionic cell surface [94].

In an attempt to enhance binding by using the synergy between two ligands, Gunawan and Auguste [95] prepared immunoliposomes bearing two distinct antibodies directed against intracellular cell adhesion molecule 1 (aICAM) and E-selectin (aELAM). The presence of the two Abs increased the cellular uptake of immunoliposomes by IL-1β-activated HUVECs compared with the uptake of liposomes bearing only aICAM or aELAM-labeled. They reported greater binding and internalization of DOPC immunoliposomes in which the lipids are in a fluid state at temperatures above -20°C than DPPC immunoliposomes in which the lipids are in a gel state at physiological temperature [95]. This

influence of lipid mobility the aICAM: aE-selectin ratio on cell binding only occurred in conditions under which lipid rafts were present. When the formation of lipid rafts was prevented by depleting the cell membrane of cholesterol, binding of both DOPC and DPPC immunoliposomes was reduced to the nonspecific binding level, suggesting that the presence of lipid rafts in ECs is critical for targeted drug delivery [96].

3.1.1.2 Microspheres

Microspheres of poly (ε-caprolactone) (PCL), on which the humanized monoclonal antibody (mAb) for E- and P-selectin, (HuEP5C7.g2) was adsorbed, exhibited specific adhesion to IL-1β-activated human umbilical vein endothelial cells (HUVEC) expressing E-selectin, while binding to inactivated cells was very low [90]. It is important to note that the attachment efficiency to the selectin substrates in this study was quite low (<0.17% that of leukocytes), with appreciable attachment occurring only at low shear (0.3 dyn/cm^2). This was attributed to a low level of HuEP5C7.g2 adsorbed onto the microspheres. It should be kept in mind that particles of micrometric size have limited applications on systemic administration. The authors proposed these particles to deliver drugs in conjunction with balloon angioplasty [90].

To improve the coupling of the antibody onto polystyrene microspheres and nanospheres Blackwell et al first adsorbed Protein A before binding its F_c portion with HuEP5C7.g2 mAb, allowing a correct orientation of the mAb on the particle surface. *In vitro* adhesion assays revealed augmented and specific adhesion to selectin-bearing CHO Chinese hamster ovary (CHO) and HUVECs stimulated by IL-1β, while reduced adhesion was observed when the incubation was carried out at 4 °C [91].

PLA-PEG microparticles conjugated to with anti-human E-selectin mAb (68-5H11) via a biotin-neutravidin bridge with high densities (>200,000 mAbs per particle) demonstrated significant selective adhesion (up to 15-fold more) to inflamed endothelium compared with noninflamed endothelium, under physiologically relevant *in vitro* flow conditions (1.5 dyn/cm^2) [92], which is strikingly more avid than was achieved previously with passive adsorption of mAbs onto biodegradable particles [90]. In an *in vivo* model, the intrascrotal injection of TNF-α which elicits E-selectin expression [93], followed by injection of particles two hours later showed a significant (6-fold higher) selective adhesion for cytokine-inflamed endothelium than for non-cytokine-treated endothelium [92].

All these findings have demonstrated the effectiveness of specific antibodies in the targeting of E-selectin using liposomes and polymeric particles. The key factors that determine the efficiency of such systems is the position of the antibody on the surface of the

vector and the way with which it is conjugated to the lipidic or polymeric backbone. More studies are needed to evaluate the *in vivo* toxicity of these systems, including the immunogenicity after antibodies administration especially with long term treatment.

3.1.2 Targeting with E-selectin ligands and analogs

Minaguchi et al have used liposomes on which SLE^x moieties were bound via human serum albumin, encapsulating a fluorescent marker. After intravenous injection in mouse model of arthritis induced by an anti-collagen-antibody, fluorescent imaging showed a signal confined to the inflammatory site in an inflammation-dependent manner and with colocalisation with the vascular endothelial cell marker (CD31) and E-selectin [97].

Banquy et al prepared nanoparticles from poly (lactic acid) covalently linked to a mannose based analog of SLE^x. *In vitro* adhesion tests showed strong adhesion of nanoparticles mediated specifically by E- and P-selectin because the pretreatment of activated cells with free ligand inhibited the adhesion of the particles [29].

Our group has prepared nanoparticles from an amphiphilic block copolymer composed of poly (lactic acid), PEG methacrylate (PEGMA) and functionalized at the distal end of the PEG chains with the mannose-based analog mentioned above. These nanoparticles allowed efficient targeting of TNF-α-stimulated E-selectin-expressing HUVECs with subsequent internalization (unpublished data). In these experiments, approximately two-thirds of the observed cell association was inhibited by pretreatment with anti-E-selectin antibody, suggesting that nanoparticles entered cells mainly in an E-selectin-mediated way, the remaining internalization may be mediated by interaction with P-selectin which was not blocked by the specific E-selectin antibody.

Peptide-quinic acid derivatives have been developed as non carbohydrate analogs of SLE^x. These constructions antagonized the adhesion of SLE^x-expressing HL-60 cells to both E-selectin and P-selectin-coated plates. When these analogs were conjugated to Hydroxypropyl methacrylamide (HPMA) copolymers, they showed about 3 orders of magnitude higher affinity than the monomolecular ligand and were internalized E-selectin expressing endothelial cells majoratly through majorital mechanism of copolymer entry was found to be endocytosis [98].

In order to design a targeted ultrasound diagnostic tool, lipidic microparticles based on phosphatidylcholine were functionalized with thiolated peptide ligands for E-selectin. These particles showed effective binding to human bladder carcinoma cells expressing E-selectin under flow conditions. Reduced binding in the presence of free ligand demonstrated the specificity of the binding, however, this was inhibited by serum proteins. Increasing the

phospholipid chain length from 18 carbons to 22 carbons improved the stability of the particles during ultrasound exposure, without compromising their acoustic properties [99].

In conclusion, Small molecules ligand-based targeting systems seem to be safer than antibodies based ones and probably much cheaper. Although they have given very good results in both *in vitro* and *in vivo* models but the clinical trials are still missing compared with system targeting other receptors by small ligands such as folic acid based carriers targeting folic acid receptor.

Table 1 Summary of published work describing delivery systems targeting E-selectin

system	**Recognition element**	**Linking method**	**Evaluation**	**Reference**
Liposomes	E-sel Ab	Direct linkage	*In vitro* : (static and shear conditions	[87]
Liposomes	E-sel Ab (rat IgG)	Covalent linkage direct or through PEG spacer	*In vitro* static	[88]
Liposomes	E-sel Ab murine anti human E-sel mAB (BBA 26)	Covalent linkage through PEG spacer	*In vitro* : static conditions	[89]
Microspheres poly (ε-caprolactone)	E-sel and P-sel humanized mAB (HuEP5C7.g2)	Simple adsorption	*In vitro :* shear conditions	[90]
Microsphere/ nanospheres polystyrene	E-sel and P-sel humanized mAb (HuEP5C7.g2)	Coupled with the Fc portion of Protein A adsorbed to particles	*In vitro* : static conditions	[91]
Microspheres PLA-PEG	murine biotinylated mAb 68–5H11 (anti-human E-sel IgG1)	Neutravidin-biotin interaction	*In vitro :* shear conditions *In vivo* (intrascrotal injection of TNF-α)	[92]
Liposomes	Murine IgG2a E-sel mAb (H18/7)	Covalent linkage with lipids forming liposomes	*In vitro* : static conditions	[94]
Liposomes	mouse anti-human E-sel mAbs	Covalent linkage through N-dod-PE anchor	*In vitro* : static conditions	[95]
Liposomes	SLE^x	Via human serum albumin	*In vivo* : collagen induced arthritis	[97]
Nanoparticles PLA	Mannose based SLE^x	Covalent linkage with polymer backbone	*In vitro* : static conditions	[29]
HPMA copolymers	Peptide-quinic acid derivatives analogs of SLE^x	Covalent linkage with polymer backbone	*In vitro* : static conditions	[98]
lipidic microparticles	E-sel thiolated peptide ligands	Covalent linkage through PEG spacer	*In vitro* : shear conditions	[99]

3.2 Targeting therapeutic agents

3.2.1 Targeting inflammation

Dexamethasone (DXM) is widely used to treat inflammatory and autoimmune diseases due to its broad spectrum of pharmacological effects. The various adverse effects of corticotherapy, especially during long-term treatment, suggest that targeting by E-selectin could be advantageous in dexamethasone therapy. This drug has often been used as a model in studies of anti-inflammatory drug targeting to activated endothelium.

In the work of Everts et al, DXM was covalently attached to H18/7 anti-E-selectin mAb. This conjugate selectively bound to TNF-α-stimulated endothelial cells, was internalized and routed to lysosomes, allowing DXM to be released and to down-regulate the the expression of the proinflammatory IL-8 gene [100]. It is noteworthy that the antibody carrying an average of two conjugated dexamethasone molecules per antibody molecule, still recognized its target antigen. However, higher dexamethasone loading ratios (up to 10 dexamethasone molecules per Ab molecule) reduced the solubility of the conjugate and diminished its recognition of E-selectin [100].

Further work from the same group reported the internalization and lysosomal degradation of an Iodine-125 (^{125}I-radiolabeled) dexamethasone-anti-E-selectin immunoconjugate in activated endothelial cells. The binding, internalization and degradation of the conjugate followed the kinetics of E-selectin expression and internalization. In contrast, free DXM entered both resting and activated endothelial cells by passive diffusion [101].

Immunoliposomes encapsulating DXM and bearing anti-E-selectin Ab, were selectively internalized by activated endothelial cells, but their binding to E-selectin was saturated at a slightly lower concentration than the molecular immunoconjugate described above, probably because of the presence of multiple Ab molecules on the surface of one liposome [102]. In an *in vivo* model of murine delayed-type hypersensitivity known to induce E-selectin expression in the affected skin, both immunoconjugates and immunoliposomes accumulated in activated endothelial cells in the inflamed area. However, the liposomes were also detected in control skin, although to a lesser extent, and in macrophages of the liver and the spleen. The authors argued that this behavior could be explained by the coupling of intact antibody molecules in a random orientation to the liposomes, allowing recognition by the F_c-receptors on macrophages because of clustering of F_c portions of the antibody on the liposomal membrane [102]. This important issue of specificity should be treated with special attention for any further clinical trials.

Similar liposomes conjugated with MES-1 anti-E-selectin Ab were internalized by activated mouse endothelial cells *in vitro* through E-selectin-mediated endocytosis. After intravenous administration in mice afflicted with anti-glomerular basement membrane glomerulonephritis, accumulation of targeted liposomes in the kidney was 3.6 times higher than that of nontargeted IgG liposomes, whereas the accumulation of both types of liposomes in the liver, spleen, heart and lungs was comparable. In glomeruli, targeted delivery of dexamethasone reduced expression of P-selectin, E-selectin, and vascular cell adhesion molecule-1 on the glomerular endothelial by 60–70% [103]. These liposomes reduced renal injury, improved glomerular function, strongly inhibited the formation of crescents in glomeruli and did not affect blood glucose levels In contrast to free dexamethasone [103].

Instead of antibodies, SLE^x itself has also been used as a targeting ligand for DXM-loaded liposomes. In a model of murine experimental autoimmune uveoretinitis, intravenous injection of these conjugated liposomes led to their accumulation in the retina of EAU mice. Pretreatment with anti-E-selectin antibody inhibited the accumulation. Again, liposomes were detected in the liver as well as in inflamed tissue. Two-fold higher dexamethasone concentration was achieved in the inflamed eyes after administration of 2 µg of encapsulated drug than that obtained with 1 mg of free dexamethasone [56].

3.2.2 Cancer targeting

Two strategies based on E-selectin targeting have been developed: inhibition of cancer cell adhesion by competition with ligand-bearing particles, and delivery of anti-cancer drugs to tumor cells via neighbouring activated endothelial cells expressing E-selectin (Table 2).

As mentioned above, E-selectin is involved in the first step of the adhesion cascade taking place on the endothelial cell surface metastasic process [9, 82, 104]. Therefore, occupation of this receptor by targeted structures could prevent this adhesion and thereby inhibit metastasis. Zeising et al reported the preparation of several formulations of liposomes functionalized with SLE^x which inhibited in vitro adhesion of HT29 colon and Lewis lung carcinoma LL cancer cells expressing SLE^x and/or SLE^a to the endothelium [105]. Similarly multivalent sialyl $Lewis^x$-peptide ligands and SLE^x-bearing liposomes were used to block E-selectin-mediated binding of HEpG2 hepatoma cells. Their ability to inhibit tumor cell binding to activated HUVECs was as follows (SLE^x = $(SLE^x)_2$-peptides < ($SLE^x)_3$-peptides (2fold) <<< SLE^x liposomes (2000 fold)). In the case of glycopeptides, if the first bond between one SLE^x residue and a receptor has been formed, the free mobility of the other residues is

strongly restricted, while the mobility of glycolipids in the liposome bilayer renders them almost independent of one other, making them very active inhibitors [106].

A trisaccharide analog of SLE^x known as GSC-150 inhibited the adhesion of a human colon carcinoma-derived cell line (KH12-HX) over-expressing SLE^x to HUVECs activated with TNF-α. Coadministration of GSC-150 with these cells into the spleens of BALB/c nude mice reduced the number of cells distributed to the liver and the number of cancer nodules in the liver even in mice injected with lipopolysaccharide (LPS), which is known to induce high E-selectin expression [107].

Mann et al have identified a thioaptamer ligand (ESTA-1) that selectively recognizes E-selectin, thus allowing it to bind specifically to the inflamed tumor-associated vasculature of human carcinomas derived from breast, ovarian, and skin, but not to normal organs. It is able to block the adhesion (over 75% inhibition) of SLE^x-positive HL-60 selectin on endothelial cells. Intravenously injected ESTA-1 was detected binding to the tumor vasculature in a breast cancer xenograft model [108]. The advantage of this thioaptamer compared with SLE^x is its nanomolar binding affinity (KD = 47 nM) combined with minimal cross reactivity with P- and L-selectin making it a selective ligand compared with many others including SLE^x itself that may interact with other selectins.

Inhibition of the E-selectin-mediated adhesion of metastatic cells could be used to prevent or at least to reduce metastatic tumor spread under certain conditions of high risk of dissemination such as during tumor surgery.

Carriers targeting E-selectin have also been used to deliver anti-tumor drugs. Liposomes conjugated with the anti-E-selectin H18/7 mAb and loaded with the cytotoxic agent doxorubicin caused a marked decrease of survival of activated cells, whereas nonactivated HUVECs were unaffected by this treatment [94].

Hydroxypropyl methacrylamide (HPMA) functionalized with a high-affinity E-selectin binding peptide (ESBP) bound to E-selectin on the surface of vascular endothelial cells with an affinity in the low nano-molar range, 10-fold higher than that of non-targeted copolymers. Once bound, E-selectin facilitated rapid internalization and lysosomal trafficking of the copolymers. When these immunopolymers were conjugated to doxorubicin they had 150-fold higher cytotoxicity than non targeted HPMA–DOX conjugates [109].

Two studies have been based on the fact that E-selectin vascular expression is significantly increased in malignant breast cancer. Mice bearing transplanted mammary tumors showed a significant increase in E-selectin expression on endothelial cells after tumor irradiation [110]. Immunoliposomes conjugated with anti-E-selectin mAb (10E9.6), loaded

with the angiogenesis inhibitor combretastatin disodium phosphate and injected after a single dose of radiation, inhibited the growth of blood vessels, which led to an inhibition of tumor growth. Fractionated radiation plus fractionated doses of immunoliposomes resulted in further tumor growth delay [110].

Table 2 Summary of delivery systems directed towards E-selectin for cancer therapy

System	Type of cancer/ cancer cells	Recognition element	Target	Evaluation	Reference
liposomes (several formulations)	HT29 colon and Lewis lung carcinoma LL cancer cells	SLE^x	Inhibition of cancer cells adhesion to endothelium	*In vitro*	[106]
multivalent peptide ligands and liposomes	HEpG2 hepatoma cells	SLE^x	Inhibition of cancer cells adhesion to endothelium	*In vitro*	[106]
Free ligand	Human colon carcinoma-derived cell line (KH12-HX)	SLE^x trisaccharide analog	Inhibition of cancer cells adhesion to endothelium	*In vitro* *In vivo*	[107]
Free ligand	1) HL-60 2) breast, ovarian, and skin carcinomas	thioaptamer ligand	1) Inhibition of cancer cells adhesion to endothelium 2) Targeting inflamed tumor-associated vasculature	*In vitro* *In vivo*	[108]
Liposomes	-	anti-E-selectin H18/7 mAb	Targeting endothelial cells with doxorubicin	*In vitro*	[94]
HPMA polymer	-	E-sel binding peptide	Targeting endothelial cells with doxorubicin	*In vitro*	[109]
Liposomes	Transplanted mammary tumors	anti-E-selectin mAb (10E9.6)	inhibition of angiogenesis with combretastatin disodium phosphate	*In vivo*	[110]
Liposomes	Mammary adenocarcinoma	SLE^x	Treat cancer and increase survival time with Merphalan	*In vivo*	[111]
Liposomes	Ehrlich's ascites tumors	SLE^x	Treat cancer and increase survival time with cisplatin	*In vivo*	[112]

In another study, mice bearing spontaneous mammary adenocarcinoma were treated with SLE^x-targeted liposomes loaded with the anticancer agent merphalan prodrug [76]. The treated mice showed higher average time before palpable tumors could be detected and higher average survival time than mice treated with non-targeted Merphalan-loaded liposomes. As well as the essential influence of the glycoconjugate itself, the authors

highlight the role of its hydrophilic nature in the stabilization of liposomes in the circulation [111].

3.2.3 Cardiovascular targeting

Targeting endothelial cells is a potential strategy for treating cardiovascular anomalies. An example of drug delivery by targeted carriers is the treatment of restenosis, which remains a serious complication after angioplasty. In accord with the observation that E-selectin is expressed on the endothelium of atherosclerotic lesions [113, 114], Tsuruta et al detected E-selectin in the carotid artery after balloon angioplasty in rats. When this local inflammation was targeted with SLE^X-conjugated liposomes carrying doxorubicin, significant accumulation of the drug was observed in the injured vessel walls. The residual lumen area in rats treated with these liposomes was significantly larger than those in all other groups, demonstrating that such a system could effectively prevents restenosis after angioplasty [115].

Thrombin is a mediator in vascular pathologies involving activation of the endothelium. In order to deliver hirudin, a potent and specific inhibitor of thrombin, it was covalently cross-linked to the H18/7 mAb. This immunoconjugate selectively bound to IL-1-activated but not to non activated HUVECs. During the process of cell activation with IL-1, immunoconjugate binding increased in parallel with cell-surface procoagulant activity. When bound to activated cells, the immunoconjugate significantly inhibited endogenous thrombin activity, and down regulated cellular responses that are mediated via the thrombin receptor [116].

3.3 Gene transfer

Endothelial cells are an attractive target for gene therapy because they are intimately involved in disease processes associated with inflammation and angiogenesis and because they are readily accessible to gene therapy vectors via the circulation. Successful gene delivery requires good cellular targeting, internalization, endosomal escape and translocation to the nucleus. Targeted delivery systems can help to increase the specificity through promoting entry and intracellular trafficking of the genetic material.

One of the first reports using E-selectin as a targeting ligand for gene transfer was the work of Wickham et al [117] in which an adenovirus was coupled to a bispecific antibody (bsAb) (recognizing both an epitope of adenovirus and an anti-E-selectin antibody). This bsAb was able to direct binding and entry of adenovirus into TNF-α-activated endothelial cells increasing then β-galactosidase transduction, while non activated cells were not

efficiently transduced. The targeting was E-selectin specific, since the majority of transduction was blocked by preincubating the HUVECs with the anti-E-selectin mAb [117].

In further work with the adenovirus vector, the anti-E-selectin mAb (1.2B6) was coupled directly to the virus. Gene transduction of cultured endothelial cells was increased 20-fold compared with a non-specific control Ab coupled to the virus. The vector transduced around 30% of the intimal endothelial cells in segments of pig aorta cultured with cytokines *ex vivo*, compared with less than 0.1% of transduced cells with the control [118].

In an attempt to improve the specificity of viral gene carriers, Ogawara et al carried out PEGylation of the adenovirus to inhibit its interaction with the coxsackie-adenovirus receptor and conjugated an E-selectin Ab to the ends of the PEG chains. This system showed longer persistence in the circulation with plasma concentrations 12-fold higher than those of unmodified virus, and selectively localized in inflamed skin in mice exhibiting a delayed-type hypersensitivity inflammation, resulting in local expression of the reporter transgene luciferase [119].

Another strategy to prolong the circulation time of viral vectors was proposed by Bachtarzi et al. who coated adenovirus with an amino-reactive polymer based on poly [N-(2-hydroxypropyl) methacrylamide. H18/7 mAb was conjugated to these particles via protein G to provide optimal antibody orientation. This construction enhanced the transduction of TNF-α-activated endothelium *in vitro* and in a human umbilical vein cord model *ex vivo*. When the virus was targeted using a chimeric P-selectin Glycoprotein Ligand-1-Fc fusion (PSGL-1) protein (that recognized both P- and E-selectin), it showed significant uptake into HepG2 xenografts following systemic administration in mice, with 36-fold more genome copies than non-modified virus. [120].

Although viral vectors are efficient at transfecting cells *in vitro* and *in vivo*, there are still some safety issues to be resolved. Therefore, much research has been devoted to non viral vectors, based on lipids or on polymers which are safer than viral vectors, relatively non immunogenic, may not be pro-inflammatory and generally easy to make. Targeting strategies towards E-selectin have also been applied to these systems.

George et al proposed a method of coupling anti-E-selectin 1.2B6 Ab to liposomes already complexed with DNA, using mild heat treatment to aggregate the immunoglobulin G (IgG). The transfection rate was increased in CHO cells transfected to express E-selectin, TNF-α-activated endothelial cells, and TNF-*α*-stimulated human saphenous veins *ex vivo.* Transfection was inhibited by an excess of free antibody, demonstrating the specificity of targeting [121].

Amido amine dendrimers (PAMAM) carry a large number of positively charged terminal amines and hence bind DNA electrostatically, condensing and protecting it from various cellular, extracellular and bacterial nucleases [124 and thus represent an alternative to liposomes for non viral gene delivery]. When the anti-selectin 1.2B6 Ab was conjugated to PAMAM by means of biotin/avidin interaction, the transfection efficacy of complexed DNA increased 4-7 fold in CHO cells expressing E-selectin, in primary human saphenous vein endothelial cells activated with TNF-α and in human saphenous vein segments compared to plain dendrimers [124].

These *in vitro* trials of E-selectin-mediated targeting of viral and non-viral gene delivery seem to be promising. However, no data are available from *in vivo* studies of such systems. Future development will have to deal with general issues of gene delivery *in vivo* such as gene activation, integrating the gene into the cellular genome and avoiding harmful side effects.

Another aspect of nucleic acid delivery is, the use of smaller sequences (antisense oligonucleotides and siRNA) to silence genes. One example of this strategy in the treatment of inflammation was the use of SLE^x–bearing liposomes loaded with antisense oligonucleotides (AS-ODNs) directed against the adhesion molecule ICAM-1 to activated vascular endothelial cells [122]. Two different AS-ODNs were tested and both were able to reach their target in the cytoplasm and inhibit protein expression. The AS-ODN concentrations needed to inhibit ICAM-1 protein expression were ten-fold lower than those required when lipofectin was used as the vector for ODN transport [122]. A similar approach to silence the gene for a cellular adhesion molecule was the addition of siRNA targeting the gene for VE-cadherin to the cationic amphiphilic lipid known as “SAINT” which has been conjugated to the H18/7 anti-selectin mouse Ab. These lipoplexes delivered significantly more siRNA to activated endothelial cells *in vitro* and in human kidney tissue slices subjected to inflammatory conditions *ex vivo*. The enhanced uptake of siRNA was combined with improved silencing of both gene and protein expression of VE-cadherin in activated HUVECs, indicating that SAINT delivered functionally active siRNA. The association of the lipid complex with cells was correlated with the expression pattern of E-selectin [123]. This is an important result because endothelial cells are notoriously difficult to transfect.

3.4 Applications for imaging

E-selectin has been used to improve the specificity of various types of imaging agents including radioactive (Table 3), fluorescent and MRI (Table 4) markers. We present below

some published data in this domain, including *in vitro* and *in vivo*approaches and clinical trials.

3.4.1 Radioactive agents

Early pioneering work was done by Peters, Haskard and co-workers using Indium (^{111}In)-radiolabeled E-selectin mAb 1.2B6 or its $F(Ab)_2$ fragment (^{111}1n-F(Ab)'1.2B6) for the imaging of vascular endothelial activation [125-127]. After intravenous injection of these imaging agents, they could be clearly detected 20-24h later associated with the inflamed tissues in models of phytohaemagglutinin (PHA)-induced arthritis [125] and urate crystal-induced arthritis [126] in pigs. The *in vivo* accumulation was many folds higher than controls and was correlated with E-selectin expression in the inflamed tissue.

Pig skin sites injected with IL-1, TNF-α, phytohemagglutinin, or phorbol myristate acetate showed specific accumulation of technetium-99(^{99m}Tc)-labeled anti-selectin 1.2B6 mAb after intravenous injection [128]. This approach allowed changes in vascular luminal expression of E-selectin to be quantified and leukocyte traffic and other signs of inflammatory responses to be detected *in vivo* [128].

An E-selectin–binding peptide (ESbp) conjugated with ^{99m}Tc had high affinity for E-selectin *in vitro*. *In vivo* imaging in a rat adjuvant-induced arthritis model showed specific binding of ^{99m}Tc-ESbp to the rat ankle joint which preceded clinical manifestations of inflammation [129].

Garrood et al described imaging of human synovial tissue transplanted into SCID mice using a radiolabeled 1.2B6 mAb and nano *single photon emission computed tomography* / computed tomography (NanoSPECT/CT). The tissue vasculature was stimulated with TNF-α by an intra-graft injection 5 h prior to intravenous injection of ^{111}In-labeled anti E-selectin. A significant difference in graft radioactivity was observed at 4 h and 24 h with a significantly higher uptake of ^{111}In-anti-E-selectin compared with control antibody of the same isotype [130].

In a clinical study carried out with patients suffering from rheumatoid arthritis, prominent and well defined uptake of ^{111}In-labeled $F(ab')_2$ fragments of 1.2B6 anti-E-selectin mAb was clearly visible in inflamed joints of all patients as compared with nonspecific immunoglobulin which was not specifically localized. Targeted ^{111}In-1.2B6 scintigraphy is a sensitive method which yielded more intense and specific imaging than technetium-99 labeled human immunoglobulin (^{99m}Tc-HIg). However, the optimum time for imaging ^{111}In-1.2B6 was 24 h after injection, whereas good results are obtained with ^{99}Tc-HIg as soon as 4 h post injection. Furthermore, Tc is a more suitable isotope for scintigraphy than In [131].

Based on the fact that E-selectin is expressed in venules of actively inflamed mucosa in inflammatory bowel disease (IBD), scintigraphy using ^{111}In-labeled F(ab')$_2$ mAb was carried out. This technique yielded comparable results to the standard technique with Tc-99m labelled leucocytes in 14 patients out of 17, with those positive for both (10/17) showing similar disease localization and extent [71].

A similar approach was applied to rheumatoid arthritis. When a fragment of 1.2B6 anti-E-selectin was labeled with ^{99m}Tc, image contrast in RA patients was slightly better at 4 h than ^{111}In-labelled 1.2B6 F(ab')$_2$, showing a clear advantage of the ^{99m}Tc-Fab as it could be used in a one-day protocol. Plasma clearance of ^{99m}Tc-Fab was faster and its diagnostic accuracy was better than that of ^{111}In-F (ab')(2) and the commonly used tracer ^{99}mTc-oxidronate (^{99m}Tc-HDP) [132]. It should be mentioned that ^{99m}Tc-Fab appeared somewhat unstable *in vivo*, as shown by radioactivity in the thyroid gland and bowel [132].

Table 3 Summary of radioactive imaging agents directed towards E-selectin

system	Imaging agent	Recognition element	Model	Reference
Immunoconjugate	(^{111}In)	E-sel mAb 1.2B6	*In vivo* : phyto-haemagglutinin induced arthritis	[125]
Immunoconjugate	(^{111}In)	E-sel mAb F(Ab)$_2$ fragment (1.2B6)	*In vivo* : urate crystal-induced arthritis	[126]
Immunoconjugate	^{99m}Tc	E-sel mAb 1.2B6 mAb	*In vivo* :skin sites injected with IL-1, TNF-α, phytohema-glutinin, or phorbol myristate acetate	[128]
immunoconjugate	^{99m}Tc	E-sel binding peptide	*in vitro*. *In vivo* adjuvant-induced arthritis	[129]
Immunoconjugate	(^{111}In)	E-sel mAb 1.2B6	*In vivo* : tissue vasculature stimulated with TNF-α	[130]
Immunoconjugate	(^{111}In)	E-sel mAb F(Ab)$_2$ fragment (1.2B6)	Clinical study: rheumatoid arthritis	[131]
Immunoconjugate	(^{111}In)	E-sel mAb F(Ab)$_2$ fragment (1.2B6)	Clinical study :inflammatory bowel disease	[71]
Immunoconjugate	^{99m}Tc	E-sel mAb F(Ab) fragment (1.2B6)	Clinical study: rheumatoid arthritis	[132]
Immunoconjugate	^{111}In	E-sel mAb F(Ab)$_2$ fragment (1.2B6)	Clinical study: rheumatoid arthritis	[132]

3.4.2 Fluorescent agents

Recently, fluorescence has become to replace radioactivity as a means of imaging pathological tissues. Near-infrared labels are necessary for *in vivo* studies to avoid excessive absorbance of the emitted fluorescence by the tissues.

Graft copolymers of poly-(L-lysine) and methyl-PEG were covalently conjugated with a mAb fragment, F $(Ab)_2$ of the H18/7 Ab and labeled with near-infrared indocyanine fluorophores (Cy5.5). The system was employed for *in vitro* imaging of E-selectin expression on human endothelial cells activated with IL-1, it showed high binding specificity (20–30 fold more than non-specific uptake) [133].

Small E-Selectin-binding ligands have also been used to target fluorescent markers. The E-selectin–binding peptide (ESBP) was conjugated to crosslinked dextran-coated iron oxide (CLIO) nanoparticles labeled with (Cy5.5). Internalization by activated HUVECs was rapid and mediated by E-selectin. *In vivo*, the fluorescent targeted particles bound both to Lewis lung carcinoma cells and endothelial cells, although the cancer cells had a much lower expression of E-selectin. This suggests that the system was a very sensitive detector of E-selectin expression [134]. Wittmann et al have reported chemoenzymatic synthesis of a fluorescently labeled mono and bivalent SLE^x conjugates. The staining of CHO and HUVEC cell lines expressing E-selectin was comparable to that for fluorescent anti E-selectin mAb [135].

Liposomes have been used as a carrier for fluorescent imaging with anti-E-selectin Ab. A Cy5.5 fluorescent marker was encapsulated. These liposomes efficiently recognized HUVECs after cytokine activation *in vitro, and were able to localize in an Ehrlich ascites tumor in mice* [77]. The same formulation also localized in arthritic joints in a mouse model [136].

3.4.3 Magnetic resonance imaging

MRI can give much useful information about the structure and function of soft tissues *in vivo* by recording changes in the state of water protons in a magnetic field. However, since water is ubiquitous, this technique has limited sensitivity and specificity unless appropriate contrast agents are used to highlight the tissue of interest. Direct targeting of MR contrast agents to receptors within the pathological region could provide greater specificity than “passive” targeting approaches. Therefore, a number of systems utilizing E-selectin targeting have been developed for MRI. The contrast agents that have been used most frequently are diethylene triamine pentaacetic acid (DTPA) coupled with gadolinium (Gd) and superparamagnetic iron oxide particles.

Mulder et al. prepared pegylated liposomes labeled with H18/7 mAb covalently coupled to the distal end of the PEG-chains incorporating 20-30 mol % of Gd-DTPA -bis(stearyl amide). The encapsulation of the contrast agent did not affect the stability of the liposomes. A rhodamine derivative was also incorporated in order to follow the liposomes by

fluorescence microscopy. Both MRI and fluorescence microscopy revealed the specific association of the liposomal MR contrast agent with TNF-α-stimulated HUVECs [137]. The same group synthesized a molecular conjugate consisting of an analog of SLE^X coupled to DTPA in order to target sites of inflammation. They complexed this ligand with gadolinium to prepare a new contrast agent known as (Gd-DTPA-B (SLE^x) [138]. When this agent was evaluated in mice and rats in a model of fulminating hepatitis induced by the co-administration of D-galactosamine and *E. coli* lipopolysaccharide, an efficient enhancement of contrast was obtained, rendering the liver blood vessels to clearly visible in the affected animals [139]. Accumulation of both specific and non specific contrast agent was also observed in other organs (liver, kidneys, and spleen), which the authors attributed to tissue damage as a result of inflammation leading to extravasation.

A similar contrast agent (Gd-DTPA- SLE^x A) increased the MRI signal intensity in murine models of brain injury stimulated by intracerebral injection of cytokines [140], and focal ischemia [141]. Nonselective contrast agents did not increase the contrast in either model, indicating that the results were not due to nonspecific leakage of the agent across the blood–brain barrier (BBB) or nonselective binding to the endothelium. However, in these models, the enhancement of contrast was slight [141].

Despite these encouraging results, it is known that Gd-based contrast agents generally have low sensitivity, therefore a large number of paramagnetic centers are often needed to obtain adequate contrast. On the other hand, superparamagnetic nanoparticles of iron oxide containing a large number of iron atoms clustered in the same particle have better relaxation properties and are thereby detectable at very low concentrations and provide increased contrast.

Hence Muller et al. grafted the sialyl Lewis x analog described above [138] onto the dextran coating of ultra small particles of iron oxide (USPIO) [142]. Extensive retention of USPIO-SLE^x on TNF-α-stimulated HUVECs was observed *in vitro*. To create an *in vivo* model, hepatitis was induced in NMRI mice by injection of Concanavalin A (Con A), known to stimulate the expression of E-selectin on the endothelium of liver vessels [143]. USPIO are able to pass through the fenestrate of the liver and to be captured by Kupffer cells [144], leading to a loss of signal intensity on MR images. When USPIO-SLE^x were injected intravenously to Con A-treated mice, they induced a significantly lower attenuation of liver signal intensity than USPIO-SLE^x injected to healthy mice, or USPIO injected to ConA-treated mice, suggesting that the specific contrast media is retained extracellularly as a result of interaction with E-selectin overexpressed on the vascular endothelium [142].

Table 4 Summary of delivery systems of MRI imaging agents directed towards E-selectin

System	Imaging agent	Recognition element	Model	Reference
Liposomes	Gd-DTPA	H18/7 mAb	*In vitro*	[137]
Ligand - conjugate	Gd-DTPA	Analogue of SLE^x	*In vivo* fulminating hepatitis	[139]
Ligand - conjugate	Gd-DTPA	Analogue of SLE^x	*In vivo* : brain injury	[140]
Ligand - conjugate	Gd-DTPA	Analogue of SLE^x	*In vivo* : focal ischemia	[141]
Dextran coated iron oxide nanoparticles	Iron oxide	Analogue of SLE^x	*In vitro* *In vivo*: hepatitis	[142]
dextran coated iron Oxide nanoparticles	Iron oxide	E-sel mAb $F(Ab)_2$ fragment (H18/7)	*In vitro*	[145]
Dextran coated iron oxide nanoparticles	Iron oxide	E-sel mAb $F(Ab)_2$ fragment (H18/7)	*In vivo* : adoptive human endothelial cell (HUVEC) implanted in athymic mice	[146]
Iron oxide nanoparticles	Iron oxide	E-sel mAb $F(Ab)_2$ fragment (1.2B6)	*In vitro* *In vivo* : hypersensitivity to oxazolone in the ear	[147]
Iron oxide nanoparticles	Iron oxide	SLE^x	In vitro *In vivo* : multiple sclerosis and stroke	[148]

Cross-linked iron oxide nanoparticles (CLIO) have been decorated with anti-human E-selectin $F(Ab)_2$ fragments. These particles showed 100-200 times higher binding to HUVECs treated with IL-1β than to control cells, and as a result the HUVECs became intensely superparamagnetic [145]. This system was evaluated *in vivo* using a model of adoptive human endothelial cell (HUVEC) implanted in athymic mice in a Matrigel scaffold. E-selectin was induced by IL-1β treatment. The MR high-resolution images recorded after injection of the nanoparticles revealed a three-fold higher accumulation and six-fold stronger contrast effect than with unmodified CLIO [146].

In another study, Reynolds et al. used USPIO nanoparticles conjugated to the anti–murine E-selectin $F(Ab)_2$ 1.2B6 mAb. These nanoparticles were shown to bind to CHO cells expressing mouse E-selectin *in vitro* [147]. In an *in vivo* mouse model of contact hypersensitivity to oxazolone in the ear, the injection of functionalized nanoparticles resulted in their accumulation in the affected ear but not in the noninflammed ear. Accumulation of antibody-directed nanoparticles in the liver and spleen was also observed [147].

Nanoparticles with an iron oxide core coated with more complex polysaccharides were prepared by van Kasteren et al. [148]. These particles each contained 10^5 to 10^7 sugars

per particle. In fact, only nanoparticles carrying the tetra saccharide SLE^x showed strong and selective binding to an E-selectin-F_c chimeric protein in an *in vitro* binding assay. These SLE^x nanoparticles were able to provide good MRI contrast in a model of acute inflammation induced by microinjection of interleukin-1β into the left striatum of rats as well as in model reproducing the clinical features of multiple sclerosis and stroke [148]. Nanoparticles were cleared at later time-points, which indicate that they could be used safely. Therefore, this type of particle could be used in early, preclinical detection of MS and other neuropathologies including multi-infarct dementia, HIV-associated encephalitis, or Parkinson's disease [148].

4 Discussion

Targeting therapeutic agents by means of specific molecular recognition is a very promising strategy for the treatment of complex diseases such as cancer, inflammation, autoimmune disorders, and neuropathologies. These systems could be expected to be more effective and to reduce side effects as well as allowing more accurate and earlier diagnosis by the development of more specific imaging agents.

The body of work described above shows how E-selectin has become one of the molecular targets for this type of specific therapy because of its expression during different disease states.

One of the most important features of targeted delivery systems is their surface properties. Several factors have emerged as important: steric stabilization using PEG [88, 105, 119], dextran [134, 142], or methacrylamide [149] chains; the manner in which the antibody or ligand is attached to the surface (it is clear that covalent linking is more efficient than physical adsorption [90, 91]), ligand accessibility and flexibility, where the positioning of the ligand/antibodyat the end of the chain of PEG stabilizing chain has often been observed to be more effective than direct connection to the surface of the carrier [88, 105] and antibody attached to mobile lipids rather than gel-forming lipids aids effective binding [95, 96]; the number of drug molecules attached to each antibody molecule in the particular case of immunoconjugates that may affect their solubility [100] and the density of the antibody or ligand on the surface in, the case of particulate system [92, 123, 136].

The multivalency or "cluster" effect due to the presence of several copies of antibody or ligand carried by the conjugate/vector has been found to be an important factor that improves the adhesion with E-selectin [148]*. This multivalency enhanced the binding of immunoconjugates compared with free antibody fragments* [133]*, polymers carrying 7-8 copies of E-selectin-binding peptide compared with free peptide* [109]*, immunoliposomes compared with immunoconjugate* [94, 102]*, and nanoparticles carrying antibody fragments*

compared with free antibody fragments [145]*. In all these examples, c*ooperative binding occurs when multiple weak bonds result in overall strong adhesion, mimicking the adhesion of leukocytes to the endothelium.

Negative charge has been claimed to be an advantageous property for injectable systems because it leads to electrostatic repulsion with cells such as vascular endothelial cells, erythrocytes and leucocytes which are also negatively charged. This repulsion is expected to limit non specific interaction with these cells [56, 77, 112, 136].

Different systems have been used for targeting, including simple conjugates, functionalized polymers, liposomes, micro and nanoparticles. Each platform has its own advantages and limits.

Conjugates are small molecules that can be prepared with relatively few steps of preparation and a smaller amount of adjuvant material administered, but their solubility could be an issue [100] and in most cases they have only one recognition element by molecule, so there is no multivalency effect. Liposomes and nanoparticles can carry a wide variety of both hydrophilic and hydrophobic therapeutic or diagnostic agents, provide a larger drug payload per particle, protect encapsulated agents from metabolic processes, and allow a high degree of cooperative binding to target cell antigens. In addition, the lipid composition of liposomes or the polymer composition of the nanoparticles can be modified to obtain other desirable properties such as prolonged circulation in the blood by adding PEG or polysaccharides to their surface.

Liposomes have a phospholipid bilayer structure that mimics the cell membrane and renders them biocompatible and non toxic, but suffer from poor stability on storage (complicated freeze drying) and after administration (interactions with serum proteins and lipoproteins). Progress in polymer chemistry over the last few decades has allowed polymer-based systems with very large spectrum of physico-chemical and biological proprieties to be synthesized. Polymeric nanoparticles are usually more stable than liposomes but their biocompatibility is an important issue that should be always well evaluated in the development of therapeutic or diagnostic agents.

It is clear that the choice of recognition element that will guide the delivery system is as important as the target itself. Monoclonal antibodies are still the most specific tool for molecular recognition, but their immunogenicity and the large size of the final system have prompted an evolution towards antibody fragments (i.e. $F[ab]_2$ and Fab fragments) and even antigen-binding domain fragments. These fragments can be excreted rapidly, and minimize the risk of an undesirable immunological reaction. Another disadvantage of antibodies is that

some of them may have restricted species specificity, i.e they are active in animal models but does not cross-react with the human epitope. In all cases, the complex purification and high cost of antibody production remains a practical problem.

Peptides are easily prepared in large quantity and high purity by solid-phase synthesis, and the sequence can be modified to change their biological half-life; however; very few studies of targeting E-selectin using binding peptides have been reported [98, 99, 109].

Recent progress in glycobiology and the determination of the mechanism by which E-selectin binds to its biological ligands have rendered the use of saccharide ligands an attractive alternative to overcome the problems mentioned above. The use of a proven, small molecule ligand such as SLE^x and its analogs has the advantage of transferable cross-species activity. However, it should be mentioned that SLE^x has a weak affinity for E-selectin, and the system will be in completion with leukocytes carrying SLE^x.

Synthetic analogs of SLE^x could be an advantageous solution, especially because some of these molecules have been reported to have higher affinity than the natural ligands [47, 48]; hence they can bind E-selectin more effectively than leucocytes. Moreover, the hydrophilization of the carrier surface due to the presence of sugar derivatives can participate, to a limited but non negligible extent, to the protection of the delivery system against the adsorption of opsonin proteins in blood plasma and phagocytosis by macrophages [109, 111, 136]. On the other hand, it should be kept in mind that the synthesis of these saccharide molecules is complex but not very expensive.

Most *in vitro* tests under static conditions were carried out using HUVECs or Chinese hamster ovary cells. A number of dynamic methods have been developed and used to simulate circulation conditions; these systems are reviewed elsewhere [50]. Although the *in-vitro* flow models provide useful information and allow some phenomena to be studied in a more relevant way than in static adhesion assays, they represent an approximation and do not completely simulate *in vivo* conditions where the presence of other blood components such as erythrocytes and blood proteins in circulation [150], as well as the modification of vasculature and flow profile within different disease settings [151], may affect interactions with endothelial cells.

The most important concern for the development of clinically acceptable system is to tackle problems of specificity and selectivity of targeting. Although most systems tested *in vitro* have showed very good results, *in-vivo* data often shows a lack of specificity since the targeted conjugate/carrier could be detected in sites other than those to which is was

targeted, especially in the liver [56, 102, 132, 147], spleen [102, 139, 147] , heart and lungs [103] and sometimes the skin [102]. This could be due to formulation issues such as the use of ligands that can recognize other structures in addition to selectins [142], or the use of excess antibody or ligand in the formulation that was not firmly attached to the conjugate or carrier and could serve to mask the target receptor [124].

Future development will depend mainly on how such systems can improve the therapeutic index in the treatment of serious inflammatory disease and cancer compared with conventional therapies.

Conclusion

Although many clinical trials have been carried out in the field of medical imaging, targeted systems for drug delivery to E-selectin are still mostly at the level of laboratory research with animal models. At the same time, new high-affinity ligands have been developed over the last few years and these could be interesting tools for targeting strategies. Much work is now needed to screen these ligands to confirm their specificity before clinical studies. The question of large-scale production for such innovative molecular drug delivery systems also needs to be addressed.

References

[1] M.P. Bevilacqua, J.S. Pober, D.L. Mendrick, R.S. Cotran, M.A. Gimbrone, Jr., Identification of an inducible endothelial-leukocyte adhesion molecule. Proc Natl Acad Sci U S A 84(24) (1987) 9238-9242.

[2] M.P. Bevilacqua, S. Stengelin, M.A. Gimbrone, Jr., B. Seed, Endothelial leukocyte adhesion molecule 1: an inducible receptor for neutrophils related to complement regulatory proteins and lectins. Science 243(4895) (1989) 1160-1165.

[3] S. Hsu-Lin, C.L. Berman, B.C. Furie, D. August, B. Furie, A platelet membrane protein expressed during platelet activation and secretion. Studies using a monoclonal antibody specific for thrombin-activated platelets. J Biol Chem 259(14) (1984) 9121-9126.

[4] P.E. Stenberg, R.P. McEver, M.A. Shuman, Y.V. Jacques, D.F. Bainton, A platelet alpha-granule membrane protein (GMP-140) is expressed on the plasma membrane after activation. J Cell Biol 101(3) (1985) 880-886.

[5] R.P. McEver, J.H. Beckstead, K.L. Moore, L. Marshall-Carlson, D.F. Bainton, GMP-140, a platelet alpha-granule membrane protein, is also synthesized by vascular endothelial cells and is localized in Weibel-Palade bodies. J Clin Invest 84(1) (1989) 92-99.

[6] R. Bonfanti, B.C. Furie, B. Furie, D.D. Wagner, PADGEM (GMP140) is a component of Weibel-Palade bodies of human endothelial cells. Blood 73(5) (1989) 1109-1112.

[7] D.M. Lewinsohn, R.F. Bargatze, E.C. Butcher, Leukocyte-endothelial cell recognition: evidence of a common molecular mechanism shared by neutrophils, lymphocytes, and other leukocytes. J Immunol 138(12) (1987) 4313-4321.

[8] C. Kneuer, C. Ehrhardt, M.W. Radomski, U. Bakowsky, Selectins - potential pharmacological targets? Drug Discov Today 11(21-22) (2006) 1034-1040.

[9] R.P. McEver, Selectin-carbohydrate interactions during inflammation and metastasis. Glycoconj J 14(5) (1997) 585-591.

[10] M.B. Lawrence, T.A. Springer, Leukocytes roll on a selectin at physiologic flow rates: distinction from and prerequisite for adhesion through integrins. Cell 65(5) (1991) 859-873.

[11] T.N. Mayadas, R.C. Johnson, H. Rayburn, R.O. Hynes, D.D. Wagner, Leukocyte rolling and extravasation are severely compromised in P selectin-deficient mice. Cell 74(3) (1993) 541-554.

[12] M.S. Mulligan, M.J. Polley, R.J. Bayer, M.F. Nunn, J.C. Paulson, P.A. Ward, Neutrophil-dependent acute lung injury. Requirement for P-selectin (GMP-140). J Clin Invest 90(4) (1992) 1600-1607.

[13] M.P. Schon, C. Drewniok, W.H. Boehncke, Targeting selectin functions in the therapy of psoriasis. Curr Drug Targets Inflamm Allergy 3(2) (2004) 163-168.

[14] A.J. Littler, C.D. Buckley, P. Wordsworth, I. Collins, J. Martinson, D.L. Simmons, A distinct profile of six soluble adhesion molecules (ICAM-1, ICAM-3, VCAM-1, E-selectin, L-selectin and P-selectin) in rheumatoid arthritis. Br J Rheumatol 36(2) (1997) 164-169.

[15] M. Subramaniam, P.S. Frenette, S. Saffaripour, R.C. Johnson, R.O. Hynes, D.D. Wagner, Defects in hemostasis in P-selectin-deficient mice. Blood 87(4) (1996) 1238-1242.

[16] G. Wu, F. Li, P. Li, C. Ruan, Detection of plasma alpha-granule membrane protein GMP-140 using radiolabeled monoclonal antibodies in thrombotic diseases. Haemostasis 23(2) (1993) 121-128.

[17] R. Lotan, A. Raz, Endogenous lectins as mediators of tumor cell adhesion. J Cell Biochem 37(1) (1988) 107-117.

[18] R.J. Ludwig, B. Boehme, M. Podda, R. Henschler, E. Jager, C. Tandi, W.H. Boehncke, T.M. Zollner, R. Kaufmann, J. Gille, Endothelial P-selectin as a target of heparin action in experimental melanoma lung metastasis. Cancer Res 64(8) (2004) 2743-2750.

[19] R.J. Ludwig, M.P. Schon, W.H. Boehncke, P-selectin: a common therapeutic target for cardiovascular disorders, inflammation and tumour metastasis. Expert Opin Ther Targets 11(8) (2007) 1103-1117.

[20] O. Spertini, B. Schleiffenbaum, C. White-Owen, P. Ruiz, Jr., T.F. Tedder, ELISA for quantitation of L-selectin shed from leukocytes *in vivo*. J Immunol Methods 156(1) (1992) 115-123.

[21] E.R. Lampeter, T.K. Kishimoto, R. Rothlein, E.A. Mainolfi, J. Bertrams, H. Kolb, S. Martin, Elevated levels of circulating adhesion molecules in IDDM patients and in subjects at risk for IDDM. Diabetes 41(12) (1992) 1668-1671.

[22] A. Stucki, A.S. Cordey, N. Monai, J.C. de Flaugergues, M. Schapira, O. Spertini, Cleaved L-selectin concentrations in meningeal leukaemia. Lancet 345(8945) (1995) 286-289.

[23] H.P. Hartung, K. Reiners, J.J. Archelos, M. Michels, P. Seeldrayers, F. Heidenreich, K.W. Pflughaupt, K.V. Toyka, Circulating adhesion molecules and tumor necrosis factor receptor in multiple sclerosis: correlation with magnetic resonance imaging. Ann Neurol 38(2) (1995) 186-193.

[24] K. Fassbender, R. Mossner, L. Motsch, U. Kischka, A. Grau, M. Hennerici, Circulating selectin- and immunoglobulin-type adhesion molecules in acute ischemic stroke. Stroke 26(8) (1995) 1361-1364.

[25] P. Pahlsson, J. Strindhall, U. Srinivas, A. Lundblad, Role of N-linked glycosylation in expression of E-selectin on human endothelial cells. Eur J Immunol 25(9) (1995) 2452-2459.

[26] M.P. Bevilacqua, Endothelial-leukocyte adhesion molecules. Annu Rev Immunol 11 (1993) 767-804.

[27] K.F. Montgomery, L. Osborn, C. Hession, R. Tizard, D. Goff, C. Vassallo, P.I. Tarr, K. Bomsztyk, R. Lobb, J.M. Harlan, et al., Activation of endothelial-leukocyte adhesion molecule 1 (ELAM-1) gene transcription. Proc Natl Acad Sci U S A 88(15) (1991) 6523-6527.

[28] D. Wong, K. Dorovini-Zis, Regualtion by cytokines and lipopolysaccharide of E-selectin expression by human brain microvessel endothelial cells in primary culture. J Neuropathol Exp Neurol 55(2) (1996) 225-235.

[29] X. Banquy, G.g. Leclair, J.-M. Rabanel, A. Argaw, J.-F.o. Bouchard, P. Hildgen, S. Giasson, Selectins Ligand Decorated Drug Carriers for Activated Endothelial Cell Targeting. Bioconjugate Chemistry 19(10) (2008) 2030-2039.

[30] E.J. von Asmuth, E.F. Smeets, L.A. Ginsel, J.J. Onderwater, J.F. Leeuwenberg, W.A. Buurman, Evidence for endocytosis of E-selectin in human endothelial cells. Eur J Immunol 22(10) (1992) 2519-2526.

[31] M. Subramaniam, J.A. Koedam, D.D. Wagner, Divergent fates of P- and E-selectins after their expression on the plasma membrane. Mol Biol Cell 4(8) (1993) 791-801.

[32] H. Setiadi, R.P. McEver, Clustering endothelial E-selectin in clathrin-coated pits and lipid rafts enhances leukocyte adhesion under flow. Blood 111(4) (2008) 1989-1998.

[33] J.F. Leeuwenberg, E.F. Smeets, J.J. Neefjes, M.A. Shaffer, T. Cinek, T.M. Jeunhomme, T.J. Ahern, W.A. Buurman, E-selectin and intercellular adhesion molecule-1 are released by activated human endothelial cells *in vitro*. Immunology 77(4) (1992) 543-549.

[34] R.R. Lobb, G. Chi-Rosso, D.R. Leone, M.D. Rosa, S. Bixler, B.M. Newman, S. Luhowskyj, C.D. Benjamin, I.G. Dougas, S.E. Goelz, Expression and functional characterization of a soluble form of endothelial-leukocyte adhesion molecule 1. The Journal of Immunology 147(1) (1991) 124-129.

[35] C.J. Cummings, Curtis N. Sessler, L.D. Beall, Bernard J. Fisher, Al M. Best, Alpha A. Fowler, III, Soluble E-Selectin Levels in Sepsis and Critical Illness . Correlation with Infection and Hemodynamic Dysfunction. Am. J. Respir. Crit. Care Med. 156(2) (1997) 431-437.

[36] M. Steegmaier, A. Levinovitz, S. Isenmann, E. Borges, M. Lenter, H.P. Kocher, B. Kleuser, D. Vestweber, The E-selectin-ligand ESL-1 is a variant of a receptor for fibroblast growth factor. Nature 373(6515) (1995) 615-620.

[37] K.L. Moore, S.F. Eaton, D.E. Lyons, H.S. Lichenstein, R.D. Cummings, R.P. McEver, The P-selectin glycoprotein ligand from human neutrophils displays sialylated, fucosylated, O-linked poly-N-acetyllactosamine. J Biol Chem 269(37) (1994) 23318-23327.

[38] L.J. Picker, R.A. Warnock, A.R. Burns, C.M. Doerschuk, E.L. Berg, E.C. Butcher, The neutrophil selectin LECAM-1 presents carbohydrate ligands to the vascular selectins ELAM-1 and GMP-140. Cell 66(5) (1991) 921-933.

[39] M. Matsumoto, K. Atarashi, E. Umemoto, Y. Furukawa, A. Shigeta, M. Miyasaka, T. Hirata, CD43 functions as a ligand for E-Selectin on activated T cells. J Immunol 175(12) (2005) 8042-8050.

[40] C.J. Dimitroff, J.Y. Lee, S. Rafii, R.C. Fuhlbrigge, R. Sackstein, CD44 is a major E-selectin ligand on human hematopoietic progenitor cells. J Cell Biol 153(6) (2001) 1277-1286.

[41] P. Kotovuori, E. Tontti, R. Pigott, M. Shepherd, M. Kiso, A. Hasegawa, R. Renkonen, P. Nortamo, D.C. Altieri, C.G. Gahmberg, The vascular E-selectin binds to the leukocyte integrins CD11/CD18. Glycobiology 3(2) (1993) 131-136.

[42] S. Gout, C. Morin, F. Houle, J. Huot, Death receptor-3, a new E-Selectin counter-receptor that confers migration and survival advantages to colon carcinoma cells by triggering p38 and ERK MAPK activation. Cancer Res 66(18) (2006) 9117-9124.

[43] M.L. Phillips, E. Nudelman, F.C. Gaeta, M. Perez, A.K. Singhal, S. Hakomori, J.C. Paulson, ELAM-1 mediates cell adhesion by recognition of a carbohydrate ligand, sialyl-Lex. Science 250(4984) (1990) 1130-1132.

[44] G. Walz, A. Aruffo, W. Kolanus, M. Bevilacqua, B. Seed, Recognition by ELAM-1 of the sialyl-Lex determinant on myeloid and tumor cells. Science 250(4984) (1990) 1132-1135.

[45] W.S. Somers, J. Tang, G.D. Shaw, R.T. Camphausen, Insights into the molecular basis of leukocyte tethering and rolling revealed by structures of P- and E-selectin bound to SLe(X) and PSGL-1. Cell 103(3) (2000) 467-479.

[46] F. Pichierri, Molecular orbital study of the E-selectin/sialyl LewisX interaction. RIKEN Rev 46 (2002) 50-51.

[47] E.E. Simanek, G.J. McGarvey, J.A. Jablonowski, C.H. Wong, ChemInform Abstract: Selectin—Carbohydrate Interactions: From Natural Ligands to Designed Mimics. ChemInform 29(25) (1998).

[48] N. Kaila, B.E.t. Thomas, Design and synthesis of sialyl Lewis(x) mimics as E- and P-selectin inhibitors. Med Res Rev 22(6) (2002) 566-601.

[49] A.M. Olofsson, K.E. Arfors, L. Ramezani, B.A. Wolitzky, E.C. Butcher, U.H. von Andrian, E-selectin mediates leukocyte rolling in interleukin-1-treated rabbit mesentery venules. Blood 84(8) (1994) 2749-2758.

[50] C. Ehrhardt, C. Kneuer, U. Bakowsky, Selectins-an emerging target for drug delivery. Adv Drug Deliv Rev 56(4) (2004) 527-549.

[51] S.R. Barthel, J.D. Gavino, L. Descheny, C.J. Dimitroff, Targeting selectins and selectin ligands in inflammation and cancer. Expert Opin Ther Targets 11(11) (2007) 1473-1491.

[52] J.J. Grailer, M. Kodera, D.A. Steeber, L-selectin: Role in regulating homeostasis and cutaneous inflammation. Journal of Dermatological Science 56(3) (2009) 141-147.

[53] D.H. Adams, S.G. Hubscher, N.C. Fisher, A. Williams, M. Robinson, Expression of E-selectin and E-selectin ligands in human liver inflammation. Hepatology 24(3) (1996) 533-538.

[54] L. Stefanovic, M. Bogic, J. Balaban, O. Mitrovic, R. Stosovic, S. Andrejevic, [The role of endothelial cells in allergic inflammation reactions]. Srp Arh Celok Lek 126(3-4) (1998) 138-144.

[55] S.A. Asgeirsdottir, J.A. Kamps, H.I. Bakker, P.J. Zwiers, P. Heeringa, K. van der Weide, H. van Goor, A.H. Petersen, H. Morselt, H.E. Moorlag, E. Steenbergen, C.G. Kallenberg, G. Molema, Site-specific inhibition of glomerulonephritis progression by targeted delivery of dexamethasone to glomerular endothelium. Mol Pharmacol 72(1) (2007) 121-131.

[56] N. Hashida, N. Ohguro, N. Yamazaki, Y. Arakawa, E. Oiki, H. Mashimo, N. Kurokawa, Y. Tano, High-efficacy site-directed drug delivery system using sialyl-Lewis X conjugated liposome. Experimental Eye Research 86(1) (2008) 138-149.

[57] S.P. Jones, S.D. Trocha, M.B. Strange, D.N. Granger, C.G. Kevil, D.C. Bullard, D.J. Lefer, Leukocyte and endothelial cell adhesion molecules in a chronic murine model of myocardial reperfusion injury. Am J Physiol Heart Circ Physiol 279(5) (2000) H2196-2201.

[58] G. Kulig, K. Pilarska, [The role od adhesion molecules in the pathogenesis of Graves ophthalmopathy]. Klin Oczna 103(2-3) (2001) 147-150.

[59] R. Wikaningrum, J. Highton, A. Parker, M. Coleman, P.A. Hessian, P.J. Roberts-Thompson, M.J. Ahern, M.D. Smith, Pathogenic mechanisms in the rheumatoid nodule: comparison of proinflammatory cytokine production and cell adhesion molecule expression in rheumatoid nodules and synovial membranes from the same patient. Arthritis Rheum 41(10) (1998) 1783-1797.

[60] J. Kriegsmann, G.M. Keyszer, T. Geiler, A.S. Lagoo, S. Lagoo-Deenadayalan, R.E. Gay, S. Gay, Expression of E-selectin messenger RNA and protein in rheumatoid arthritis. Arthritis Rheum 38(6) (1995) 750-754.

[61] M.M. Corkill, B.W. Kirkham, D.O. Haskard, C. Barbatis, T. Gibson, G.S. Panayi, Gold treatment of rheumatoid arthritis decreases synovial expression of the endothelial leukocyte adhesion receptor ELAM-1. J Rheumatol 18(10) (1991) 1453-1460.

[62] T. Garrood, L. Lee, C. Pitzalis, Molecular mechanisms of cell recruitment to inflammatory sites: general and tissue-specific pathways. Rheumatology (Oxford) 45(3) (2006) 250-260.

[63] P.P. Tak, P.C. Taylor, F.C. Breedveld, T.J. Smeets, M.R. Daha, P.M. Kluin, A.E. Meinders, R.N. Maini, Decrease in cellularity and expression of adhesion molecules by anti-tumor necrosis factor alpha monoclonal antibody treatment in patients with rheumatoid arthritis. Arthritis Rheum 39(7) (1996) 1077-1081.

[64] T. Kobayashi, S. Hashimoto, K. Imai, E. Amemiya, M. Yamaguchi, A. Yachi, T. Horie, Elevation of serum soluble intercellular adhesion molecule-1 (sICAM-1) and sE-selectin levels in bronchial asthma. Clin Exp Immunol 96(1) (1994) 110-115.

[65] L. Kowalzick, A. Kleinheinz, K. Neuber, M. Weichenthal, I. Kohler, J. Ring, Elevated serum levels of soluble adhesion molecules ICAM-1 and ELAM-1 in patients with severe atopic eczema and influence of UVA1 treatment. Dermatology 190(1) (1995) 14-18.

[66] C. Wenisch, D. Myskiw, B. Parschalk, T. Hartmann, K. Dam, W. Graninger, Soluble endothelium-associated adhesion molecules in patients with Graves' disease. Clin Exp Immunol 98(2) (1994) 240-244.

[67] N. Oka, I. Akiguchi, T. Kawasaki, K. Ohnishi, J. Kimura, Elevated serum levels of endothelial leukocyte adhesion molecules in Guillain-Barre syndrome and chronic inflammatory demyelinating polyneuropathy. Ann Neurol 35(5) (1994) 621-624.

[68] D.S. Kim, K.Y. Lee, Serum soluble E-selectin levels in Kawasaki disease. Scand J Rheumatol 23(5) (1994) 283-286.

[69] W. Czech, E. Schopf, A. Kapp, Soluble E-selectin in sera of patients with atopic dermatitis and psoriasis--correlation with disease activity. Br J Dermatol 134(1) (1996) 17-21.

[70] D. Krasowska, A. Pietrzak, B. Lecewicz-Torun, Serum level of sELAM-1 in psoriatic patients correlates with disease activity. J Eur Acad Dermatol Venereol 12(2) (1999) 140-142.

[71] M. Bhatti, P. Chapman, M. Peters, D. Haskard, H.J. Hodgson, Visualising E-selectin in the detection and evaluation of inflammatory bowel disease. Gut 43(1) (1998) 40-47.

[72] I.P. Witz, The selectin-selectin ligand axis in tumor progression. Cancer Metastasis Rev 27(1) (2008) 19-30.

[73] K. Kiriyama, C. Ye, [E-selectin expression in serum and tissue correlates with distant metastasis of colorectal cancer]. Nippon Rinsho 53(7) (1995) 1760-1764.

[74] B. Mayer, H. Spatz, I. Funke, J.P. Johnson, F.W. Schildberg, De novo expression of the cell adhesion molecule E-selectin on gastric cancer endothelium. Langenbecks Arch Surg 383(1) (1998) 81-86.

[75] J. Renkonen, A. Makitie, T. Paavonen, R. Renkonen, Sialyl-Lewis(x/a)-decorated selectin ligands in head and neck tumours. J Cancer Res Clin Oncol 125(10) (1999) 569-576.

[76] M. Nguyen, C.L. Corless, B.M. Kraling, C. Tran, T. Atha, J. Bischoff, S.H. Barsky, Vascular expression of E-selectin is increased in estrogen-receptor-negative breast cancer: a role for tumor-cell-secreted interleukin-1 alpha. Am J Pathol 150(4) (1997) 1307-1314.

[77] M. Hirai, Y. Hiramatsu, S. Iwashita, T. Otani, L. Chen, Y.-g. Li, M. Okada, K. Oie, K. Igarashi, H. Wakita, M. Seno, E-selectin targeting to visualize tumors *in vivo*. Contrast Media & Molecular Imaging 5(2) (2010) 70-77.

[78] R. Kannagi, M. Izawa, T. Koike, K. Miyazaki, N. Kimura, Carbohydrate-mediated cell adhesion in cancer metastasis and angiogenesis. Cancer Sci 95(5) (2004) 377-384.

[79] A. Takada, K. Ohmori, T. Yoneda, K. Tsuyuoka, A. Hasegawa, M. Kiso, R. Kannagi, Contribution of carbohydrate antigens sialyl Lewis A and sialyl Lewis X to adhesion of human cancer cells to vascular endothelium. Cancer Res 53(2) (1993) 354-361.

[80] P. Brodt, L. Fallavollita, R.S. Bresalier, S. Meterissian, C.R. Norton, B.A. Wolitzky, Liver endothelial E-selectin mediates carcinoma cell adhesion and promotes liver metastasis. Int J Cancer 71(4) (1997) 612-619.

[81] A. Tozeren, H.K. Kleinman, D.S. Grant, D. Morales, A.M. Mercurio, S.W. Byers, E-selectin-mediated dynamic interactions of breast- and colon-cancer cells with endothelial-cell monolayers. Int J Cancer 60(3) (1995) 426-431.

[82] M.A. Moss, S. Zimmer, K.W. Anderson, Role of metastatic potential in the adhesion of human breast cancer cells to endothelial monolayers. Anticancer Res 20(3A) (2000) 1425-1433.

[83] M.H. Eichbaum, T.M. de Rossi, S. Kaul, G. Bastert, Serum levels of soluble E-selectin are associated with the clinical course of metastatic disease in patients with liver metastases from breast cancer. Oncol Res 14(11-12) (2004) 603-610.

[84] C.J. Dimitroff, M. Lechpammer, D. Long-Woodward, J.L. Kutok, Rolling of human bone-metastatic prostate tumor cells on human bone marrow endothelium under shear flow is mediated by E-selectin. Cancer Res 64(15) (2004) 5261-5269.

[85] T. Nakashio, T. Narita, M. Sato, S. Akiyama, Y. Kasai, M. Fujiwara, K. Ito, H. Takagi, R. Kannagi, The association of metastasis with the expression of adhesion molecules in cell lines derived from human gastric cancer. Anticancer Res 17(1A) (1997) 293-299.

[86] Y. Izumi, Y. Taniuchi, T. Tsuji, C.W. Smith, S. Nakamori, I.J. Fidler, T. Irimura, Characterization of Human Colon Carcinoma Variant Cells Selected for Sialyl Lex Carbohydrate Antigen: Liver Colonization and Adhesion to Vascular Endothelial Cells. Experimental Cell Research 216(1) (1995) 215-221.

[87] G. Bendas, A. Krause, R. Schmidt, J. Vogel, U. Rothe, Selectins as new targets for immunoliposome-mediated drug delivery. A potential way of anti-inflammatory therapy. Pharm Acta Helv 73(1) (1998) 19-26.

[88] G. Bendas, A. Krause, U. Bakowsky, J. Vogel, U. Rothe, Targetability of novel immunoliposomes prepared by a new antibody conjugation technique. International Journal of Pharmaceutics 181(1) (1999) 79-93.

[89] S. Kessner, A. Krause, U. Rothe, G. Bendas, Investigation of the cellular uptake of E-Selectin-targeted immunoliposomes by activated human endothelial cells. Biochim Biophys Acta 1514(2) (2001) 177-190.

[90] J.B. Dickerson, J.E. Blackwell, J.J. Ou, V.R. Shinde Patil, D.J. Goetz, Limited adhesion of biodegradable microspheres to E- and P-selectin under flow. Biotechnol Bioeng 73(6) (2001) 500-509.

[91] J.E. Blackwell, N.M. Dagia, J.B. Dickerson, E.L. Berg, D.J. Goetz, Ligand coated nanosphere adhesion to E- and P-selectin under static and flow conditions. Ann Biomed Eng 29(6) (2001) 523-533.

[92] H.S. Sakhalkar, M.K. Dalal, A.K. Salem, R. Ansari, J. Fu, M.F. Kiani, D.T. Kurjiaka, J. Hanes, K.M. Shakesheff, D.J. Goetz, Leukocyte-inspired biodegradable particles that selectively and avidly adhere to inflamed endothelium *in vitro* and *in vivo*. Proc Natl Acad Sci U S A 100(26) (2003) 15895-15900.

[93] E.J. Kunkel, K. Ley, Distinct phenotype of E-selectin-deficient mice. E-selectin is required for slow leukocyte rolling *in vivo*. Circ Res 79(6) (1996) 1196-1204.

[94] D.D. Spragg, D.R. Alford, R. Greferath, C.E. Larsen, K.D. Lee, G.C. Gurtner, M.I. Cybulsky, P.F. Tosi, C. Nicolau, M.A. Gimbrone, Jr., Immunotargeting of liposomes to activated vascular endothelial cells: a strategy for site-selective delivery in the cardiovascular system. Proc Natl Acad Sci U S A 94(16) (1997) 8795-8800.

[95] R.C. Gunawan, D.T. Auguste, The role of antibody synergy and membrane fluidity in the vascular targeting of immunoliposomes. Biomaterials 31(5) (2009) 900-907.

[96] R.C. Gunawan, D.T. Auguste, Immunoliposomes That Target Endothelium *In Vitro* Are Dependent on Lipid Raft Formation. Molecular Pharmaceutics 7(5) (2010) 1569-1575.

[97] J. Minaguchi, T. Oohashi, K. Inagawa, A. Ohtsuka, Y. Ninomiya, Transvascular accumulation of Sialyl Lewis X conjugated liposome in inflamed joints of collagen antibody-induced arthritic (CAIA) mice. Arch Histol Cytol 71(3) (2008) 195-203.

[98] Y. Shamay, D. Paulin, G. Ashkenasy, A. David, Multivalent display of quinic acid based ligands for targeting E-selectin expressing cells. J Med Chem 52(19) (2009) 5906-5915.

[99] A.H. Myrset, H.B. Fjerdingstad, R. Bendiksen, B.E. Arbo, R.M. Bjerke, J.H. Johansen, M.A. Kulseth, R. Skurtveit, Design and Characterization of Targeted Ultrasound Microbubbles for Diagnostic Use. Ultrasound in Medicine & Biology 37(1) (2011) 136-150.

[100] M. Everts, R.J. Kok, S.A. Asgeirsdottir, B.N. Melgert, T.J. Moolenaar, G.A. Koning, M.J. van Luyn, D.K. Meijer, G. Molema, Selective intracellular delivery of dexamethasone into activated endothelial cells using an E-selectin-directed immunoconjugate. J Immunol 168(2) (2002) 883-889.

[101] R.J. Kok, M. Everts, S.A. Asgeirsdottir, D.K. Meijer, G. Molema, Cellular handling of a dexamethasone-anti-E-selectin immunoconjugate by activated endothelial cells: comparison with free dexamethasone. Pharm Res 19(11) (2002) 1730-1735.

[102] M. Everts, G.A. Koning, R.J. Kok, S.A. Ásgeirsdóttir, D. Vestweber, D.K.F. Meijer, G. Storm, G. Molema, *In Vitro* Cellular Handling and *in Vivo* Targeting of E-Selectin-Directed Immunoconjugates and Immunoliposomes Used for Drug Delivery to Inflamed Endothelium. Pharmaceutical Research 20(1) (2003) 64-72.

[103] S.A. Asgeirsdottir, P.J. Zwiers, H.W. Morselt, H.E. Moorlag, H.I. Bakker, P. Heeringa, J.W. Kok, C.G.M. Kallenberg, G. Molema, J.A.A.M. Kamps, Inhibition of proinflammatory genes in anti-GBM glomerulonephritis by targeted dexamethasone-loaded AbEsel liposomes. Am J Physiol Renal Physiol 294(3) (2008) F554-561.

[104] R. Kannagi, Molecular mechanism for cancer-associated induction of sialyl Lewis X and sialyl Lewis A expression-The Warburg effect revisited. Glycoconj J 20(5) (2004) 353-364.

[105] R. Zeisig, R. Stahn, K. Wenzel, D. Behrens, I. Fichtner, Effect of sialyl Lewis X-glycoliposomes on the inhibition of E-selectin-mediated tumour cell adhesion *in vitro*. Biochim Biophys Acta 1660(1-2) (2004) 31-40.

[106] R. Stahn, H. Schafer, F. Kernchen, J. Schreiber, Multivalent sialyl Lewis x ligands of definite structures as inhibitors of E-selectin mediated cell adhesion. Glycobiology 8(4) (1998) 311-319.

[107] K. Shirota, Y. Kato, T. Irimura, H. Kondo, Y. Sugiyama, Anti-metastatic effect of the sialyl Lewis-X analog GSC-150 on the human colon carcinoma derived cell line KM12-HX in the mouse. Biol Pharm Bull 24(3) (2001) 316-319.

[108] A.P. Mann, A. Somasunderam, R. Nieves-Alicea, X. Li, A. Hu, A.K. Sood, M. Ferrari, D.G. Gorenstein, T. Tanaka, Identification of thioaptamer ligand against E-selectin: potential application for inflamed vasculature targeting. PLoS One 5(9) (2010) 13050.

[109] Y. Shamay, D. Paulin, G. Ashkenasy, A. David, E-selectin binding peptide-polymer-drug conjugates and their selective cytotoxicity against vascular endothelial cells. Biomaterials 30(32) (2009) 6460-6468.

[110] C. Pattillo, B. Venegas, F. Donelson, L. Del Valle, L. Knight, P. Chong, M. Kiani, Radiation-Guided Targeting of Combretastatin Encapsulated Immunoliposomes to Mammary Tumors. Pharmaceutical Research 26(5) (2009) 1093-1100.

[111] E.L. Vodovozova, E.V. Moiseeva, G.K. Grechko, G.P. Gayenko, N.E. Nifant'ev, N.V. Bovin, J.G. Molotkovsky, Antitumour activity of cytotoxic liposomes equipped with selectin ligand SiaLe(X), in a mouse mammary adenocarcinoma model. Eur J Cancer 36(7) (2000) 942-949.

[112] M. Hirai, H. Minematsu, Y. Hiramatsu, H. Kitagawa, T. Otani, S. Iwashita, T. Kudoh, L. Chen, Y. Li, M. Okada, D.S. Salomon, K. Igarashi, M. Chikuma, M. Seno, Novel and simple loading procedure of cisplatin into liposomes and targeting tumor endothelial cells. International Journal of Pharmaceutics 391(1-2) (2010) 274-283.

[113] D.T. Price, J. Loscalzo, Cellular adhesion molecules and atherogenesis. Am J Med 107(1) (1999) 85-97.

[114] T.M. Carlos, J.M. Harlan, Leukocyte-endothelial adhesion molecules. Blood 84(7) (1994) 2068-2101.

[115] W. Tsuruta, H. Tsurushima, T. Yamamoto, K. Suzuki, N. Yamazaki, A. Matsumura, Application of liposomes incorporating doxorubicin with sialyl Lewis X to prevent stenosis after rat carotid artery injury. Biomaterials 30(1) (2009) 118-125.

[116] J.-M. Kiely, M.I. Cybulsky, F.W. Luscinskas, M.A. Gimbrone, Jr., Immunoselective Targeting of an Anti-Thrombin Agent to the Surface of Cytokine-Activated Vascular Endothelial Cells. Arterioscler Thromb Vasc Biol 15(8) (1995) 1211-1218.

[117] T.J. Wickham, D. Haskard, D. Segal, I. Kovesdi, Targeting endothelium for gene therapy via receptors up-regulated during angiogenesis and inflammation. Cancer Immunol Immunother 45(3-4) (1997) 149-151.

[118] O.A. Harari, T.J. Wickham, C.J. Stocker, I. Kovesdi, D.M. Segal, T.Y. Huehns, C. Sarraf, D.O. Haskard, Targeting an adenoviral gene vector to cytokine-activated vascular endothelium via E-selectin. Gene Ther 6(5) (1999) 801-807.

[119] K. Ogawara, M.G. Rots, R.J. Kok, H.E. Moorlag, A.M. Van Loenen, D.K. Meijer, H.J. Haisma, G. Molema, A novel strategy to modify adenovirus tropism and enhance transgene delivery to activated vascular endothelial cells *in vitro* and in vivo. Hum Gene Ther 15(5) (2004) 433-443.

[120] H. Bachtarzi, M. Stevenson, V. Subr, K. Ulbrich, L.W. Seymour, K.D. Fisher, Targeting adenovirus gene delivery to activated tumour-associated vasculature via endothelial selectins. J Control Release 150(2) (2011) 196-203.

[121] P.H. Tan, M. Manunta, N. Ardjomand, S.A. Xue, D.F.P. Larkin, D.O. Haskard, K.M. Taylor, A.J.T. George, Antibody targeted gene transfer to endothelium. The Journal of Gene Medicine 5(4) (2003) 311-323.

[122] R. Stahn, C. Grittner, R. Zeisig, U. Karsten, S.B. Felix, K. Wenzel, Sialyl Lewis(x)-liposomes as vehicles for site-directed, E-selectin-mediated drug transfer into activated endothelial cells. Cell Mol Life Sci 58(1) (2001) 141-147.

[123] S.A. Ásgeirsdóttir, E.G. Talman, I.A. de Graaf, J.A.A.M. Kamps, S.C. Satchell, P.W. Mathieson, M.H.J. Ruiters, G. Molema, Targeted transfection increases siRNA uptake and gene silencing of primary endothelial cells *in vitro* -- A quantitative study. Journal of Controlled Release 141(2) (2010) 241-251.

[124] S. Theoharis, U. Krueger, P.H. Tan, D.O. Haskard, M. Weber, A.J.T. George, Targeting gene delivery to activated vascular endothelium using anti E/P-Selectin antibody linked to PAMAM dendrimers. Journal of Immunological Methods 343(2) (2009) 79-90.

[125] E.T.M. Keelan, A.A. Harrison, P.T. Chapman, R.M. Binns, A.M. Peters, D.O. Haskard, Imaging Vascular Endothelial Activation: An Approach Using Radiolabeled Monoclonal Antibodies Against the Endothelial Cell Adhesion Molecule E-Selectin. J Nucl Med 35(2) (1994) 276-281.

[126] P.T. Chapman, F. Jamar, A.A. Harrison, R.M. Binns, A.M. Peters, D.O. Haskard, Noninvasive imaging of E-selectin expression by activated endothelium in urate crystal-induced arthritis. Arthritis Rheum 37(12) (1994) 1752-1756.

[127] F. Jamar, P.T. Chapman, A.A. Harrison, R.M. Binns, D.O. Haskard, A.M. Peters, Inflammatory arthritis: imaging of endothelial cell activation with an indium-111-labeled F(ab')2 fragment of anti-E-selectin monoclonal antibody. Radiology 194(3) (1995) 843-850.

[128] E.T. Keelan, S.T. Licence, A.M. Peters, R.M. Binns, D.O. Haskard, Characterization of E-selectin expression *in vivo* with use of a radiolabeled monoclonal antibody. Am J Physiol Heart Circ Physiol 266(1) (1994) H278-290.

[129] K.R. Zinn, T.R. Chaudhuri, C.A. Smyth, Q. Wu, H.G. Liu, M. Fleck, J.D. Mountz, J.M. Mountz, Specific targeting of activated endothelium in rat adjuvant arthritis with a 99mTc-radiolabeled E-selectin-binding peptide. Arthritis Rheum 42(4) (1999) 641-649.

[130] T. Garrood, M. Blades, D.O. Haskard, S. Mather, C. Pitzalis, A novel model for the pre-clinical imaging of inflamed human synovial vasculature. Rheumatology (Oxford) 48(8) (2009) 926-931.

[131] F. Jamar, P.T. Chapman, D.H. Manicourt, D.M. Glass, D.O. Haskard, A.M. Peters, A comparison between 111In-anti-E-selectin mAb and 99Tcm-labelled human non-specific immunoglobulin in radionuclide imaging of rheumatoid arthritis. Br J Radiol 70(833) (1997) 473-481.

[132] F. Jamar, F.A. Houssiau, J.P. Devogelaer, P.T. Chapman, D.O. Haskard, V. Beaujean, C. Beckers, D.H. Manicourt, A.M. Peters, Scintigraphy using a technetium 99m-labelled anti-E-selectin Fab fragment in rheumatoid arthritis. Rheumatology (Oxford) 41(1) (2002) 53-61.

[133] H.W. Kang, R. Weissleder, A. Bogdanov, Jr., Targeting of MPEG-protected polyamino acid carrier to human E-selectin *in vitro*. Amino Acids 23(1-3) (2002) 301-308.

[134] M. Funovics, X. Montet, F. Reynolds, R. Weissleder, L. Josephson, Nanoparticles for the optical imaging of tumor E-selectin. Neoplasia 7(10) (2005) 904-911.

[135] V. Wittmann, A.K. Datta, K.M. Koeller, C.-H. Wong, Chemoenzymatic Synthesis and Fluorescent Visualization of Cell-Surface Selectin-Bound Sialyl Lewis X Derivatives. Chemistry – A European Journal 6(1) (2000) 162-171.

[136] M. Hirai, H. Minematsu, N. Kondo, K. Oie, K. Igarashi, N. Yamazaki, Accumulation of liposome with Sialyl Lewis X to inflammation and tumor region: Application to *in vivo* bio-imaging. Biochemical and Biophysical Research Communications 353(3) (2007) 553-558.

[137] W.J. Mulder, G.J. Strijkers, A.W. Griffioen, L. van Bloois, G. Molema, G. Storm, G.A. Koning, K. Nicolay, A liposomal system for contrast-enhanced magnetic resonance imaging of molecular targets. Bioconjug Chem 15(4) (2004) 799-806.

[138] Y. Fu, S. Laurent, Robert N. Muller, Synthesis of a Sialyl LewisX Mimetic Conjugated with DTPA, Potential Ligand of New Contrast Agents for Medical Imaging. European Journal of Organic Chemistry 2002(23) (2002) 3966-3973.

[139] S. Boutry, C. Burtea, S. Laurent, G. Toubeau, L. Vander Elst, R.N. Muller, Magnetic resonance imaging of inflammation with a specific selectin-targeted contrast agent. Magn Reson Med 53(4) (2005) 800-807.

[140] N.R. Sibson, A.M. Blamire, M. Bernades-Silva, S. Laurent, S. Boutry, R.N. Muller, P. Styles, D.C. Anthony, MRI detection of early endothelial activation in brain inflammation. Magn Reson Med 51(2) (2004) 248-252.

[141] P.A. Barber, T. Foniok, D. Kirk, A.M. Buchan, S. Laurent, S. Boutry, R.N. Muller, L. Hoyte, B. Tomanek, U.I. Tuor, MR molecular imaging of early endothelial activation in focal ischemia. Ann Neurol 56(1) (2004) 116-120.

[142] S. Boutry, S. Laurent, L.V. Elst, R.N. Muller, Specific E-selectin targeting with a superparamagnetic MRI contrast agent. Contrast Media & Molecular Imaging 1(1) (2006) 15-22.

[143] H. Morikawa, K. Hachiya, H. Mizuhara, H. Fujiwara, S. Nishiguchi, S. Shiomi, T. Kuroki, K. Kaneda, Sublobular veins as the main site of lymphocyte adhesion/transmigration and adhesion molecule expression in the porto-sinusoidal-hepatic venous system during concanavalin A-induced hepatitis in mice. Hepatology 31(1) (2000) 83-94.

[144] B.E. Van Beers, C. Sempoux, R. Materne, M. Delos, A.M. Smith, Biodistribution of ultrasmall iron oxide particles in the rat liver. J Magn Reson Imaging 13(4) (2001) 594-599.

[145] H.W. Kang, L. Josephson, A. Petrovsky, R. Weissleder, A. Bogdanov, Magnetic Resonance Imaging of Inducible E-Selectin Expression in Human Endothelial Cell Culture. Bioconjugate Chemistry 13(1) (2002) 122-127.

[146] H.W. Kang, D. Torres, L. Wald, R. Weissleder, A.A. Bogdanov, Targeted imaging of human endothelial-specific marker in a model of adoptive cell transfer. Lab Invest 86(6) (2006) 599-609.

[147] P.R. Reynolds, D.J. Larkman, D.O. Haskard, J.V. Hajnal, N.L. Kennea, A.J. George, A.D. Edwards, Detection of vascular expression of E-selectin *in vivo* with MR imaging. Radiology 241(2) (2006) 469-476.

[148] S.I. van Kasteren, S.J. Campbell, S. Serres, D.C. Anthony, N.R. Sibson, B.G. Davis, Glyconanoparticles allow pre-symptomatic in vivo imaging of brain disease. Proc Natl Acad Sci U S A 106(1) (2009) 18-23.

[149] H. Bachtarzi, M. Stevenson, L.W. Seymour, K.D. Fisher, Targeting adenovirus gene delivery to activated tumour-associated vasculature via endothelial selectins. Journal of Controlled Release In Press, Uncorrected Proof.

[150] H.L. Goldsmith, V.T. Turitto, Rheological aspects of thrombosis and haemostasis: basic principles and applications. ICTH-Report--Subcommittee on Rheology of the International Committee on Thrombosis and Haemostasis. Thromb Haemost 55(3) (1986) 415-435.

[151] J.R. Less, T.C. Skalak, E.M. Sevick, R.K. Jain, Microvascular architecture in a mammary carcinoma: branching patterns and vessel dimensions. Cancer Res 51(1) (1991) 265-273.

Travaux expérimentaux

Chapitre I

Synthèse, caractérisation et reconnaissance moléculaire des nanoparticules ornées de ligand saccharidique

Comme il a été souligné dans l'introduction de cette thèse, l'objectif de notre travail était d'élaborer un système vecteur de troisième génération type cœur-couronne composé d'une partie hydrophobe centrale entourée d'une couronne hydrophile de poly(éthylène glycol) modifiée à son extrémité par un ligand glucidique.

L'enjeu a été de développer une structure macromoléculaire amphiphile fonctionnalisée dont la composition chimique est biocompatible pour une administration *in-vivo*, et permet de préparer des nanosphères stables de taille inférieure à 200nm. La structure des nanosphères doit également adoptée une conformation favorable en suspension aqueuse pour rendre les molécules de sucre accessibles vis-à-vis de leur cible.

Aujourd'hui, les avancées considérables de la chimie organique et des polymères offrent beaucoup de possibilités pour la construction de structures extrêmement variées selon l'application finale désirée. Toutes ces avancées nous ont permis dans ce travail de développer une stratégie de synthèse pour l'obtention d'un copolymère amphiphile avec une architecture à bloc munie sur sa partie hydrophile d'une unité saccharidique. Pour montrer la faisabilité de notre stratégie, nous avons commencé cette étude avec le glucopyranoside comme modèle d'un ligand glucidique.

Avec le double objectif de contrôler le taux d'insertion du ligand ainsi que sa position sur la surface des nanoparticules, nous avons choisi de l'insérer en amont de notre synthèse directement sur l'extrémité du monomère hydrophile. Pour cela, il était nécessaire d'avoir une méthode efficace et spécifique pour la réalisation de ce couplage.

Le concept de la « click chemistry » (schéma 1), surtout celle catalysée par le cuivre pour former un cycle triazole à partir des azides et des acétylènes [1], a attiré l'attention de nombreux chercheurs ces dernières années grâce à sa spécificité, son efficacité, ses conditions simples de réaction et son rendement élevé. Pour toutes ses raisons, nous avons séléctionné cette méthode de couplage pour incorporer le glucopyranoside via une cycloaddition d'un alcyne (R-C ≡ C) greffé sur le monomère et d'un azide ($-N_3$) porté par la molécule de sucre.

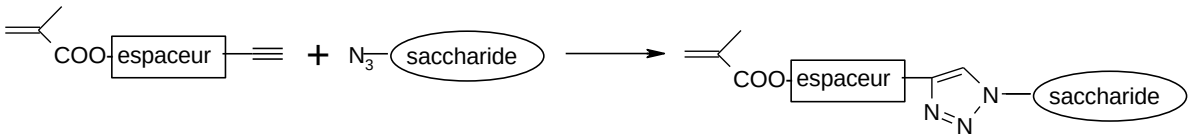

Schéma.1 Mécanisme de la méthode de « click chemistry » appliqué au PEGMA

La polymérisation par ouverture de cycle (ROP) des lactones (schéma 2) est classiquement utilisée pour la préparation des polyesters dégradables et plus récemment

pour préparer des polymères à bloc complexes en combinant la ROP avec d'autres méthodes de polymérisation. Nous l'avons utilisé pour la préparation de la partie hydrophobe de copolymère amphiphile composé de polylactide PLA.

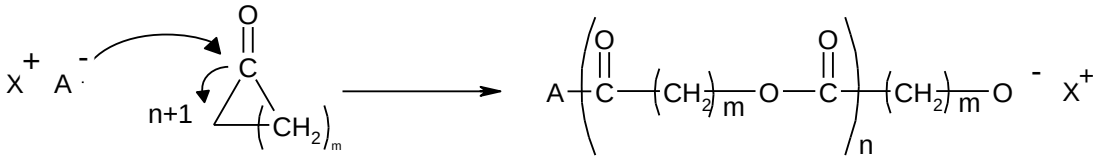

Schéma.2 Mécanisme de la ROP

Dans le but d'obtenir un copolymère de structure définie, les techniques de synthèse par polymérisation radicalaire contrôlée nous semblaient les plus indiquées en raison de leur facilité de mise en œuvre. La littérature rapporte principalement la voie par polymérisation radicalaire par transfert d'atome (ATRP) (schéma 3). Dans ce procédé, le mécanisme est basé sur un équilibre réversible entre une espèce dormante halogénée et une espèce active en présence d'un complexe métalique. Seule l'espèce active est capable d'amorcer la polymérisation et d'additionner un monomère. Ceci a pour conséquence de réduire la concentration en radicaux dans le milieu et donc de limiter les réactions de terminaison. Il est donc aisé par ce procédé de contrôler la masse molaire des polymères ainsi que leur architecture selon l'amorceur utilisé.[2]

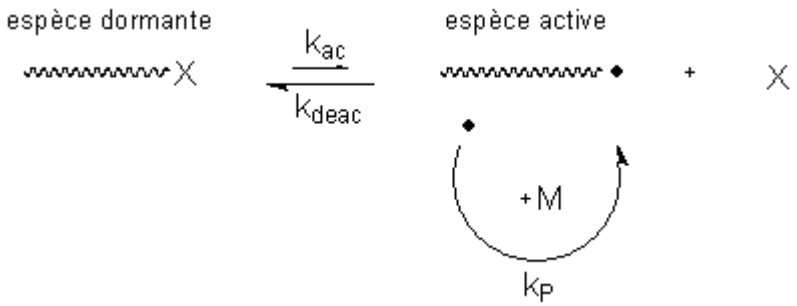

Schéma 3. Mécanisme de l'ATRP.

Une copolymérisation par ATRP a donc été envisagée pour synthétiser la partie hydrophile de nos nanoparticules.

Dans le travail présenté dans ce chapitre, nous avons mis au point les conditions opératoires pour coupler le glucopyranoside avec le poly (éthylène glycol) méthacrylate (PEGMA) par « click chemistry ». Ensuite, la construction du copolymère amphiphile a été

faite par une combinaison de la ROP pour la partie hydrophobe et l'ATRP pour la partie hydrophile.

La caractérisation chimique des polymères a été réalisée par résonance magnétique nucléaire (RMN ^{1}H), chromatographie d'exclusion stérique (SEC) et spectroscopie Infrarouge.

Les nanoparticules ont été préparées à partir de ce copolymère par la méthode de nanoprécipitation introduite par Fessi et al [3]. Ces nanoparticules ont été caractérisées au niveau de leur taille par la diffusion quasi élastique de la lumière et de leur morphologie par la microscopie électronique à transmission.

La présence des résidus de glucopyranoside à la surface des nanoparticules et leurs accessibilités ont été confirmées par réaction avec la Concanavalin A (Con A). Cette dernière est une lectine qui contient plusieurs sites de reconnaissance des molécules saccharidiques comme le α-mannopyranosyl et le α-glucopyranosyl. La présence de Con A avec les nanoparticules a provoqué leurs agrégations indiquant l'interaction des glucopyranosides à la surface des particules avec la molécule de lectine.

L'évaluation de leur cytotoxicité a été réalisée sur des cultures de cellules endothéliales de la veine ombilicale humaine en utilisant le test MTT.

Références bibliographiques

1. Huisgen, R., *Kinetics and Mechanism of 1,3-Dipolar Cycloadditions.* Angewandte Chemie International Edition in English, 1963. **2**(11): p. 633-645.
2. Matyjaszewski, K. and J. Xia, *Atom Transfer Radical Polymerization.* Chem. Rev., 2001. **101**(9): p. 2921-2990.
3. H. Fessi, J.P.Devissaguet., F. Puieux et C. Thies, *Procédé de préparation de systèmes colloïdaux dispersibles d'une substance sous forme de nanoparticules.* Brevet Français N° 8618444 1986: France.

Synthesis, Characterization and Molecular Recognition of Sugar-Functionalized Nanoparticles Prepared by a Combination of ROP, ATRP and Click Chemistry

Emile Jubeli, Laurence Moine* and Gillian Barratt

Université Paris-Sud11, UMR 8612 CNRS, IFR 141, Faculté de Pharmacie 5 rue J.B. Clément CHATENAY-MALABRY , FR 92296

Journal of Polymer Science Part A:
Polymer Chemistry

Vol. 48, 3178–3187 (2010) Wiley Periodicals, Inc.

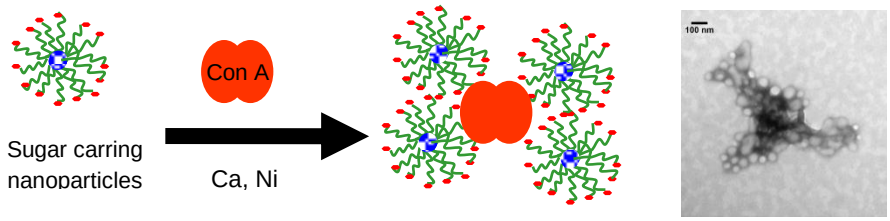

* To whom correspondence should be addressed: Tel: +33 1 46 83 59 94 ; Fax: +33 1 46 83 53 12 ; e-mail: laurence.moine@u-psud.fr

Keywords

Nanoparticles, Click chemistry, ROP/ATRP, Carbohydrate ligand

Abstract

The aim of this work was to prepare nanoparticles bearing sugar residues at their surface through the synthesis of amphiphilic block copolymer of PLA and PEGMA, with the hydrophilic part terminating with glucopyranoside molecules as a model for any carbohydrate ligand. The construction was achieved by a combination of click chemistry, ring-opening polymerization and atom transfer radical polymerization. The modified monomer and resulting copolymer were characterized by NMR, SEC and FT-IR. Nanoparticles with a mean hydrodynamic diameter of less than 200nm as determined by quasi-elastic light scattering were prepared from the amphiphilic copolymer by nanoprecipitation using DMF as water-miscible solvent. In the range of 2.5-10 mg copolymer/mL DMF, the polymer concentration did not have much effect on the size of the nanoparticles. Accessibility of glucopyranoside molecules on the surface of the nanoparticles was confirmed by formation of aggregates from nanoparticles in the presence of Concanavalin A observed by transmission electronic microscopy. Finally, no significant cytotoxicity towards human umbilical vein endothelial cells was detected for the final nanoparticles.

Introduction

Nanosized particles as drug delivery systems [1-4] have attracted increasing interest over the last two decades because of their advantageous properties, such as their high surface-to-mass ratio, their ability to protect labile drugs and to carry poorly soluble ones. It has been clearly demonstrated that surface properties of colloids are a key factor which determines their *in vivo* fate and, in particular, their interactions with blood proteins which can lead to rapid opsonisation and uptake by cells of the reticuloendothelial system. To reduce this uptake and obtain long-circulating nanoparticles, surface-modified colloids have been developed by grafting hydrophilic chains of poly (ethylene glycol) [5-8] or polysaccharides [9, 10] onto their surface. More site-specific drug targeting can be achieved by using specific bimolecular recognition such as antibody-antigen and sugar-protein binding.

Recent progress in glycobiology shows that specific interactions between cell surface oligosaccharides and a large number of known lectins play important roles in various biological recognition process including inflammation, fertilization, cell-cell contacts, signal transmission [11-16]. Thus, sugar-bearing molecules or macromolecules are a very attractive tool for drug targeting compared with other strategies such as antigen-antibody recognition that possess drawbacks such as possible immunogenicity, large size of the final delivery system and the high cost of antibody production. Moreover pendant saccharides on a polymer backbone can enhance the affinity towards cell-surface lectins because of the multivalent recognition, known as the “cluster effect” [11, 17].

Polymeric nanoparticles carrying saccharide moieties have been developed for liver-specific drug delivery [18, 19] and for targeting drugs to activated endothelium [20]. The development of new strategies to functionalize materials and/or to formulate them as drug delivery systems is of a major interest for pharmaceutical applications. To prepare such systems, well-defined glycopolymers should be synthesized. Most glycopolymers reported in the literature were prepared by post-functionnalization of preformed polymers using sugar moieties. [21-24] In this way it was possible to prepare libraries of different copolymers with various proportions of different carbohydrate epitopes using click chemistry (termed co-clicking by Haddleton and coworkers [21, 25, 26]). A smaller number of reports have used another strategy of polymerizing sugar-containing monomers [27-30].

Azide-alkyne dipolar cycloaddition proposed by Huisgen results in a triazole heterogenic cycle [31]. Now referred to as “click chemistry”, this is a powerful, high reliable and very selective reaction which can be carried out under mild experimental conditions [32]. Moreover, the azide and acetylene groups have weak acid-base properties, so they are

almost inert toward biological molecules under conditions found inside living cells [33, 34]. It is now evident that this click process is an excellent tool for the synthesis of glycopolymers. We report here its use to synthesize a bioactive and stable glycomonomer that can be polymerized to generate glycolfunctionalized polymers.

In order to synthesize a biocompatible polymer with a defined structure that can be used in the formulation of nanoparticles, we chose to base this on poly DL-lactide (PdLL), which is a well-known biodegradable polymer, widely used in surgical repair, to formulate carriers for drug delivery and other biomedical applications. As well as its biodegradability, it has good mechanical properties and excellent shaping and modeling properties.

Among the methods for the preparation of tailor-made polymers, atom transfer radical polymerization (ATRP) is a well established controlled living method based on an equilibrium between a large number of dormant halogenated species and a small number of active propagating radicals [35]. In this way, the degree of polymerization can be controlled and a narrow molecular weight distribution can be obtained, especially for the polymerization of methacrylate derivatives [36, 37].

In the light of these considerations, the aim of this work was the preparation of nanoparticles bearing adaptable saccharide molecules as a model for a carbohydrate ligand on a drug carrier surface. Firstly, the coupling of the azide-terminated monosaccharide molecules with the alkyne-functionalized poly (ethylene glycol) methacrylate (PEGMA) was achieved by a click reaction, followed by the synthesis of amphiphilic block copolymer bearing a monosaccharide residue by a combination of ring-opening polymerization of lactide and atom transfer radical polymerization of PEGMA.

These amphiphilic block copolymers were used successfully to prepare surfactant-free glucosylated nanoparticles by the nanoprecipitation method. The effect of the copolymer concentration in the organic solvent on the formation of nanoparticles was investigated and the accessibility of glucose moieties on their surface was proved by their agglutination in the presence of Concanavalin (A), a protein known for its affinity for glucose and mannose molecules. The cytotoxicity of these nanoparticles towards endothelial cells was also evaluated.

Experimental section

Materials

Poly (ethylene glycol) methacrylate PEGMA (*M*n ≈ 526), 1-azido-1-deoxy-β-D-glucopyranoside tetra acetate, tin (II) 2-ethylhexanoate ($Sn(Oct)_2$ 95%) and *N*, *N′*, dicyclohexyl carbodiimide (DCC 99%), sodium methoxide approximately 25 wt.% solution in methanol, HEPES (*N*-2-hydroxyethylpiperazine-*N*'-2-ethanesulfonic acid) and Concanavaline A type IV (jack bean) were purchased from Sigma-Aldrich. 2-bromo-2-methylpropionyl bromide (98%) and *N*,*N*,*N′*,*N″*,*N″*-pentamethyldiethylenetriamine (PMDETA), amberlite@ IR120 resin were obtained from Acrôs organics (Belgium). Trimethylamine (99.5%) and 4-pentynoic acid 98% were purchased from Alfa Aesar-UK. $NiCl_2$ and $CaCl_2$ were obtained from VWR international. D-Lactide (Biovalley) was recrystallized from ethyl acetate twice then dried under vacuum. Copper (I) bromide Cu (I) Br (Sigma-Aldrich) was washed with glacial acetic acid, filtered, washed with ethanol and dried under vacuum. PEGMA was purified before use as described previously [36].

Instruments:

^{1}H-NMR measurements were performed with a Bruker 300MHz spectrometer. Tetramethylsilane was used as an internal standard and $CDCl_3$ as a solvent unless otherwise mentioned.

Size exclusion chromatography was performed with a double detector 270 dual viscosimeter and light scattering detector 90° (Viscotek®- France) and a refractometer (Waters® 410). THF was used as the mobile phase with a TOSOH BIOSCIENCE TSKgel 5µm bead size Guard pre-column, and two TOSOH BIOSCIENCE TSKgel 5µm bead size GMHHR-M columns, operated at 1 mL/min with the column temperature set at 30°C. Omnisec® software (Viscotek) was used to process the data.

The mean hydrodynamic diameter and polydispersity of the nanoparticles were measured by quasi-elastic light scattering with a Zetasizer NanoZS90 (Malvern Instruments) after appropriate dilution with MilliQ® water. For each sample, the measurement was performed three times at a temperature of 25°C with a detection angle of 90°.

Transmission electron microscopy (Philips EM 208 equipped with an acquisition camera CCD ATM) was used to visualize the morphology and the structure of nanoparticles and their aggregates with Con A. 3µL of each simple was placed on a copper mesh grid and images were obtained after carbon coating.

Synthesis of the bifunctional initiator

β-hydroxyl ethyl α-bromoisobutyrate [HEBIB] was synthesized according to a procedure reported in the literature [38, 39]. It was obtained as a colorless liquid with a yield of 60 %.

^{1}H-NMR ($CDCl_3$): 1.96 (6H, BrC (C**H$_3$)$_2$**-), 3.95 (2H, CH_2-C**H$_2$**-OH), 4.15 (4H, C**H$_2$**-C**H2**-OH).

Synthesis of the PLA macroinitiator (1)

D,L-lactide (8.64g ; 60mmol), $Sn(Oct)_2$ (10.4mg ; 0.013mmol) and the synthesized bifunctional initiator HEBIB (30mg ; 0.28mmol) were introduced in a schlenk tube and the mixture was bubbled with nitrogen for 30min. The schlenk tube was placed in a thermostated oil bath at 130 °C and stirred for 2 hours. The resulting solid crude product was dissolved in chloroform and precipitated in a cold mixture of 1:1 petroleum ether/diethyl ether and dried in a vacuum oven at 40°C to give a white solid (yield 96%).

^{1}H-NMR (300MHz, $CDCl_3$, δ ppm) 1.55 (3H, C**H$_3$**), 5.2 **(**1H, -C**H** main chain). Mn_{NMR}= 32400, Mn_{SEC} = 32400, Mw/Mn=1.02.

Synthesis of acetylene-terminated PEGMA. (Pentynoate- PEGMA) (3):

PEGMA (7.5g; 14.3mmol), 4-pentynoic acid (2.8g; 28.5mmol) and DMAP (0.17g; 1.4mmol) were put in a schlenk tube with 35 ml of methylene chloride (CH_2Cl_2). DCC (5.6g; 27.2mmol) was solubilized in 5 mL of CH_2Cl_2 and then added to the schlenk tube. The mixture was stirred overnight at room temperature. After elimination of DCU crystals by filtration, the organic solvent was evaporated under reduced pressure. The resulting yellow oil-like product was purified by column chromatography with a mixture of ethyl acetate/methanol (9:1) as eluant to yield the acetylene-terminated PEGMA (yield =82%).

^{1}H-NMR (300MHz, $CDCl_3$, δ ppm): 1.92 (3H, CH_2=C-C**H$_3$**), 1.96 (1H, ≡ C**H**), 2.50 (2H, -C**H$_2$**-CH_2-C≡CH), 2.51 (2H, -CH_2-C**H$_2$**-C≡CH), 3.65 (36H, -C**H$_2$**-, PEG), 4.26 (4H, 2 x -CH_2-COO), 5.55 (1H, - **H**HC= C), 6.1 (1H , -H**H**C = C). IR (cm^{-1}): 3260 (-C≡CH), 2870 (alkyl), 1620 (-C=C-).

Synthesis of glucopyranoside tetra acetate-grafted PEGMA (4)

Acetylene-terminated PEGMA (**3**) (1.2g; 2mmol), 1-azido-1-deoxy-β-D-glucopyranoside tetra acetate (1.49g; 4mmol), CuBr (0.29g; 2mmol) and PMDETA (0.35mg; 2mmol) were introduced in a schlenk tube with 5 mL of DMF. The mixture was degassed by

three freeze-pump-thaws. After stirring for the mentioned time at room temperature, the reaction was stopped and the content was diluted with CH_2Cl_2 before being submitted to column chromatography with a mixture of CH_2Cl_2/methanol (95:5). The resulting PEGMA-glucopyranoside tetra acetate (**4**) was dried under vacuum (yield= 79%).

^{1}H-NMR (300MHz, $CDCl_3$, δ ppm): 1.91 (3H, CH_2=C-C**H$_3$**), 1.83_1.99_2.03_2.05 (4 x 3H, 4 COO-C**H$_3$**), 2.72 (2H, -C**H$_2$**-CH_2-C=CH), 3 (2H, -CH_2-C**H$_2$**-C=CH), 3.62 (36H, -CH_2- of PEG), 3.98 (1H, -N-C**H**-, glucose ring), 4.27 (4H, 2x -C**H$_2$**-COO), 5.19_5.37_5.81 (1H,2H,1H, 4 –C**H**- glucose ring), 5.54 (1H , **H**HC= CH-, vinyl), 6.1 (1H , H**H**C = CH vinyl), 7.58 (1H, -C=C**H**-N triazole ring). IR (cm^{-1}): 2870 (alkyl), 1720 (-C=O-), 1640 (-C=C).

Synthesis of glucopyranoside-grafted PEGMA (5)

The deprotection of the glucopyranoside was done as described in literature with slight modifications [24]. Product (**4**) (0.536g; 0.55mmol) was dissolved in methanol (5mL), then sodium methoxide (10µL, 0.05mmol) was added and the mixture was stirred for 8 minutes before neutralization with Amberlite$^@$ IR120. After filtration and evaporation of the methanol under reduced vacuum, the deprotected product (**5**) was obtained with a 96% yield.

^{1}H-NMR (300MHz, DMSO d6, δ ppm): 1.88 (3H, CH_2=C-C**H$_3$**), 2.69 (2H, -C**H$_2$**-CH_2-C=CH), 2.89 (2H, -CH_2-C**H$_2$**-C=CH), 3.2-3.9 (4H,–C**H**- glucose cycle and 36H, -C**H$_2$**- of PEG), 4.12 (4H, 2x -C**H$_2$**-COO), 5.55 (–C**H**- anomeric g- lucose cycle), 5.67 (1H , **H**HC= CH-, vinyl), 6.02 (1H , H**H**C = CH vinyl), 8.05 (1H, -C=C**H**-N triazole ring). IR (cm^{-1}): 30600-3050 (-OH), 2870 (alkyl), 1720 (-C=O-), 1640 (-C=C).

Synthesis of PLA-block-PEGMA-glucopyranoside by ATRP (6)

PLA (**1**) (0.64g; 0.02mmol) PEGMA-glucopyranoside (**5**) (0.81 mg; 0.1mmol), CuBr (5.72mg; 0.04mmol), PMDETA (6.9mg; 0.04mmol) were introduced to a schlenk tube with 4 ml of anisole. After three freeze-pump-thaws, the schlenk tube was placed in a thermostated oil bath at 60 °C and stirred for 3h. The content was then purified by column chromatography with CH_2Cl_2/methanol (9:1) to remove the copper complex. After precipitation by adding polymer solution in chloroform to a cold mixture of petroleum ether/ diethyl ether (1:1), the product was dried in a vacuum oven at 40°C to yield 56%.

^{1}H-NMR (300MHz, DMSO, δ ppm): 1.2-1.4 (-C**H$_2$-** main chain of PEGMA), 1.45 (3H, -C**H$_3$** PLA), 2.71 (2H, -C**H$_2$**-CH_2-C=CH), 2.89 (2H, -CH_2-C**H$_2$**-C=CH),), 3.2-3.9 (4H,–C**H**-glucose ring and 36, -C**H$_2$**- of PEG), 4.14 (4H, 2x -C**H$_2$**-COO), 5.19 (-C**H**- main chain of PLA),

5.5 (C**H**- anomeric glucose cycle), 8.05 (1H, -C=C**H**-N triazole ring). Mn_{NMR} = 35400, Mn_{SEC}= 36400 and *M*w/*M*n = 1.21.

Preparation of nanoparticles:

Nanoparticles were prepared by nanoprecipitation: 5, 10 or 20mg of the copolymer (**6**) were dissolved in 2 mL of DMF. This solution was added dropwise to 4ml of water under moderate stirring through a needle (0.8mm internal diameter) over 1min. The crude nanoparticles suspension was centrifuged (Centrifuge Eppendorf 5804 R) at 4500 x g for 10 min at 20 °C to separate larger polymer aggregates from nanoparticles that remained in the supernatant, then DMF was removed by 4 hours dialysis (MWCO 15000 Da) against deionized water. After measuring nanoparticles size by light scattering, nanoparticles suspensions were freeze-dried (freeze-drier Christ Alpha 2-4 LD plus, Bioblock scientific) and the resulting dry lyophilizates were weighed to determine the yield of nanoparticles (NP) formation as follows: NP % = (M_{NP}/ M_{total}) x100.

Concanavalin A binding assay:

Nanoparticles containing approximately 20µM of surface glucopyranoside residues (based on copolymer composition determined by ^{1}H-NMR) were prepared in 10 mM HEPES buffer solution containing 1mM $CaCl_2$, and 1mM $NiCl_2$. The pH was adjusted to 7.4 by addition of NaOH 1M. Concanavalin A (Con A) solutions were prepared in an identical buffer solution.

2 mL of nanoparticles suspension were added to 2 mL of different concentrations of Con A solution (0-10 µM) directly into the cuvette in a UV-Visible spectrometer and absorbance data were recorded every 2 minutes at 340 nm for 20 min under continuous stirring. Then the apparent size of the aggregates resulting from the interaction between glucopyranoside-decorated nanoparticles and Con A was measured by quasi-elastic light scattering, and samples of these suspensions were observed by TEM.

Cell culture and cytotoxicity assay

Human umbilical vein endothelial cells (HUV-EC-C cell line, ATCC reference CRL-1730) were cultured in Dulbecco modified Eagle's medium (DMEM, Lonza, Vervier, Belgium) supplemented with 2 mM L-glutamine, 10% fetal calf serum (FCS), 50 U/ml penicillin, and 50 µg/mL streptomycin. Cells were maintained at 37 °C under a humidified atmosphere containing 5% CO_2.

The cytotoxicity of nanoparticles prepared from the copolymer (**6**) was determined by assessing cell viability on HUVEC cell line using the 3-[4,5-dimethylthiazol-2-yl]-2,5-diphenyltetrazolium) bromide (MTT) assay measuring mitochondrial dehydrogenase cell activity. Cells were seeded in DMEM into 96-well plates at a density of 10^4 cells/well. After an adherence period of 24h, different dilutions of nanoparticles (0.1-0.5 mg polymer/mL of culture medium) were added to the cells. Each dilution was tested in at least 5 wells. After 48 hours of incubation at 37°C, 20µL of a MTT (Sigma-Aldrich, Saint Quentin Fallavier, France) in PBS (5mg/mL) were added to each well. After further incubation for 2 hours at 37°C, culture medium was removed and formazan crystals were dissolved in 200 µL DMSO. The absorbance of converted dye, correlated with the number of viable cells was measured at 570 nm using a microplate reader (Labsystems multiscan MS). The percentage of survival cells was calculated as the absorbance ratio of treated to untreated cells.

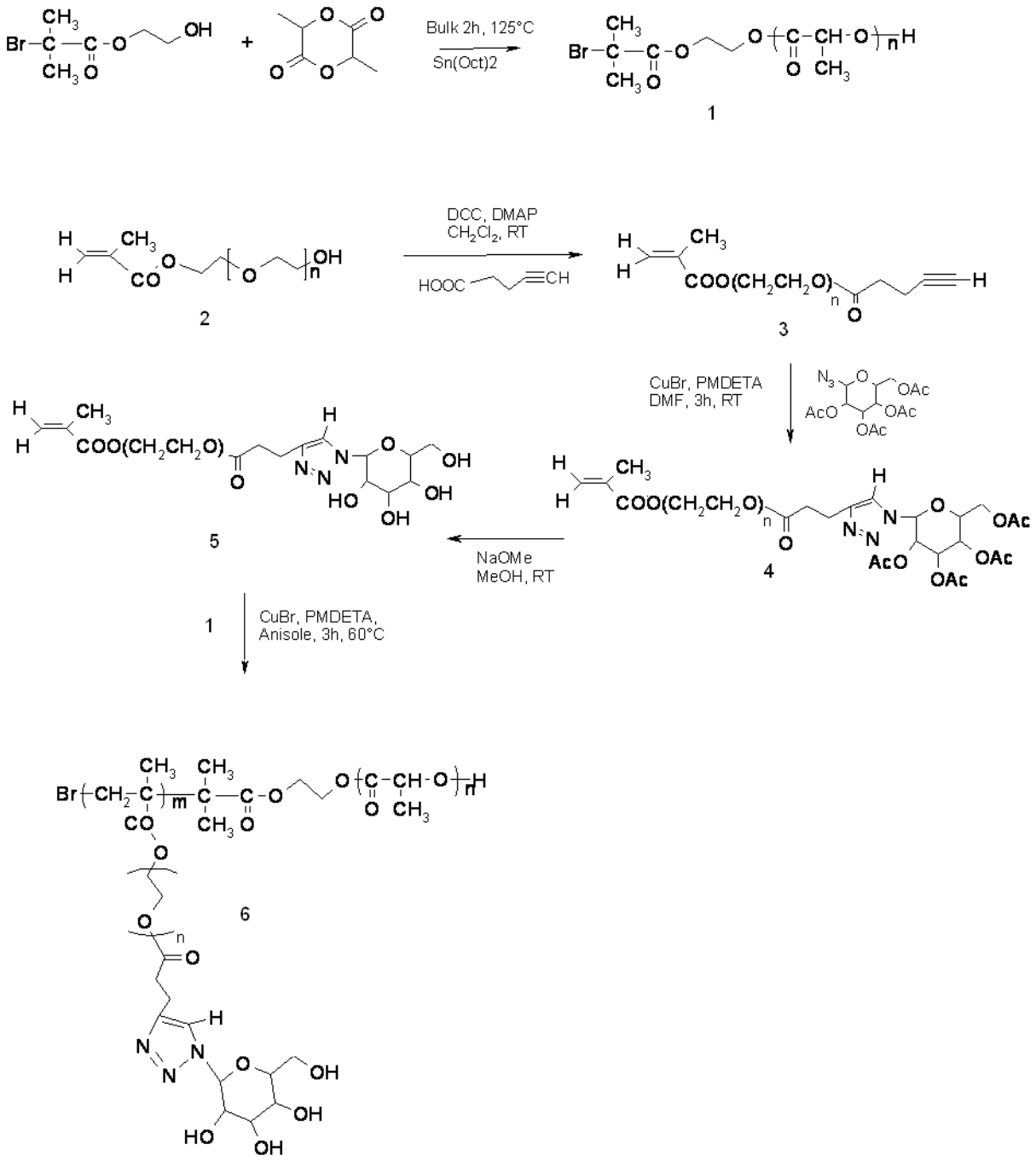

Figure 1: Synthesis of the amphiphilic copolymer.

Results and Discussion

Synthesis of glucopyranoside grafted PEGMA

Cu(I)-catalyzed click reactions as proposed by Wang et al [34] have been used efficiently in recent years in a wide range of applications [40] such as bioconjugates [41] and dendrimer [42] synthesis, polymer ligation [43] and surface fictionalization of liposomes [44] and nanoparticles [45].

The aim of our work was to prepare biodegradable nanoparticles bearing sugar residues that could be adapted to the specificity of the targeted receptor. Our synthesis strategy was first to conjugate the glucopyranoside with a methacrylic monomer bearing PEG chain (PEGMA), so that the PEG chain would be a spacer allowing better molecular recognition as well as rendering the nanoparticles surface hydrophilic.

The preparation of the glucopyranoside macromonomer was carried out by click chemistry. As shown in Figure 1, PEGMA was first reacted with 4-pentynoic acid by an esterification reaction leading to the alkyne-terminated PEGMA (**3**) (Fig. S2 in the supporting information).

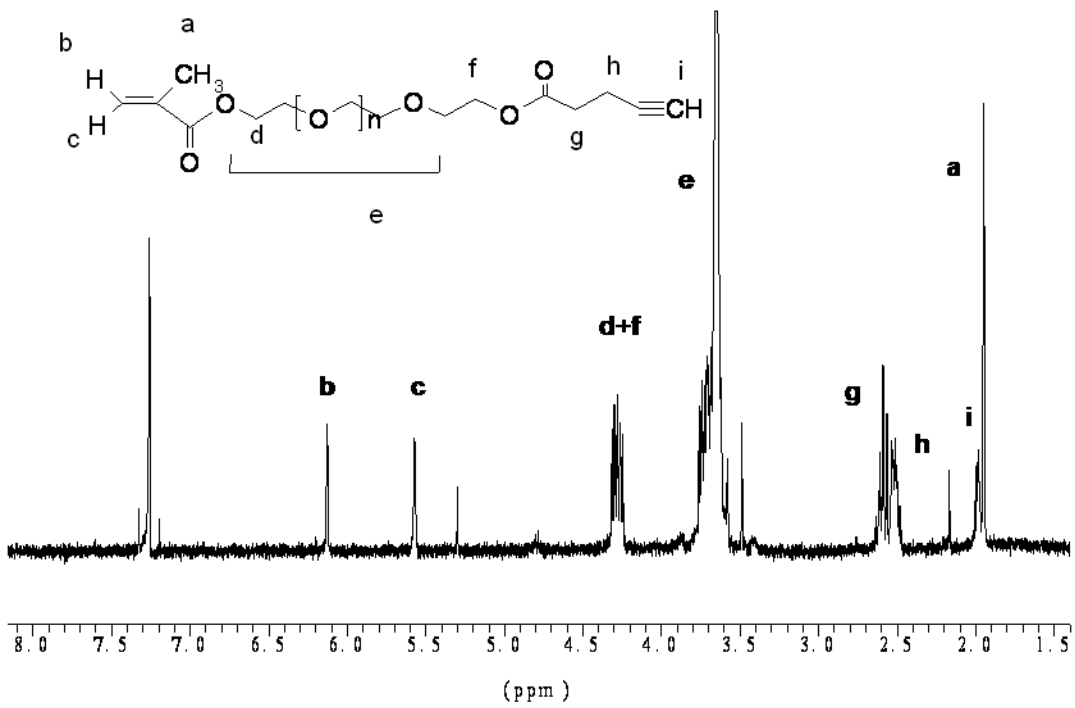

Figure S2: ^{1}H-NMR (CDCl3, 300MHz) acetylene-terminated PEGMA (**3**)

Thereafter, 1-azido-1-deoxy-β-D-glucopyranoside tetraacetate was introduced by Cu-catalyzed [2 + 3] cycloaddition to provide the glucopyranoside macromonomer (**4**) (Fig 2). The efficiency of the click reaction was estimated by ^{1}H-NMR measurement; the integration values of a newly appeared methine proton (i) on the triazole ring observed around δ 7.5 ppm were compared with those of the methylene protons (h) at the α-position of triazole ring observed at δ 2.7 ppm.

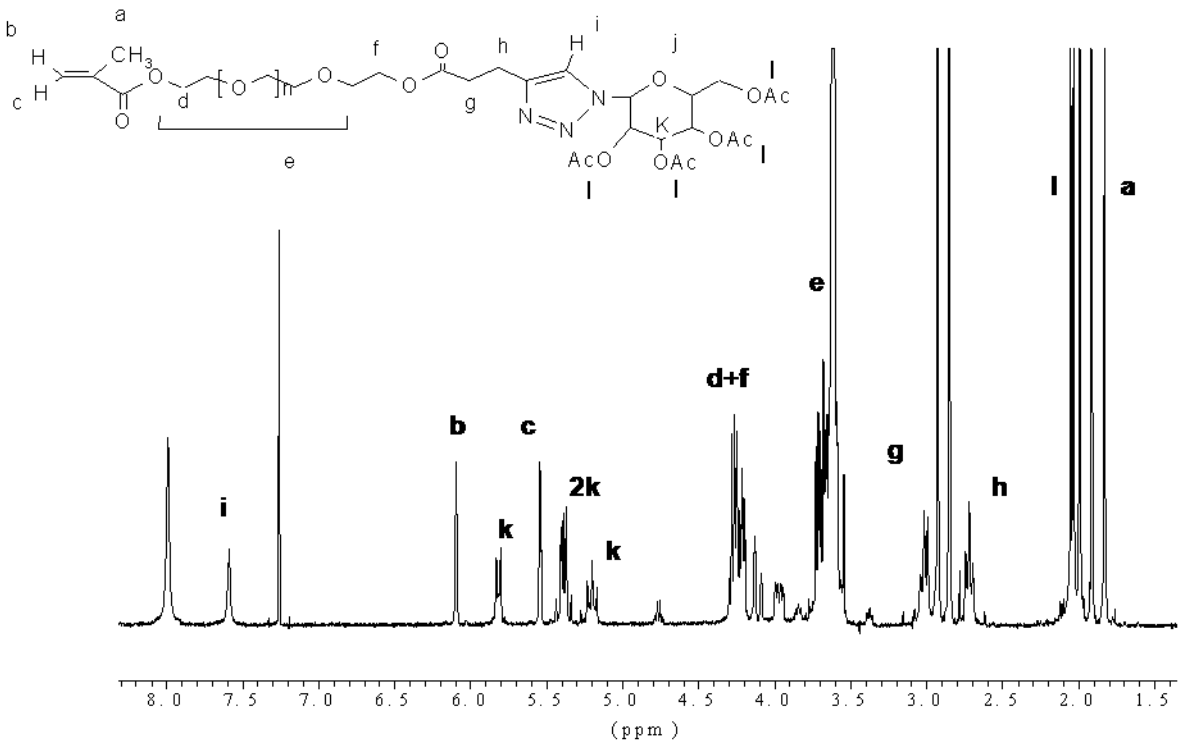

Figure 2: ^{1}H-NMR (CDCl3, 300MHz) of glucopyranoside tetra acetate-grafted PEGMA (**4**).

To evaluate the influence of the reaction time on the efficiency of glucopyranoside linking reaction, the cycloaddition was carried out for different periods (Table 1). Whatever the reaction time, the efficiency of azide acetylene cycloaddition was higher than 95%, but for reaction times higher than 3h, the proportion of intact vinyl group decreased according to ^{1}H-NMR. One paper [46] has already mentioned this side reaction, which the authors attributed to the cycloaddition of excess azides to electron-deficient olefins such as methacrylate derivatives. To limit this side reaction and preserve the methacrylic moiety, the reaction time was fixed at 3 hours.

Table 1: Efficiency of the click reaction between glycopyranoside and PEGMA

Time	Grafted monomer [a)]	Intact vinyl group [b)]
h	%	%
3	97	100
12	98	1.6
24	98	22
72	96	13

[a)] = Ii /Ib where Ii and Ib are the integral values of peaks i and b respectively (Fig.2)
[b)] = [Ib / (Ig/2)] where Ib and Ig are the integral values of peaks b and g respectively (Fig.2).

Deprotection of the sugar residues at the extremity of macromonomer (**4**) was achieved under mild conditions using sodium methoxide at ambient temperature for 8 min to avoid hydrolysis of the ester function [24]. Characterization by ^{1}H-NMR of the deprotected macromonomer (**5**) (Fig 3) showed the persistence of the triazol ring at 8.05 ppm and the disappearance of acetate peaks (δ~1.9-2 ppm) indicating the deacetylation of sugar residues. Peaks of glucopyranoside cycle were shifted to the region δ~3-4 ppm, except for the anomeric proton (δ=5.45) (Deprotection of the glucopyranoside alone under similar conditions have led also to a shift of the ring protons peaks to the region δ~3-4 ppm).

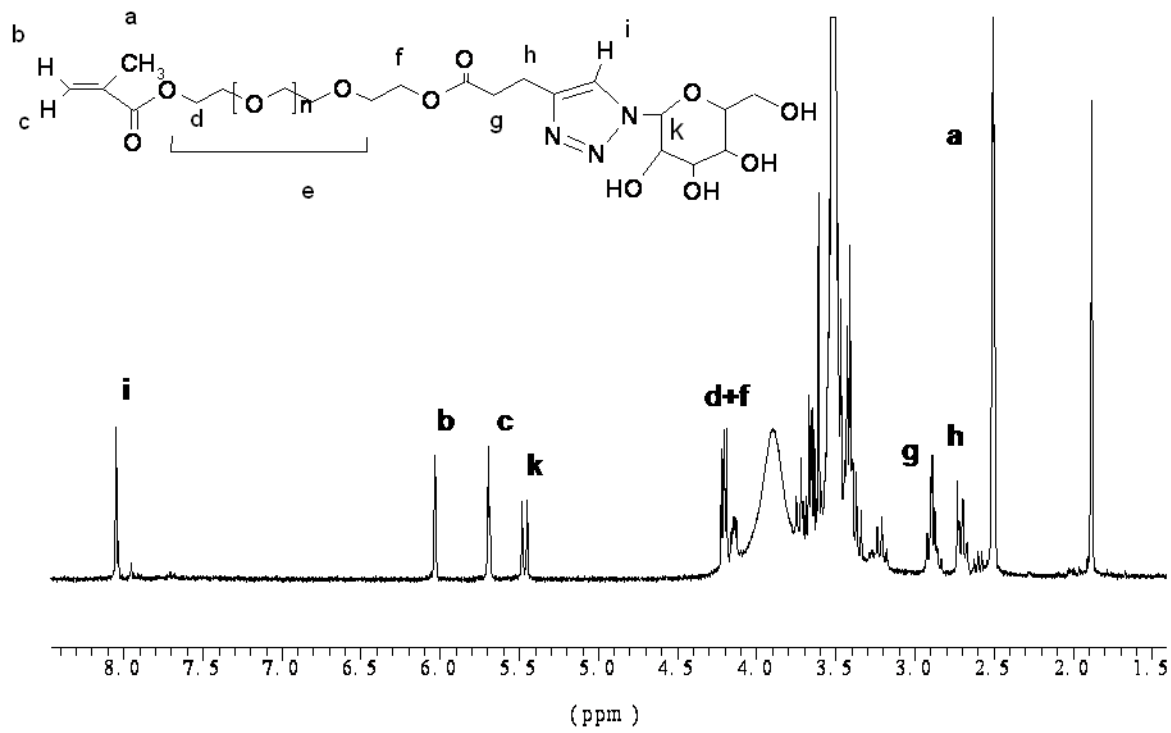

Figure 3: ^{1}H-NMR (DMSO-d^{6}, 300MHz) of glucopyranoside -grafted PEGMA (**5**)

No hydrolysis of the two ester bonds within the monomer took place during deprotection, as could be affirmed by the presence of the double bond protons at δ=5.67, 6.02 and that of methylene protons at the α and β-position of triazole ring (δ= 2.69, 2.89 ppm) in the ^{1}H-NMR spectrum of the deprotected monomer (Fig 3).

The infrared spectra of (**5**) and of its precursor (**4**) confirmed the deprotection by the decrease of the absorption intensity corresponding to the carbonyl band of the acetate ester at v = 1672 cm^{-1} and the appearance of a broad band ranging from 3050 to 3600 cm^{-1} corresponding to the hydroxyl groups of the deprotected glucopyranoside ring (Fig S3 in the supporting information).

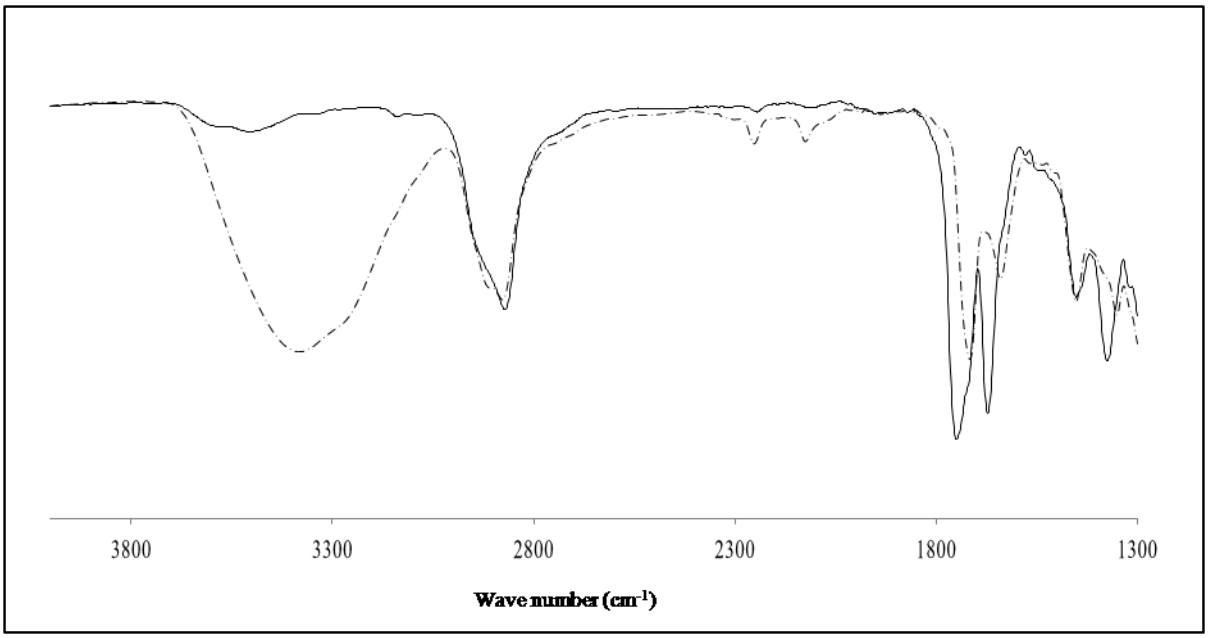

Figure S3: FT-IR of glucopyranoside tetra acetate-grafted PEGMA (**4**) (continuous line) and glucopyranoside -grafted PEGMA (**5**) (discontinuous line).

Synthesis of the amphiphilic block copolymer

The combination of different polymerization techniques allows polymeric materials with well-defined and complex architecture to be obtained, leading to great advances in the synthesis of graft and block copolymers in recent years. In particular, a combination of ring-opening polymerization (ROP) with (ATRP) has been widely used to prepare different structures such as block [47], random [39], graft [48] and star [49] copolymers.

In order to synthesize an amphiphilic block copolymer using two different methods of controlled polymerization, we synthesized an asymmetric bifunctional initiator, HEBIB. This contains a primary hydroxyl group that could be used to initiate the ring opening polymerization as well as an α-bromobutyrate group which is an efficient initiator for the ATRP of vinyl monomers.

The PLA block was first prepared by ROP using HEBIB as initiator and $Sn(Oct)_2$ as a bulk catalyst at 130 °C. The resultant linear HO-PLA-Br polymer (Mn = 32400 g/mol, *M*w/*M*n = 1.02) retained the alkyl halide function of the initiator, as observed on the ^{1}H-NMR spectrum by the presence of the peak at 1.9 ppm corresponding to the two CH_3 at the □ position of bromine atom (Fig S1 in the supporting information).

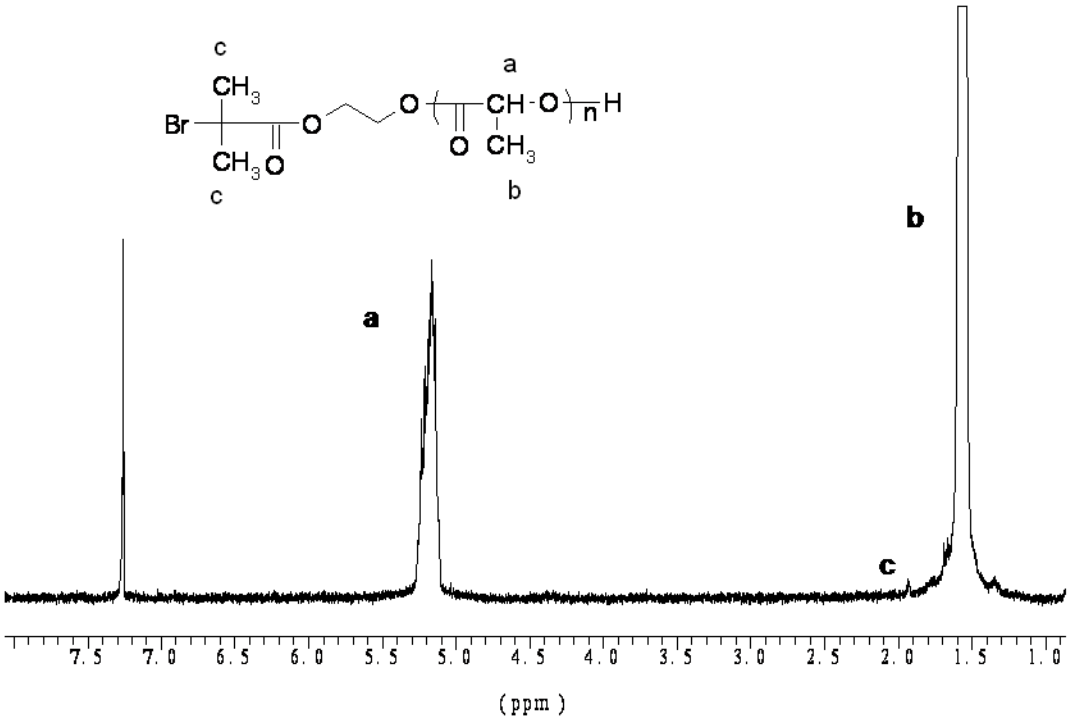

Figure S1: ^{1}H-NMR (CDCl3, 300MHz) of PLA macroinitiator (**1**)

The bromide-terminated PLA chains were subsequently employed as ATRP macroinitiators for the polymerization of PEGMA-glucopyranoside (**5**) in anisole using CuBr/PMDETA complex as a catalyst (Table 2). The polymerization was confirmed by ^{1}H-NMR (Fig 4) with the disappearance of the vinyl protons at δ =5.5 and 6.2 ppm and the appearance of the main-chain peak in the region between 1.2 and 1.4 ppm. The presence of glucose on the polymer chain could be detected by the presence of the triazole ring peak at

δ=8ppm (i) and that of the anomeric proton of glucose cycle at δ=5.5ppm. Block copolymer formation is usually corroborated by comparison of the SEC elution profile of the macroinitiator with that of the block copolymer. The SEC elution profile of (**6**) was slightly shifted to the higher molecular weight region (Fig 5). This indicates that initiation by the Br-terminated chains of PLA occurred and a block copolymer was prepared with a narrow polydispersity index (1.21).

Within the architecture of the copolymer (**6**), every chain of the hydrophobic PLA will have many hydrophilic PEG chains depending on the number of methacrylate units attached to every single chain. In order to prepare stable nanoparticles in water, the proportion of the hydrophilic part in the copolymer should not be high. For this reason we chose to use a small ratio macroinitiator/monomer =1/5 corresponding to a theoretical increase of molecular weight from *M*n=32400 to *M*n=36050. Since this increase is very small compared with the high molecular weight initiator, it is not possible to confirm that the initiation was efficient from all macroinitiator chains, but the agreement between the theoretical and experimental molecular weight obtained by SEC and ^{1}H-NMR allowed us to conclude that satisfied initiation could be achieved. That was confirmed practically by extended stability of nanoparticles prepared from the copolymer (**6**) compared with those prepared from its precursor (**2**) (data not shown).

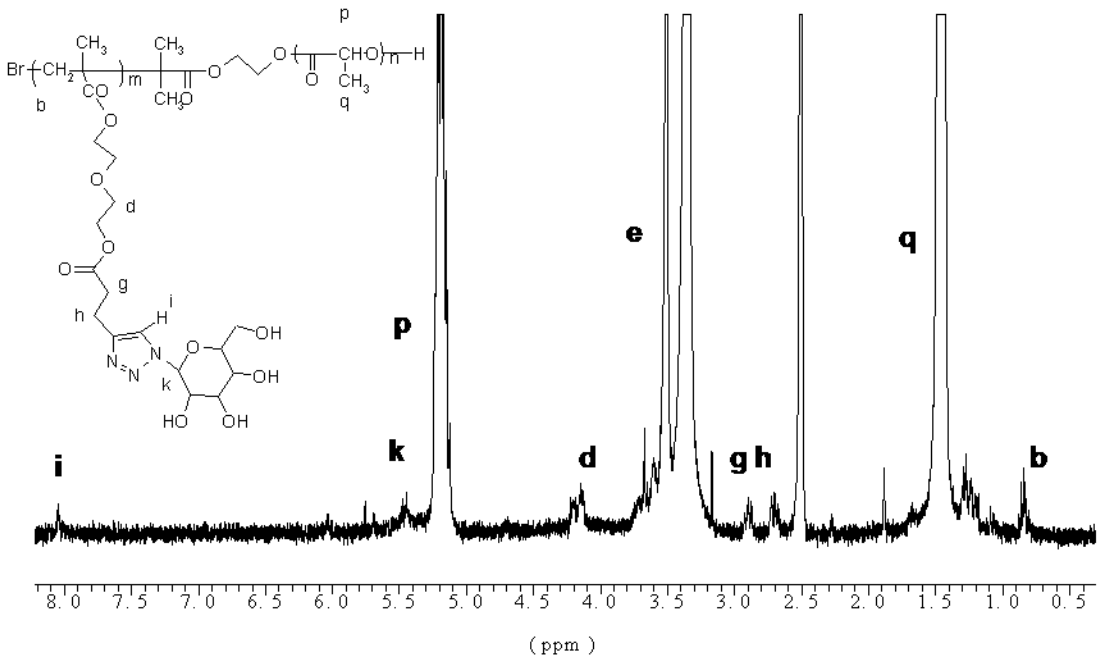

Figure 4: ^{1}H-NMR (DMSO-d^6, 300MHz) of PLA-block-PEGMA-glucopyranoside **(6)**

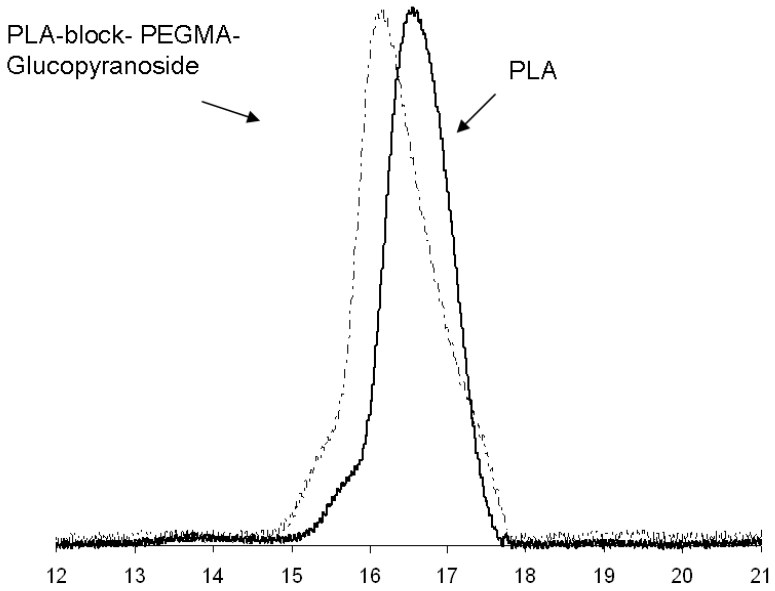

Figure5: Size exclusion chromatograms of PLA **(1)** and PLA-block- PEGMA-glucopyranoside **(6)**

Table 2: Synthesis and properties of polymers

polymer	Initiator/monomer	Conversion	Theoretical Mn	MnHNMR	MnSEC	Mw/MnSEC
		%	g.mol-1	g.mol-1	g.mol-1	g.mol-1
1	1:420	95 a)	30200	32400 b)	32200	1.02
6	1:5	76 a)	36050	35400 c)	36400	1.21

a) Obtained by ^{1}H-NMR
b) Calculated from the integration values of the CH of PLA and the two CH_3 of the initiator.
c) Calculated from the relative integration values of the main chain of PLA (Ip) and the PEGMA methylene groups (I_{d+f}).

Nanoparticle preparation

Nanoparticles were prepared by the nanoprecipitation method in which the preformed polymers are used as starting materials [50]. Acetone is the solvent most often used in this method, but here we replaced acetone with DMF for two reasons: the first being that the copolymer (**6**) was not completely soluble in acetone and the second that we intend to load these nanoparticles with a drug which is soluble in DMF but not in acetone in a further study. Very few papers have reported the use of DMF in the preparation of nanoparticles by the nanoprecipitation method and there is very little data in the literature about the cytotoxicity of such nanoparticles, thus after using DMF, we evaluated the effect of polymer concentration on the size and yield of nanoparticles formed and investigated any potential toxicity to endothelial cells *in vitro*.

A solution of 5, 10 or 20 mg of copolymer in 2 mL DMF was injected into water without any surfactant. The mixture immediately became turbid, indicating the formation of nanoparticles.

Nanoparticle size and yield were measured on three different batches prepared under identical conditions. Whatever the concentration of copolymer in DMF, the mean diameter of the nanoparticles was smaller than 200 nm and the yield was more than 75 % (Table 3). Transmission electron microscopy images showed spherical individualized particles (Fig 8a).

Table 3: Properties of nanoparticles prepared from different copolymer concentrations.

Concentration of copolymer	Size	PDI a)	NP b)
mg/2mL DMF	nm		%
5	168 ± 10.5	0.19	86 ± 2
10	169 ± 14.5	0.25	75 ± 5.7
20	152 ± 6.7	0.22	77 ± 6.9

a) PDI: Polydispersity index
b) NP%: percentage yield of nanoparticles.

Molecular recognition

Lectin-sugar interactions were used to determine the accessibility of the glucose residues at the surface of the nanoparticles. Concanavalin A is a lectin isolated from jack bean meal which is known to bind specifically to α-mannopyranosyl and α-glucopyranosyl at the level of their hydroxyl groups at positions 3, 4 and 6. Under our experimental conditions, Con A is a tetramer [51] and can interact with the hydroxyl groups of four sugar residues. Hence, the interaction of glucopyranoside groups at the end of poly (ethylene glycol) chains of nanoparticles with Con A should lead to cross-linking of the nanoparticles that would increase their light-scattering properties significantly. The subsequent turbidity in the aqueous medium could be monitored by UV/Visible spectroscopy. As seen in Figure 6, the binding of nanoparticles with Con A takes place within a few minutes. At a fixed time-point, the absorbance increased with increasing Con A concentration, in agreement with the results obtained from the measurement of apparent size of aggregates of nanoparticles formed in the presence of these different concentrations of Con A (Fig 7). It can be observed that aggregate size increases with the concentration of Con A, whereas Con A did not affect the apparent size of nanoparticles without glucopyranoside molecules on their surface (nanoparticles prepared from an identical copolymer without sugar entities on its PEGMA

block). The large standard deviations can be attributed to the random nature of the objects formed by Con A cross-linking (for example see Fig 8d).

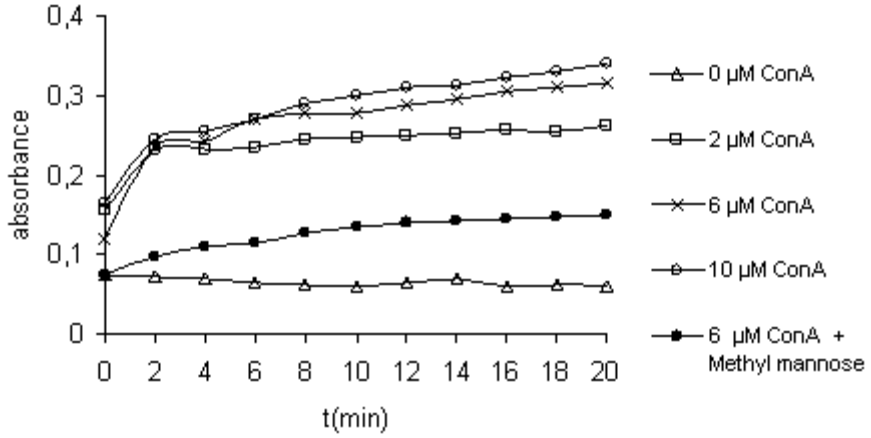

Figure 6: Absorbance measurement by UV/Vis spectroscopy of nanoparticles in presence of different concentrations of Con A.

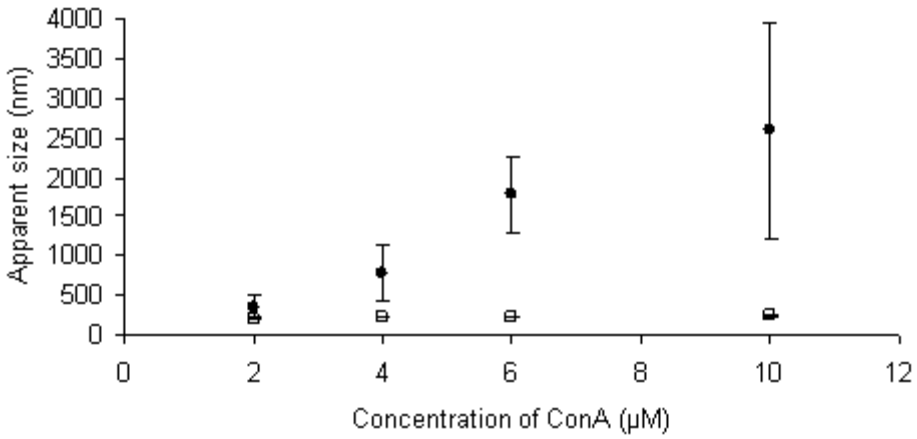

Figure 7: Apparent size measured for nanoparticles with (♦) or without (□) glucopyranoside in presence of different concentrations of Con A.

Figure 8 shows TEM images of glucopyranoside-bearing nanoparticles prepared from the copolymer (**6**) after incubation in the absence (a) or in the presence of different concentrations (b, c and d) of Con A.

When Con A was incubated with α-methyl mannopyranoside before adding the nanoparticles, a significant reduction of the turbidity was observed (Fig 6) indication the competitive binding for Con A binding sites, this is in accordance with the fact that Con A has a stronger affinity for α-methyl mannopyranoside than for glucose molecules [52].

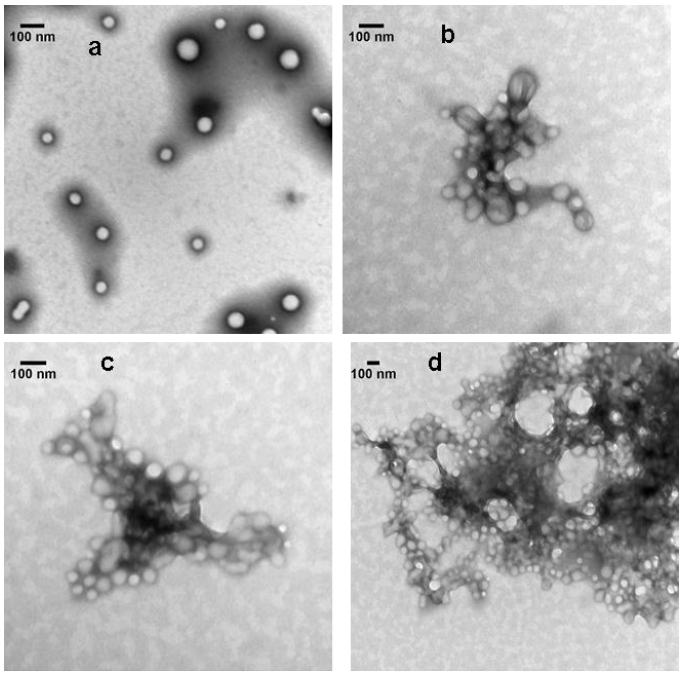

Figure 8: TEM observation of nanoparticles from polymer (**6**): without (**a)** and with 2M (a) 4M (B) and 10M (C) of Con A.

In vitro cytotoxicity of nanoparticles

In preparation for using this kind of colloid for the intravenous administration of drugs, the cytotoxicity of PLA-co-PEGMA-glucopyranoside nanoparticles was determined on the HUVEC cell line after a 48-h incubation at 37 °C using the MTT test. Although it is well established that PLA is a biodegradable polymer and the PEG as a biocompatible one, we performed this cytotoxicity assay because DMF had been used in the synthesis of polymer and the preparation of nanoparticles.

The result reported in Figure 9 show a cell viability higher than 80%, whatever the dose of nanoparticles added (in the range of 0-500µg/mL), confirming the efficient elimination of DMF by dialysis, showing that it would be possible to use this method for the formulation of drug-loaded nanoparticles with DMF-soluble drugs.

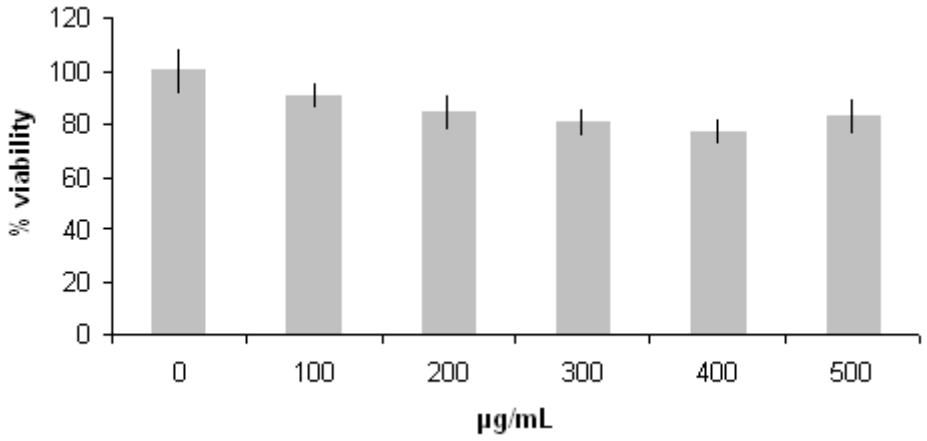

Figure 9: HUVEC cell viability determined by the MTT assay after incubation with 0-500 µg/mL polymer for 48h. Results are expressed as the mean ± SD obtained for at least three experiments

Conclusion

The development of nanosystems for site-specific drug delivery requires simple and reproducible methods of introducing ligands onto the carrier surface in a way that does not hinder their interactions with their receptors. The chemical reactions used must be compatible with the biological molecules used as drugs and for targeting and should not generate toxic by-products. In this respect, click chemistry is an extremely useful strategy. The reaction between the azide- and acetylene-derivatized precursors can be carried out under mild conditions in a highly specific way. This reaction was used to conjugate a monosaccharide to PEGMA in two steps with a good yield without affecting the methacrylate double bond. Many other potential ligands for targeting could be coupled in the same way after attachment of an azide group. Since the reaction is very efficient, the degree of substitution can be controlled by the amount of ligand in the reaction mixture, allowing an optimal ligand density at the surface of the final nanosystem.

A combination of ATRP and ROP using a single bifunctional initiator allowed us to construct a well-defined amphiphilic block polymer. The conjugation of the monosaccharide did not affect the polymerization under the reaction conditions used.

This synthesis strategy offers many points of control on the properties of the synthesized glycopolymers and nanoparticles: the length of the hydrophobic block can be modified as a function of formulation requirements such as drug loading and/or drug release profile, the length of the methacrylate block chain controls the density of the hydrophilic PEG chains on the surface, while the ratio of sugar modified /non modified monomers used can control the density of the ligand around the nanoparticles and hence could be optimized to maximize molecular recognition efficacy and reduce steric hindrance due to sugar residues being too closely spaced [11].

The resulting copolymer was successfully used to prepare spherical nanoparticles using a simple nanoprecipitation method, which allowed small-sized particles to be prepared without any surfactant. These nanoparticles did not display significant cytotoxicity to endothelial cells in the MTT assay even with the use of DMF in their formulation, suggesting that they could be safely administered by the IV route.

The accessibility of the surface ligands such as the glucose used in our study can be easily detected by the agglutination of the nanoparticles using proteins that can bind more than one molecule of the ligand in question. The small size and the presence of PEG chains should confer long-circulating properties on these nanoparticles after intravenous injection. After this proof of concept, the next step is to attach biologically relevant ligands to the surface of the nanoparticles.

Acknowledgements

The authors wish to thank *Danielle Jaillard* for technical assistance in the TEM observation and *Véronique Marsaud* for help with cytotoxicity determination.

References

1. Zhang, L., et al., *Nanoparticles in Medicine: Therapeutic Applications and Developments.* Clin Pharmacol Ther, 2007. **83**(5): p. 761-769.
2. Brigger, I., C. Dubernet, and P. Couvreur, *Nanoparticles in cancer therapy and diagnosis.* Adv Drug Deliv Rev, 2002. **54**(5): p. 631-51.
3. Ann, P.C., *Liposomes as Drug Delivery Systems.* Cancer Practice, 1998. **6**(4): p. 251-253.
4. Boyd, B.J., *Past and future evolution in colloidal drug delivery systems.* Expert Opinion on Drug Delivery, 2008. **5**(1): p. 69.
5. Gref, R., et al., *Poly(ethylene glycol)-coated nanospheres: potential carriers for intravenous drug administration.* Pharm Biotechnol, 1997. **10**: p. 167-98.
6. Gref, R., et al., *Development and characterization of CyA-loaded poly(lactic acid)-poly(ethylene glycol)PEG micro- and nanoparticles. Comparison with conventional PLA particulate carriers.* Eur J Pharm Biopharm, 2001. **51**(2): p. 111-8.
7. Bhadra, D., et al., *Pegnology: a review of PEG-ylated systems.* Pharmazie, 2002. **57**(1): p. 5-29.
8. Gref, R., et al., *'Stealth' corona-core nanoparticles surface modified by polyethylene glycol (PEG): influences of the corona (PEG chain length and surface density) and of the core composition on phagocytic uptake and plasma protein adsorption.* Colloids Surf B Biointerfaces, 2000. **18**(3-4): p. 301-313.
9. Passirani, C., et al., *Long-circulating nanoparticles bearing heparin or dextran covalently bound to poly(methyl methacrylate).* Pharm Res, 1998. **15**(7): p. 1046-50.
10. Chauvierre, C., et al., *Novel polysaccharide-decorated poly(isobutyl cyanoacrylate) nanoparticles.* Pharm Res, 2003. **20**(11): p. 1786-93.
11. Lee, Y.C. and R.T. Lee, *Carbohydrate-Protein Interactions: Basis of Glycobiology.* Accounts of Chemical Research, 2002. **28**(8): p. 321-327.
12. Andre, S., et al., *From structural to functional glycomics: core substitutions as molecular switches for shape and lectin affinity of N-glycans.* Biol Chem, 2009. **390**(7): p. 557-65.
13. Gabius, H.J., *Glycans: bioactive signals decoded by lectins.* Biochem Soc Trans, 2008. **36**(Pt 6): p. 1491-6.
14. Ehrhardt, C., C. Kneuer, and U. Bakowsky, *Selectins-an emerging target for drug delivery.* Adv Drug Deliv Rev, 2004. **56**(4): p. 527-49.

15. Kneuer, C., et al., *Selectins - potential pharmacological targets?* Drug Discov Today, 2006. **11**(21-22): p. 1034-40.
16. Hans-Joachim Gabius, H.-C.S., Sabine André, Jesús Jiménez-Barbero, Harold Rüdiger., *Chemical Biology of the Sugar Code.* ChemBioChem, 2004. **5**(6): p. 740-764.
17. Lundquist, J.J. and E.J. Toone, *The Cluster Glycoside Effect.* Chemical Reviews, 2002. **102**(2): p. 555-578.
18. Jeong, Y.-I., et al., *Cellular recognition of paclitaxel-loaded polymeric nanoparticles composed of poly([gamma]-benzyl l-glutamate) and poly(ethylene glycol) diblock copolymer endcapped with galactose moiety.* International Journal of Pharmaceutics, 2005. **296**(1-2): p. 151-161.
19. Kim, I.S. and S.H. Kim, *Development of a polymeric nanoparticulate drug delivery system. In vitro characterization of nanoparticles based on sugar-containing conjugates.* Int J Pharm, 2002. **245**(1-2): p. 67-73.
20. Banquy, X., et al., *Selectins Ligand Decorated Drug Carriers for Activated Endothelial Cell Targeting.* Bioconjugate Chemistry, 2008. **19**(10): p. 2030-2039.
21. Chen, G., et al., *A Modular Click Approach to Glycosylated Polymeric Beads: Design, Synthesis and Preliminary Lectin Recognition Studies.* Macromolecules, 2007. **40**(21): p. 7513-7520.
22. Fernandez-Megia, E., et al., *A Click Approach to Unprotected Glycodendrimers†* Macromolecules, 2006. **39**(6): p. 2113-2120.
23. Lu, C., et al., *Biodegradable Amphiphilic Triblock Copolymer Bearing Pendant Glucose Residues: Preparation and Specific Interaction with Concanavalin A Molecules.* Biomacromolecules, 2006. **7**(6): p. 1806-1810.
24. Vazquez-Dorbatt, V. and H.D. Maynard, *Biotinylated glycopolymers synthesized by atom transfer radical polymerization.* Biomacromolecules, 2006. **7**(8): p. 2297-302.
25. Ladmiral, V., et al., *Synthesis of Neoglycopolymers by a Combination of â€œClick Chemistryâ€ and Living Radical Polymerization.* Journal of the American Chemical Society, 2006. **128**(14): p. 4823-4830.
26. Nurmi, L., et al., *Glycopolymers via catalytic chain transfer polymerisation (CCTP), Huisgens cycloaddition and thiol-ene double click reactions.* Chem Commun (Camb), 2009(19): p. 2727-9.
27. Vazquez-Dorbatt, V. and H.D. Maynard, *Biotinylated Glycopolymers Synthesized by Atom Transfer Radical Polymerization.* Biomacromolecules, 2006. **7**(8): p. 2297-2302.

28. Martin, H., et al., *Neoglycopolymers Based on 4-Vinyl-1,2,3-Triazole Monomers Prepared by Click Chemistry.* Macromolecular Bioscience, 2009. **9999**(9999): p. NA.
29. Albertin, L., et al., *Effect of an added base on (4-cyanopentanoic acid)-4-dithiobenzoate mediated RAFT polymerization in water.* Polymer, 2006. **47**(4): p. 1011-1019.
30. Gao, C., et al., *Linear and Hyperbranched Glycopolymer-Functionalized Carbon Nanotubes: Synthesis, Kinetics, and Characterization.* Macromolecules, 2007. **40**(6): p. 1803-1815.
31. Huisgen, R., *Kinetics and Mechanism of 1,3-Dipolar Cycloadditions.* Angewandte Chemie International Edition in English, 1963. **2**(11): p. 633-645.
32. Hartmuth C. Kolb, M.G.F.K.B.S., *Click Chemistry: Diverse Chemical Function from a Few Good Reactions.* Angewandte Chemie International Edition, 2001. **40**(11): p. 2004-2021.
33. Manetsch, R., et al., *In Situ Click Chemistry: Enzyme Inhibitors Made to Their Own Specifications.* Journal of the American Chemical Society, 2004. **126**(40): p. 12809-12818.
34. Wang, Q., et al., *Bioconjugation by Copper(I)-Catalyzed Azide-Alkyne [3 + 2] Cycloaddition.* Journal of the American Chemical Society, 2003. **125**(11): p. 3192-3193.
35. Matyjaszewski, K. and J. Xia, *Atom transfer radical polymerization.* Chem Rev, 2001. **101**(9): p. 2921-90.
36. Ali, M.M. and H.D.H. Stover, *Well-Defined Amphiphilic Thermosensitive Copolymers Based on Poly(ethylene glycol monomethacrylate) and Methyl Methacrylate Prepared by Atom Transfer Radical Polymerization.* Macromolecules, 2004. **37**(14): p. 5219-5227.
37. T. Erdogan, Z.O.G.H.U.T., *Facile synthesis of AB-type miktoarm star polymers through the combination of atom transfer radical polymerization and ring-opening polymerization.* Journal of Polymer Science Part A: Polymer Chemistry, 2004. **42**(10): p. 2313-2320.
38. Jayachandran, K.N., A. Takacs-Cox, and D.E. Brooks, *Synthesis and Characterization of Polymer Brushes of Poly(N,N-dimethylacrylamide) from Polystyrene Latex by Aqueous Atom Transfer Radical Polymerization.* Macromolecules, 2002. **35**(11): p. 4247-4257.
39. Wojciech Jakubowski, J.-F.L.S.S.K.M., *Block and random copolymers as surfactants for dispersion polymerization. I. Synthesis via atom transfer radical polymerization*

and ring-opening polymerization. Journal of Polymer Science Part A: Polymer Chemistry, 2005. **43**(7): p. 1498-1510.

40. Lutz, J.F. and Z. Zarafshani, *Efficient construction of therapeutics, bioconjugates, biomaterials and bioactive surfaces using azide-alkyne "click" chemistry.* Adv Drug Deliv Rev, 2008. **60**(9): p. 958-70.
41. Bonnet, D., et al., *A Rapid and Versatile Method to Label Receptor Ligands Using “Click” Chemistry: Validation with the Muscarinic M1 Antagonist Pirenzepine.* Bioconjugate Chemistry, 2006. **17**(6): p. 1618-1623.
42. Malkoch, M., et al., *Structurally Diverse Dendritic Libraries: A Highly Efficient Functionalization Approach Using Click Chemistry.* Macromolecules, 2005. **38**(9): p. 3663-3678.
43. Sami Halila, M.M., Sébastien Fort, Sylvain Cottaz, Thierry Hamaide, Etienne Fleury, Hugues Driguez, *Syntheses of Well-Defined Glyco-Polyorganosiloxanes by ldquoClickrdquo Chemistry and their Surfactant Properties.* Macromolecular Chemistry and Physics, 2008. **209**(12): p. 1282-1290.
44. Said Hassane, F., B. Frisch, and F. Schuber, *Targeted Liposomes: Convenient Coupling of Ligands to Preformed Vesicles Using Click Chemistry.* Bioconjugate Chemistry, 2006. **17**(3): p. 849-854.
45. von Maltzahn, G., et al., *In Vivo Tumor Cell Targeting with “Click” Nanoparticles.* Bioconjugate Chemistry, 2008. **19**(8): p. 1570-1578.
46. Anderson, G.T., J.R. Henry, and S.M. Weinreb, *High-pressure induced 1,3-dipolar cycloadditions of azides with electron-deficient olefins.* The Journal of Organic Chemistry, 1991. **56**(24): p. 6946-6948.
47. Xiaohua He, L.L., Meiran Xie, Yiqun Zhang, Shaoliang Lin, Deyue Yan, *Synthesis of Novel Linear PEO-b-PS-b-PCL Triblock Copolymers by the Combination of ATRP, ROP, and a Click Reaction.* Macromolecular Chemistry and Physics, 2007. **208**(16): p. 1797-1802.
48. Isabelle Ydens, P.D., Philippe Dubois, Jan Libiszowski, Andrzej Duda, and Stanislaw Penczek, *Combining ATRP of Methacrylates and ROP of L,L-Dilactide and ε-Caprolactone.* Macromolecular Chemistry and Physics, 2003. **204**(1): p. 171-179.
49. Yijin Xu, C.P., Lei Tao, *Block and star block copolymers by mechanism transformation. II. Synthesis of poly(DOP-b-St) by combination of ATRP and CROP.* Journal of Polymer Science Part A: Polymer Chemistry, 2000. **38**(3): p. 436-443.

50. Legrand, P., et al., *Influence of polymer behaviour in organic solution on the production of polylactide nanoparticles by nanoprecipitation.* Int J Pharm, 2007. **344**(1-2): p. 33-43.
51. Cunningham, B.A., et al., *The covalent and three-dimensional structure of concanavalin A. II. Amino acid sequence of cyanogen bromide fragment F3.* J Biol Chem, 1975. **250**(4): p. 1503-12.
52. Shimura, K. and K. Kasai, *Determination of the Affinity Constants of Concanavalin A for Monosaccharides by Fluorescence Affinity Probe Capillary Electrophoresis.* Analytical Biochemistry, 1995. **227**(1): p. 186-194.

Chapitre II

Chargement des nanoparticules en Methotrexate en vue de les utiliser dans le traitement de polyarthrite rhumatoïdes

Chargement des nanoparticules en Méthotrexate en vue de leur utilisation dans le traitement de la polyarthrite rhumatoïde

Introduction

Les rhumatismes inflammatoires chroniques touchent près de 1% de la population mondiale. La polyarthrite rhumatoïde (PR) est le plus fréquent de ces rhumatismes, en France, environ trois cent mille personnes en souffrent. Diagnostiquée en moyenne vers l'âge de 40 ans, la PR est une pathologie très invalidante et douloureuse, elle constitue un véritable problème de santé publique, tant par la proportion croissante des personnes concernées que par ses répercussions sur la qualité de vie des patients. De plus, l'avènement des biothérapies s'est traduit par un coût de prise en charge thérapeutique très élevée, avec des coûts directs évalués à environ 20 à 25k€/an/patient sous biothérapie.

Cette maladie est d'origine encore inconnue mais elle comporte un élément auto-immune, avec des facteurs endocriniens, psychologique, environnementaux, voir génétique.

La PR se traduit par une inflammation qui touche la membrane synoviale tapissant la cavité articulaire, elle frappe surtout les extrémités des membres (mains et pieds) et le cou mais aussi les grosses articulations : genoux, chevilles, poignets, épaules, hanches et coudes. Il en résulte une déformation et une destruction articulaires invalidantes. Il existe également des manifestations extra-articulaire : rénales, cardiaque [1], neurologique [2].

Cette inflammation chronique de la membrane synoviale des articulations est amplifiée par le recrutement de leucocytes circulants vers le liquide synovial par chimiotaxie. L'extravasation des leucocytes dans les sites d'inflammation est facilitée par l'expression de molécules d'adhésion comme la E-selectine sur les cellules endothéliales [3-5]. L'expression de l'E-sélectine permet l'immobilisation des leucocytes sur les cellules endothéliales [6] par l'intermédiaire de liaisons faibles entre l'E-sélectine et ses ligands (motifs glucidiques comme le sialyl Lewis X) [7].

Les objectifs de traitement médicamenteux de la PR sont de soulager les douleurs grâce aux traitements symptomatiques (antalgiques et anti-inflammatoires) et de ralentir l'évolution de la maladie grâce à des traitements de fond qui diminuent la fréquence et l'intensité des poussées et peuvent même limiter ou arrêter la progression de l'endommagement articulaire.

Le méthotrexate (MTX) est un antagoniste de l'acide folique qui intervient dans le métabolisme des purines et la synthèse de l'acide désoxyribonucléique (ADN). Il est donc

utilisé en cancérologie à fortes doses, mais la découverte de son efficacité à faible dose (5 à 20 mg/semaine) dans la polyarthrite rhumatoïde a constitué un grand progrès dans le traitement de cette maladie. Il est devenu le médicament de choix parmi les traitements de fond grâce à son efficacité et son bas coût.

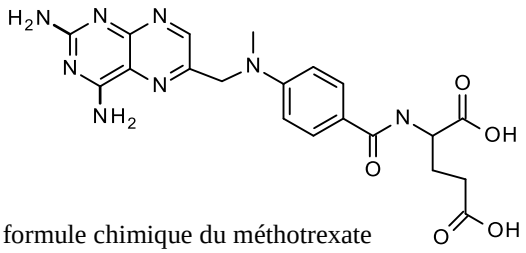

Fig. 1 formule chimique du méthotrexate

Le mécanisme selon lequel le MTX agit sur la PR n'est pas tout à fait clair [8]. Les données scientifiques provenant des études *in vitro*, *in vivo* ainsi que des études cliniques montrent une variété d'effets pharmacologiques qui pourraient être responsables de son efficacité.

Au niveau cellulaire, le MTX inhibe l'action de l'enzyme 5-aminoimidazole-4-carboxamide ribonucléotide (AICAR) formyltransférase, ce qui entraine une augmentation de la concentration intracellulaire de l'adénosine 5-Phosphate (AMP) et de l'adénosine [9-11]. Ces deux composés se retrouvent dans le milieu extracellulaire où l'AMP est transformée en adénosine. Quand cette adénosine extracellulaire se lie à son récepteur A2, le niveau de l'adénosine monophosphate cyclique intracellulaire (AMPc) augmente et induit un certain nombre d'effets anti-inflammatoires, dont principalement l'inhibition de la production [12-14] et de l'activité d'interleukine 1 (IL-1) [15]. Les autres interleukines inhibées par le MTX comprennent le TNF-α, interféron (IFN-γ), IL-4, IL-6, IL-8, IL-12, et de IL-13 [8, 10, 14, 16-19]. Une inhibition de la prolifération des lymphocytes et la phagocytose ont été aussi décrites [20-22]

La destruction des articulations au cours de la PR est liée en partie à l'augmentation de la synthèse et l'activité des enzymes protéolytiques libérées par l'inflammation. Certaines études ont montré que le MTX diminuait de façon significative l'activité de l'enzyme neutre métallocollagénolytique (NMCE) [23], la production de protéinase [24], ainsi que l'expression du gène collagénase [25], l'ensemble de ces effets limite la destruction articulaire. Cette réduction de l'activité protéolytique est probablement causée par l'inhibition d'IL-1 comme ce dernier induit la protéinase dans les fibroblastes synoviaux [26].

Le MTX diminue également l'expression de certaines molécules d'adhésion cellulaire comme l'antigène lymphocytaire cutanious (CLA)[27-29], l'E-sélectine [29-31], la molécule d'adhésion intracellulaire-1 (ICAM-1) [27, 28, 30-32] et la molécule d'adhésion vasculaire

cellulaire (VCAM) [31, 32]. Cet effet est indirect puisque il est lié à la diminution des cytokines [22].

D'autres effets cités dans des études publiées incluent une diminution du nombre de lymphocytes B et T circulants [33], une inhibition de la chemotaxis [34], une inhibition de l'activation de macrophage [35], une inhibition de la production de prostaglandine E2 stimulée par IL-β1[36], une inhibition de la prolifération de fibroblastes synoviaux [34] et une inhibition de la néo-vascularisation [14, 37].

Le MTX est administré généralement par voie orale, plusieurs études cliniques proposent le passage aux traitements parentérales avant de passer à la biothérapie chez les patients qui ne montrent pas une réponse à la forme orale [38, 39].

Malgré l'efficacité incontestée du MTX par l'une ou l'autre de ces formes actuelles dans le traitement de la PR, ses effets secondaires assez conséquents freinent son utilisation à long terme. Les patients traités par MTX sont plus susceptibles d'interrompre le traitement en raison des effets indésirables qu'à cause de son inefficacité [40, 41]. Les anomalies hématologiques comprennent la leucopénie [42, 43], thrombopénie [42], une anémie mégaloblastique, et une pancytopénie. Un cas d'érythro leucémie a été détecté [44] . Au niveau hépatique, les études montrent une augmentation des enzymes hépatiques alanine amino transférase (ALT) et aspartate amino transférase (AST)[43, 45]. Le MTX peut être responsable de pneumopathie interstitielle [43, 46], et peut favoriser la nodulose [47, 48]. Le MTX est tératogène dû à ses propriétés anti-folate et il est contre-indiqué pendant la grossesse. Il doit être associé à une contraception très efficace chez les femmes en âge de procréer.

Pour diminuer les effets secondaires systémiques et optimiser l'effet anti-inflammatoire, le MTX libre a été administré par voie intra-articulaire [49, 50] mais son efficacité a été faible en raison d'une élimination rapide du médicament de la cavité articulaire.

Le MTX a fait l'objet de plusieurs essais d'encapsulation dans des systèmes de vectorisation (tableau 1). A notre connaissance, aucun système de vectorisation du MTX par des véhicules ciblant un récepteur moléculaire n'a été développé pour le traitement de la PR.

Dans ce contexte, notre projet a pour objectif de développer des nanoparticules furtives pouvant jouer le rôle de vecteur du MTX. Leur particularité sera de s'immobiliser sur l'endothélium vasculaire par l'intermédiaire d'un système récepteur-ligand afin de libérer le MTX encapsulé proche de ses sites d'action. Dans ce but, l'E-sélectine a été choisie comme une cible interessante pour un tel vecteur comme développée précedamment dans le

chapitre I. En ce qui concerne la dose à administrer chez les souris, notre object a été d'avoire une dose moyenne requise de 0,5mg/kg (10µg pour un souris de 20g).

Dans ce chapitre, la synthèse et la caractérisation de copolymère utilisé pour encapsuler le MTX sont présentées, ainsi que les résultats et les conclusions concernant l'association du MTX à ces nanoparticules.

Tableau 1 systèmes de vectorisation encapsulant le MTX

Forme	**Matériaux**	**Voies d'utilisation**	**Pathologie**	**ref**
microsphères	PLA	Intra-articulaire	Polyarthrites rhumatoïde	[51, 52]
Nanosphères	PLA-polyacide sébacique	sous-cutanée	ND	[53]
Nanosphères	Chitosane- méthoxy PEG	ND	Cancer	[54]
Nanosphères	polybutylcyanoacrylate couvertes de polysorbane	Intra veineuse	Cancers du cerveau	[55]
Nanocapsules à cœur huileux	PLA ou PLA-PEG	ND	ND	[56]
Liposomes	Lécithine de soja ou lécithine hydrogéné / di potassium glycerrhizinate	Cutanée	psoriasis	[57]
Microémulsions E/H	Huile de soja / eau	orale	Cancer du sein	[58]
dendrimères	Acide dihydroxy benzoïque / POE Ou acide gallique - POE	Parentérale	cancers gliales	[59]

Matériel et méthodes

Le méthacrylate de poly (éthylène glycol) méthyle éther (PEGMA Mn≈ 300), le CuBr, le 4- diméthylaminopyridine (DMAP), l'étain (II) de 2-éthyl hexanoate ($Sn(Oct)_2$) (95%) ont été obtenus auprès de Sigma-Aldrich. Le 2-bromo-2méthylpropionyle bromide (98%) et le penta-méthylediéthylènetriamine (PMDETA) ont été obtenus auprès de Acrôs organics-Belgique. Le d-l-Lactide provient de Biovalley. Le méthotrexate a été fourni par TCI europe.

Tous les solvants organiques utilisés lors des synthèses chimiques (dichlorométhane, diméthyle éther, éthanol, méthanol, acétate d'éthyle, tétrahydrofurane) ont été obtenus auprès de Carlo Erba, et le diméthyle formamide auprès de Acrôs organics.

Spectroscopie par résonance magnétique nucléaire (RMN).

Les spectres RMN ^{1}H ont été enregistrés sur un spectromètre Brucker 300MHz, les analyses ont été effectuées en tube de 5 mm à température ambiante.

Chromatographie d'exclusion stérique

Les polymères ont été analysés à l'aide d'un appareil Viscotek muni d'une pompe type 1122, d'une pré-colonne TOSOH BIOSCIENCE TSKgel 5µm Guard, de deux colonnes TOSOH BIOSCIENCE TSKgel 5µm GMHHR-M, d'un double détecteur 270 dual (viscosimètre, diffusion de la lumière 90°) et d'un refractomètre WATERS 410. Les données ont été traitées avec le logiciel Omnisec.

Les échantillons de polymère sont préparés dans le THF à une concentration de 10 mg/mL, filtrés avant injection sur un filtre seringue Millipore Millex® - FG constitué d'une membrane FluoroporeTM hydrophobique (PTF) dont la limite de filtration est de 0,2 µm. L'éluant utilisé est le THF avec un débit de 1 mL/min.

Synthèse de l'amorceur β-hydroxylethyl α- bromoisobutyrate (HEBIB)

Un amorceur bifonctionnel a été synthétisé pour pouvoir combiner deux types de polymérisation : la polymérisation radicalaire par transfert d'atome (ATRP) et celle par ouverture de cycle (ROP). Les détails expérimentaux de cette synthèse sont disponibles dans notre précédente publication [60]. Le rendement était de 70%. ^{1}H-NMR ($CDCl_3$): 1,96 (6H, BrC(C**H$_3$)**$_2$-), 3,95 (2H, CH_2-C**H**$_2$-OH), 4,15 (2H, C**H$_2$**-CH_2-OH).

Polymérisation du lactide par ouverture de cycle

Le d,l-lactide (8,64g ; 60mmol), HEBIB (30mg ; 0,28mmol) et le $Sn(Oct)_2$ (10,4mg; 0,013mmol) sont introduits dans un schlenck. L'ensemble est dégazé avec un courant d'azote pendant 30 min, et ensuite agité à 130°C pendant 6h, le polymère est précipité dans un mélange diéthyle éther/éther de pétrole (50/50). Le rendement était de 92%. ^{1}H-RMN (300MHz, $CDCl_3$, δ en ppm) 1,55 (3H, -CH_3), 5,1 (1H, -CH- de la chaîne principale). MnNMR= 29700, MnSEC = 28500, Mw/Mn=1,05.

Préparation du copolymère à partir du PLA

Le macroamorceur PLA (0,96g; 0,03mmol), le PEGMMA (0,2g; 2,78mmol), le CuBr (9,5mg;0,06mmol) et le PMDETA (11mg; 0,06 mmol) ont été introduits dans un schlenck avec 4mL d'anisole. L'ensemble est dégazé par 3 cycles de vide/azote puis le mélange a été agité 6h à 60°C. Ensuite, la solution a été filtrée sur silice en utilisant un mélange CH_2Cl_2/ méthanol (9:1) pour eliminer le cuivre. Après évaporation du méthanol sous vide, le copolymère a été précipité dans l'éther. ^{1}H-RMN (300MHz, $CDCl_3$, δ en ppm), δ = 0,75_1 (-C**H**$_2$- chaîne principale de PEGMMA),1,55 (3H, -C**H**$_3$ de PLA), 1,78_2 (3H, -C**H**$_3$), 3,36 (-OC**H**$_3$), 3,61 (36H, -C**H**$_2$- du PEG), 4,05 (2H, COO-CH$_2$), 5,2 (1H, -CH de la chaîne principale de PLA). SEC : Mn =38 000, Mw= 44 600 et Ip = 1,14 (conversion$_{RMN}$ = 89%).

Préparation des nanoparticules

Les nanoparticules ont été préparées par nanoprécipitation. 10 mg de polymère (PLA ou PLA-PEGMMA) avec la quantité désirée de MTX (0, 1, 2, 5, et 10 mg) ont été dissous dans 2 mL de DMF. Cette solution a été ajoutée goutte à goutte à 4 ml d'eau sous agitation modérée à travers une aiguille (0,8 mm interne de diamètre) pendant 1min. La suspension brute de nanoparticules a été centrifugée (centrifugeuse Eppendorf 5804 R) à 4500 g pendant 10 min pour séparer les agrégats de polymère. Le DMF a été éliminé par dialyse pendant 4 heures (MWCO 15000 Da) contre 500 ml de l'eau déminéralisée. A la fin de la dialyse, le volume de dialysat a été ajusté pour avoir 10 ml de suspension de nanoparticules. Chaque formulation a été préparée trois fois pour le dosage de principe actif

Dosage du MTX par HPLC

La quantité totale de méthotrexate (MTX_{tot}) en suspension a été déterminée par HPLC après dissolution des nanoparticules dans du DMF (1/10 v/v), et une dilution appropriée dans la phase mobile. Pour déterminer la quantité de médicament non associée aux nanoparticules (MTX_{libre}), la suspension de nanoparticules a été ultrafiltrée dans des tubes microcon centrifuge équipés d'un filtre (30000 Da) (10min, 6000*g*) qui permettent de retenir les nanoparticules en laissant passer le surnageant travers la membrane (Schéma. 1).

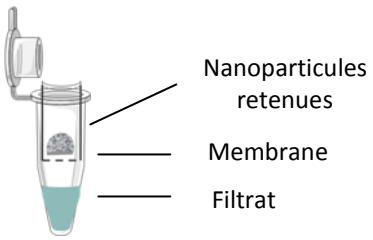

Schéma.1 Ultrafiltration par microcon

Le surnageant récupéré dans la partie inférieure du microcon a été dosé par HPLC après une dilution appropriée. La quantité de médicament associé (MTX_{ass}) aux nanoparticules a été calculée comme suit: $MTX_{ass} = MTX_{tot} – MTX_{libre}$

Conditions analytiques de l'HPLC

Le dosage quantitatif du méthotrexate a été réalisé par HPLC en phase inversée avec une colonne Aptisphere strategy 100Å C18-2 (150 mm x 3 mm ID, 3 µm) (Interchim, France) thermostatée à 30°C avec un four (7956R, Grace, Etats-Unis). Un débit de 0,5 mL/min est assuré par une pompe (600 Controller, Waters, France). Les injections (20 µL) sont effectuées au moyen d'un injecteur automatique (717 Autosampler, Waters, France). La phase mobile est composée d'un mélange eau/acétonitrile (85/15 v/v) acidifié avec 0,1% d'acide trifluoroacétique. La détection est réalisée par spectrophotométrie (Waters 470 Guyancourt, France) dans l'ultraviolet à 304 nm, ce qui correspond au maximum d'absorbance du méthotrexate. Les pics ont fait l'objet d'une intégration par le logiciel Azure (France). Dans ces conditions, le temps de rétention du méthotrexate est environ de 5 minutes. La méthode de dosage est linéaire entre 0,1 et 20 µg/mL, le coefficient de corrélation R^2 est de 0,9991.

Résultats

Ce travail a été réalisé sur des nanoparticules pegylées sans ligand, dans le but d'utiliser par la suite les paramètres optimisés d'encapsulation du MTX pour la préparation des nanoparticules porteuses du ligand de l'E-sélectine.

Synthèse et caractérisation du copolymère

La synthèse du bloc hydrophobe de notre copolymère à été réalisée par polymerisation par ouverture de cycle du lactide en présence d'un amorceur bifonctionel (HEBIB) (LA/A =420) et de $Sn(Oct)_2$ comme catalyseur (Schéma. 2).

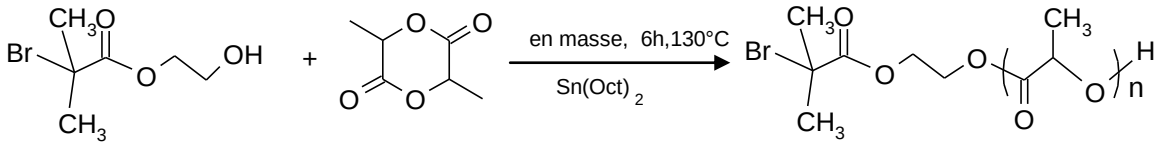

Schèma . 2 synthèses du PLA par ouverture de cycle

Le spectre RMN ^{1}H du polymère après précipitation nous indique la formation de polymère via l'élargissement du pic méthyle et le changement de position du pic -CH- qui passe de 5 ppm dans le monomère à 5,2 ppm dans le polymère.

La synthèse du copolymère PLA-PEGMMA a été réalisée par ATRP du PEGMMA à partir du PLA préalablement synthétisé.

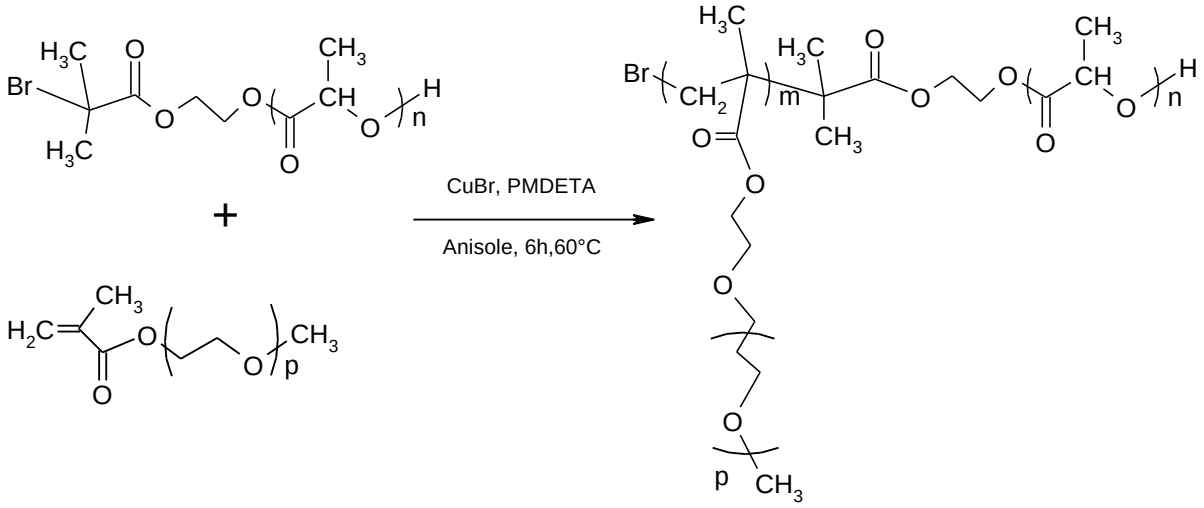

Schèma. 3 Préparation du copolymère à partir du PLA

Le spectre RMN ^{1}H du copolymère avant précipitation nous a permis d'estimer le pourcentage de conversion du PEGMMA à environ 90%. Le spectre RMN ^{1}H du copolymère après précipitation (Fig. 2) montre la disparition des pics des protons vinyliques à 5,5 et 6,2ppm ainsi que l'apparition des pics correspondant au PEGMMA polymérisé (CH_2 de la chaîne principale entre 0,7 et 1,1 ppm et le CH_2 en position α de la liaison ester à 4,05ppm).

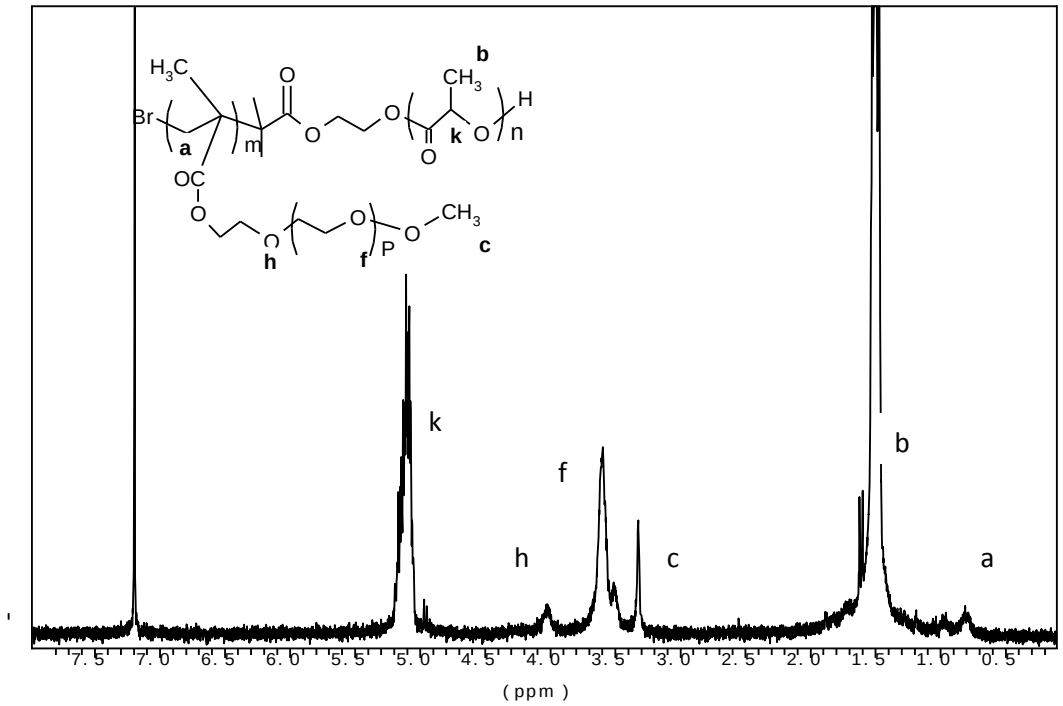

Fig. 2 Spectre RMN ^{1}H du PLA-PEGMMA

Après avoir montré par RMN la polymérisation du PEGMMA, la chromatographie d'exclusion stérique (SEC) nous a permis de vérifier si cette polymérisation a bien conduit à la formation d'un copolymère à bloc ou à deux polymères séparés. D'après le chromatogramme (Fig. 3), nous constatons bien la formation d'un copolymère de plus forte masse molaire que le macroamorceur de PLA. L'indice de polymolécularité (Ip) est de 1,14. Cette faible valeur indique la bonne homogénéité de la taille des chaînes du copolymère formé.

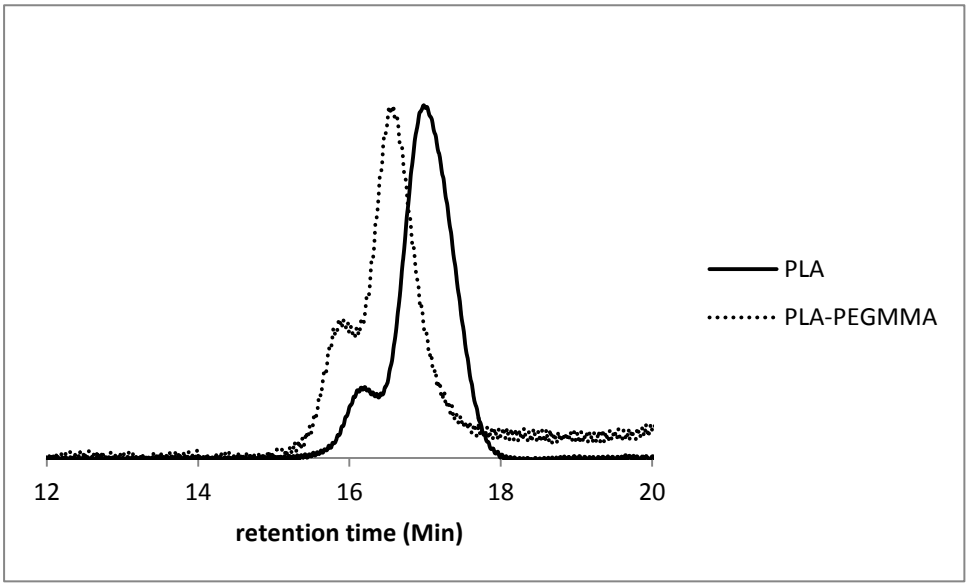

Fig. 3 Superposition des chromatogrammes du PLA et du PLA-PEGMA

Préparation et caractérisation des nanoparticules

Des nanoparticules ont été préparées à partir de ce copolymère par un simple procédé de nanoprécipitation sans l'utilisation de tensioactifs. Les solvants classiquement utilisés pour la préparation des nanosphères par cette technique sont l'acétone et le THF[61]. Le DMF et le DMSO sont très rarement utilisés dus à leurs toxicités. Seulement, pour notre étude, nous avons dû choisir le DMF car il est un des rares solvants à solubiliser parfaitement le MTX (>30mg/ml à 25°C). De plus, il permet également de solubiliser le copolymère amphiphile portant une molécule saccharidique.

Les nanoparticules ont donc été préparées dans le DMF dans les mêmes conditions opératoires que précédemment décrites (chapitre I). La présence de surfactant n'a pas été nécessaire pour permettre une bonne stabilisation.

Avant de pouvoir caractériser les nanoparticules et déterminer la dose encapsulée de MTX, il est nécessaire d'éliminer le DMF. Son haut point d'ébullition (T_{eb} = 153 °C) ne permet pas de l'évaporer simplement comme le THF ou l'acétone. Nous avons donc dû effectuer une dialyse qui a le double avantage d'éliminer le DMF mais également le MTX non absorbé par le polymère (tout du moins partiellement). Après 4h de dialyse (pendant lesquelles l'eau de dialyse a été remplacée 4 fois), nous avons vérifié que le DMF n'était plus détectable par RMN. Cela a été confirmé par les résultats de cytotoxicité des nanoparticles

sur des cellules endothéliales en culture [60]. L'absence de cytotoxicité confirme en effet l'élimination efficace du DMF par dialyse. Ainsi, nous avons fixé le temps de dialyse à 4h pour éviter une éventuelle libération de MTX pendant des durées plus longues.

Les nanoparticules ont toute une taille inférieure à 200 nm (tableau. 2). La présence des chaînes de PEG dans les nanoparticules de PLA-PEGMMA a induit une diminution de leur taille comparée aux nanoparticules de PLA due à l'effet tensioactif du copolymère amphiphile qui participe à la stabilisation de surface. Les nanoparticules sont stables en suspension aqueuse pendant 14 jours grâce à la nature amphiphile du copolymère utilisé (Fig 4).

Tableau. 2 Caractérisation des nanoparticules utilisées dans cette étude

	Taille (nm)	PZ (mV)
PLA	150 ± 8,2	- 44
PLA-PEGMMA	110 ± 3,4	-21
PLA-PEGMMA-MTX*	124 ± 4,9	-29

*en présence de 1 mg de MTX dans la formulation

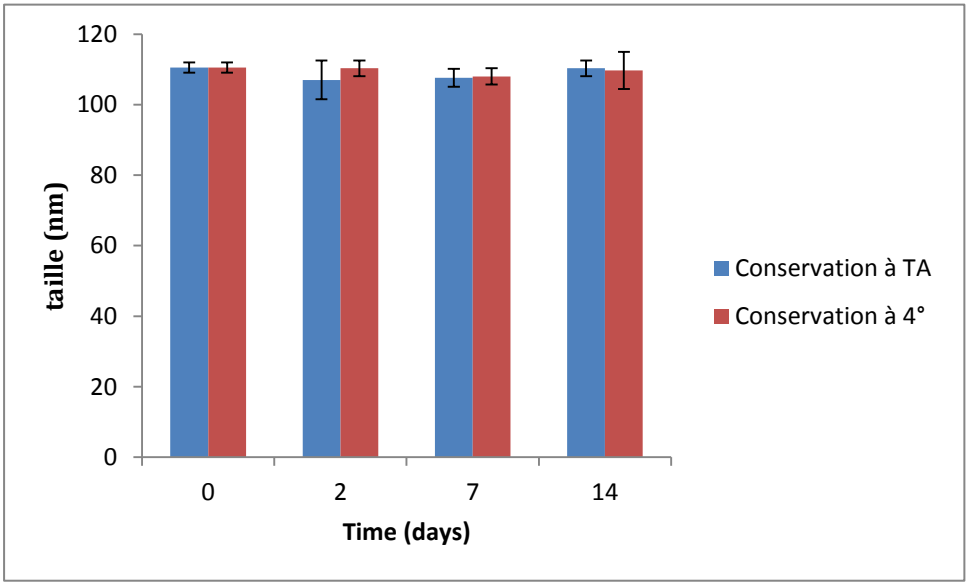

Fig. 4 Stabilité des nanoparticules pendant 14 jours

L'augmentation de la quantité de MTX dans la formulation entraine un accroissement de la taille moyenne des nanoparticules (Fig 5). Cet effet a déjà été observé avec des nanoparticules de PLGA préparées par nanoprécipitation [62], les auteurs ont

distribué cette augmentation de la taille à une adsorption de principe actif à la surface des particules. Dans notre cas, le MTX semble être adsorbé à la surface, d'où la modification de la charge de surface détectée par la mesure du potentiel zêta qui a montré une charge plus négative pour les nanoparticules chargées en méthotrexate (tableau. 2). Mais Il serait étonnant que cela aie un effet sur la taille des nanoparticules, vu les valeurs modestes d'encapsulation obtenue (voir paragraphe : effet de la quantité initiale de MTX sur l'encapsulation**).** Une possible explication à cette observation est la cinétique de diffusion de DMF dans l'eau au moment de nanoprécipitation, qui se diffère quand la charge de DMF en MTX est modifiée, puisque la vitesse de diffusion du solvant et de la nucléation des nanoparticules sont les paramètres clés qui contrôlent la taille des particules formées.

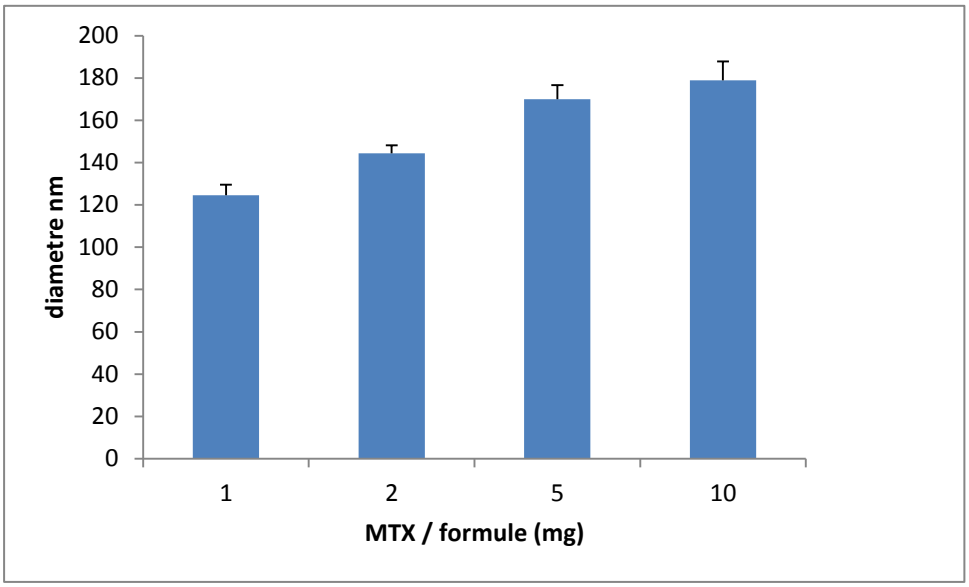

Fig. 5 Effet de la quantité de MTX sur la taille des nanoparticules

Effet de la quantité initiale de MTX sur l'encapsulation

La quantité de MTX dans la formulation a été variée entre 1 et 10 mg. Après dialyse des suspensions des nanoparticules chargées, le surnageant a été isolé par ultrafiltration à l'aide de unités de ultrafiltration-centrifugation. L'estimation de la quantité encapsulée a été réalisé d'une manière indirecte par la différence entre la quantité totale de MTX dans la suspension des nanoparticules et le MTX dans le surnageant.

Les résultats d'encapsulation n'ont pas permis d'établir une relation directe entre la quantité de MTX initiale dans la formulation et la quantité encapsulée (Fig. 6 et 7). De plus, des valeurs d'écart-type assez importantes ont été trouvées ce qui nous indique la non-reproductibilité de nos résultats.

Comme la quantité de MTX présente dans le surnageant est assez importante, la séparation de ce surnageant représente une étape indispensable pour construire une forme d'administration ciblée du MTX. L'ultrafiltration en utilisant les unités de ultrafiltration-centrifugation pour la séparation du surnageant ne permet pas de récupérer les nanoparticules chargées qui restent collées sur la membrane. La méthode classiquement utilisée est l'ultracentrifugation. Nous avons testé cette méthode avec ces nanoparticules (ultracentrifugeuse Ultra Optima L 90 ; 111000g pendant 2h) mais cela a conduit à la formation d'un culot non- redispersable dans l'eau. La petite taille des nanoparticules, les courtes chaînes de PEG qui les entourent (5 unités PEG = 220Da) ainsi que l'absence de tensioactif dans la formulation sont certainement à l'origine de ce résultat. Par conséquent nous n'avons pas pu récupérer de nanoparticules chargées suspendues dans un surnagent sans MTX. Si ces nanoparticules doivent être utilisées pour l'évaluation biologique, il serait nécessaire de développer une méthode pour pouvoir séparer les nanoparticules chargées du surnageant, par exemple, la chromatographie d'exclusion sur gel.

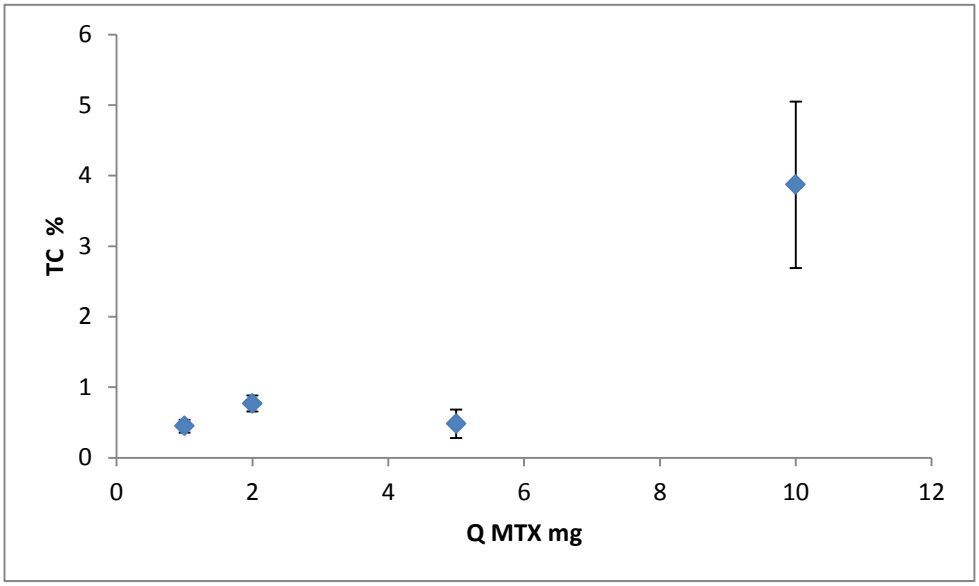

Fig. 6 Taux de chargement (moyenne ± SD, n=3)

(TC %) = (MTX_{nano}/polymère) *100

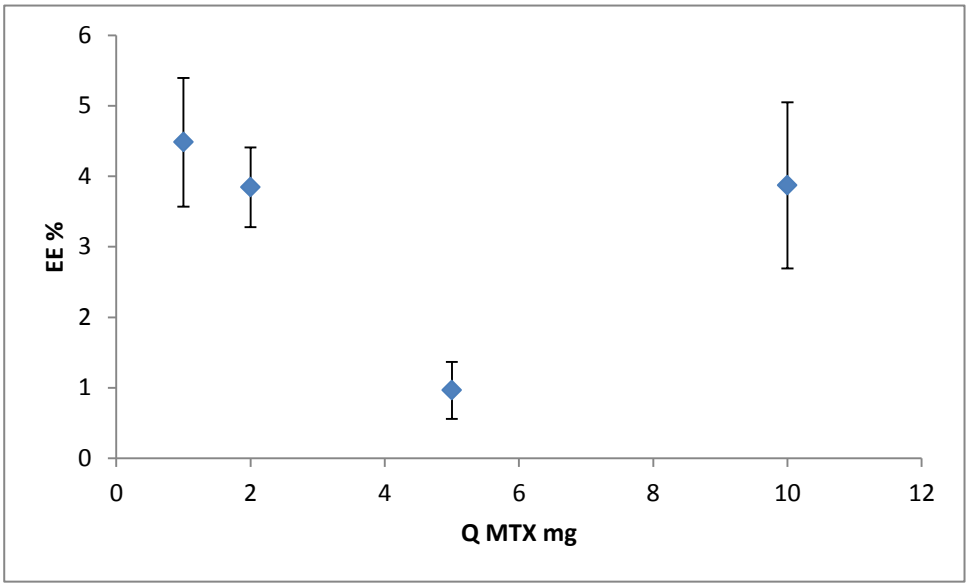

Fig. 7 Efficacité d'encapsulation (moyenne ± SD, n=3)

(EE%) = (MTXnano/MTXtot)*100

Discussion

Ce travail sur l'efficacité d'encapsulation du MTX a été réalisé sur les nanoparticules sans ligand afin de transposer les résultats optimisés aux nanoparticules fonctionnalisées avec le ligand de l'E-sélectine.

Nous n'avons pas rencontré de difficultés particulières lors de la synthèse du copolymère amphiphile suite au travail d'optimisation réalisé dans notre précédent travail [60].

Les nanoparticules ont été préparées par nanoprécipitation sans utilisation de tensioactif malgré tout elles se sont avérées stables en suspension aqueuse pendant 14 jours grâce à la nature amphiphile du copolymère utilisé.

L'encapsulation du MTX s'est avérée difficile. De nombreux problèmes de purification et de reproductibilité des résultats ont été rencontrés. Une des raisons principales est la nature avérée hydrophile du méthotrexate. Les données relatives à sa solubilité dans la littérature sont contradictoires. Selon la fiche technique du fournisseur, le MTX est insoluble dans l'eau mais soluble dans des solutions d'acide minéral et des solutions diluées de carbonate et des hydroxydes alcalins. Dans une seule publication, la solubilité dans l'eau a été mesurée et trouvée à 59µg/mL [53]. Cependant, lors de nos dosages par HPLC, une concentration de 226µg/ml a été détectée dans le surnageant. Dans une banque de données de principes actifs (www.drugbank.ca), deux valeurs de la solubilité du MTX sont fournies, ce

sont la solubilité théorique « Predicted Water Solubility » estimée par des outils bioinformatiques à 171µg/ml et la solubilité expérimentale « Experimental Water Solubilité » mesurée à 2,6 mg/ml [63].

Comme nous pouvons le constater, il existe certaines contradictions entre les différentes valeurs de solubilité du MTX. En débutant cette étude, nous avons considéré que ce principe actif n'était que faiblement soluble dans l'eau et que son encapsulation ne poserait pas ou peu de problèmes dans une nanoparticule à cœur hydrophobe. Pourtant, dans différentes études portant sur l'encapsulation de MTX dans des systèmes de vectorisation (voir le Tableau ci-dessus), le médicament se trouvait dans un environnement hydrophile de la forme finale du vecteur comme la phase aqueuse d'une émulsion eau/huile [58], les cavités de dendrimère riche en groupements PEG [64] ou POE [59], ou encore le cœur hydrophile de liposomes [57]. Seule une étude présente l'encapsulation dans le cœur hydrophobe de nanoparticules composées de polymère méthoxyPEG-chitosane [54]. De façon plus générale, plusieurs études ont montré une faible association médicament hydrophile / nanoparticules de PLGA préparées par nanoprécipitation. Cela a été attribué à une répartition plus favorable du médicament dans l'eau que dans la matrice polymère. De plus, la surface spécifique élevée des nanosphères favorise la désorption du médicament adsorbé à cette surface vers la phase aqueuse environnante [62, 65, 66].

Dans notre travail, l'hydrophile du MTX a favorisée sa répartition dans l'eau plutôt que dans les nanoparticules dont le cœur composé de PLA est hydrophobe.

A cela s'ajoute l'effet de charge. Le MTX possède trois valeurs de pKa (3,8/4,8/5,6) donc à pH≈6,5 de l'eau ultra pure (utilisée dans notre préparation), le MTX est sous sa forme non protonée (négative) ce qui entraîne une répulsion électrique avec les nanoparticules qui possèdent elles aussi une charge négative de surface.

Dans la littérature, plusieurs vecteurs particulaires à base de PLA ont été développés pour encapsuler le MTX. Des résultats légèrement supérieurs aux nôtres ont été obtenus avec des microparticules de PLA, mais les auteurs ont utilisé la méthode d'évaporation de solvant avec une solution de 2,5% de tensioactif [51, 52]. En outre, la séparation des microparticules chargées se fait aisément par simple centrifugation ou filtration mais il ne faut pas oublier que ces particules ne peuvent être injectées que par voie intra-articulaire et non par voie parentérale.

Dans une autre étude, le PLA, au lieu de servir de matrice pour adsorber le MTX, a été utilisé pour la formation de nanocapsules à cœur huileux (Mygliol 812) où le MTX a été préalablement suspendu [56]. Toutefois, pour obtenir des nanocapsules stables, une quantité de tensioactifs deux fois plus importantes que le polymère a été nécessaire.

En prenant en compte nos résultats d'encapsulation, ainsi que la très grande solubilité du MTX dans le DMF, nous avons conclu que la majeure partie du MTX restait dans le mélange eau/DMF pendant la nanoprécipitation avec seulement une faible fraction qui s'adsorbait sur le polymère. De plus, cette faible fraction se libère partiellement pendant les quatre heures de dialyse. Tout ceci justifie les valeurs aléatoires d'encapsulation obtenues avec des écart-types élevés.

Un autre élément important est la longueur des chaînes de PEG, dans cette étude, elle est relativement faible (environ 5 unités de PEG/Chaîne = 220 Da). Une masse molaire plus importante serait nécessaire à l'avenir pour améliorer la stabilisation de ces nanoparticles après ultracentrifugation.

Nos résultats indiquent la nécessité de modifier notre formulation pour améliorer l'encapsulation du MTX dans ces nanoparticules. L'utilisation d'un tensioactif pourrait améliorer le rendement d'encapsulation et donner la possibilité de remettre en suspension les nanoparticules après ultracentrifugation. Seulement, notre objectif initial était d'encapsuler le MTX sans l'utilisation de tensioactif. Cette stratégie aurait permis d'éviter les effets indésirables des tensioactifs, et d'avoir une formulation simple qui contiendrait que le polymère et le principe actif. L'encapsulation pourrait être améliorée en utilisant une autre méthode de préparation des nanoparticules. Parmi ces méthodes alternatives, nous pouvons citer la préparation de nanocapsules avec un cœur aqueux dans lequel le MTX est soluble, dans ce cas là l'utilisation d'un sel de MTX encore plus soluble dans l'eau pourrait améliorer d'avantage l'efficacité de chargement. Une autre possibilité est la préparation de nanosphères par évaporation de solvant où le MTX serait suspendu dans un solvant non miscible avec l'eau (comme le dichlorométhane) pour former une émulsion, ce qui favorise le contact du MTX non soluble avec les chaînes de polymère. Lors de l'évaporation du solvant pour former les nanosphères, le MTX serait déjà adsorbé sur les chaînes macromoléculaires limitant ainsi la perte liée à sa solubilité dans l'eau.

Toutefois, il nous semblerait plus judicieux de remplacer le PLA constituant le cœur hydrophobe des nanoparticules par un autre polymère qui posséderait une plus grande affinité vis-à-vis du MTX. Nous pouvons citer par exemple les dérivés du poly (acide malique)[67] qui sont aisément modifiables et qui permettrait de greffer latéralement des chaînons compatibles avec la structure du MTX comme des structures aromatiques (malolactonate de Benzyle). Ce polymère a déjà été utilisé pour préparer des nanocapsules à cœur aqueux encapsulant du Si-RNA [68].

Conclusion

Dans ce travail, le copolymère à bloc développé précédemment (chapitre II) a été utilisé pour le chargement du MTX. La technique de nanoprécipitation nous semblait la plus adaptée pour la préparation des nanosphères à partir de ce type de polymère de nature amphiphile. Le DMF a été choisi comme solvant car il permet de solubiliser parfaitement le polymère ainsi que le principe actif.

La quantité encapsulée de principe actif s'est révélée insuffisante pour pouvoir utiliser ces nanoparticules dans des applications *in vivo*. En outre, nous n'avons pas pu séparer le MTX non encapsulé. Ces difficultés viennent de la méthode utilisée, de la composition du copolymère ainsi que des propriétés physico-chimiques du MTX.

L'utilisation de chaînes de PEG plus longues s'avère nécessaire pour stabiliser d'avantage les nanoparticules après ultracentrifugation. Les choix de la méthode de fabrication et la nature chimique du polymère hydrophobe utilisé reste à explorer. Finalement une étude plus approfondie de la formulation des nanosphères est nécessaire, notamment la possibilité d'utiliser un tensioactif permettrait certainement d'améliorer l'efficacité d'encapsulation du MTX.

Références

1. Kitas, G., M.J. Banks, and P.A. Bacon, *Cardiac involvement in rheumatoid disease.* Clinical Medicine, Journal of the Royal College of Physicians, 2001. **1**: p. 18-21.
2. Berkanovic, E. and M.L. Hurwicz, *Rheumatoid arthritis and comorbidity.* J Rheumatol, 1990. **17**(7): p. 888-92.
3. Wikaningrum, R., et al., *Pathogenic mechanisms in the rheumatoid nodule: comparison of proinflammatory cytokine production and cell adhesion molecule expression in rheumatoid nodules and synovial membranes from the same patient.* Arthritis Rheum, 1998. **41**(10): p. 1783-97.
4. Kriegsmann, J., et al., *Expression of E-selectin messenger RNA and protein in rheumatoid arthritis.* Arthritis Rheum, 1995. **38**(6): p. 750-4.
5. Corkill, M.M., et al., *Gold treatment of rheumatoid arthritis decreases synovial expression of the endothelial leukocyte adhesion receptor ELAM-1.* J Rheumatol, 1991. **18**(10): p. 1453-60.
6. Garrood, T., L. Lee, and C. Pitzalis, *Molecular mechanisms of cell recruitment to inflammatory sites: general and tissue-specific pathways.* Rheumatology (Oxford), 2006. **45**(3): p. 250-60.
7. Phillips, M.L., et al., *ELAM-1 mediates cell adhesion by recognition of a carbohydrate ligand, sialyl-Lex.* Science, 1990. **250**(4984): p. 1130-2.
8. Swierkot, J. and J. Szechinski, *Methotrexate in rheumatoid arthritis.* Pharmacol Rep, 2006. **58**(4): p. 473-92.
9. Cronstein, B.N., D. Naime, and E. Ostad, *The antiinflammatory mechanism of methotrexate. Increased adenosine release at inflamed sites diminishes leukocyte accumulation in an in vivo model of inflammation.* J Clin Invest, 1993. **92**(6): p. 2675-82.
10. Cutolo, M., et al., *Anti-inflammatory mechanisms of methotrexate in rheumatoid arthritis.* Annals of the Rheumatic Diseases, 2001. **60**(8): p. 729-735.
11. Riksen, N.P., et al., *Methotrexate modulates the kinetics of adenosine in humans in vivo.* Annals of the Rheumatic Diseases, 2006. **65**(4): p. 465-470.
12. Hu, S.K., et al., *Studies on the effect of methotrexate on macrophage function.* J Rheumatol, 1988. **15**(2): p. 206-9.
13. Connolly, K.M., et al., *Alteration of interleukin-1 production and the acute phase response following medication of adjuvant arthritic rats with cyclosporin-A or methotrexate.* Int J Immunopharmacol, 1988. **10**(6): p. 717-28.

14. Seitz, M., et al., *methotrexate action in rheumatoid arthritis: stimulation of cytokine inhibitor and inhibition of chemokine production by peripheral blood mononuclear cells.* Rheumatology, 1995. **34**(7): p. 602-609.
15. Brody, M., I. Bohm, and R. Bauer, *Mechanism of action of methotrexate: experimental evidence that methotrexate blocks the binding of interleukin 1 beta to the interleukin 1 receptor on target cells.* Eur J Clin Chem Clin Biochem, 1993. **31**(10): p. 667-74.
16. Crilly, A., et al., *Interleukin 6 (IL-6) and soluble IL-2 receptor levels in patients with rheumatoid arthritis treated with low dose oral methotrexate.* J Rheumatol, 1995. **22**(2): p. 224-6.
17. Straub, R.H., et al., *Decrease of interleukin 6 during the first 12 months is a prognostic marker for clinical outcome during 36 months treatment with disease-modifying anti-rheumatic drugs.* Rheumatology, 1997. **36**(12): p. 1298-1303.
18. Gerards, A.H., et al., *Inhibition of cytokine production by methotrexate. Studies in healthy volunteers and patients with rheumatoid arthritis.* Rheumatology (Oxford), 2003. **42**(10): p. 1189-96.
19. Kraan, M.C., et al., *Differential effects of leflunomide and methotrexate on cytokine production in rheumatoid arthritis.* Ann Rheum Dis, 2004. **63**(9): p. 1056-61.
20. Strauss, G., W. Osen, and K.M. Debatin, *Induction of apoptosis and modulation of activation and effector function in T cells by immunosuppressive drugs.* Clin Exp Immunol, 2002. **128**(2): p. 255-66.
21. Genestier, L., et al., *Mechanisms of action of methotrexate.* Immunopharmacology, 2000. **47**(2-3): p. 247-57.
22. Wessels, J.A., T.W. Huizinga, and H.J. Guchelaar, *Recent insights in the pharmacological actions of methotrexate in the treatment of rheumatoid arthritis.* Rheumatology (Oxford), 2008. **47**(3): p. 249-55.
23. Martel-Pelletier, J., J.M. Cloutier, and J.P. Pelletier, *In vivo effects of antirheumatic drugs on neutral collagenolytic proteases in human rheumatoid arthritis cartilage and synovium.* J Rheumatol, 1988. **15**(8): p. 1198-204.
24. Haraoui, B., et al., *Synovial membrane histology and immunopathology in rheumatoid arthritis and osteoarthritis. In vivo effects of antirheumatic drugs.* Arthritis Rheum, 1991. **34**(2): p. 153-63.
25. Firestein, G.S., M.M. Paine, and D.L. Boyle, *Mechanisms of methotrexate action in rheumatoid arthritis. Selective decrease in synovial collagenase gene expression.* Arthritis Rheum, 1994. **37**(2): p. 193-200.

26. Dayer, J.M., et al., *Human recombinant interleukin 1 stimulates collagenase and prostaglandin E2 production by human synovial cells.* The Journal of Clinical Investigation, 1986. **77**(2): p. 645-648.
27. Johnston, A., et al., *The anti-inflammatory action of methotrexate is not mediated by lymphocyte apoptosis, but by the suppression of activation and adhesion molecules.* Clin Immunol, 2005. **114**(2): p. 154-63.
28. Montesinos, M.C., et al., *Adenosine A2A or A3 receptors are required for inhibition of inflammation by methotrexate and its analog MX-68.* Arthritis Rheum, 2003. **48**(1): p. 240-7.
29. Majumdar, S. and B.B. Aggarwal, *Methotrexate suppresses NF-kappaB activation through inhibition of IkappaBalpha phosphorylation and degradation.* J Immunol, 2001. **167**(5): p. 2911-20.
30. Bunescu, A., et al., *Enhanced Fcgamma receptor I, alphaMbeta2 integrin receptor expression by monocytes and neutrophils in rheumatoid arthritis: interaction with platelets.* J Rheumatol, 2004. **31**(12): p. 2347-55.
31. Parker, A., et al., *Peripheral blood expression of nuclear factor-kappab-regulated genes is associated with rheumatoid arthritis disease activity and responds differentially to anti-tumor necrosis factor-alpha versus methotrexate.* J Rheumatol, 2007. **34**(9): p. 1817-22.
32. Szekanecz, Z. and A.E. Koch, *Cell-cell interactions in synovitis. Endothelial cells and immune cell migration.* Arthritis Res, 2000. **2**(5): p. 368-73.
33. Wascher, T.C., et al., *Cell-type specific response of peripheral blood lymphocytes to methotrexate in the treatment of rheumatoid arthritis.* Clin Investig, 1994. **72**(7): p. 535-40.
34. Kremer, J.M., *The mechanism of action of methotrexate in rheumatoid arthritis: the search continues.* J Rheumatol, 1994. **21**(1): p. 1-5.
35. Segal, R., M. Yaron, and B. Tartakovsky, *Methotrexate: mechanism of action in rheumatoid arthritis.* Semin Arthritis Rheum, 1990. **20**(3): p. 190-200.
36. Vergne, P., et al., *Methotrexate and cyclooxygenase metabolism in cultured human rheumatoid synoviocytes.* J Rheumatol, 1998. **25**(3): p. 433-40.
37. Seitz, M., *Molecular and cellular effects of methotrexate.* Curr Opin Rheumatol, 1999. **11**(3): p. 226-32.
38. Bingham, S.J., et al., *Parenteral methotrexate should be given before biological therapy.* Rheumatology (Oxford), 2003. **42**(8): p. 1009-10.

39. Bharadwaj, A., et al., *Use of parenteral methotrexate significantly reduces the need for biological therapy.* Rheumatology (Oxford), 2008. **47**(2): p. 222.
40. Morand, E.F., P.I. McCloud, and G.O. Littlejohn, *Life table analysis of 879 treatment episodes with slow acting antirheumatic drugs in community rheumatology practice.* J Rheumatol, 1992. **19**(5): p. 704-8.
41. Suarez-Almazor, M.E., et al., *Methotrexate for rheumatoid arthritis.* Cochrane Database Syst Rev, 2000(2): p. CD000957.
42. Schnabel, A. and W.L. Gross, *Low-dose methotrexate in rheumatic diseases--efficacy, side effects, and risk factors for side effects.* Semin Arthritis Rheum, 1994. **23**(5): p. 310-27.
43. McKendry, R.J. and P. Dale, *Adverse effects of low dose methotrexate therapy in rheumatoid arthritis.* J Rheumatol, 1993. **20**(11): p. 1850-6.
44. Choi, B.R., et al., *Acute erythroleukemia in a rheumatoid arthritis patient during low-dose methotrexate therapy.* Rheumatol Int, 2005. **25**(4): p. 311-3.
45. Kremer, J.M., R.G. Lee, and K.G. Tolman, *Liver histology in rheumatoid arthritis patients receiving long-term methotrexate therapy. A prospective study with baseline and sequential biopsy samples.* Arthritis Rheum, 1989. **32**(2): p. 121-7.
46. Barrera, P., et al., *Methotrexate-related pulmonary complications in rheumatoid arthritis.* Ann Rheum Dis, 1994. **53**(7): p. 434-9.
47. Patatanian, E. and D.F. Thompson, *A review of methotrexate-induced accelerated nodulosis.* Pharmacotherapy, 2002. **22**(9): p. 1157-62.
48. Kerstens, P.J., et al., *Accelerated nodulosis during low dose methotrexate therapy for rheumatoid arthritis. An analysis of ten cases.* J Rheumatol, 1992. **19**(6): p. 867-71.
49. Hall, G.H., et al., *Intra-articular methotrexate. Clinical and laboratory study in rheumatoid and psoriatic arthritis.* Ann Rheum Dis, 1978. **37**(4): p. 351-6.
50. Wigginton, S.M., et al., *Methotrexate pharmacokinetics after intraarticular injection in patients with rheumatoid arthritis.* Arthritis Rheum, 1980. **23**(1): p. 119-22.
51. Liang, L.S., et al., *Methotrexate loaded poly(L-lactic acid) microspheres for intra-articular delivery of methotrexate to the joint.* J Pharm Sci, 2004. **93**(4): p. 943-56.
52. Liang, L.S., et al., *Intra-articular treatment of inflammatory arthritis with microsphere formulations of methotrexate: pharmacokinetics and efficacy determination in antigen-induced arthritic rabbits.* Inflamm Res, 2009. **58**(8): p. 445-56.
53. Modi, S., et al., *Copolymers of pharmaceutical grade lactic acid and sebacic acid: drug release behavior and biocompatibility.* Eur J Pharm Biopharm, 2006. **64**(3): p. 277-86.

54. Yang, X., et al., *Self-aggregated nanoparticles from methoxy poly(ethylene glycol)-modified chitosan: synthesis; characterization; aggregation and methotrexate release in vitro.* Colloids Surf B Biointerfaces, 2008. **61**(2): p. 125-31.
55. Gao, K. and X. Jiang, *Influence of particle size on transport of methotrexate across blood brain barrier by polysorbate 80-coated polybutylcyanoacrylate nanoparticles.* Int J Pharm, 2006. **310**(1-2): p. 213-9.
56. Sartori, T., et al., *Development and validation of a fast RP-HPLC method for determination of methotrexate entrapment efficiency in polymeric nanocapsules.* J Chromatogr Sci, 2008. **46**(6): p. 505-9.
57. Trotta, M., et al., *Deformable liposomes for dermal administration of methotrexate.* Int J Pharm, 2004. **270**(1-2): p. 119-25.
58. Karasulu, H.Y., et al., *Controlled release of methotrexate from w/o microemulsion and its in vitro antitumor activity.* Drug Deliv, 2007. **14**(4): p. 225-33.
59. Dhanikula, R.S., et al., *Methotrexate loaded polyether-copolyester dendrimers for the treatment of gliomas: enhanced efficacy and intratumoral transport capability.* Mol Pharm, 2008. **5**(1): p. 105-16.
60. Jubeli, E., L. Moine, and G. Barratt, *Synthesis, characterization, and molecular recognition of sugar-functionalized nanoparticles prepared by a combination of ROP, ATRP, and click chemistry.* Journal of Polymer Science Part A: Polymer Chemistry. **48**(14): p. 3178-3187.
61. Legrand, P., et al., *Influence of polymer behaviour in organic solution on the production of polylactide nanoparticles by nanoprecipitation.* Int J Pharm, 2007. **344**(1-2): p. 33-43.
62. Govender, T., et al., *PLGA nanoparticles prepared by nanoprecipitation: drug loading and release studies of a water soluble drug.* J Control Release, 1999. **57**(2): p. 171-85.
63. Wishart, D.S., et al., *DrugBank: a knowledgebase for drugs, drug actions and drug targets.* Nucleic Acids Research, 2008. **36**(suppl 1): p. D901-D906.
64. Natali, S. and J. Mijovic, *Dendrimers as Drug Carriers: Dynamics of PEGylated and Methotrexate-Loaded Dendrimers in Aqueous Solution.* Macromolecules. **43**(6): p. 3011-3017.
65. Barichello, J.M., et al., *Encapsulation of hydrophilic and lipophilic drugs in PLGA nanoparticles by the nanoprecipitation method.* Drug Dev Ind Pharm, 1999. **25**(4): p. 471-6.

66. Eric Allémann, R.G., and Eric Doelker, *drug loaded nanoparticles preparation methodes and drug targeting issues* European Journal of Pharmaceutics and Biopharmaceutics, 1993. **39**: p. 173-191.
67. Cammas-Marion, S. and P. Guérin, *Design of malolactonic acid esters with a large spectrum of specified pendant groups in the engineering of biofunctional and hydrolyzable polyesters.* Macromolecular Symposia, 2000. **153**(1): p. 167-186.
68. Bouclier, C., et al., *Physicochemical characteristics and preliminary in vivo biological evaluation of nanocapsules loaded with siRNA targeting estrogen receptor alpha.* Biomacromolecules, 2008. **9**(10): p. 2881-90.

Chapitre III

Préparation des nanoparticules ciblant l'E-sélectine

Evaluation in-vitro dans un modèle d'endothélium activé

Après avoir développé dans le premier chapitre une stratégie de synthèse d'un copolymère amphiphile fonctionnalisé capable de former par un procédé simple de nanoprécipitation, des nanoparticules de type cœur/couronne avec une orientation favorable des molécules de ligand à leur surface, notre mission par la suite a été de remplacer ces molécules modèles de glucopyranoside par un mime du sialyl lewis x pour construire le vecteur fonctionnel capable de cibler activement l'E-sélectine.

Dans cette partie de la thèse, nous avons étendu la méthodologie de préparation des copolymères et des particules à un mime du sialyl lewis x : Man-glu (Fig I). La structure de ce dernier est basée sur le mannose où les principaux groupements impliqués dans l'interaction avec l'E-sélectine sont présents. La molécule de fucose a été également remplacée par le mannose qui est moins onéreux.

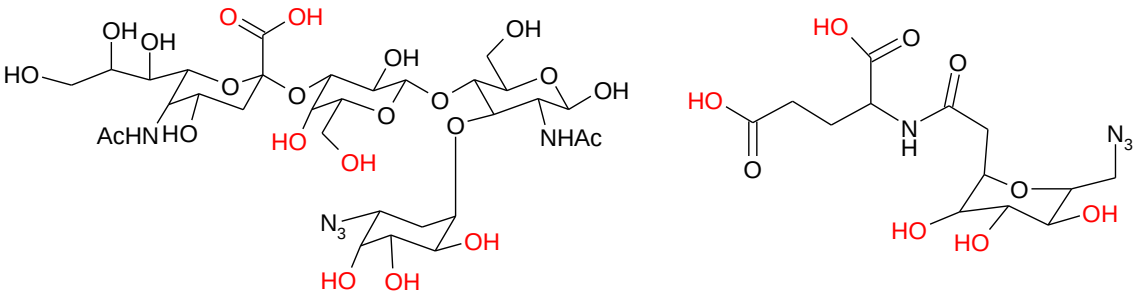

Fig. I structure du SLEx (gauche) et de son mime Man-glu (droit) utilisé dans notre travail
Les groupements impliqués dans l'interaction avec l'E-sélectine sont en rouge

Certains paramètres de la polymérisation par ATRP ont du être modifiés pour permettre une meilleure polymérisation de ce nouveau glyco-monomère préparé par « click chemistry ». Dans ce travail, nous avons également dû mettre au point les conditions de déprotection par hydrogénolyse des groupements benzyle protecteurs des fonctions hydroxyle et carboxyle du ligand. La caractérisation chimique des polymères a été réalisée par résonance magnétique nucléaire (RMN ^{1}H), chromatographie d'exclusion stérique (SEC) et spectroscopie infrarouge.

Afin de préparer des nanoparticules fluorescentes, nous avons synthétisé un copolymère amphiphile fluorescent grâce à l'insertion de molécules de rhodamine dans sa structure. Ce copolymère a été préparé à partir des chaines de PLA par polymérisation du PEGMMA par ATRP en présence d'un faible pourcentage de monomère méthacrylique rhodaminé (methacryloxyethyl thiocarbamoyl rhodamine B) dans le milieu réactionnel.

Une association de ce copolymère fluorescent et du copolymère fonctionnalisé avec le mime a été utilisée pour préparer des nanoparticules fluorescentes et porteuses du ligand. Les propriétés de fluorescence du copolymère et des nanoparticules qui en résultent ont été étudiées.

Après avoir testé la biocompatibilité de ces nanoparticules vis-à-vis des cellules endothéliales de veine ombilicale (HUVECs) en culture, ces cellules ont été traitées avec le TNF-α, et l'expression de l'E-sélectine a été confirmée par immunodétection grâce à un anticorps monoclonal anti E-sélectine.

L'efficacité des nanoparticules fluorescentes décorées de ce mime du sialyl Lewis X à interagir avec l'E-sélectine a été étudiée *in vitro* avec les HUVECs préalablement activées par un traitement au TNF-α. L'analyse en microscopie confocale a permis de visualiser l'association des nanoparticules avec les cellules.

La localisation cytoplasmique de la fluorescence sous forme de spots brillants montre une incorporation par endocytose médiée par l'E-sélectine. La quantification de la fluorescence associée aux cellules a été réalisée en spectrofluorimétrie après une lyse complète des cellules à l'aide d'une solution diluée de Triton-X100. Cela nous a permis de confirmer les observations faites par microscopie. Les résultats démontrent l'efficacité du ciblage des cellules endothéliales activées à l'aide du mime de sialyl lewis X.

Preparation of E-selectin-targeting nanoparticles and preliminary *in vitro* evaluation

Emile Jubeli[‡], Laurence Moine[‡]* Valérie Nicolas[†] and Gillian Barratt[‡]

[‡]Université Paris-Sud11, Faculté de Pharmacie 5 rue J.B. Clément CHATENAY-MALABRY FR 92296 UMR 8612 CNRS, IFR 141, [†] Plateforme d'Imagerie Cellulaire IFR141, France

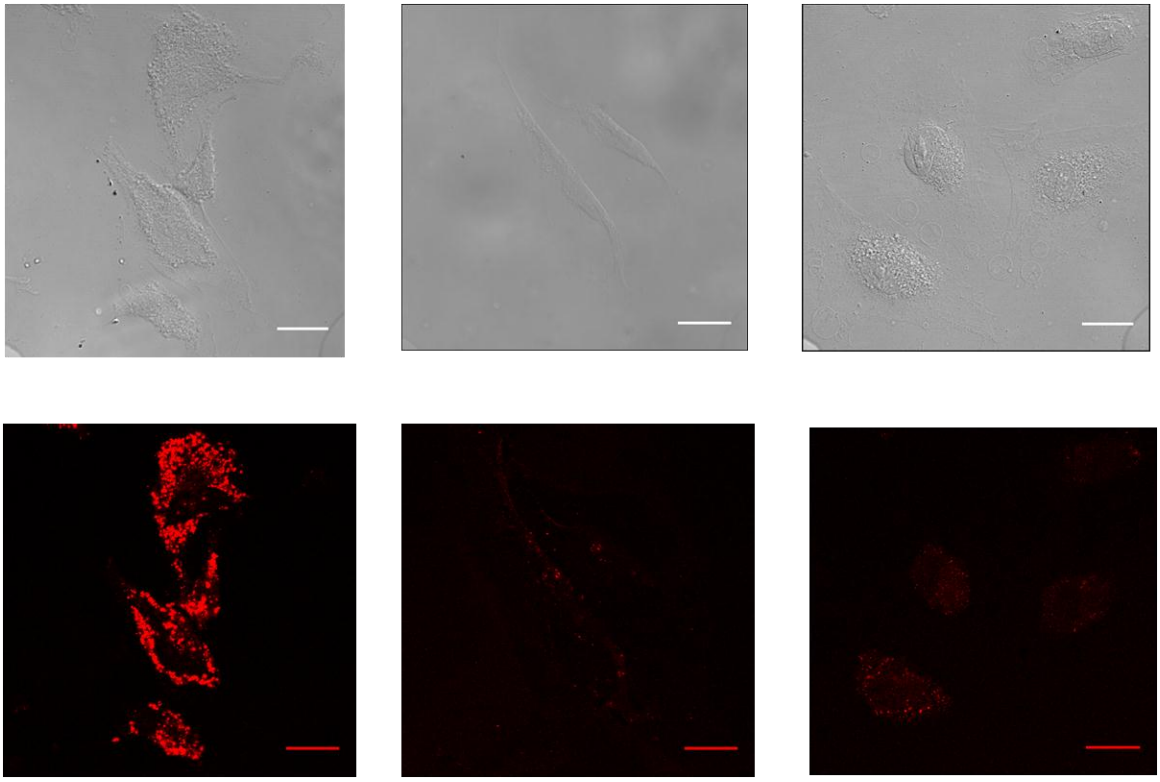

* To whom correspondence should be addressed: Tel: +33 1 46 83 59 94 ; Fax: +33 1 46 83 53 12 ; e-mail: Laurence.moine@u-psud.fr

Keywords: Nanoparticles, E-selectin, HUVECs, targeting, Carbohydrate ligand.

Abstract

Targeted delivery aims to concentrate therapeutic agents at their site of action and thereby enhance treatment and limit side-effects. E-selectin on endothelial cells is markedly up-regulated by cytokine stimulation of inflamed and some tumoral tissues, promoting the adhesion of leukocytes and metastatic tumor cells, thus making it an interesting molecular target for drug delivery systems.

We report here the preparation of targeted nanoparticles from original amphiphilic block copolymers functionalized with an analog of sialyl Lewis X (SLE^x), the physiological ligand of E-selectin. Nanoparticles, prepared by nanoprecipitation, caused no significant cytotoxicity. Ligand-functionalized nanoparticles were specifically recognized and internalized better by tumor necrosis factor α (TNF-α)-activated human umbilical vein endothelial cells (HUVECs) than control nanoparticles or HUVECs with low E-selectin expression. These nanoparticles are designed to carry the ligand at the end of a PEG spacer to improve accessibility. This system has potential for the treatment of inflammation, inhibition of tumor metastasis, and for molecular imaging.

Introduction

Colloidal carriers for intravenous drug delivery represent a promising approach to achieve controlled release and/or site specific targeting. This necessitates careful tuning of the chemical structure and hence the surface properties of the drug delivery systems. One of the major prerequisites is to render their surface hydrophilic in order to avoid rapid elimination from the blood stream by the macrophages of the mononuclear phagocyte system and the consequent accumulation of the delivery system in the liver and the spleen [1]. It is well documented that this can be achieved by grafting hydrophilic flexible chains of poly (ethylene glycol) [2, 3] or polysaccharides onto their surface [4, 5].

In order to avoid passive distribution of nanoparticles and hence of the drug they carry, they can be equipped with specific elements able to recognize molecules overexpressed or exclusively present on targeted cells, tissues or organs. Recognition elements include antibodies [6, 7], antibody fragments [8, 9], peptides [10-12], or folic acid[13, 14]. Such strategies promote site-specific targeting, i.e allow a controlled distribution of the drug and limit the side effects caused by its non specific distribution.

Among potential targets are the selectins: a family of three calcium-dependent transmembrane glycoproteins. They are classified by their site of expression as E-selectin (activated endothelium), P-selectin (platelets), and L-selectin (lymphocytes)[15]. E-selectin, also known as ELAM-1, is markedly up-regulated in endothelial cells when they are activated by proinflammatory factors such as TNF-α (tumor necrosis factor), interleukin-1 (IL-1) and bacterial lipopolysaccharide (LPS) [16, 17]. Once expressed on the surface of cell, it is efficiently internalized by endocytosis [18]. The expression of selectins, including E-selectin, allows the immobilization of leukocytes on endothelial cells. It has been demonstrated that E-selectin specifically recognizes the tetrasaccharide sialyl Lewis X (SLE^X) which is the terminal epitope of the structure of glycoproteins and glycolipids located on the surface of leukocytes and tumor cells [19, 20]. The E-selectin-SLE^x interaction via weak bonds initiates leukocyte “rolling”, the first step in leukocyte adhesion and infiltration into tissues undergoing inflammation, cancer or ischemic events. Therefore, E-selectin is a very interesting target for the site-specific delivery of colloids.

In the literature there are some reports of the use of this receptor as a therapeutic target for colloids bearing anti-E-selectin antibodies [21, 22] but this strategy is limited by possible immunogenicity, the large size of the final delivery system and the high cost of antibody production. A further disadvantage of antibodies is that some of them may have restricted species specificity, i.e they are active in animal models but do not cross-react with

the human epitope. Another approach to targeting E-selectin is the use of its physiological ligand SLE^x coupled to drug carriers such as liposomes [23, 24] or nanoparticles [25] but, as well as the complex and expensive synthesis of this ligand, these drug delivery systems could be in competition with SLE^x found on leukocytes that would be, in their turn, concentrated in the targeted region because of chemotaxis.

A way to overcome these problems is to use a small saccharidic ligand with a simple structure that would be non-immunogenic and recognize E-selectin with higher affinity than its natural ligand. Moreover, it is well documented that the presence of many copies of pendant saccharides on a polymer backbone can enhance the affinity towards cell-surface lectins because of multivalent recognition, known as the “cluster effect” [26, 27].

Drugs encapsulated in such carriers could be expected to be concentrated in the sites where nanoparticles are retained i.e. in the sites where the pharmacological effect should take place.

Our goal in the present work was to mimic the interaction of leukocyte/endothelial cells throughout the design of novel biodegradable nanoparticles that can target endothelial cells with up-regulated E-selectin in inflammatory pathologies diseases such as rheumatoid arthritis [28, 29], liver inflammation [30], autoimmune uveoretinitis[31], or even some cancers where E-selectin is present on the vasculature of tumor tissue; for example, human colorectal cancer [32], gastric cancer [33] head and neck [34] or breast tumors [35]. These nanoparticles are composed of poly (d,l-lactide) (PLA) surrounded with pendant chains of poly (ethylene glycol) to confer a long circulation time on them. In order to target E-selectin specifically, our choice was to use a SLE^x analog, proposed by Wong et al[36] that has a small structure and five times higher affinity for E-selectin than SLE^x in a cell-free test [37]. This ligand was attached to the end of PEG chains using “click chemistry”, resulting in a stable covalent link to the nanoparticles surface in physiological media.

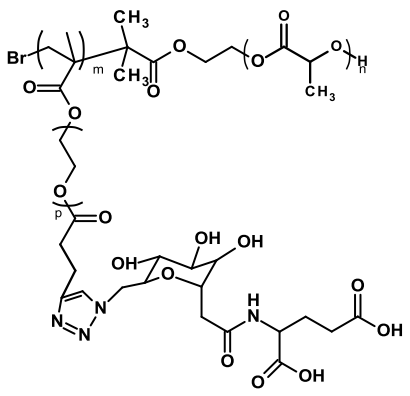

Figure 1: Structure of the copolymer PLA-PEGMA-Man-glu-OH (**5**)

In this work, we report the preparation of these nanoparticles, their characterization, *in vitro* cytotoxicity and *in vitro* interactions with activated endothelial cells. Fluorescent nanoparticles were prepared from a fluorescently tagged copolymer. Their association with endothelial cells was evaluated qualitatively through observation by confocal microscopy and quantitatively by measuring cell-associated fluorescence by spectrofluorimetry.

Materials and methods

Chemicals

Poly(ethylene glycol) methacrylate PEGMA (Mn ≈ 526 g/mol), Poly(ethylene glycol) methyl ether methacrylate (300 g/mol), tin (II) 2-ethylhexanoate ($Sn(Oct)_2$ 95%) and N,N′,dicyclohexyl carbodiimide (DCC 99%), 3-[4,5-dimethylthiazol-2-yl]-2,5-diphenyltetrazolium) bromide were purchased from Sigma-Aldrich. 2-bromo-2-methylpropionyl bromide (98%) and N,N,N′,N″,N″-pentamethyldiethylenetriamine (PMDETA) were obtained from Acrôs organics (Belgium). Trimethylamine (99.5%) and 4-pentynoic acid 98% were purchased from Alfa Aesar-UK. Methacryloxyethyl thiocarbamoyl rhodamine B and d,l-lactide were purchased from Biovalley. Palladium hydroxide 20% on carbon was obtained from TCI. Copper (I) bromide (Cu (I)Br) (Sigma-Aldrich) was washed with glacial acetic acid, filtered, washed with ethanol and dried under vacuum. PEGMA was purified before use as described previously [38]. Dibenzyl N – [(6-azido–6-deoxy–2,3,4–tri–O-benzyle-α-D-mannopyranosyl)]-L-glutamic acid (referred to as Man-glu in the text) was synthesized by Symphabase (Switzerland).

For the synthesis and characterization of the bifunctional initiator, PLA-PEGMA (**7**) and PLA-PEGMMA-Rhodamine (**8**), see the Supporting Information.

Instruments:

^{1}H-NMR measurements were performed with a Bruker 300MHz spectrometer. Size exclusion chromatography was performed with a double detector: 270 dual viscosimeter and light scattering detector 90° (Viscotek®- France) and a refractometer (Waters® 410). THF was used as the mobile phase with a TOSOH BIOSCIENCE TSKgel 5µm bead size Guard pre-column; and two TOSOH BIOSCIENCE TSKgel 5µm bead size GMHHR-M columns, operated at 1 mL/min with the column temperature set at 30 °C. Omnisec® software (Viscotek) was used to process the data.

The mean hydrodynamic diameter and polydispersity of the nanoparticles were measured by quasi-elastic light scattering with a Zetasizer NanoZS90 (Malvern Instruments). For each sample, the measurement was performed three times at a temperature of 25 °C

with a detection angle of 90°. Nanoparticle surface charge was investigated by ζ-potential measurement at 25 °C after dilution with 1 mM NaCl.

The fluorescence properties of nanoparticles were evaluated using a Perkin-Elmer LS50B spectrofluorometer with a 10 mm optical quartz cuvette.

Confocal laser scanning microscopy (Zeiss LSM-510, Carl Zeiss, Germany) was used for *in-vitro* imaging studies. All images were acquired with an air-cooled ion laser at 488 nm (FITC) and 543 nm (rhodamine), performed using Plan Apochromat 63 × /1.4NA oil objective lens. Fluorescence was collected by using a 505–550 nm band pass filter for FITC and a long pass filter beginning at 560 nm for rhodamine. It was checked that autofluorescence of HUVECs was negligible under the acquisition settings and did not interfere with the fluorescence coming from the nanoparticles.

Synthesis of acetylene-terminated PEGMA (Pentynoate- PEGMA) (3)

An acetylene group was conjugated with PEGMA as described in our previous work [39]. Briefly PEGMA (7.5g; 14.3mmol), 4-pentynoic acid (2.8g; 28.5mmol) and DMAP (0.17g; 1.4mmol) were put in a schlenk tube with 35 mL of methylene chloride (CH_2Cl_2). DCC (5.6g; 27.2mmol) was solubilized in 5 mL of CH_2Cl_2 and then added to the schlenk tube. The mixture was stirred overnight at room temperature. After elimination of dicyclohexylurea (DCU) crystals by filtration, the organic solvent was evaporated under reduced pressure. The resulting yellow oil-like product was purified by column chromatography with a mixture of ethyl acetate/methanol (9:1) as eluant to yield the acetylene-terminated PEGMA (yield =82%).

^{1}H-NMR (300MHz, $CDCl_3$, δ ppm): 1.92 (3H, CH_2=C-C**H**$_3$), 1.96 (1H, ≡ C**H**), 2.50 (2H, -C**H**$_2$-CH_2-C≡CH), 2.51 (2H, -CH_2-C**H**$_2$-C≡CH), 3.65 (36H, -C**H**$_2$-, PEG), 4.26 (4H, 2 x -C**H**$_2$-COO), 5.55 (1H, - **H**HC= C), 6.10 (1H, -H**H**C = C). IR (cm^{-1}): 3260 (-C≡CH), 2870 (alkyl), 1620 (-C=C-).

Synthesis of PEGMA-Man-glu-Bz (4)

Acetylene-terminated PEGMA (**3**) (0.3g; 0.5mmol), Man-glu-Bz (0.62g; 0.75mmol), CuBr (0.071g; 0.5mmol) and PMDETA (0.086mg; 0.5mmol) were introduced in a schlenck tube with 4 mL of DMF. The mixture was stirred for 3 hours at room temperature, the reaction was stopped and the content was diluted with ethyl acetate before being submitted to column chromatography using gradient mixtures of cyclohexane / ethyl acetate then ethyl acetate /methanol. The resulting PEGMA-Man-glu-Bz (**4**) was dried under vacuum (yield= 55%).

^{1}H-NMR (300MHz, $(CD_3)_2O$, δ ppm): 1.79 (3H, CH_2=C-C**H$_3$**), 2.10 (1H, C**H**H-CO-NH-), 2.52 (2H, -CH_2- C**H$_2$**-COO), 2.65 (CH, -C**H$_2$**-CH_2-C=CH), 2.95 (2H, -CH_2-C**H$_2$**-C=CH), 3.62 (36H, -C**H$_2$**-C**H$_2$** of PEG + 3H –C**H**- mannose ring), 3.80-4.15 (1H, O-C**H**-CH_2, mannose ring), 4.15-4.32 (4H, 2x -C**H$_2$**-COO), 4.52-4.80 (6H, -C**H$_2$**-Bz, protecting mannose hydroxyl groups), 5.08-5.20 (4H, -C**H$_2$**-Bz, protecting glutamate carboxyl groups), 5.65 (1H, **H**HC=CH-, vinyl), 6.08 (1H, H**H**C=CH vinyl), 7.2-7.45 (25H, aromatic protons), 7.80 (1H, -C=C**H**-N triazole ring). IR (cm^{-1}): 3650 (-NH-), 2870 (alkyl), 1720 (-C=O-), 1640 (-C=C), 700 (aromatic C-H).

Synthesis of the PLA macroinitiator (1)

D, l-lactide (8.64g; 60mmol), Sn $(Oct)_2$ (10.4mg; 0.013mmol) and the synthesized bifunctional initiator β-hydroxyl ethyl α-bromoisobutyrate (HEBIB) (30mg; 0.28mmol) were introduced in a schlenk tube and the mixture was bubbled with nitrogen for 30 min. The schlenk tube was placed in a thermostated oil bath at 130 °C and stirred for 6 hours. The resulting solid crude product was solubilized with chloroform, and precipitated in a cold mixture of 1:1 petroleum ether/diethyl ether and dried in a vacuum oven at 40 °C to give a white solid (yield 92%). ^{1}H-NMR (300MHz, $CDCl_3$, δ ppm): 1.55 (3H, C**H$_3$**), 5.2 (1H, -C**H** main chain). Mn$_{NMR}$= 29700, Mn$_{SEC}$ = 28500, Mw/Mn=1.02.

Synthesis of PLA-block- PEGMA-Man-glu-Bz (5) by ATRP

PLA (**1**) (0.320g; 0.01mmol), PEGMA-Man-glu-Bz (**3**) (0.311 mg; 0.22mmol), CuBr (3.1mg; 0.02mmol), PMDETA (3.8mg; 0.02mmol) were introduced to a schlenk tube with 1 mL of DMSO. After three freeze-pump-thaws, the schlenk tube was placed in a thermostated oil bath at 60 °C and stirred for 24h. The content was then purified by column chromatography with CH_2Cl_2/methanol (9:1) to remove the copper complex. After evaporation of solvents, product (**5**) was dried in a vacuum oven at 45 °C for 48h, (yield 78%).

^{1}H-NMR (300MHz, DMSO, δ ppm): 0.7-1.3 (-C**H$_2$-** main chain of PEGMA), 1.35-1,65 (3H, -C**H$_3$** PLA), 1.95 (1H, C**H**H-CO-NH-), 2.40 (4H, -C**H$_2$**- C**H$_2$**-COO + 2H -C**H$_2$**-CH_2-C=CH), 2.8 (2H, -CH_2-C**H$_2$**-C=CH), 3.20-3.70 (36H, -C**H$_2$**- of PEG + 4H,–C**H**- mannose ring and), 4.14 (4H, 2x -C**H$_2$**-COO), 4.32-4.72 (6H, -C**H$_2$**-Bz, protecting mannose hydroxyl groups), 4.9-5.30 (4H, -C**H$_2$**-Bz, protecting glutamate carboxyl groups + 1H, -C**H**- main chain of PLA), 7.15-7.4 (25H, aromatic protons), 7.7 (1H, -C=C**H**-N triazole ring). IR (cm^{-1}): 3650 (-NH-), 2870 (alkyl), 1720 (-C=O-), 700 (aromatic C-H). Mn$_{NMR}$ = 44700, Mn$_{SEC}$=38200 and Mw/Mn = 1.09.

Deprotected PLA-block- PEGMA-Man-glu-OH (6)

The benzyl groups protecting the three hydroxyl groups of mannose and the two carboxyl groups of glutamate in the structure of Man-glu-Bz were reduced by catalytic debenzylation in the presence of hydrogen gas. Product (**5**) (0.450g) was dissolved in a 10 ml mixture of THF: glacial acetic acid (1:4) in a cylindrical tube, then 400 mg of palladium hydroxide 20% on carbon was dispersed in the solution. After degassing with argon for 10 min, the tube was introduced to a special cell, filled with hydrogen gas and maintained under a pressure of 6 bars. The mixture was stirred vigorously with a magnetic stirrer for 72 hours. After filtration through celite to remove the palladium-carbon, solvents were evaporated under vacuum at 45 °C; the deprotected product (**6**) was obtained with a 91% yield (Fig 1). ^{1}H-NMR (300MHz, $(CD_3)_2CO$, δ ppm): 0.8-1.3 (-C**H$_2$-** main chain of PEGMA), 1.45-1.70 (3H, -C**H$_3$** PLA), 2.25 (1H, C**H**H-CO-NH-), 2.60 (4H, -C**H$_2$**- C**H$_2$**-COO + 2H -C**H$_2$**-CH_2-C=CH), 3.00 (2H, -CH_2-C**H$_2$**-C=CH), 3.50-3.78 (36H, -C**H$_2$**- of PEG + 4H,–C**H**- mannose ring), 4.14-4.42 (4H, 2x -C**H$_2$**-COO), 5.15-5.38 (1H, -C**H**- main chain of PLA), 7.33 (1H, -C=C**H**-N triazole ring). IR (cm^{-1}): 3000-3600 (-OH-), 2870 (alkyl), 1720 (-C=O-).

Preparation of nanoparticles

Nanoparticles were prepared by nanoprecipitation. 10 mg of a 1:1 mixture of PLA-PEGMA-Rhod (**8**) and PLA-PEGMMA (**7**) or PLA-PEGMA-Man-glu-OH (**6**) were dissolved in 2 ml of DMF. This solution was added dropwise to 4 mL of water under moderate stirring through a needle (0.8 mm internal diameter) over 1 min. The crude nanoparticle suspension was centrifuged (Centrifuge Eppendorf 5804 R) at 4500 x g for 10 min at 20 °C to separate larger polymer aggregates from nanoparticles that remained in the supernatant, then DMF was removed by 4 hours dialysis (MWCO 15000 Da) against deionized water.

Fluorescent properties of labeled copolymer and nanoparticles

The fluorescent properties of copolymer (**8**) and nanoparticles containing this copolymer were studied by fluorescence spectroscopy. Excitation and emission wavelengths were determined for a solution (5 mg/mL) of copolymer (**8**) in THF and for a suspension of nanoparticles in water (5 mg/mL) prepared from a 1:1 mixture of copolymers (**7** and **8**). Calibration curves of fluorescence emission intensity as a function of the concentration of polymers in THF and of nanoparticles in water were drawn in the range of 0.01-1 mg/mL.

Cell culture and cytotoxicity assay

Freshly isolated human umbilical vein endothelial cells (HUVECs) (Hospital Bichat – Paris-France), were cultured in Endothelial Cell Growth Medium (Promocell - Germany) supplemented with 2% fetal calf serum (FCS), 0.1 ng/ml epidermal growth factor, 1ng/ml basic fibroblast growth factor, 90 µg/ml heparin, 1µg/ml hydrocortisone, 50 U/ml penicillin, and 50 µg/ml streptomycin. Cells were maintained at 37 °C under a humidified atmosphere containing 5% CO_2.

The cytotoxicity of nanoparticles was determined by assessing cell viability on HUVECs using the 3-[4,5-dimethylthiazol-2-yl]-2,5-diphenyltetrazolium) bromide (MTT) assay measuring mitchondrial dehydrogenase cell activity. Cells were seeded in the above mentioned medium into 96-well plates at a density of 10^4 cells/well. After an adherence period of 24h, different dilutions of nanoparticles (0.05-0.5 mg polymer/mL of culture medium) were added to the cells. Each dilution was tested in at least 5 wells. After 48 hours of incubation at 37 °C, 20µL of MTT (Sigma-Aldrich, Saint Quentin Fallavier, France) in PBS (5 mg/mL) were added to each well. After further incubation for 2 hours at 37 °C, culture medium was removed and formazan crystals were dissolved in 200 µL DMSO. The absorbance of converted dye, correlated with the number of viable cells, was measured at 570 nm using a microplate reader (Labsystems multiscan MS). The percentage of surviving cells was calculated as the absorbance ratio of treated to untreated cells.

Immunodetection of E-selectin

HUVEC cells were seeded on sterile round coverslips at a density of $5x10^4$ cells/well into 24-well plates and grown for 48h prior to activation by 50ng/ml of recombinant human TNF-α (R&D systems) for 4 hours. After rinsing with PBS, cells were fixed with 4% solution of paraformaldehyde (Sigma-Aldrich), then free aldehyde groups were quenched with 50mM solution NH_4Cl in PBS. Unspecific sites were blocked with 5% bovine serum albumin solution (BSA - Sigma-Aldrich). Cells were then incubated overnight at 4 °C with monoclonal anti-human E-selectin antibody (R&D systems) (10µg/mL in BSA 5%). After washing with PBS, cells were incubated for 2 hours with a 1:300 dilution of secondary anti-mouse Alexa 546-labeled antibody (Invitrogen). In order to stain cell lipids and particularly the cell membrane, cells were incubated with a 100µL solution (2:100) in PBS of FITC-PKH67 fluorescent dye (Sigma-Aldrich). Imaging was carried out with the laser scanning confocal microscope as described above.

Observation and quantification of nanoparticles association with HUVEC

HUVECs were seeded in 24-well plates and activated as described above, then fluorescent nanoparticles (100 µg/well) with or without ligand were incubated with cells for 0.5, 2 and 21h in 37 °C or 4 °C. For laser scanning confocal microscope observation, cells were fixed with 4% paraformaldehyde as described above after elimination of non associated nanoparticles by repeating washing with PBS.

For quantification of nanoparticles association with cells, the monolayer was lysed with 1ml of 0.2% Triton X-100 in 1M NaOH. The nanoparticles content was quantified by spectrofluorimetry (λ_{ex}=560 nm, λ_{em}=580 nm). HUVECs incubated with known concentrations of nanoparticles were lysed in 1mL of 0.2% Triton X-100 in 1M NaOH and these lysats were used to calibrate the spectrofluorometer. Linear calibration curves were obtained for nanoparticles with and without ligand (r = 0.9993 and 0.9997 respectively), over a nanoparticles concentration range of 2 to 100 µg/mL. This linear calibration confirmed that the autofluorescence of HUVECs was negligible and did not interfere with nanoparticles fluorescence under our experimental conditions.

To determine the specificity of E-selectin binding, a similar procedure was used in which monoclonal anti-human E-selectin antibody was preincubated with cells (10 µg/mL) for 1 hour before determining the association of nanoparticles with the cells.

Results

During the early stages of our work, we successfully synthesized an amphiphilic copolymer with block architecture carrying on its hydrophilic part a monosaccharide as a model of a carbohydrate ligand[39]. The glucopyranoside used was first coupled with a poly (ethylene glycol) methacrylate macromonomer by "click chemistry". Thereafter, the construction of the copolymer was carried out by a combination of two types of polymerization: ATRP (Atom Transfer Radical Polymerization) for the hydrophilic part and ROP (Ring Opening Polymerization) for the hydrophobic part. The presence of glucopyranoside residues on the surface of nanoparticles formed from this copolymer was demonstrated through their interactions with Concanavalin A.

In the present work, we have extended our methodology to the preparation of particles carrying a sialyl Lewis X analog in place of monosaccharide to study their ability to mimic the interactions between leukocytes and activated endothelial cells. Our choice was to use a mannose-based SLE^x analog, synthesized for the first time by Wong et al[36], due to its simple structure and its moderate cost as well as its high affinity for E-selectin estimated by the authors as five times greater than SLE^x in a cell-free test [37]. The use of this analog

makes these nanoparticles a very interesting candidate for a drug delivery system targeting E-selectin.

Synthesis of PEGMA-Man-glu-Bz (**4**)

The preparation of the ligand-functionalized macromonomer was carried out by click chemistry. PEGMA was first reacted with 4-pentynoic acid by an esterification reaction leading to the alkyne-terminated PEGMA (**3**) (Figure S1). Thereafter, N–(6-deoxy–6 azido α-D-Mannopyranosyl)]-L-glutamic acid (Man-glu) was introduced by Cu-catalyzed [2 + 3] cycloaddition to provide the macro monomer (**4**). The time of this reaction was fixed at 3 hours, leading to a high conversion ratio while maintaining the integrity of methacrylate double bond. ^{1}H-NMR spectroscopy was used to assess the efficiency of the click reaction by measurement of the integration values of a newly appeared methine proton on the triazole ring observed around δ = 7.8 ppm compared with those of the methylene protons at the α-position of triazole ring observed at δ = 2.95 ppm.

Synthesis of amphiphilic copolymers

In order to evaluate this nanoparticulate system, we have synthesized different copolymers including a non functionalized copolymer (**7**), a ligand-functionalized one (**6**) and fluorescent copolymers (**8**). Different combinations of these copolymers were used to prepare nanoparticles for the cytotoxicity studies and *in vitro* interaction with cells.

For the synthesis of copolymers (**7**) and (**8**)**,** we were guided by our previous work using anisole as solvent. However, our first attempts at ATRP polymerization with the ligand-based PEGMA monomer in anisole resulted in a very low conversion rate according to ^{1}H-NMR (<30%). The limited solubility of PLA in polar solvents and PEG and ligand in apolar ones necessitated the use of solvents with a moderate dielectric constant. Other solvents reported in the literature for the polymerization of methacrylic monomers initiated by hydrophobic macroinitiators include tetrahydrofuran (THF) [40, 41], dimethylformamide (DMF), dimethyl sulfoxide (DMSO)[42] N-methylpyrrolidone (NMP) [43, 44], with dielectric constants of 7, 36, 47 and 170, respectively. Polymerization carried out in NMP, THF and DMF did not give better conversion rate than anisole (results not shown), while the use of DMSO allowed us to obtain a conversion rate of more than 75% (Table 1) keeping CuBr/PMDETA complex as catalyst but with a longer polymerization time of 24h [42].

Although DMSO is rarely used in the preparation of polymers, it is quite efficient for solubilizing the PLA and ligand-functionalized pegylated monomer, which allowed a high conversion rate in this system.

Table 1: Synthesis and properties of polymers.

	polymer	M/I	% conv NMR	Mn Theo	Mn NMR	Mn SEC	PDI Mw/Mn
1	PLA	1/420	92	30200	29700[a]	28500	1.05
5	PLA-PEGMA-Man-glu-Bz	1/20	80	57600	44700[b]	38200	1.10
6	PLA-PEGMA-Man-glu-OH	-	-	42000	35500[c]	ND	ND
7	PLA-PEGMMA	1/20	89	35000	36000[d]	44600	1.14
8	PLA-PEGMMA-Rhod	1/20	72	31000	28000[d]	28900	1.12

[a)] Calculated from the relative integration values of the main chain (-CH-) of PLA and the two ($-CH_3-$) of the initiator.
[b)] Calculated from the relative integration values of the main chain (-CH-) of PLA and the (-CH-) of triazole ring.
[c)] Calculated from the relative integration values of the main chain (-CH-) of PLA and the ($-CH_2-$) of PEG chain.
[d)] Calculated from the relative integration values of the main chain (-CH-) of PLA and the ($-OCH_3$) of PEGMMA.

The structure of the resulting copolymer was confirmed by a combination of ^{1}H-NMR, IR and SEC. In ^{1}H-NMR spectrum (Figure 2), the disappearance of the peaks of vinyl protons (δ = 5.5 and 6.2 ppm) and the appearance of the peak of the main chain in the region between 0.75 and 1.4 ppm confirmed the polymerization. Incorporation of Man-glu-Bz on the copolymer chain could be attested by the presence of triazole peak (δ = 7.7 ppm), aromatic protons (δ = 7.35) and methylene protons of benzyl groups (δ = 4.32-4.72 ppm and 4.9-5.3 ppm). The SEC elution profile of (**5**) was shifted to the higher molecular weight region (Figure S4) compared with its PLA precursor, indicating that initiation by the Br-terminated chains of PLA had occurred and a block copolymer was prepared with a narrow polydispersity index (1.1). It could be shown on the SEC traces of copolymers, presence of a shoulder at the lower retention volume meaning occurrence of bimolecular termination by combination. Nevertheless, as shown in Table 1, presence of this shoulder does not lead to a large deviation of the polydispersity which remains narrow (≤1.1). Since the overall chromatogram was shifted towards the higher masses, this indicates that the initiation was satisfactory with regard to our final application. Presence of some polymeric chains with higher molecular weight will not affect the formation of nanoparticles.

Pendant benzyl groups were removed by catalytic hydrogenolysis using severe conditions (6 bars pressure, 72 h, and high amount of palladium). In fact, with milder conditions, the deprotection could not take place. The IR spectrum of the copolymer (Figure S3) showed a large broad band from 3000 to 3500 cm^{-1}, which demonstrated the presence of hydroxyl groups on the mannose. The characteristic bands of aromatic C-H stretching (at 690-750 cm^{-1}) were absent. In the ^{1}H-NMR spectrum (Figure S2), no peak was found either at 7.35 ppm or at 4.32-4.72 ppm or 4.9-5.3 ppm, showing the disappearance of the protecting groups, while the presence of peaks of PLA at 5.1 ppm and 1.5 ppm confirmed the integrity of the polyester backbone under our experimental conditions.

The SEC chromatogram of the deprotected polymer showed a broad signal beginning from a shorter elution time and finishing at a longer elution time than that of the macroinitiator (PLA) (Figure S6). As this was not the case for the copolymer bearing the benzyl-protected ligand, we attributed this wider peak to the poor solubility of the glycopolymer in THF and the possible interaction of the two carboxylic groups of the ligand with the column.

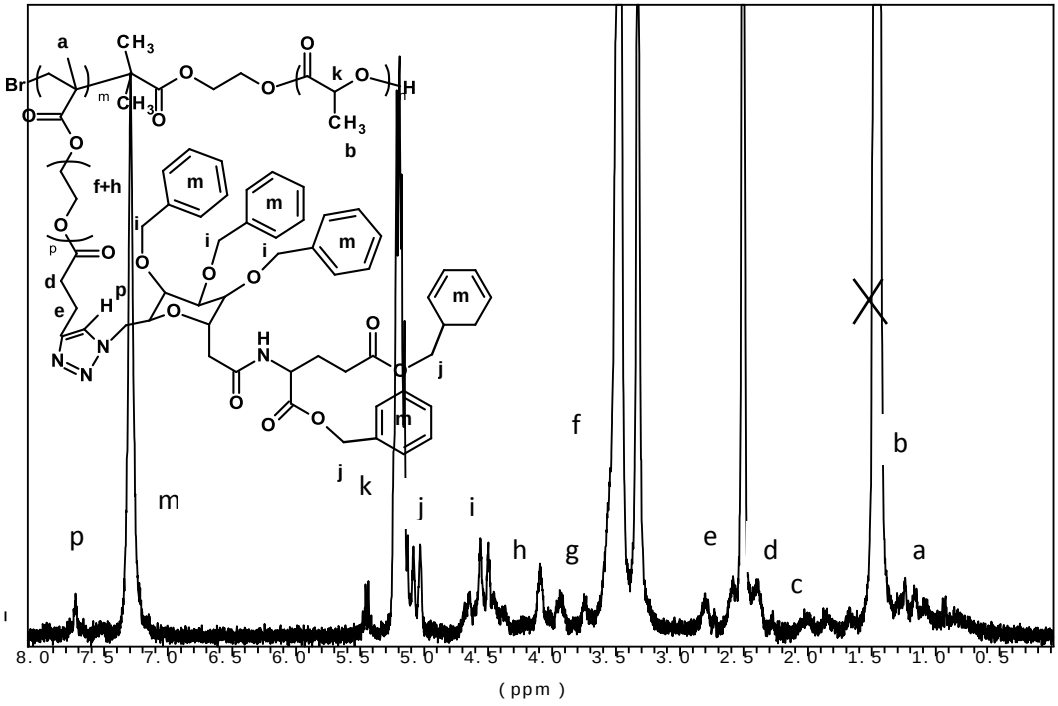

Figure 2: ^{1}H-NMR spectrum of PLA-PEGMA-Man-glu-Bz (**5**)

Characterization of nanoparticles

Nanoparticles were prepared in a single step by nanoprecipitation. Nanoparticles both with and without ligand (Figure 3) showed a homogeneous mean diameter of around 170 nm with a unimodal size distribution (Table 2). After two weeks of storage at 4 °C in water, no significant size change was detected and no aggregation was observed.

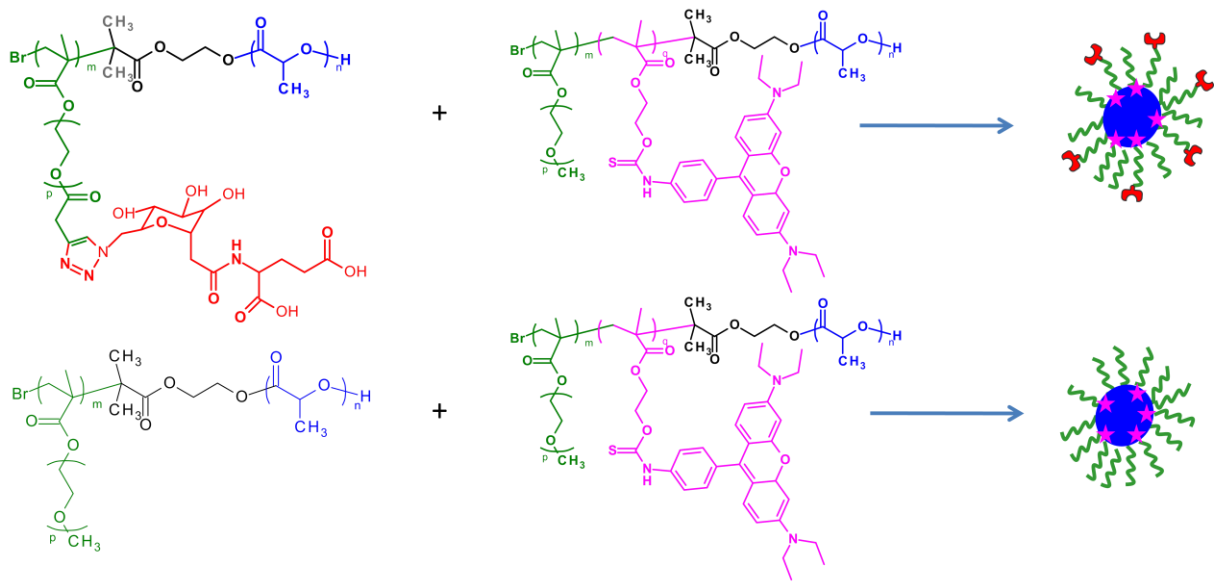

Figure 3. Composition of the two types of nanoparticles prepared for this study

Negative zeta potential values were observed for both types of nanoparticles, due to the end groups of PLA block of the copolymer, even in the presence of PEG chains. It has been reported that high PEG weight content are needed to completely mask the charge of PLA[45] which is not the case for the nanoparticles prepared in this study. The more negative values obtained for Man-glu-OH carrying nanoparticles could be attributed to the two carboxylic groups present in the ligand.

Table 2: Properties of nanoparticles prepared with and without ligand

	Copolymers	Size (nm)	PDI*	Zeta potential (mV)
NP-Ligand-Rhod	(6 + 8)	178±10.9	0.167	-21.9
NP-Rhod	(7 + 8)	165±1.6	0.124	-28.4

*Polydispersity index

Characterization of fluorescently labeled copolymer and nanoparticles

The fluorescence spectra of a solution of rhodamine polymer (**8**) in THF were studied. The excitation and emission maxima wavelengths were found to be λex = 559.5 nm and λem = 580.5 nm (Figure S7) which are in agreement with results obtained with other rhodamine-labeled polymers in solution [46].

Similar values were observed for a 5 mg/mL suspension of nanoparticles prepared from a 1:1 mixture of copolymers (**7**) and (**8**): λex = 560 nm and λem = 579 nm (Figure S8). A linear relationship between the fluorescence intensity and concentration were observed for polymer in THF (0.01-1 mg/mL R^2=0.9993) and for nanoparticles in water (0.01-0.8 mg/mL R^2=0.9997).

Nanoparticle cytotoxicity studies

The *in vitro* cytotoxicity of fluorescent nanoparticles prepared with and without the ligand was determined on freshly isolated HUVECs after 48 h of incubation at 37 °C using the MTT test. The results reported in Figure 4 show cell viability higher than 60% in the range of (0-500 µg/mL), for both types of fluorescent nanoparticles.

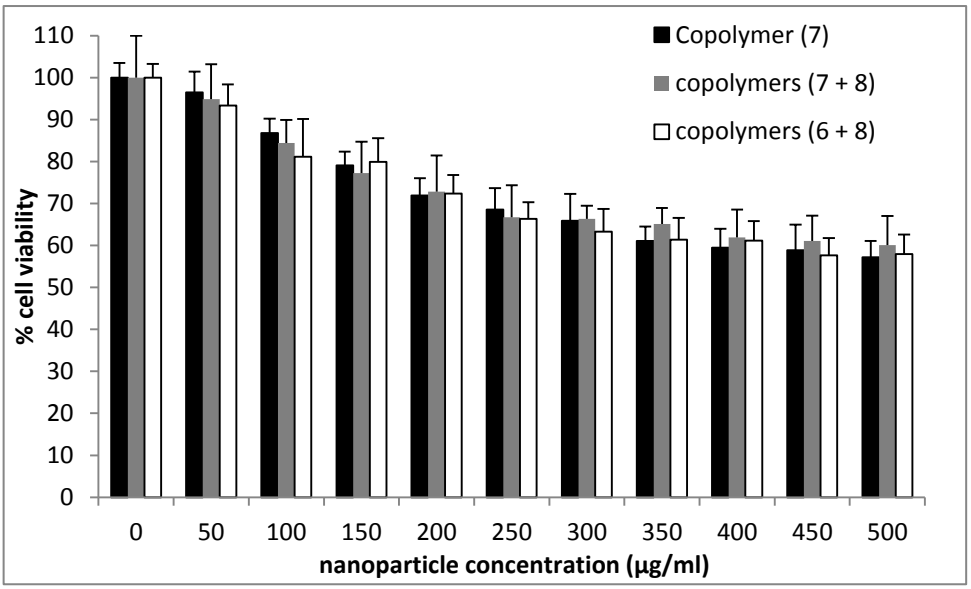

Figure 4: HUVEC cell viability determination by the MTT assay after incubation with 0-500 µg/ml of different kinds of nanoparticles for 48h. NP without rhodamine (black columns), NP-Rhod (gray columns) and NP-ligand-Rhod (white columns)

Nanoparticles prepared only from copolymer (**7**) (without rhodamine) were also tested to assess any additional toxicity of the rhodamine incorporated in the polymer backbone. It is evident from Figure 4 that rhodamine-containing nanoparticles have an identical cytotoxicity profile to that of non-fluorescent nanoparticles.

In the light of these results, we chose 100 µg/mL of nanoparticles in the culture medium - at which cell viability is higher than 80% - as the concentration to be used for the evaluation of nanoparticles association with HUVEC cells.

In the light of these results, we chose 100 µg/mL of nanoparticles in the culture medium - at which cell viability is higher than 80% - as the concentration to be used for the evaluation of nanoparticle association with HUVEC cells.

Immunodetection of E-selectin

HUVECs were used as an endothelial cell model because of their human origin, and also because they are well characterized, widely used to investigate vascular events *in vitro*, and can be treated with cytokines to generate an *in vitro* model of activated endothelium.

Pro-inflammatory TNF-α-activated HUVECs and non activated HUVECs were incubated with anti-human E-selectin antibody and examined with confocal microscopy in order to detect the basic and stimulated expression of the receptor. Activated cells were fixed 4 hours after incubation with TNF-α as it was reported that E-selectin expression was maximal after 4 hours of activation [16].

High fluorescence could be observed in the level of the membrane of TNF-α-activated HUVECs (Figure 5, upper panels) while a very weak fluorescence was detected on cells that were not pre-treated with the pro-inflammatory agent (Figure 5, lower panels). The lipophilic dye PKH67 was used to label the cell membrane and thus help to localize the E-selectin staining. This dye did not remain in the plasma membrane but also stained the membranes of intracellular structures. However, it allowed the cell contours to be visualized and did not interfere with the interpretation of E-selectin localization.

Nanoparticles association with HUVECs

Association of nanoparticles with stimulated and non-stimulated HUVECs was observed by laser scanning confocal microscope and quantified by measuring cell-associated fluorescence by spectrofluorimetry.

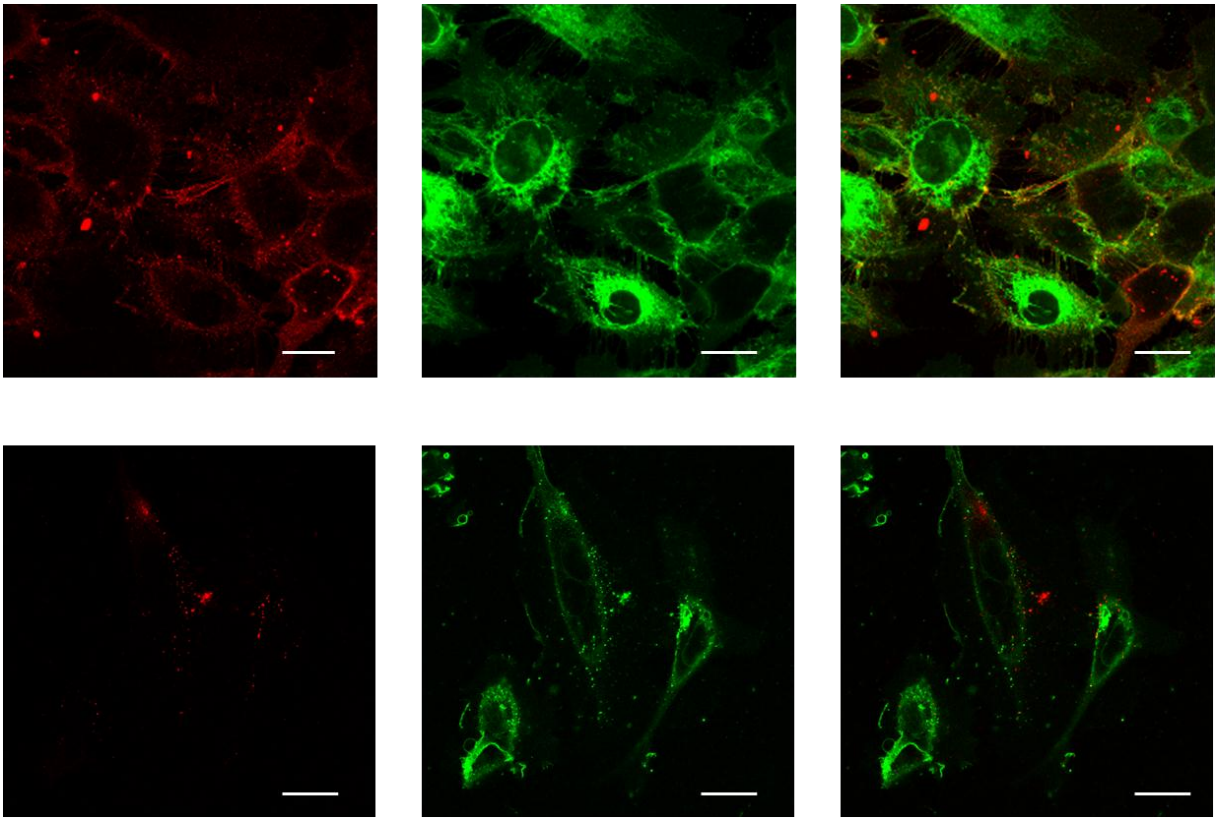

Figure 5: Fluorescence imaging of activated HUVECs (upper panels) and non activated ones (lower panels). The red channel shows E-selectin localization. The green channel shows cellular lipids stained with PKH67. (scale bar 22µm)

Cells were incubated with nanoparticles for different times (30 min, 2 h and 21 h). Figure 6 shows confocal micrographs of the cell monolayers incubated with nanoparticles for 21 h, The fluorescence of TNF-α-activated cells incubated with ligand-bearing nanoparticles was significantly higher than that observed with bare nanoparticles (Figure 6a and 6b), indicating a predominantly selective uptake mediated by E-selectin. Moreover, the fluorescence was mainly distributed through the cytoplasm, as bright red spots. Cells incubated with fluorescently labelled bare nanoparticles displayed only very weak fluorescence that can be attributed to low non specific uptake of the particles. The nuclear area remained non fluorescent in all cases.

Some cell-associated fluorescence was also observed when ligand-carrying nanoparticles were incubated with non activated cells (Figure 6c).

In order to quantify the association of nanoparticles with HUVECs, we measured the cell-associated fluorescence after different times of incubation with nanoparticles.

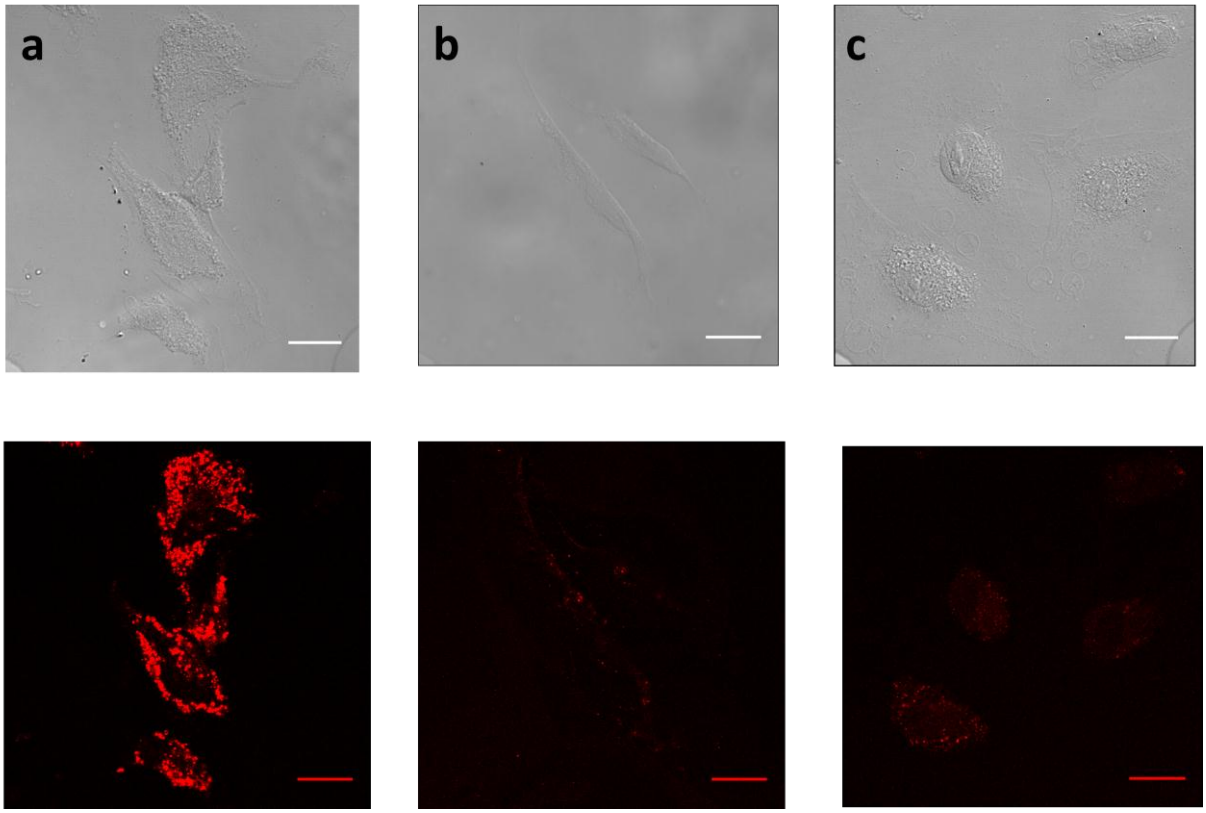

Figure 6: Fluorescence imaging of nanoparticles incubated for 24h with HUVECs in different conditions. Activated cells with ligand-bearing nanoparticles (left panels), activated cells with bare nanoparticles (middle panels) and non-activated cells with ligand nanoparticles (right panels). Differential contrast images (upper panels); red fluorescent channel (lower panels) (scale bar 22µm)

As shown in Figure 7, the association of ligand-bearing nanoparticles by TNF-á-activated HUVECs was higher than that of bare nanoparticles or targeted nanoparticles added to unstimulated HUVECs. For example, after 2h of incubation with ligand-bearing nanoparticles the cellular fluorescence was about 6 times higher than that of cells incubated with bare nanoparticles and 3 times higher than that of non activated cells incubated with ligand-bearing nanoparticles. Association of ligand bearing nanoparticles with non activated cells is the sum of non specific association and the specific association related to the basic levels of E-selectin expression, but this association is still many times lower than the one with activated cell. These results are in agreement with the observations by confocal microscopy. The level of ligand-bearing nanoparticles association with stimulated cells incubated at 4 °C was greatly reduced compared to 37 °C for all incubation times, indicating energy-dependent endocytosis of the functionalized nanoparticles.

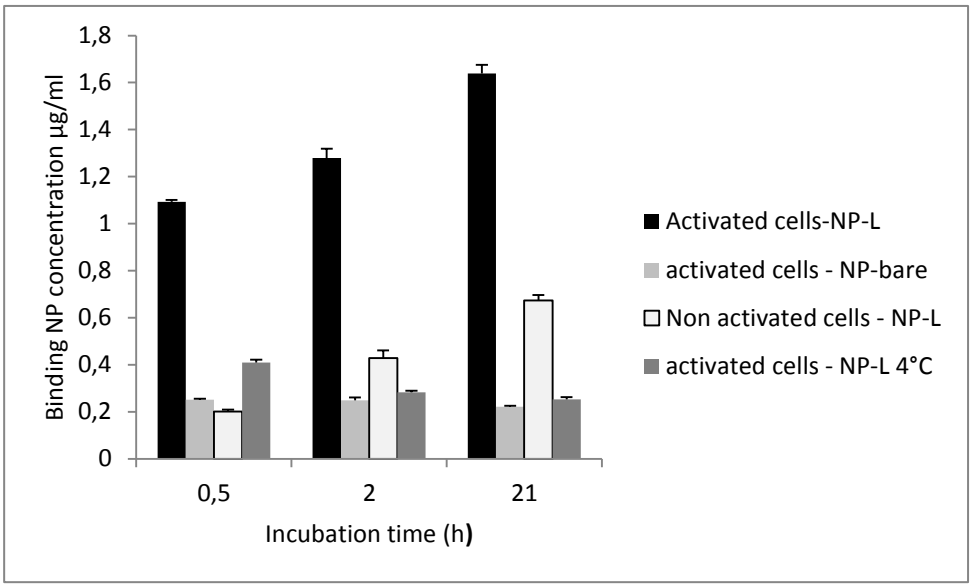

Figure 7: Nanoparticles association with HUVEC under different conditions, measured by spectrofluorimetry as described in Materials and Methods. Mean ± SD (n=3).

When an anti-E-selectin monoclonal antibody was applied prior to incubation with ligand-bearing nanoparticles, the cell associated fluorescence was reduced by about 65% (results not shown). From this result we can conclude that nanoparticles enter cells mainly through an E-selectin-mediated mechanism but that this is not the only mechanism of interaction.

Discussion

The vascular endothelium is a major target for drug delivery systems since these are the first cells in contact with these systems when they are administered by a parenteral route. Among the surface molecules expressed on endothelial cells, E-selectin is an attractive candidate for targeting to treat inflammation [47, 48] and inhibit tumor metastasis[49, 50], as well as for *in vivo* imaging[51-54].

Since up-regulation of this receptor as a result of tissue damage facilitates the recruitment of circulating leukocytes, we hypothesized that nanocarriers functionalized with an analog of SLE^x would allow the carriers to accumulate in these regions.

It has been found that the six functional groups required for E-selectin binding are the 2-, 3- and 4-OH groups of fucose, the 4- and 6-OH groups of galactose and the CO_2- group of NeuAc[55]. Intensive research was done, especially in the 1990s, to synthesize molecules

that could be used as inhibitors of selectin binding and thereby be potential drug candidates for the treatment of inflammatory diseases. Hence libraries of different SLE^x analogs were proposed, including mono, bi, tri or tetrasaccharide-based structures [56, 57]. These molecules are very useful as recognition elements to functionalize drug delivery systems that could carry cargo such as anti-inflammatory drugs, immunomodulators, anti-cancer drugs or imaging agents.

Among these analogs of sialyl Lewis, we have chosen a mannose-based SLE^x analog (Man-glu) developed by Wong et al [36]. This molecule has been successfully used as a recognition element connected directly to nanoparticles surface without a spacer [58]. In this study, the authors showed with docking experiments that the hydroxyl group at the 6-O position of the mannose is not essential for E-selectin-ligand binding; hence this oxygen could be used to connect the molecule to another structure such as a macromolecular chain from a drug delivery system.

In a previous report we demonstrated that nanoparticles prepared from an amphiphilic copolymer with a similar structure to the one used here (glucose at the extremity of a hydrophilic PEG chain) can adopt an appropriate conformation in water where the sugar moieties are present on the surface and accessible to interact with a neighboring protein. In the present work we used the same strategy of synthesis to conjugate the Man-glu ligand to a PEG chain bearing a methacrylic monomer (PEGMA), so that the PEG chain would become a spacer, both allowing better molecular recognition and rendering the nanoparticle surface hydrophilic.

The reaction between the azide- and acetylene-derivatized precursors could be carried out under mild conditions in a highly specific way with a good yield without affecting the methacrylate double bond. A combination of ATRP and ROP using a single bifunctional initiator allowed us to construct a well-defined amphiphilic block polymer. ATRP conditions have been modified to polymerize the Man-glu-Bz-conjugated monomer, and to deprotect benzyl groups with a good yield.

In this way, a functionalized copolymer, a nonfunctionalized copolymer and a fluorescent copolymer with homologous structures were synthesized. Mixtures with different ratios of these copolymers can be used to prepare nanoparticles with varying surface ligand density, and varying fluorescence intensities. The use of copolymers with pre-conjugated ligand allows control of the ligand density on the nanoparticles surface, which is more difficult when methods of post-functionalization of pre-formed nanoparticles are used. It also ensures

that the copper ions necessary for the click chemistry reaction are absent from the final preparation.

Man-glu-OH-functionalized nanoparticles did not display significant cytotoxicity to endothelial cells over a large range of nanoparticles concentrations, suggesting that they could be safely administered by the IV route.

Endothelial cells have only low expression of E-selectin in normal physiological condition, but this expression is strongly up-regulated by factors such as TNF-α, IL-1 and LPS.

Functionalized nanoparticles, in contrast to the non functionalized ones, were effectively internalized by the cells and this cell association was enhanced upon activation of HUVECs with TNF-α. This result confirms the specific binding properties of these nanoparticles which make them a very good drug targeting system. 65% of association was inhibited by pretreatment with anti-E-selectin antibody. These results suggest that our nanoparticles enter cells mainly by an E-selectin-mediated route. In fact the ligand used in this work may also interact with P-selectin[58] which was not blocked by the specific anti E-selectin antibody. The nanoparticles used here are negatively charged and it has been reported that negatively charged carriers can limit nonspecific adsorption with endothelial cells that are also negatively charged[59, 60], which could explain the low uptake of non functionalized nanoparticles.

These findings suggest that this type of system could have the double advantage of limiting immune cell adhesion by occupying their receptors on one hand and by concentrating an encapsulated drug in sites where the receptor is highly expressed.

Conclusion

Leukocyte-endothelial cells adhesion mechanisms were exploited to target biodegradable nanoparticles. We have used macromolecular chemistry techniques to construct a well-defined amphiphilic block polymer that was successfully used to prepare spherical nanoparticles using a simple nanoprecipitation method without any surfactant. These nanoparticles did not display significant cytotoxicity to endothelial cells.

Coupling of a sialyl Lewis X analog onto the surface of nanoparticles allowed efficient targeting of human endothelial cells overexpressing E-selectin with subsequent internalization by the cells.

These results suggest that such targeting systems could have the double action of inhibiting leukocyte infiltration into tissues beneath activated endothelium (since the receptor

would be already occupied by particles), with the ability to concentrate a drug encapsulated within these particles within the targeted tissue.

The next steps will be to evaluate interaction of these nanoparticles *in vitro* with serum proteins as an indicator of their ability to avoid uptake by the reticuloendothelial system. Their loading with an anti-inflammatory drug and their *in vivo* fate after intravenous administration will also be evaluated.

Supporting Information Available. Supplementary experimental details and figures are available including: the scheme of synthesis of (**6**) (Scheme S1), ^{1}H- NMR spectra of (**4**) (Figure S1), (**6**) (figure S2), (**7**) (figure S3), infra-red spectra of (**5**) and (**6**) (Figure S5), SEC chromatograms of (**1**), (**5**) and (**7**) (Figure S4), SEC chromatograms of (**1**) and (**6**) (Figure S6), fluorescence spectrum of (**8**) (Figure S7) and fluorescence spectra of nanoparticles prepared from polymers (**7**) and (**8**) (Figure S8). This material is available free of charge via the Internet at HTTP://pubs.acs.org

Acknowledgements

The authors wish to thank Dr. Didier Desmaele (UMR CNRS 8076 Université Paris-Sud 11, France) for help in the deprotection of benzyl groups and Dr. Catherine Le Visage (Inserm U698 for supplying HUVECs. This work was supported by CNRS (programme: INTERFACE Physique-Chimie Biologie: aide à la prise de risque).

References and notes

[1] I. Brigger, C. Dubernet, P. Couvreur, Nanoparticles in cancer therapy and diagnosis. Adv Drug Deliv Rev 54(5) (2002) 631-651.

[2] R. Gref, Y. Minamitake, M.T. Peracchia, A. Domb, V. Trubetskoy, V. Torchilin, R. Langer, Poly(ethylene glycol)-coated nanospheres: potential carriers for intravenous drug administration. Pharm Biotechnol 10 (1997) 167-198.

[3] R. Gref, P. Quellec, A. Sanchez, P. Calvo, E. Dellacherie, M.J. Alonso, Development and characterization of CyA-loaded poly(lactic acid)-poly(ethylene glycol)PEG micro- and nanoparticles. Comparison with conventional PLA particulate carriers. Eur J Pharm Biopharm 51(2) (2001) 111-118.

[4] C. Passirani, G. Barratt, J.P. Devissaguet, D. Labarre, Long-circulating nanoparticles bearing heparin or dextran covalently bound to poly(methyl methacrylate). Pharm Res 15(7) (1998) 1046-1050.

[5] C. Chauvierre, D. Labarre, P. Couvreur, C. Vauthier, Novel polysaccharide-decorated poly(isobutyl cyanoacrylate) nanoparticles. Pharm Res 20(11) (2003) 1786-1793.

[6] G. Bendas, A. Krause, U. Bakowsky, J. Vogel, U. Rothe, Targetability of novel immunoliposomes prepared by a new antibody conjugation technique. International Journal of Pharmaceutics 181(1) (1999) 79-93.

[7] M. Everts, G.A. Koning, R.J. Kok, S.A. Ásgeirsdóttir, D. Vestweber, D.K.F. Meijer, G. Storm, G. Molema, *In Vitro* Cellular Handling and *in Vivo* Targeting of E-Selectin-Directed Immunoconjugates and Immunoliposomes Used for Drug Delivery to Inflamed Endothelium. Pharmaceutical Research 20(1) (2003) 64-72.

[8] H.W. Kang, L. Josephson, A. Petrovsky, R. Weissleder, A. Bogdanov, Magnetic Resonance Imaging of Inducible E-Selectin Expression in Human Endothelial Cell Culture. Bioconjugate Chemistry 13(1) (2002) 122-127.

[9] H.W. Kang, R. Weissleder, A. Bogdanov, Jr., Targeting of MPEG-protected polyamino acid carrier to human E-selectin *in vitro*. Amino Acids 23(1-3) (2002) 301-308.

[10] Y. Shamay, D. Paulin, G. Ashkenasy, A. David, Multivalent display of quinic acid based ligands for targeting E-selectin expressing cells. J Med Chem 52(19) (2009) 5906-5915.

[11] A.H. Myrset, H.B. Fjerdingstad, R. Bendiksen, B.E. Arbo, R.M. Bjerke, J.H. Johansen, M.A. Kulseth, R. Skurtveit, Design and Characterization of Targeted Ultrasound Microbubbles for Diagnostic Use. Ultrasound in Medicine & Biology 37(1) (2011) 136-150.

[12] N. Zhang, C. Chittasupho, C. Duangrat, T.J. Siahaan, C. Berkland, PLGA nanoparticle--peptide conjugate effectively targets intercellular cell-adhesion molecule-1. Bioconjug Chem 19(1) (2008) 145-152.

[13] B. Stella, V. Marsaud, S. Arpicco, G. Geraud, L. Cattel, P. Couvreur, J.M. Renoir, Biological characterization of folic acid-conjugated poly(H2NPEGCA-co-HDCA) nanoparticles in cellular models. J Drug Target 15(2) (2007) 146-153.

[14] J. Wang, W. Liu, Q. Tu, N. Song, Y. Zhang, N. Nie, Folate-decorated hybrid polymeric nanoparticles for chemically and physically combined Paclitaxel loading and targeted delivery. Biomacromolecules 12(1) 228-234.

[15] C. Kneuer, C. Ehrhardt, M.W. Radomski, U. Bakowsky, Selectins - potential pharmacological targets? Drug Discov Today 11(21-22) (2006) 1034-1040.

[16] M.P. Bevilacqua, S. Stengelin, M.A. Gimbrone, Jr., B. Seed, Endothelial leukocyte adhesion molecule 1: an inducible receptor for neutrophils related to complement regulatory proteins and lectins. Science 243(4895) (1989) 1160-1165.

[17] K.F. Montgomery, L. Osborn, C. Hession, R. Tizard, D. Goff, C. Vassallo, P.I. Tarr, K. Bomsztyk, R. Lobb, J.M. Harlan, et al., Activation of endothelial-leukocyte adhesion molecule 1 (ELAM-1) gene transcription. Proc Natl Acad Sci U S A 88(15) (1991) 6523-6527.

[18] E.J. von Asmuth, E.F. Smeets, L.A. Ginsel, J.J. Onderwater, J.F. Leeuwenberg, W.A. Buurman, Evidence for endocytosis of E-selectin in human endothelial cells. Eur J Immunol 22(10) (1992) 2519-2526.

[19] M.L. Phillips, E. Nudelman, F.C. Gaeta, M. Perez, A.K. Singhal, S. Hakomori, J.C. Paulson, ELAM-1 mediates cell adhesion by recognition of a carbohydrate ligand, sialyl-Lex. Science 250(4984) (1990) 1130-1132.

[20] G. Walz, A. Aruffo, W. Kolanus, M. Bevilacqua, B. Seed, Recognition by ELAM-1 of the sialyl-Lex determinant on myeloid and tumor cells. Science 250(4984) (1990) 1132-1135.

[21] S.A. Asgeirsdottir, P.J. Zwiers, H.W. Morselt, H.E. Moorlag, H.I. Bakker, P. Heeringa, J.W. Kok, C.G.M. Kallenberg, G. Molema, J.A.A.M. Kamps, Inhibition of proinflammatory genes in anti-GBM glomerulonephritis by targeted dexamethasone-loaded AbEsel liposomes. Am J Physiol Renal Physiol 294(3) (2008) F554-561.

[22] C. Pattillo, B. Venegas, F. Donelson, L. Del Valle, L. Knight, P. Chong, M. Kiani, Radiation-Guided Targeting of Combretastatin Encapsulated Immunoliposomes to Mammary Tumors. Pharmaceutical Research 26(5) (2009) 1093-1100.

[23] J. Minaguchi, T. Oohashi, K. Inagawa, A. Ohtsuka, Y. Ninomiya, Transvascular accumulation of Sialyl Lewis X conjugated liposome in inflamed joints of collagen antibody-induced arthritic (CAIA) mice. Arch Histol Cytol 71(3) (2008) 195-203.

[24] R. Stahn, C. Grittner, R. Zeisig, U. Karsten, S.B. Felix, K. Wenzel, Sialyl Lewis(x)-liposomes as vehicles for site-directed, E-selectin-mediated drug transfer into activated endothelial cells. Cell Mol Life Sci 58(1) (2001) 141-147.

[25] S.I. van Kasteren, S.J. Campbell, S. Serres, D.C. Anthony, N.R. Sibson, B.G. Davis, Glyconanoparticles allow pre-symptomatic *in vivo* imaging of brain disease. Proc Natl Acad Sci U S A 106(1) (2009) 18-23.

[26] Y.C. Lee, R.T. Lee, Carbohydrate-Protein Interactions: Basis of Glycobiology. Accounts of Chemical Research 28(8) (1995) 321-327.

[27] J.J. Lundquist, E.J. Toone, The Cluster Glycoside Effect. Chemical Reviews 102(2) (2002) 555-578.

[28] R. Wikaningrum, J. Highton, A. Parker, M. Coleman, P.A. Hessian, P.J. Roberts-Thompson, M.J. Ahern, M.D. Smith, Pathogenic mechanisms in the rheumatoid nodule: comparison of proinflammatory cytokine production and cell adhesion molecule expression in rheumatoid nodules and synovial membranes from the same patient. Arthritis Rheum 41(10) (1998) 1783-1797.

[29] J. Kriegsmann, G.M. Keyszer, T. Geiler, A.S. Lagoo, S. Lagoo-Deenadayalan, R.E. Gay, S. Gay, Expression of E-selectin messenger RNA and protein in rheumatoid arthritis. Arthritis Rheum 38(6) (1995) 750-754.

[30] D.H. Adams, S.G. Hubscher, N.C. Fisher, A. Williams, M. Robinson, Expression of E-selectin and E-selectin ligands in human liver inflammation. Hepatology 24(3) (1996) 533-538.

[31] N. Hashida, N. Ohguro, N. Yamazaki, Y. Arakawa, E. Oiki, H. Mashimo, N. Kurokawa, Y. Tano, High-efficacy site-directed drug delivery system using sialyl-Lewis X conjugated liposome. Experimental Eye Research 86(1) (2008) 138-149.

[32] K. Kiriyama, C. Ye, [E-selectin expression in serum and tissue correlates with distant metastasis of colorectal cancer]. Nippon Rinsho 53(7) (1995) 1760-1764.

[33] B. Mayer, H. Spatz, I. Funke, J.P. Johnson, F.W. Schildberg, De novo expression of the cell adhesion molecule E-selectin on gastric cancer endothelium. Langenbecks Arch Surg 383(1) (1998) 81-86.

[34] J. Renkonen, A. Makitie, T. Paavonen, R. Renkonen, Sialyl-Lewis(x/a)-decorated selectin ligands in head and neck tumours. J Cancer Res Clin Oncol 125(10) (1999) 569-576.

[35] M. Nguyen, C.L. Corless, B.M. Kraling, C. Tran, T. Atha, J. Bischoff, S.H. Barsky, Vascular expression of E-selectin is increased in estrogen-receptor-negative breast cancer: a role for tumor-cell-secreted interleukin-1 alpha. Am J Pathol 150(4) (1997) 1307-1314.

[36] C.-H. Wong, F. Moris-Varas, S.-C. Hung, T.G. Marron, C.-C. Lin, K.W. Gong, G. Weitz-Schmidt, Small Molecules as Structural and Functional Mimics of Sialyl Lewis X Tetrasaccharide in Selectin Inhibition: A Remarkable Enhancement of Inhibition by Additional Negative Charge and/or Hydrophobic Group. Journal of the American Chemical Society 119(35) (1997) 8152-8158.

[37] G. Weitz-Schmidt, D. Stokmaier, G. Scheel, N.E. Nifant'ev, A.B. Tuzikov, N.V. Bovin, An E-selectin binding assay based on a polyacrylamide-type glycoconjugate. Anal Biochem 238(2) (1996) 184-190.

[38] M.M. Ali, H.D.H. Stover, Well-Defined Amphiphilic Thermosensitive Copolymers Based on Poly(ethylene glycol monomethacrylate) and Methyl Methacrylate Prepared by Atom Transfer Radical Polymerization. Macromolecules 37(14) (2004) 5219-5227.

[39] E. Jubeli, L. Moine, G. Barratt, Synthesis, characterization, and molecular recognition of sugar-functionalized nanoparticles prepared by a combination of ROP, ATRP, and click chemistry. Journal of Polymer Science Part A: Polymer Chemistry 48(14) 3178-3187.

[40] J.L. Hedrick, M. Trollsas, C.J. Hawker, B. Atthoff, H. Claesson, A. Heise, R.D. Miller, D. Mecerreyes, R. Jerome, P. Dubois, Dendrimer-like Star Block and Amphiphilic Copolymers by Combination of Ring Opening and Atom Transfer Radical Polymerization. Macromolecules 31(25) (1998) 8691-8705.

[41] W. Yuan, J. Yuan, S. Zheng, X. Hong, Synthesis, characterization, and controllable drug release of dendritic star-block copolymer by ring-opening polymerization and atom transfer radical polymerization. Polymer 48(9) (2007) 2585-2594.

[42] F.F. Wolf, N. Friedemann, H. Frey, Poly(lactide)-block-Poly(HEMA) Block Copolymers: An Orthogonal One-Pot Combination of ROP and ATRP, Using a Bifunctional Initiator. Macromolecules 42(15) (2009) 5622-5628.

[43] X.-H. Dai, C.-M. Dong, Synthesis, self-assembly and recognition properties of biomimetic star-shaped poly(ε-caprolactone)-b-glycopolymer block copolymers. Journal of Polymer Science Part A: Polymer Chemistry 46(3) (2008) 817-829.

[44] S. Qiu, H. Huang, X.-H. Dai, W. Zhou, C.-M. Dong, Star-shaped polypeptide/glycopolymer biohybrids: Synthesis, self-assembly, biomolecular recognition, and controlled drug release behavior. Journal of Polymer Science Part A: Polymer Chemistry 47(8) (2009) 2009-2023.

[45] R. Gref, M. Luck, P. Quellec, M. Marchand, E. Dellacherie, S. Harnisch, T. Blunk, R.H. Muller, 'Stealth' corona-core nanoparticles surface modified by polyethylene glycol (PEG): influences of the corona (PEG chain length and surface density) and of the core composition on phagocytic uptake and plasma protein adsorption. Colloids Surf B Biointerfaces 18(3-4) (2000) 301-313.

[46] D. Brambilla, J. Nicolas, B. Le Droumaguet, K. Andrieux, V. Marsaud, P.-O. Couraud, P. Couvreur, Design of fluorescently tagged poly(alkyl cyanoacrylate) nanoparticles for human brain endothelial cell imaging. Chemical Communications 46(15) (2010) 2602-2604.

[47] M. Everts, R.J. Kok, S.A. Asgeirsdottir, B.N. Melgert, T.J. Moolenaar, G.A. Koning, M.J. van Luyn, D.K. Meijer, G. Molema, Selective intracellular delivery of dexamethasone into activated endothelial cells using an E-selectin-directed immunoconjugate. J Immunol 168(2) (2002) 883-889.

[48] R.J. Kok, M. Everts, S.A. Asgeirsdottir, D.K. Meijer, G. Molema, Cellular handling of a dexamethasone-anti-E-selectin immunoconjugate by activated endothelial cells: comparison with free dexamethasone. Pharm Res 19(11) (2002) 1730-1735.

[49] R. Zeisig, R. Stahn, K. Wenzel, D. Behrens, I. Fichtner, Effect of sialyl Lewis X-glycoliposomes on the inhibition of E-selectin-mediated tumour cell adhesion *in vitro*. Biochim Biophys Acta 1660(1-2) (2004) 31-40.

[50] R. Stahn, H. Schafer, F. Kernchen, J. Schreiber, Multivalent sialyl Lewis x ligands of definite structures as inhibitors of E-selectin mediated cell adhesion. Glycobiology 8(4) (1998) 311-319.

[51] F. Jamar, P.T. Chapman, A.A. Harrison, R.M. Binns, D.O. Haskard, A.M. Peters, Inflammatory arthritis: imaging of endothelial cell activation with an indium-111-labeled F(ab')2 fragment of anti-E-selectin monoclonal antibody. Radiology 194(3) (1995) 843-850.

[52] P.A. Barber, T. Foniok, D. Kirk, A.M. Buchan, S. Laurent, S. Boutry, R.N. Muller, L. Hoyte, B. Tomanek, U.I. Tuor, MR molecular imaging of early endothelial activation in focal ischemia. Ann Neurol 56(1) (2004) 116-120.

[53] W. Tsuruta, H. Tsurushima, T. Yamamoto, K. Suzuki, N. Yamazaki, A. Matsumura, Application of liposomes incorporating doxorubicin with sialyl Lewis X to prevent stenosis after rat carotid artery injury. Biomaterials 30(1) (2009) 118-125.

[54] T. Garrood, M. Blades, D.O. Haskard, S. Mather, C. Pitzalis, A novel model for the pre-clinical imaging of inflamed human synovial vasculature. Rheumatology (Oxford) 48(8) (2009) 926-931.

[55] R. Wang, C.-H. Wong, Synthesis of sialyl Lewis X mimetics: Use of O-[alpha]-fucosyl-(1R, 2R)-2-aminocyclohexanol as core structure. Tetrahedron Letters 37(31) (1996) 5427-5430.

[56] E.E. Simanek, G.J. McGarvey, J.A. Jablonowski, C.H. Wong, ChemInform Abstract: Selectin—Carbohydrate Interactions: From Natural Ligands to Designed Mimics. ChemInform 29(25) (1998).

[57] N. Kaila, B.E.t. Thomas, Design and synthesis of sialyl Lewis(x) mimics as E- and P-selectin inhibitors. Med Res Rev 22(6) (2002) 566-601.

[58] X. Banquy, G.g. Leclair, J.-M. Rabanel, A. Argaw, J.-F.o. Bouchard, P. Hildgen, S. Giasson, Selectins Ligand Decorated Drug Carriers for Activated Endothelial Cell Targeting. Bioconjugate Chemistry 19(10) (2008) 2030-2039.

[59] M. Hirai, H. Minematsu, N. Kondo, K. Oie, K. Igarashi, N. Yamazaki, Accumulation of liposome with Sialyl Lewis X to inflammation and tumor region: Application to *in vivo* bio-imaging. Biochemical and Biophysical Research Communications 353(3) (2007) 553-558.

[60] M. Hirai, H. Minematsu, Y. Hiramatsu, H. Kitagawa, T. Otani, S. Iwashita, T. Kudoh, L. Chen, Y. Li, M. Okada, D.S. Salomon, K. Igarashi, M. Chikuma, M. Seno, Novel and simple loading procedure of cisplatin into liposomes and targeting tumor endothelial cells. International Journal of Pharmaceutics 391(1-2) (2010) 274-283.

Supporting information for "Preparation of E-selectin-targeting nanoparticles and preliminary *in vitro* evaluation"

Emile Jubeli[1], Laurence Moine[1]* Valérie Nicolas[2] and Gillian Barratt[1]

Université Paris-Sud11, Faculté de Pharmacie 5 rue J.B. Clément CHATENAY-MALABRY FR 92296 [1]UMR 8612 CNRS, IFR 141, [2] Plat Form d'Imagerie Cellulaire IFR141, France

Submitted to *Bioconjugates chemistry*

* To whom correspondence should be addressed: Tel: +33 1 46 83 59 94 ; Fax: +33 1 46 83 53 12 ; e-mail: Laurence.moine@u-psud.fr

Keywords : Nanoparticles, E-selectin, HUVECs, targeting, Carbohydrate ligand

Supporting information for "Preparation of E-selectin-targeting nanoparticles and preliminary *in vitro* evaluation"

Emile Jubeli[1], Laurence Moine[1]* Valérie Nicolas[2] and Gillian Barratt[1]

Université Paris-Sud11, Faculté de Pharmacie 5 rue J.B. Clément CHATENAY-MALABRY FR 92296 [1]UMR 8612 CNRS, IFR 141, [2] PlateForme d'Imagerie Cellulaire IFR141, France

* To whom correspondence should be addressed: Tel: +33 1 46 83 59 94 ; Fax: +33 1 46 83 53 12 ; e-mail: Laurence.moine@u-psud.fr

Synthesis of the bifunctional initiator

β-hydroxyl ethyl α-bromoisobutyrate [HEBIB] was synthesized according to a procedure reported in the literature [(1, 2)]. It was obtained as a colorless liquid with a yield of 60 %.

^{1}H-NMR (300MHz, $CDCl_3$, δ ppm): 1.96 (6H, $BrC(C\mathbf{H}_3)_2$-), 3.95 (2H, $C\mathbf{H}_2$-CH_2-OH), 4.15 (2H, $C\mathbf{H}_2$-CH_2-OH).

Synthesis of PLA-block- PEGMMA by ATRP (7)

PLA (**1**) (0.96g; 0.03mmol), PEGMMA (0.2 g; 0.1mmol), CuBr (9.5mg; 0.06mmol), PMDETA (11mg; 0.06mmol) were introduced to a schlenk tube with 4 ml of anisole. After three freeze-thaw cycles the schlenk tube was placed in a thermostated oil bath at 60 °C and stirred for

6h. The content was then purified by column chromatography with CH_2Cl_2/methanol (9:1) to remove the copper complex. After precipitation by adding polymer solution in chloroform to a cold mixture of petroleum ether/ diethyl ether (1:1), the product was dried in a vacuum oven at 40°C to yield 83%.^{1}H-NMR (300MHz, $CDCl_3$, δ ppm): 0.75-1 (-C**H$_2$-** main chain of PEGMA), 1.55 (3H, C**H$_3$**), 3.3 (3H, -OC**H**$_3$), 3.61 (36H, -C**H$_2$**- of PEG), 4.05 (2H, -C**H$_2$**-COO), 5.2 (1H, -C**H** main chain). Mn_{NMR}= 36000, Mn_{SEC} = 44600, Mw/Mn=1.14.

Synthesis of PLA-PEGMMA-Rhod by ATRP (8)

PLA (**1**) (0.5g; 0.02mmol), PEGMMA (0.12 g; 0.4mmol), methacryloxyethyl thiocarbamoyl rhodamine B (2.7mg, 0,004mmol), CuBr (5.72mg; 0.04mmol), PMDETA (6.9mg; 0.04mmol) were introduced to a schlenk tube with 4 ml of anisole. After three freeze-thaw cycles, the schlenk tube was placed in a thermostated oil bath at 60 °C and stirred for 6h. The content was then purified by column chromatography with CH_2Cl_2/methanol (9:1) to remove the copper complex. After precipitation by adding polymer solution in chloroform to a cold mixture of petroleum ether/ diethyl ether (1:1), the product was dried in a vacuum oven at 40°C to yield 56%. ^{1}H-NMR (300MHz, $CDCl_3$, δ ppm): 0.8-1 (-C**H$_2$-** main chain of PEGMA), 1.58 (3H, C**H$_3$**), 3.4 (3H, -OC**H**$_3$), 3.65 (36H, -C**H$_2$**- of PEG), 4.1 (2H, -C**H$_2$**-COO), 5.2 (1H, -C**H** main chain). Mn_{NMR}= 28000, Mn_{SEC} = 28900, Mw/Mn=1.12.

Results of synthesis and characterization of polymers (7) and (8)

The primary nature of the hydroxyl group and the tertiary α-carboxyl halogenide of the bifunctional initiator used ensure fast initiation for both ROP and ATRP.

PLA-block-PEGMMA (**7**) was first synthesized as a control for the preparation of PEGylated nanoparticles without ligand molecules on their surface. Characterizations by ^{1}H

NMR and SEC (Figures S3 and S4) show that a block copolymer with a narrow polydispersity index (1.14) was efficiently prepared

To prepare fluorescent nanoparticles, we chose the strategy of inserting covalently linked fluorescent units into the backbone of the polymer, rather than incorporating a lipophilic fluoresent dye within the nanoparticles. That was to avoid technical problems and inaccurate interpretation of fluorescence measurements that could be caused by the release of the dye from nanoparticles, as has been highlighted in the literature[(3)]. To synthesize PLA-block-PEGMMA-Rhod (**8**), the fluorophore was incorporated during the synthesis of the amphiphilic copolymer using a small amount of a rhodaminated derivative of methacrylate that could be inserted randomly into the methacrylate chain [(4)]. The polymerization of (**8**) was followed by ^{1}H-NMR and SEC as for the synthesis of (**7**).

References

(1). Jayachandran, K. N.; Takacs-Cox, A.; Brooks, D. E., Synthesis and Characterization of Polymer Brushes of Poly(N,N-dimethylacrylamide) from Polystyrene Latex by Aqueous Atom Transfer Radical Polymerization. *Macromolecules* **2002,** 35, (11), 4247-4257.

(2). Wojciech Jakubowski, J.-F. L. S. S. K. M., Block and random copolymers as surfactants for dispersion polymerization. I. Synthesis via atom transfer radical polymerization and ring-opening polymerization. *Journal of Polymer Science Part A: Polymer Chemistry* **2005,** 43, (7), 1498-1510.

(3). Xu, P.; Gullotti, E.; Tong, L.; Highley, C. B.; Errabelli, D. R.; Hasan, T.; Cheng, J.-X.; Kohane, D. S.; Yeo, Y., Intracellular Drug Delivery by Poly(lactic-co-glycolic acid) Nanoparticles, Revisited. *Molecular Pharmaceutics* **2008,** 6, (1), 190-201.

(4). Brambilla, D.; Nicolas, J.; Le Droumaguet, B.; Andrieux, K.; Marsaud, V.; Couraud, P.-O.; Couvreur, P., Design of fluorescently tagged poly(alkyl cyanoacrylate) nanoparticles for human brain endothelial cell imaging. *Chemical Communications***2010** 46, (15), 2602-2604.

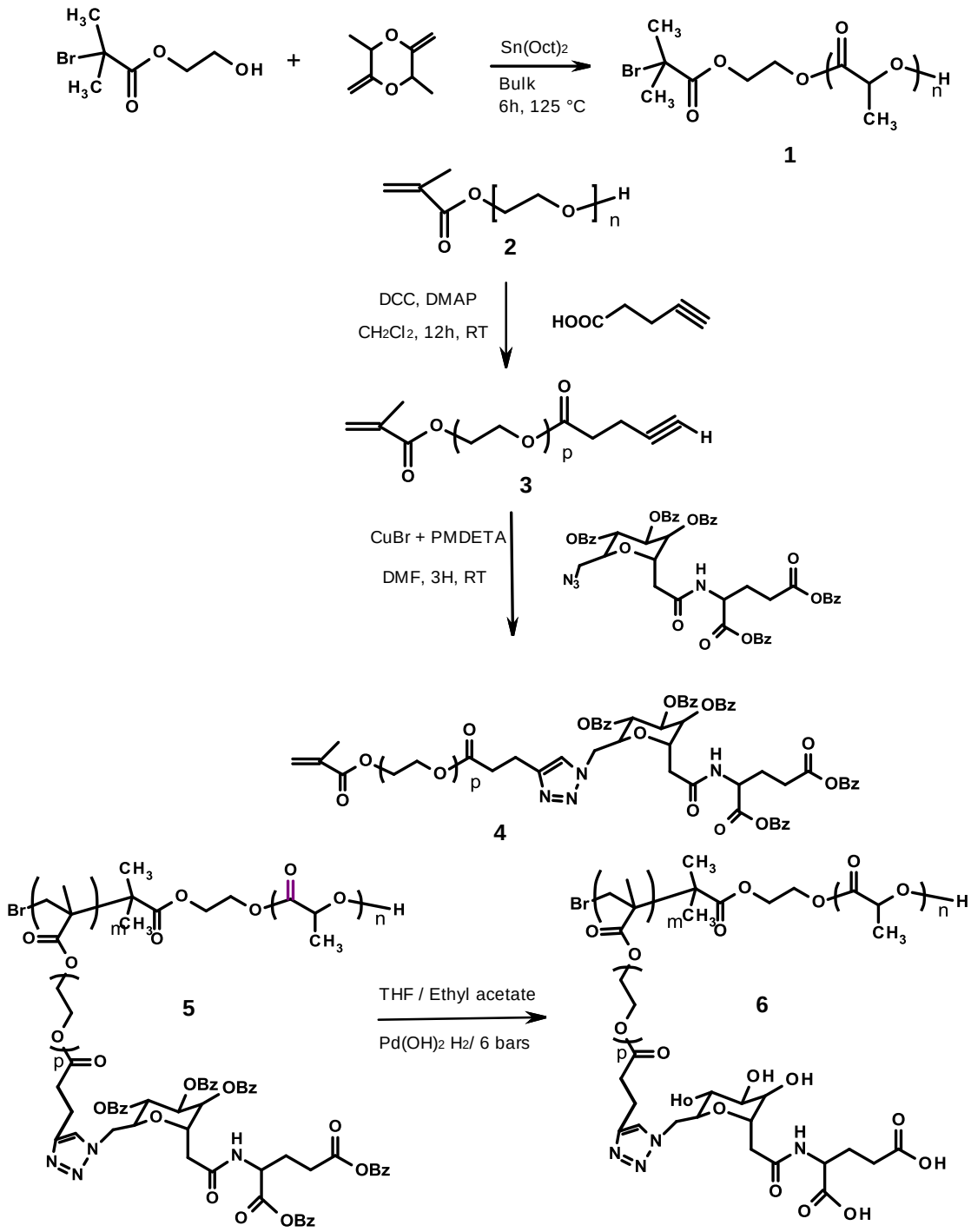
Sn(Oct)2
Bulk
6h, 125 °C
1
2
DCC, DMAP
CH2Cl2, 12h, RT
HOOC
3
CuBr + PMDETA
DMF, 3H, RT
4
5
THF / Ethyl acetate
Pd(OH)2 H2/ 6 bars
6

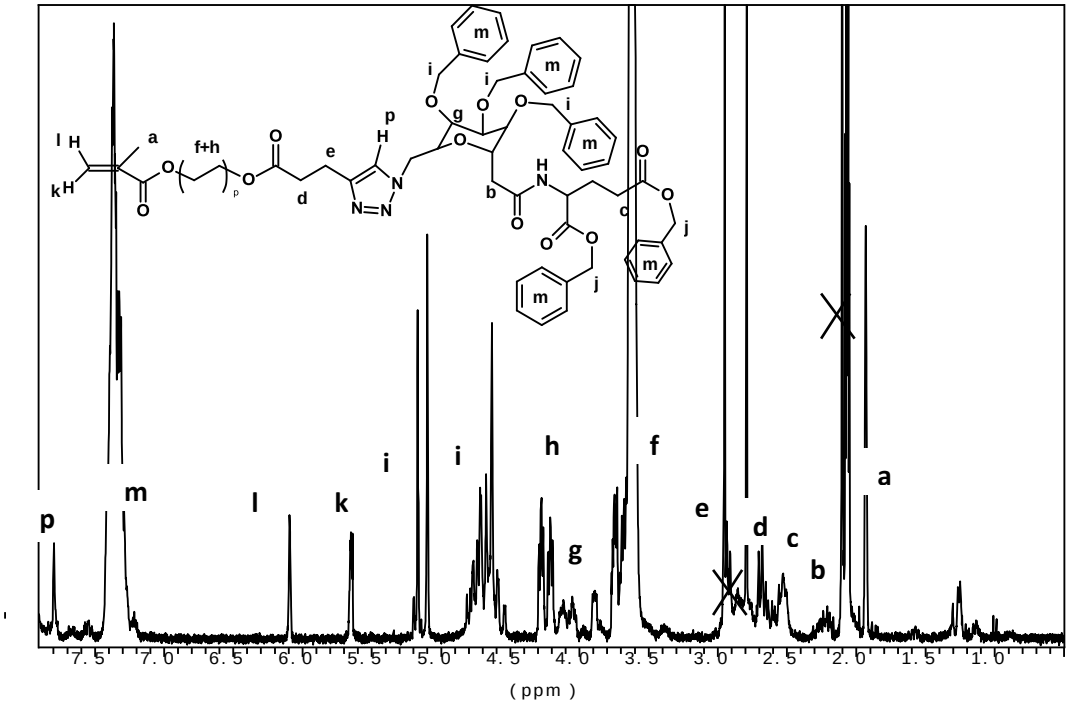

Figure S1: ^{1}H-NMR spectrum of PEGMA-Man-glu-Bz (**4**)

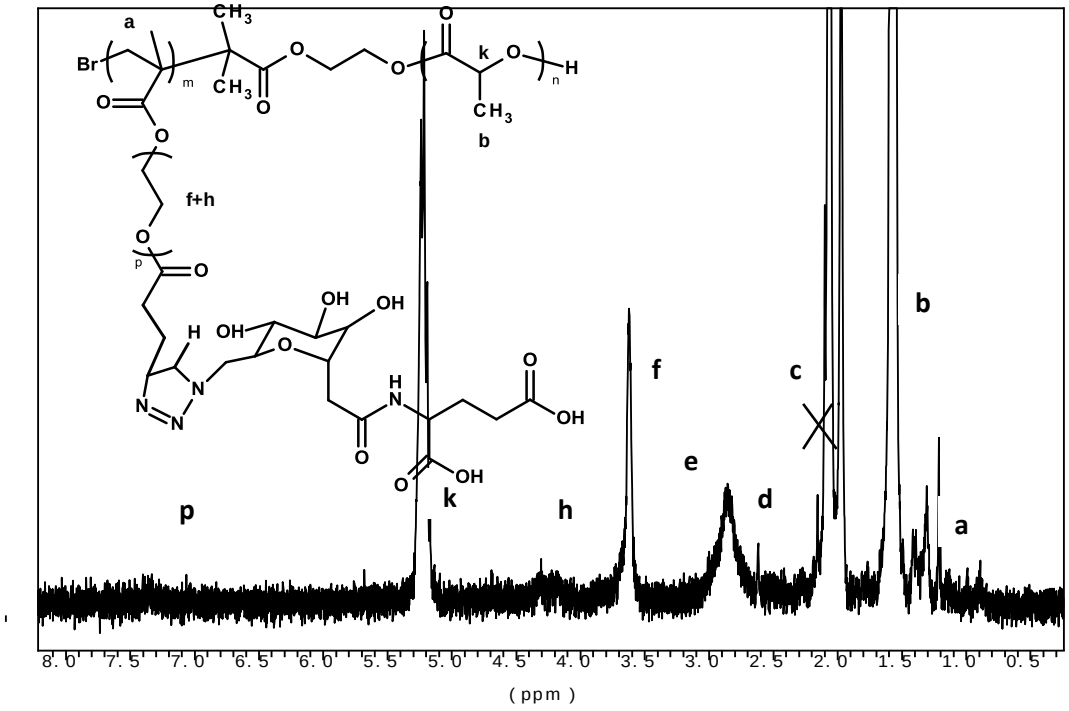

Figure S2: ^{1}H-NMR spectrum of PLA-PEGMA-Man-glu-OH (**6**)

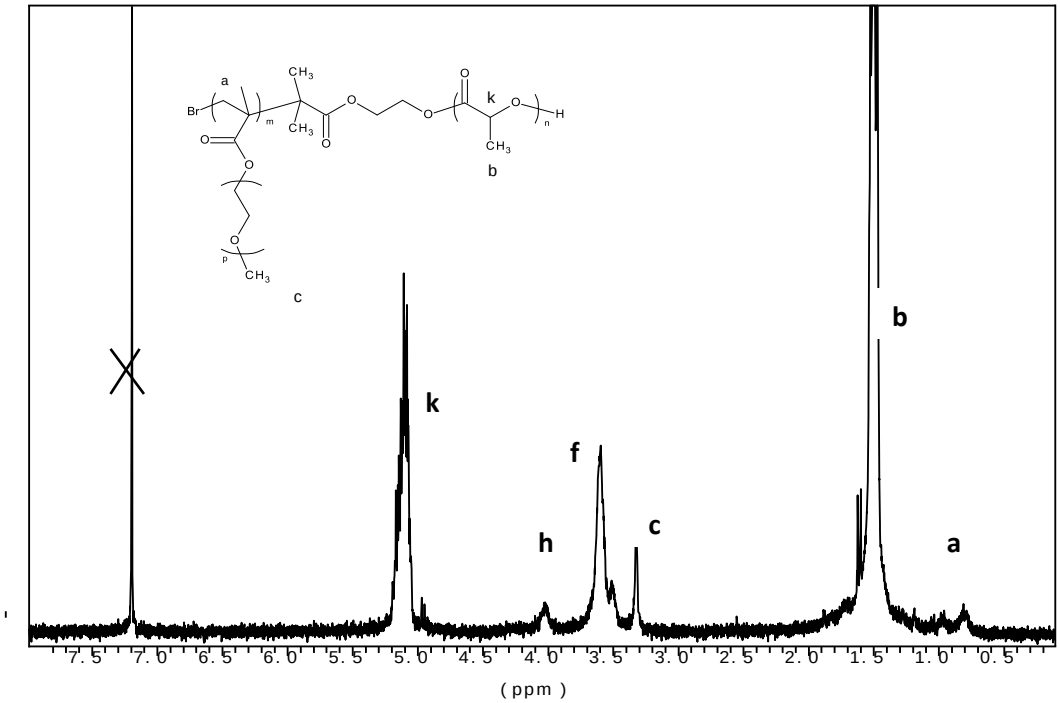

Figure S3. ^{1}H-NMR spectrum of PLA-PEGMMA (**7**)

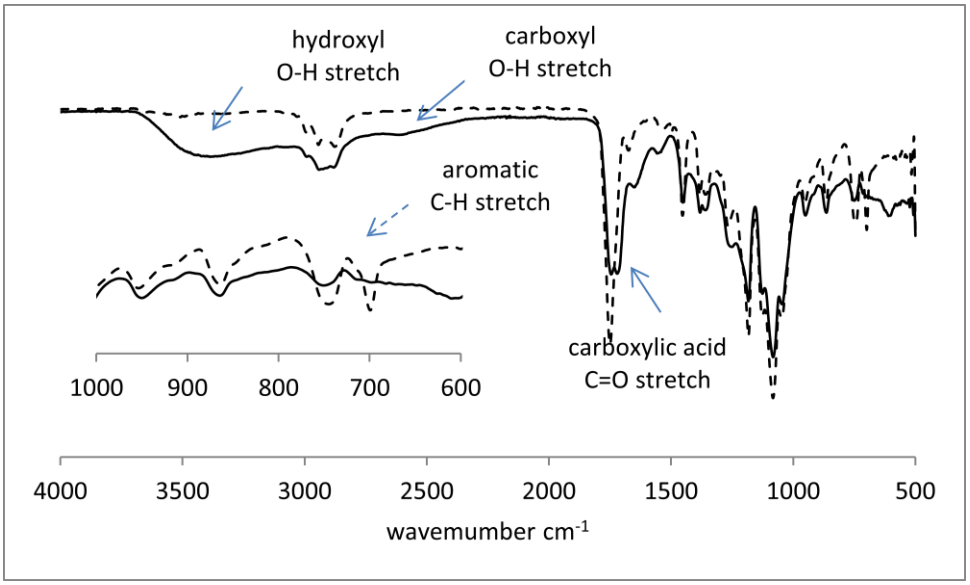

Figure S5 FT-IR of protected (discontinuous line) and deprotected PLA-PEGMA-Man-glu-OH (continuous line)

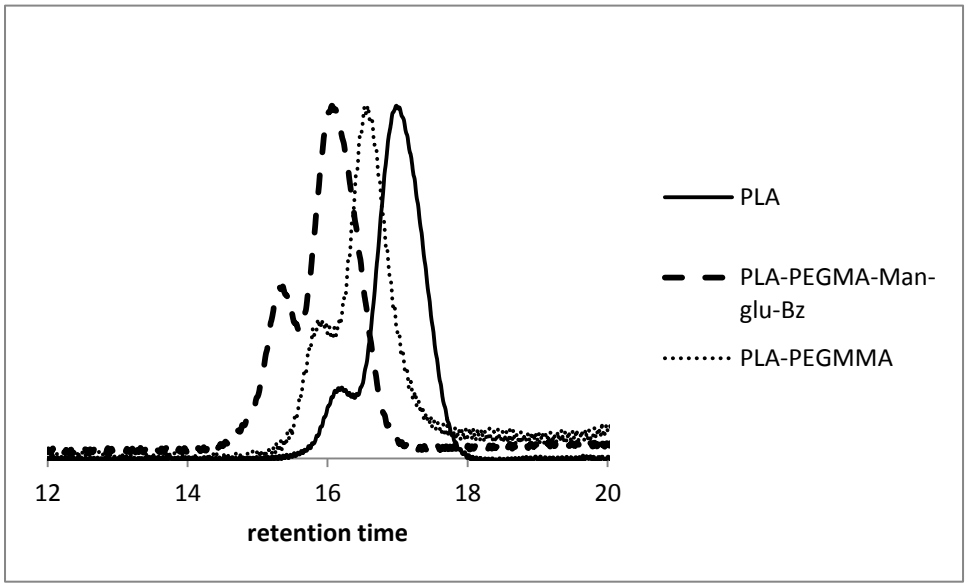

Figure S4 Size exclusion chromatograms of PLA **(1),** block-PEGMA-Man-glu-Bz (**5**) and PLA-block-PEGMMA (**7**)

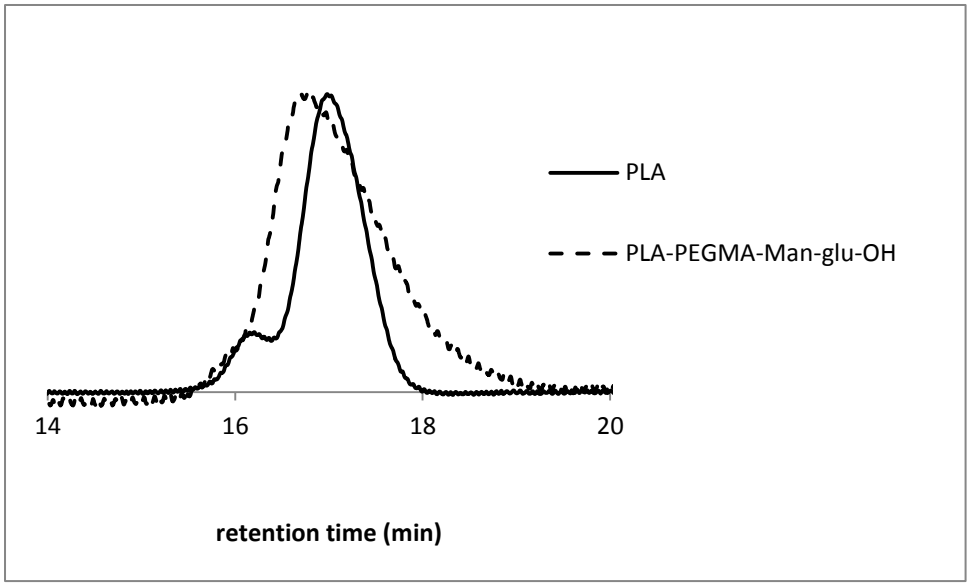

Figure S6 Size exclusion chromatograms of PLA **(1),** PLA-PEGMA-Man-glu-OH (**6**)**.**

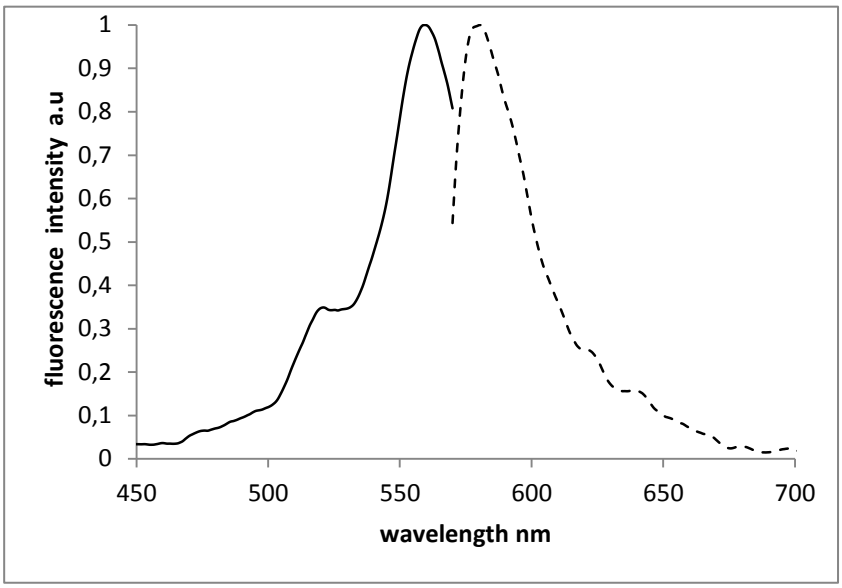

Figure S7 Normalized excitation (continuous line) and emission (discontinuous line) spectra of PLA- -PEGMMA- Rhod (**8**) in THF.

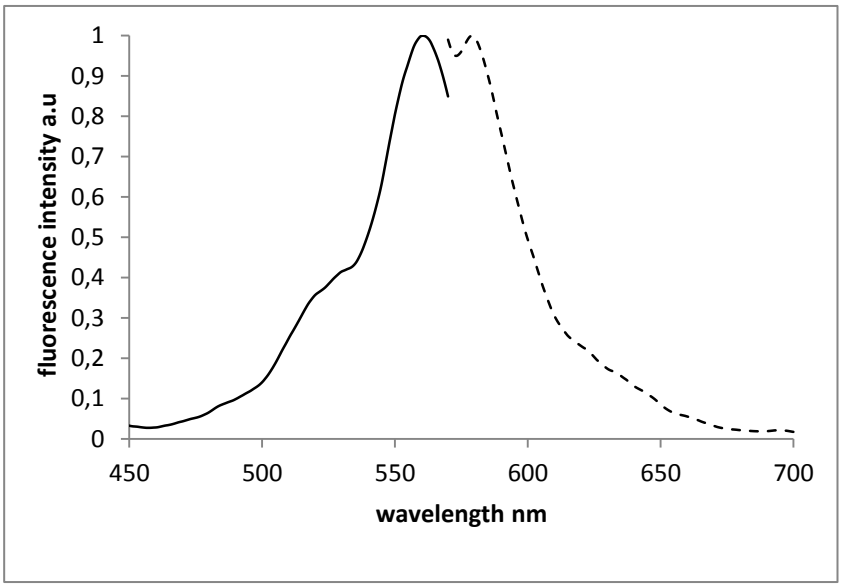

Fig S8. Normalized excitation (continuous line) and emission (discontinuous line) spectra of nanoparticles prepared from a mixture of (**7**) and (**8**) suspended in water

Appendices

In vitro studies of complement activation and *in vivo* evaluation of functionalized nanoparticles

Preparation of concentrated suspensions of nanoparticles

In order to obtain concentrated suspensions, nanoparticles were prepared by nanoprecipitation using 40 mg of polymer instead of 10mg used previously. Other parameters were unchanged (2mL DMF and 4mL water) (Table 1).

Table 1: Composition of nanoparticles prepared for this study.

Type of nanoparticles	Polymers used
Non pegylated NP	(**4**)* 40 mg
Fluorescent - Pegylated- NP with ligand	(**6**) 20mg + (**8**) 20mg
Fluorescent-Pegylated-NP without ligand	(**7**) 20mg + (**8**) 20mg

The numbering of the polymers corresponds to that in the publication in this chapter

Evaluation of complement activation by 2D-immunoelectrophoresis of C3

The C3 protein is a major plasma protein of the complement system. It circulates in a functionally inactive form and is involved in non-specific recognition, i.e. opsonization of foreign bodies [1]. A critical step of complement activation consists in the cleavage of C3 into a large fragment C3b and a small fragment C3a that can only occur in the presence of divalent ions. The activation of this process by nanoparticles can be evaluated *in vitro* by incubating them with human serum in the presence of calcium and magnesium, followed by evaluating the conversion of C3 into C3b and C3a by 2-D immune-electrophoresis using a polyclonal antibody to human C3 [2]. The method used for the 2-D immunoelectrophoresis has been previously described by Kazatchkine [3].

Human serum was obtained after calcifying plasma from healthy donors, and stored at -80 °C until use. Veronal Buffer Saline (VBS) containing 0.15 mM Ca^{+2} and 0.5 mM Mg^{+2} ions (VBS^{+2}) and VBS containing 40 mM ethylenediaminetetraacetic acid (VBS–EDTA) were prepared as described by Kazatchkine et al [3]. Nanoparticle suspensions (100 µL) were incubated under gentle agitation for 1 h at 37 °C with 50 µL human serum and 50 µL VBS^{+2}. To ensure a valid comparison of the different suspensions, the incubation volume (200 µL) contained a mass of nanoparticles m corresponding to a fixed surface area (300 cm^2). This mass was calculated on the basis of the average diameters (D) of the nanoparticles using the following equation: m= (S.D.d)/6 where d is the density of the polymer backbone. VBS–EDTA diluted in serum (1/4 v/v). For all assays, serum diluted in VBS^{+2} (1/4 v/v) was used as a control of the spontaneous activation of complement under the experimental conditions. After incubation, 7 µL of each sample was subjected to a first electrophoresis on 1% agarose gel in tricine buffer (pH = 8.6). The migration was achieved using a Pharmacia LKR Multiphor generator (600 V, 16 mA, and 100 W) for 50 min; bromophenol blue was used as migration indicator. Sample bands were then separated and every gel band was put at the bottom of Gelbond® film fixed to agarose gel plates containing a polyclonal antibody to human C3 (Sigma, France) aliquoted with PBS (1/5 v/v). They were then subjected to a second dimension electrophoresis for 18 h under mild conditions (500 V, 12 mA, and 100 W). This was followed by protein fixation in NaCl 0.9% and further drying. The films were finally stained with Coomassie blue to reveal the presence of C3 and C3b precipitated with the antibody. The surface of the peaks showed on the immuno-electrophoretic plate, corresponding to C3 and C3b, respectively, was measured. The complement activation was expressed by the complement activation factor (CAF), defined as the ratio of the surface of the C3b peak detected on the plate to the sum of the surfaces of the C3 and C3b peaks, using the following equation: CAF= C3b/(C3+C3b).

An increase of the ratio in the presence of nanoparticles incubated with serum diluted in $VBS+^2$ indicates that the nanoparticles possess complement activating capacity.

Mice

In house anti-type II collagen TCR transgenic DBA/1 male mice were bred in the EOPS facility of the Hôpital Cochin and were used at 7–10 week of age for *in vivo* evaluation. Animals were separated into four groups: healthy and arthritic, injected with nanoparticles with or without ligand. Every group was composed of 2 mice.

Rheumatoid arthritis was induced in mice by immunization with native bovine collagen II (100µg emulsified in CFA, id), boosted with collagen II (100mg in IFA) on day +21.

Disease onset was confirmed by clinical observation of joints (toes, tarsus, ankle, wrist and knee).

In vivo fluorescence imaging

The *in vivo* distribution was monitored by a live animal imaging system (IVIS 200 Xenogen almada, Ca, USA) equipped with gas anesthesia connections. To control for the background photon emission, the obtained data were subjected to average background subtraction. The photon radiance on the surface of an animal was expressed as photon per second per centimeter squared. The images shown in figure X are compound pictures generated by living image software.

0.1 mL of PBS (0.1M) solution were added to 0.9 ml of nanoparticle suspension to obtain a final suspension of nanoparticles (2.5mg/mL) in PBS (0.01 M). 200µL of this suspension were injected intravenously through the tail vein. Animals were imaged 5min, 2h, 24h and 48h after injection. At 48h they were sacrificed. Liver, spleen, lungs and knee bone were collected and imaged with the same imaging system.

Results and discussion

Nanoparticle preparation

The maximum volume of nanoparticles suspension that could be used in the experimental protocol of complement activation was 100µL. In order to have higher values of surface area within these 100µL, more concentrated nanoparticle suspensions were needed. To achieve this, we prepared them using 40mg of polymer rather than 10mg as previously used. This increased quantity of copolymer resulted in an increase within the size of nanoparticles which became about 200nm (Table.2). This relation between copolymer concentration and nanoparticle size using nanoprecipitation method is well established in literature [4]. Another effect was the dramatic decrease of nanoparticle yield, especially for sugar functionalized ones. That is probably due to the short PEG chains used and/or the absence of a surfactant in the formulation. This method allowed us to prepare suspensions with a slightly higher concentration of nanoparticles (2.5 mg/mL for man-glu functionalized nanoparticles) than those prepared with 10 mg of polymer previously.

It is well established that the phagocytosis of nanoparticles is mediated by opsonization. Complement proteins are a major component of the opsoninizing proteins in serum [1]. Complement activation was assessed in the presence of suspensions of PLA nanoparticles, PLA-PEGMA-Man-glu-fluorescent nanoparticles and PLA-PEGMMA fluorescent nanoparticles, incubated in human serum diluted in VBS^{2+} for 1 h at 37°C. The

amount of nanoparticles in contact with serum was adjusted to obtain equivalent contact surface areas. Cleavage of protein C3 was demonstrated by 2-D immunoelectrophoresis, and the peak surface corresponding to C3b was measured (Fig. 1). Activation of complement was expressed as the ratio of the surface of the C3 peak to the sum of the surfaces of the C3 and C3b peaks. It should be mentioned that these complement activation experiments were done only once, so the results should be considered with precaution, but they can give an idea of the properties of these nanoparticles regarding complement activation.

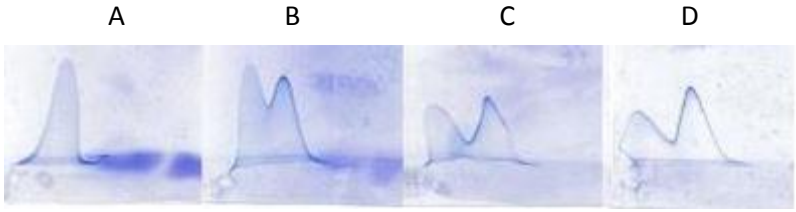

Fig 1. Profiles of complement activation for different nanoparticles (A) Serum/VBS^{+2} control of complement activation background activation;(B) Serum/VBS^{+2} with fluorescent - pegylated- nanoparticles with ligand ;(C) Serum/VBS^{+2} with fluorescent - pegylated- nanoparticles without ligand ;(D) Serum/VBS^{+2} with non- pegylated-nanoparticles

All three types of nanoparticles activated C3 in serum, but the activation was slightly higher with non pegylated nanoparticles prepared from the homopolymer PLA (65%). Pegylated ones activated it to a less extent: 50% in the case of nanoparticles without ligand and 45% for ligand carrying ones. In fact, the PEGMA used with ligand had a PEG chain composed of 10 units (440 Da) while the PEGMMA used with nanoparticles without ligand contained 5 units of PEG (220 Da). They are both considered short, although they could slightly reduce complement activation compared with non pegylated nanoparticles, but the length of the PEG chains is still insufficient to protect them from rapid opsonization and uptake by cells of the reticuloendothelial system. In the literature, it is well established that a PEG of around 5000Da is necessary to prepare stealth nanoparticles when block copolymer such as PLA-PEG or PLGA-PEG is used [5]. In the structure of our copolymers, every single PLA chain is linked to several PEGMA or PEGMMA monomer units and hence with an equal number of PEG chains, resulting in a higher density of PEG coverage compared with classical diblock copolymers. The results obtained with complement activation indicate that this high density was not sufficient to effectively protect the nanoparticles from opsonization.

Table 2: Properties of nanoparticles and their corresponding C3 activation.

	Copolymers used	Size (nm)	NP%*	CAF** %
Without NP	-	-	-	5
Non pegylated NP	(**4**)	229 ± 1.7	31.6	65
Fluorescent - pegylated- NP with ligand	(**6**) + (**8**)	189 ± 5.2	37	50
Fluorescent-pegylated-NP without ligand	(**7**) + (**8**)	231 ± 11	89.8	45

* NP%, percentage yield of nanoparticles.
** b Complement activation factor calculated from the equation, CAF = [(C3b)/(C3 b + C3)].

In vivo fluorescent imaging

In vivo fluorescent imaging was carried out in healthy and in arthritic mice after IV injection of pegylated nanoparticles with or without the E-selectin ligand Man-glu. In all groups, images of the entire animal did not show any detectable fluorescence. This was because the suspension of nanoparticles was not concentrated enough, the amount of fluorescent monomer in the copolymer structure was low and the emission wavelength was not ideal for *in vivo* imaging because of absorption in the tissues. Nevertheless, fluorescence could be detected in isolated liver, for the both types of nanoparticles. This result would be expected in the healthy animals, since there would be no E-Selectin expression to arrest the particles and their natural fate would be the organs of the reticulo-endothelial system, mainly the liver. Moreover, this finding is in agreement with the result of complement activation as these nanoparticles were not sufficiently protected by PEG chains leading to rapid complement activation and accumulation in the liver.

In the case of mice with polyarthritis, it was not possible to confirm whether nanoparticles could be accumulated in the targeted articulations or not. We believe that the low concentration of our nanoparticle suspensions and their low fluorescent intensity for animal imaging was insufficient to detect fluorescence in the targeted tissues, as well as the insufficient protection of the particles by the PEG corona.

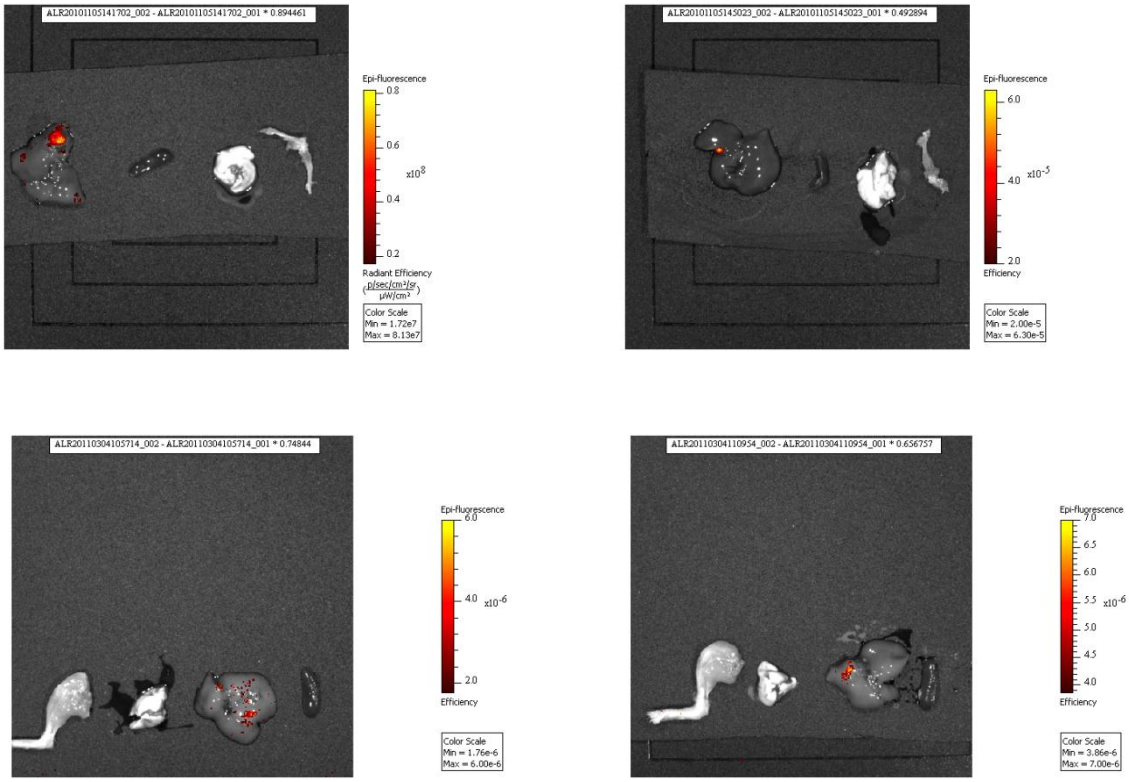

Fig. 2. Fluorescence images of organs of healthy mice (upper panels) and arthritic mice (lower panels) injected with pegylated non functionalized nanoparticles (left panels) and with Man-glu functionalized nanoparticles (right panels).

Conclusion

The nanoparticles used in this study were injected into healthy and polyarthritic mice without causing any apparent toxicity for 48 hours after injection.

Our findings suggest the need for longer PEG chains in order to obtain long-circulating nanoparticles with low activation of the complement system and to avoid the rapid accumulation in the liver evidenced by *in vivo* imaging.

In order to improve the detection of fluorescence *in vivo*, materials with a higher fluorescent intensity and a more suitable emission wavelength (>650 nm) must be prepared and the formulation should be optimized to obtain more concentrated suspensions of nanoparticles. For further *in vivo* evaluation, other means for the detection of nanoparticles such as magnetic resonance imaging or radioactivity could be used. In this case suitable contrast or radioactive agents have to be included in the formulation of nanoparticles.

Acknowledgement: we would like to thank Dr. Gilles Chiocchia Institut Cochin for providing the mice with experimental arthritis for the *in vivo* experiments, and Mlle. Anne-Laure Ramon for her help with *in vivo* imaging.

References

1. Allemann, E., et al., Kinetics of blood component adsorption on poly(D,L-lactic acid) nanoparticles: evidence of complement C3 component involvement. J Biomed Mater Res, 1997. 37(2): p. 229-34.
2. Laurell, C.B., Quantitative estimation of proteins by electrophoresis in agarose gel containing antibodies. Anal Biochem, 1966. 15(1): p. 45-52.
3. Kazatchkine MD, H.G., Nydegger UE., Techniques du complement. 1986., Paris: INSERM;.
4. Legrand, P., et al., Influence of polymer behaviour in organic solution on the production of polylactide nanoparticles by nanoprecipitation. Int J Pharm, 2007. 344(1-2): p. 33-43.
5. Gref, R., et al., 'Stealth' corona-core nanoparticles surface modified by polyethylene glycol (PEG): influences of the corona (PEG chain length and surface density) and of the core composition on phagocytic uptake and plasma protein adsorption. Colloids Surf B Biointerfaces, 2000. 18(3-4): p. 301-313.

Discussion générale

L'objectif de cette thèse a été la préparation d'un nouveau système colloïdal pour l'administration de principes actifs par voie intraveineuse. Malgré les progrès réalisés dans le domaine de la galénique, l'utilisation de nombreux médicaments dans le traitement des maladies graves comme le cancer, les maladies auto-immunes et certaines maladies inflammatoires est accompagnée d'effets secondaires importants. Ces derniers sont souvent liés à l'insuffisance de spécificité des molécules utilisées ou, autrement dit, à la biodistribution non spécifique liée à leurs propriétés physico-chimiques. Cela affecte la qualité de vie des patients et amène parfois à l'arrêt du traitement.

Parmi les stratégies thérapeutiques qui ont attirées l'attention des chercheurs pour contourner ce problème, la vectorisation de principes actifs grâce aux outils de la nanotechnologie, i.e. l'utilisation de vecteur de taille nanométrique (1-1000nm) pour véhiculer ces principes actifs vers leurs cibles, est une voie particulièrement intéressante [1, 2]. Dans ce cas, la distribution sera déterminée par les propriétés physico-chimiques du vecteur et en particulier ses propriétés de surface [3]. Cela est supposé améliorer l'index thérapeutique du principe actif en diminuant ses concentrations au niveau des sites de toxicité et en augmentant sa concentration au niveau du site d'action pharmacologique.

Les nanoparticules polymères occupent une place importante dans les recherches en vectorisation de part leur stabilité en milieu biologique comparée aux liposomes ainsi que la facilité à moduler leur structure pour avoir des propriétés adéquats en fonction de l'application recherchée [4, 5].

Comme tout vecteur injecté par voie intraveineuse, les nanoparticules polymére se heurtent à deux obstacles qui sont l'élimination rapide de la circulation et l'insuffisance de spécificité tissulaire [6].

La clairance rapide de la circulation est liée à la capture des nanoparticules par les macrophages due à l'adsorption de protéines sanguines sur leur surface, phénomène connu sous le nom d' « opsonisation ». Ainsi les particules s'accumulent dans le foie, la rate, et éventuellement dans les poumons [7-9]. Ce problème est contourné par l'élaboration de nanoparticules couvertes de polymère hydrophile comme le PEG [10] ou les polysaccharides [11, 12], qui permettent d'avoir des vecteurs avec un temps de circulation plus important que ceux possédant une surface hydrophobe. Cette stratégie permet de cibler de manière passive les sites d'inflammation ou les tumeurs où la barrière composée par les cellules endothéliales devient discontinue augmentant ainsi l'effet de la perméabilité vasculaire et la rétention tissulaire (EPR).

Des stratégies plus spécifiques pour le ciblage de principes actifs ont été proposées à travers l'utilisation de vecteurs munis d'agents capables de reconnaitre leur cible par reconnaissance moléculaire [13]. Ces agents de reconnaissance comprennent des anticorps monoclonaux, des peptides, ou des molécules de bas poids moléculaire comme les oligosaccharides ou l'acide folique. Les petites molécules appelées souvent des « ligands » permettent de contourner certains problèmes liés à l'utilisation des anticorps comme la dimension moléculaire élevée de ces derniers, leur immunogénicité et le coût de leur production et purification.

Dans l'objectif de préparer de tels systèmes dits « vecteurs de troisième génération » capables de réaliser un ciblage actif, il est nécessaire de décorer la surface du vecteur avec des molécules de reconnaissance dans une conformation active et une orientation favorable à la reconnaissance et l'interaction avec le récepteur cible.

Dans ce contexte, notre travail présenté ici avait pour objectif d'élaborer des nanoparticules polymère porteuses de ligands glycosides capables d'interagir avec l'E-sélectine, un récepteur exprimé sur les cellules endothéliales au niveau des articulations atteintes de polyarthrite rhumatoïde.

Il existe plusieurs stratégies pour introduire des ligands sur les nanoparticules. La première voie consiste à fonctionnaliser la particule en surface après sa préparation [13, 14]. Cette voie comporte de nombreux inconvénients, notamment l'imprécision des modifications et la possibilité d'altérer irréversiblement les polymères constitutifs de la particule, le manque de reproductibilité des modifications de surface, ce qui serait susceptible d'entraîner des modifications imprévisibles et délétères de la distribution *in vivo*. La deuxième voie consiste à utiliser des copolymères préformés porteurs de l'entité chimique dédiée [15]. Cette méthode est plus intéressante car elle est plus précise et utilise des matériaux préalablement purifiés. Cette technique connaît actuellement un très grand essor, notamment en raison de la parfaite maîtrise des méthodes de polymérisation et la connaissance approfondie des propriétés physico-chimiques des polymères qu'elles permettent d'obtenir. C'est pour ces raisons que nous avons adopté cette stratégie de l'utilisation de copolymères préalablement fonctionnalisés. Cela implique dans un premier temps de développer un ensemble de stratégies efficaces pour la construction des macromolécules et à partir de celles-ci de formuler des objets macromoléculaires possédant des structures décorées de motifs glycosylés placés sur les chaînes de manière contrôlée.

Les vecteurs nanoparticulaires que nous proposons ont été formulés à partir d'un copolymère amphiphile avec une architecture à blocs. La partie hydrophobe intérieure est

constituée de polylactide (PLA) et la partie hydrophile de méthacrylate de poly (éthylène glycol) (PEGMA) terminé ou non avec le ligand souhaité.

L'introduction du ligand en amont de la préparation du vecteur s'est faite grâce à la synthèse d'un nouveau monomère porteur du motif glycosylé. La première mission a donc été la mise au point d'une méthode permettant de coupler un sucre modèle (le glucopyranoside) à l'extremité hydroxy du PEGMA. Ce monomère greffé a ensuite été polymérisé pour constituer la partie hydrophile du copolymère. Cette même technique a pu être par la suite étendue au couplage du ligand de l'E-sélectine.

La stratégie de ce couplage repose sur la « click chemistry ». Ce nouveau type de chimie est basée sur la cycloaddition d'un alcyne (R-C ≡ C) et d'un azoture (R´-N_3) donnant lieu exclusivement et de manière irréversible à un cycle (1,2,3 triazole) [16]. Ainsi, en introduisant à l'extrémité alcool du PEGMA un triple liaison, il a été possible d'obtenir par réaction avec un sucre-N_3, un monomère polymérisable contenant un saccharide éloigné de la chaîne principale du polymère via un chaînon PEG. La triple liaison nécessaire à la réaction de « click » a été introduite par une réaction d'estérification sur l'extrémité alcool terminale du PEGMA. Une étude d'optimisation du temps de réaction de cycloaddition a été nécessaire afin que le macromonomère final conserve l'intégrité de ses doubles liaisons (Chapitre. I, tableau. 1). Finalement, les groupements acétate qui protégeaient les fonctions hydroxyle du glucopyranoside ont été facilement éliminées en présence de méthoxyde de sodium.

Lors de la préparation des copolymères, un équilibre de masse molaire entre les deux blocs est primordial pour la formulation des nanoparticules où la partie hydrophobe doit être de taille suffisantes pour que les chaînes de polymère s'organisent en structure nanoparticulaire en contact avec l'eau. Si le bloc hydrophile est majoritaire dans la structure, la solubilité dans l'eau des chaînes de polymère sera élevée ce qui empêchera la formation des nanoparticules. Il est donc important de maitriser les réactions de polymérisation pour contrôler la masse molaire de chaque bloc. Ainsi, nous avons fait appel à des techniques de polymérisation différentes pour chaque bloc de la chaîne. La partie hydrophobe composée du PLA a été obtenue par polymérisation par ouverture de cycle du lactide. Ce type de polymérisation est dite vivante car les réactions de transfert et de terminaison sont limitées. Cette méthode permet donc de contrôler la longueur des chaînes en jouant sur le rapport des concentrations en monomère et en amorceur.

Le bloc hydrophile a été construit par polymérisation du méthacrylate de poly (éthylène glycol). Pour ce bloc, nous avons choisi la technique de polymérisation radicalaire

par transfert d'atome (ATRP). Dans ce procédé, le mécanisme est basé sur un équilibre réversible entre une espèce dormante halogénée et une espèce active en présence d'un complexe métalique [17]. Le catalyseur stimule la formation de l'espèce active à travers une désassociation d'une liaison carbone-halogène terminale pour former un radical alors que le catalyseur lui-même passe à l'état oxydé supérieur par transfert d'un électron. Seule l'espèce active est capable d'amorcer la polymérisation et d'additionner un monomère. Ceci a pour conséquence de réduire la concentration en radicaux dans le milieu et donc de limiter les réactions de terminaison. Il est donc aisé par ce procédé de contrôler la masse molaire des polymères ainsi que son architecture selon l'amorceur utilisé. Le système Cu(I) halogène/PMDETA représente un catalyseur efficace de la polymérisation des méthacrylates de poly (éthylène glycol) par ATRP avec un taux d'amorçage qui 4 fois plus important que le taux de propagation [18]. Toutefois, pour des applications pharmaceutiques ou biologiques, une attention particulière doit être apportée à l'élimination du cuivre.

Afin de réaliser ces deux types de polymérisation, il était nécessaire de trouver un amorceur bifonctionnel capable d'amorcer les deux réactions. Le β-hydroxyl éthyl α-bromoisobutyrate (HEBIB) possède deux extrémités différenciées : un atome de Br et une fonction OH capable d'amorcer une polymérisation par ATRP et une ROP respectivement [19].

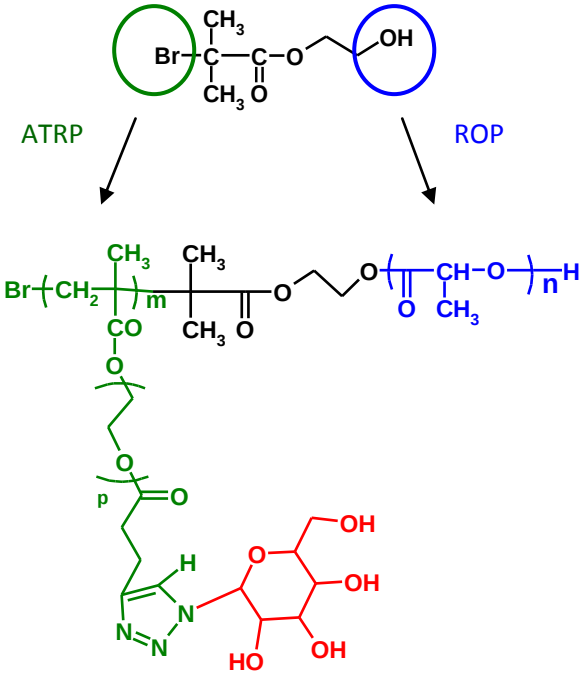

Schéma. I. structure de l'amorceur HEBIB et du copolymère amphiphile qui en résulte en utilisant deux techniques de polymérisation

Lors de la préparation des copolymères, le PLA a été synthétisé dans un premier temps puis les chaînes de polymère formées ont été utilisées comme macroamorceurs pour réaliser la polymérisation par ATRP du PEGMA fonctionalisé avec le sucre (Schéma. I).

Ce nouveau copolymère présente de nombreux avantages :

- Le ligand est lié de façon covalente avec le polymère ainsi cette liaison est stable dans les milieux biologique. En outre, la quantité de ligand présente dans le copolymère pourra être modulable en utilisant des proportions variées de monomère fonctionnalisé ou pas lors de la réaction par ATRP.
- Les techniques de polymérisation contrôlée utilisées permettent d'obtenir des blocs de taille précise et contrôlable via la détermination du rapport monomère /amorceur pour chaque bloc.
- La méthode de couplage permet de fonctionnaliser ce monomère avec une variété de ligand de bas poids moléculaire, pour cela ces derniers doivent porter une fonction azide. Ainsi, cette stratégie peut servir à fonctionnaliser différents polymères pour cibler d'autres récepteurs que l'E-sélectine (le récepteur du folate par exemple).
- La nature amphiphile du copolymère permet de préparer des nanoparticules par nanoprécipitation sans l'utilisation de tensioactif ou de stabilisant.
- Les chaînes de PEG forment une couche extérieure capable de rendre la surface des particules hydrophile, et cette couche est stable car elle est liée de façon covalente à la surface des particules.
- Comme le ligand est fixé au bout de la chaîne du PEG, la flexibilité de celle-ci facilite ultérieurement l'interaction ligand/récepteur.

L'auto assemblage des polymères est une voie extrêmement puissante qui permet de construire aisément des nanoparticules, notamment par la technique de nanoprécipitation [20]. Cette méthode est simple, rapide et facile à transposer à l'échelle industrielle). Elle permet de former spontanément des nanoparticules en une seule étape. Par ailleur aujourd'hui il est bien établi que la nanoprécipitation de copolymères amphiphiles aboutie à une orientation privilégiée, où les chaînes hydrophobes s'associent pour former une matrice tandis que, les entités hydrophiles se positionnent à l'interface entre cecoeur hydrophobe et l'eau [21, 22]. La technique de nanoprécipitation peut être appliquée aux mélanges de copolymères de façon à associer simultanément dans les mêmes particules deux ou plusieurs copolymères [23].

Dans notre étude, le copolymère synthétisé a permi de préparer des nanosphères par nanoprécipitation sans utilisation de tensioactif (Schéma. II). L'absence d'agent tensioactif pour stabiliser les suspensions nanoparticulaire représente un avantage en termes de tolérance vu la toxicité éventuelle de ces molecules. Le solvant classiquement utilisé pour la préparation de tels objets par cette technique est l'acétone dont l'élimination est rapide par une simple évaporation [24]. Toutefois, dans le but d'encapsuler le méthotrexate (MTX), nous avons dû choisir le DMF qui est à la fois un bon solvant du MTX et du copolymère amphiphile fonctionalisé. Par contre, ce choix nous a contraint à ajouter une étape supplémentaire à notre mode opératoire, à savoir l'élimination du DMF par dialyse. Malgré ce changement de solvant, nous avons obtenu des nanoparticules sphériques et de façon reproductible avec une taille inférieure à 200nm. Une caractérisation ultérieure a permis d'observer la morphologie de ces nanosphères par microscopie électronique à transmission (TEM) : les images obtenues ont montré des particules avec une forme sphérique, homogène et une surface lisse (Chapitre I Fig. 8).

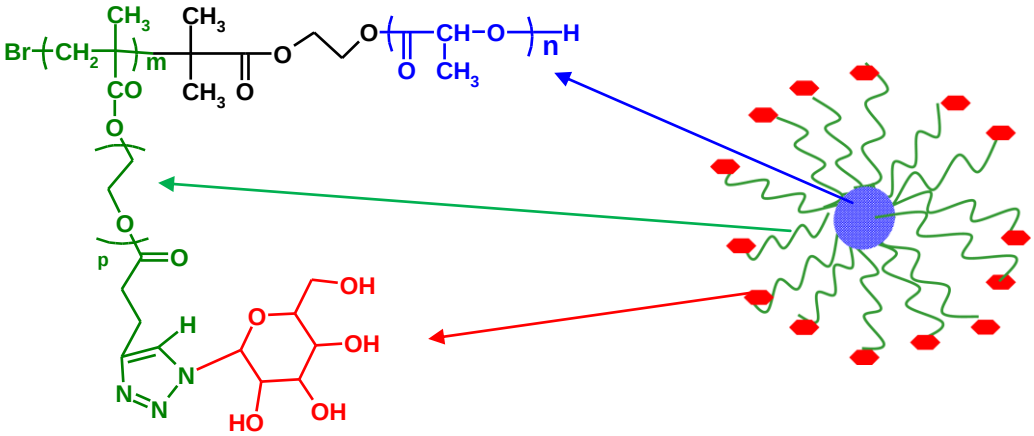

Schéma. II. Structure du copolymère avec une représentation schématique de la conformation des nanoparticules dans l'eau

La biocompatibilité de ces nanoparticules vis à vis des cellules endothéliales a été évaluée sur des cellules endothéliales de veine ombilicale humaine en culture. Aucune cytotoxicité significative n'a été détectée par le test MTT basé sur l'activité des enzymes mitochondriales. Cela nous indique d'une part la bonne biocompatibilité de nos particules ainsi que l'élimination efficace du DMF (solvant toxique) par dialyse d'autre part (Chapitre I, Fig. 9)

De manière raisonnable et comme cela a été montré pour de nombreux autres copolymères amphiphiles construits selon le même principe, il est attendu que le bloc

hydrophobe PLA forme le cœur de la particule tandis que les chaînes de PEG hydrophiles se positionnent à la surface en laissant le ligand hydrophile qu'elles portent orienté vers le milieu aqueux [14]. Afin de vérifier dans le cas de nos nanoparticules modèles l'accessibilité du ligand ainsi que sa capacité à reconnaitre une forme soluble d'un récepteur du glucose, nous les avons mises en contact avec de la Concanavaline A (ConA). Cette protéine de la famille des lectines est connue pour interagir avec les molécules de α-mannopyranosyle et de α-glucopyranosyl au niveau de leurs fonctions hydroxyle en positions 3, 4, et 6. Dans nos conditions expérimentales, cette protéine se trouve sous forme de tétramère qui lui permet d'interagir avec quatre groupements hydroxyle [25]. Lors de l'addition de Con A, une agrégation des nanoparticules a été mise en évidence par une augmentation de la turbidité des solutions (Chapitre I, Fig. 6) et de la taille des agrégats (diffusion quasi élastique de lumière) (Chapitre I, Fig. 7) ainsi que lors de leur visualisation par microscopique (TEM) (Chapitre I, Fig. 8). Cela nous indique une bonne orientation du ligand vers la surface des particules et leurs capacités à reconnaitre une forme soluble du récepteur correspondant au ligand qu'elles portent.

Dans la deuxième partie de notre travail (Chapitre II), nous avons réalisé une étude préliminaire de l'association d'un anticancéreux/anti-inflammatoire (MTX) (Schéma. III) utilisé dans le traitement de la polyarthrite rhumatoïde, avec ces nanosphères. Cela a été réalisé sur un copolymère amphiphile de structure identique mais en l'absence de ligand dans le but d'étendre par la suite les résultats d'encapsulation optimisés aux nanoparticules fonctionnalisées avec le ligand de l'E-sélectine.

La même méthode de nanoprécipitation a été utilisée mais cette fois-ci en présence du MTX solubilisé dans le DMF. De nombreux problèmes de purification et de reproductibilité des résultats ont été rencontrés. Une des raisons principales est la nature avérée hydrophile du méthotrexate. A cela s'ajoute l'effet de charge. A pH≈6,5 de l'eau ultra-pure, le MTX est sous sa forme non protonée (négative) ce qui entraine une répulsion électrique avec les nanoparticules qui ont elles aussi une charge négative de surface.

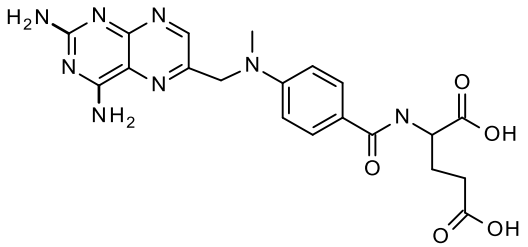

Schéma III formule chimique du méthotrexate

Nous avons conclu suite aux résultats obtenus dans cette partie de travail que la majeure partie du MTX restait dans le mélange eau/DMF pendant la nanoprécipitation avec seulement une faible fraction qui s'adsorbait sur le polymère. Cela justifie les valeurs aléatoires d'encapsulation obtenues sans aucune reproductibilité. Notre méthode de préparation et de purification des nanoparticules ne nous a donc pas permis de séparer le surnageant contenant le MTX libre des nanoparticules chargées et de récupérer ainsi des nanoparticules chargées suspendues dans un surnageant propre.

Malheureusement, faute de temps, nous n'avons pas pu allez plus loin dans nos recherches concernant l'encapsulation du MTX. L'ensemble des résultats de cette étude indiquent la nécessité de modifier la formulation pour améliorer l'association du MTX avec ces nanoparticules. L'utilisation d'un tensioactif pourrait améliorer le rendement d'encapsulation et permettre également de reprendre les nanoparticules après une ultracentrifugation ce qui n'était pas possible avec la formulation décrite dans cette thèse. D'autres possibilités sont envisageables comme changer de méthode de préparation des nanoparticules (la technique de double-émulsion, par exemple) ou bien encore d'utiliser un polymère hydrophobe possédant une meilleure affinité vis-à-vis du MTX que le PLA.

Dans la dernière partie de ce travail de thèse (Chapitre III), nous avons fonctionnalisé le PEGMA avec un analogue du sialyl lewis x, le Man-glu (Schéma. VI) à la place de glucopyranoside utilisé dans les étapes préliminaires de notre projet. Après une recherche bibliographique, cet analogue nous a semblé un bon candidat grâce à sa structure simple, et son affinité élevée vis-à-vis de l'E-sélectine [26]. Les conditions expérimentales de la synthèse du nouveau copolymère amphiphile fonctionnalisé ont été légèrement adaptées par rapport à celles décrites précédemment (Chapitre III, Schéma S1). La méthode de déprotection a due être également modifiée pour ôter dans ce cas les groupements benzyle du Man-glu au lieu des groupements acétate du glucose. Cette réaction a été effectuée après la polymérisation par ATRP car la réaction d'hydrogénation utilisée pour la déprotection risquait de réduire les doubles liaisons du méthacrylate rendant le monomère non polymérisable.

Pour pouvoir visualiser les nanoparticules *in vitro* par microscopie confocale, nous avons procédé à la préparation de copolymère amphiphile fluorescent de structure amphiphile composé de PLA-PEGMMA avec l'introduction d'un faible pourcentage de monomère méthacrylique rhodaminée dans le milieu réactionnel de la polymérisation par ATRP.

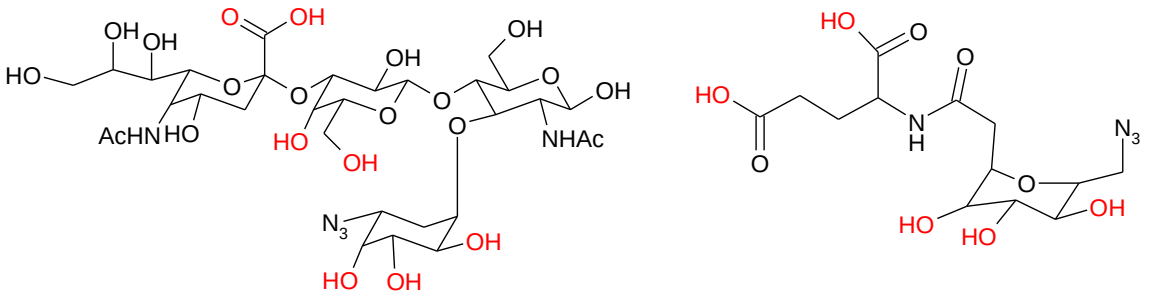

Fig. IV structure du SLEx (gauche) et de son mime Man-glu (droite) utilisé dans notre travail
Les groupements impliqués dans l'interaction avec l'E-sélectine sont en rouge

Lors de la préparation des nanoparticules par la suite, l'utilisation de deux copolymères : l'un fluorescent et l'autre fonctionnalisé avec le Man-glu dans la même formulation, a permis d'obtenir des nanoparticules à la fois fluorescentes et porteuses du ligand grâce à l'association des chaînes de PLA portées par les deux copolymères pour former le cœur hydrophobe.

Les cellules endothéliales de la veine ombilicale humaine sont couramment utilisées comme modèle pour les recherches concernant l'endothélium, de plus elles sont facilement stimulables par les cytokines ce qui entraine, entre autre, l'expression de l'E-sélectine (Chapitre. III Fig. 3). Ainsi, nous nous sommes servis de ce modèle afin d'évaluer l'efficacité des nanoparticules à interagir avec l'E-sélectine *in vitro*.

L'analyse en microscopie confocale a permis de visualiser parfaitement l'association des nanoparticules avec les cellules. La présence du ligand sur leur surface a augmenté considérablement cette association par rapport aux nanoparticules nues (Chapitre III, Fig. 4). Cela nous indique la spécificité du ciblage par l'intermédiaire du couple E-sélectine/Man-glu. Cette reconnaissance spécifique est confirmée par la diminution de l'association quand les cellules ont été préalablement incubées avec un anticorps anti E-sélectine. D'autre part, les images de microscopie confocale ont montré une localisation cytoplasmique de la fluorescence sous forme de spots brillants ce qui est considéré comme une indication de l'incorporation des particules par endocytose [14] médiée dans notre cas par l'E-sélectine qui est connue pour être internalisée par endocytose pendant les 24h qui suivent son expression à la surface des cellules endothéliales [27].

Le niveau de fluorescence mesuré par spectroscopie a montré un maximum d'association de fluorescence avec les cellules activées quand les nanoparticules fonctionnalisées avec Man-glu ont été utilisées (Chapitre III, Fig. 5). La réduction de cette

association lors de l'incubation des nanoparticules avec les cellules activées à 4 °C au lieu de 37°C est une deuxième indication que les nanoparticules peuvent être internalisées par endocytose.

Ces travaux ont permis d'élaborer une nouvelle famille de copolymères de structure bien définie avec une fonctionnalisation moléculaire. Les vecteurs formulés à partir de ces macromolécules représentent un système prometteur de ciblage tissulaire par une interaction moléculaire ligand/récepteur au niveau des cellules endothéliales.

Des tests préliminaires d'activation du complément ont été réalisés sur les nanoparticules composées d'homopolymère de PLA, de PLA-PEGMMA ou PLA PEGMA-Man-glu. La présence de poly(éthylène glycol) à la surface des nanoparticules a permis de réduire légèrement l'activation du complément, mais cela reste insuffisant pour les protéger contre une opsonisation.

Dans le cas des copolymères diblocs classiques type PLA-PEG, il est admis que des chaînes de PEG de 5000 Da sont nécessaires pour préparer des nanoparticules furtives [28]. Dans les copolymères synthétisés dans le cadre de notre travail, chaque chaîne de PLA portait un nombre de chaînes de PEG égale au nombre d'unités acryliques par chaîne de copolymère (une dizaine en moyenne) mais ces chaînes sont courtes (440Da). Celles-ci n'ont pas pu empêcher l'activation du complément. Cette reconnaissance vis-à-vis du système du complément a été confirmée lors des essais *in vivo* où les nanoparticules ont été accumulées dans le foie des souris après une administration intraveineuse. Il est donc nécessaire d'avoir une protection stérique plus efficace assurée par des chaînes de PEG plus longues.

En conclusion nous pouvons résumer les points majeurs de ce travail

- La chimie « click » a été employée avec succès pour fonctionnaliser un monomère/polymère avec des ligands de bas poids moléculaire. Cette méthode pourra être étendue à de nombreuses molécules chimiques connues pour être des ligands de récepteurs particuliers.
- une combinaison de deux méthodes de polymérisation contrôlée a été utilisée pour obtenir des copolymères de structure parfaitement maîtrisable. Ces techniques sont applicables sur une variété de monomères dont la polymérisation se fait par ROP et ATRP.
- L'application des ces méthodes chimiques pour obtenir un nouveau copolymère fonctionnalisé avec un ligand de l'E-sélectine.

- L'utilisation de ces copolymères pour la préparation de nanoparticules par une méthode très simple et reproductible. Les nanosphères obtenues ont une surface hydrophile et le ligand conjugué se trouve à l'extrémité des chaînes hydrophiles. Cette conformation des nanoparticules en milieu aqueux favorise la reconnaissance du ligand par ces récepteurs correspondants.
- La méthode utilisée pour la préparation de matériel fluorescent permet d'avoir une fluorescence émie par les matériaux eux même et non pas par une substance fluorescente encapsulée dans les nanoparticules. Nous sommes ainsi surs que la fluorescence observée par microscopie confocale ou par les appareils d'imagerie du petit animal provient du matériau et non pas de la substance encapsulée dont la diffusion dans le milieu peut complètement fausser l'interprétation.
- La reconnaissance spécifique au niveau moléculaire entre les molécules de ligand portées par les particules et le récepteur exprimé sur les cellules endothéliales confirme la réussite de notre stratégie de ciblage spécifique.
- Un tel vecteur pourra être utilisé dans une variété de pathologies caractérisée par l'expression accrue de l'E-sélectine au niveau de l'endothélium, dont la polyarthrite rhumatoïde, certains cancers et certains désordres ischémiques.

Références bibliographiques

1. Gupta, R.B., Kompella, U.B.,, *Nanoparticle technology for drug delivery* Drugs and the pharmaceutical sciences. Vol. 159. 2006, New York.: Taylor & Francis.
2. Couvreur, P. and C. Vauthier, *Nanotechnology: intelligent design to treat complex disease.* Pharm Res, 2006. **23**(7): p. 1417-50.
3. Vonarbourg, A., et al., *Parameters influencing the stealthiness of colloidal drug delivery systems.* Biomaterials, 2006. **27**(24): p. 4356-73.
4. Brigger, I., C. Dubernet, and P. Couvreur, *Nanoparticles in cancer therapy and diagnosis.* Adv Drug Deliv Rev, 2002. **54**(5): p. 631-51.
5. Nicolas, J. and P. Couvreur, *Synthesis of poly(alkyl cyanoacrylate)-based colloidal nanomedicines.* Wiley Interdiscip Rev Nanomed Nanobiotechnol, 2009. **1**(1): p. 111-27.
6. Moghimi, S.M., A.C. Hunter, and J.C. Murray, *Long-circulating and target-specific nanoparticles: theory to practice.* Pharmacol Rev, 2001. **53**(2): p. 283-318.
7. Grislain, L., et al., *Pharmacokinetics and distribution of a biodegradable drug-carrier.* International Journal of Pharmaceutics, 1983. **15**(3): p. 335-345.
8. Fernandez-Urrusuno, R., et al., *Effect of polymeric nanoparticle administration on the clearance activity of the mononuclear phagocyte system in mice.* J Biomed Mater Res, 1996. **31**(3): p. 401-8.
9. Demoy, M., et al., *Spleen Capture of Nanoparticles: Influence of Animal Species and Surface Characteristics.* Pharmaceutical Research, 1999. **16**(1): p. 37-41.
10. Peracchia, M.T., et al., *Visualization of in vitro protein-rejecting properties of PEGylated stealth® polycyanoacrylate nanoparticles.* Biomaterials, 1999. **20**(14): p. 1269-1275.
11. Passirani, C., et al., *Long-circulating nanoparticles bearing heparin or dextran covalently bound to poly(methyl methacrylate).* Pharm Res, 1998. **15**(7): p. 1046-50.
12. Chauvierre, C., et al., *Novel polysaccharide-decorated poly(isobutyl cyanoacrylate) nanoparticles.* Pharm Res, 2003. **20**(11): p. 1786-93.
13. Gref, R., et al., *Surface-engineered nanoparticles for multiple ligand coupling.* Biomaterials, 2003. **24**(24): p. 4529-4537.
14. Stella, B., et al., *Biological characterization of folic acid-conjugated poly(H2NPEGCA-co-HDCA) nanoparticles in cellular models.* J Drug Target, 2007. **15**(2): p. 146-53.
15. Banquy, X., et al., *Selectins Ligand Decorated Drug Carriers for Activated Endothelial Cell Targeting.* Bioconjugate Chemistry, 2008. **19**(10): p. 2030-2039.

16. Huisgen, R., *Kinetics and Mechanism of 1,3-Dipolar Cycloadditions.* Angewandte Chemie International Edition in English, 1963. **2**(11): p. 633-645.
17. Matyjaszewski, K. and J. Xia, *Atom Transfer Radical Polymerization.* Chem. Rev., 2001. **101**(9): p. 2921-2990.
18. Ali, M.M. and H.D.H. Stover, *Well-Defined Amphiphilic Thermosensitive Copolymers Based on Poly(ethylene glycol monomethacrylate) and Methyl Methacrylate Prepared by Atom Transfer Radical Polymerization.* Macromolecules, 2004. **37**(14): p. 5219-5227.
19. Jayachandran, K.N., A. Takacs-Cox, and D.E. Brooks, *Synthesis and Characterization of Polymer Brushes of Poly(N,N-dimethylacrylamide) from Polystyrene Latex by Aqueous Atom Transfer Radical Polymerization.* Macromolecules, 2002. **35**(11): p. 4247-4257.
20. H. Fessi, J.P.Devissaguet., F. Puisieux et C. Thies, *Procédé de préparation de systèmes colloïdaux dispersibles d'une substance sous forme de nanoparticules.* 1986: France.
21. Bouligand, J., et al., *Busulphan-loaded long-circulating nanospheres, a very attractive challenge for both galenists and pharmacologists.* Journal of Microencapsulation, 2007. **24**(8): p. 715-730.
22. Ozcan, I., et al., *Pegylation of poly(gamma-benzyl-L-glutamate) nanoparticles is efficient for avoiding mononuclear phagocyte system capture in rats.* Int J Nanomedicine. **5**: p. 1103-11.
23. Segura-Sánchez, F., et al., *Synthesis and characterization of functionalized poly([gamma]-benzyl-l-glutamate) derivates and corresponding nanoparticles preparation and characterization.* International Journal of Pharmaceutics. **387**(1-2): p. 244-252.
24. Legrand, P., et al., *Influence of polymer behaviour in organic solution on the production of polylactide nanoparticles by nanoprecipitation.* Int J Pharm, 2007. **344**(1-2): p. 33-43.
25. Cunningham, B.A., et al., *The covalent and three-dimensional structure of concanavalin A. II. Amino acid sequence of cyanogen bromide fragment .* J Biol Chem, 1975. **250**(4): p. 1503-12.
26. Wong, C.-H., et al., *Small Molecules as Structural and Functional Mimics of Sialyl Lewis X Tetrasaccharide in Selectin Inhibition:â€‰ A Remarkable Enhancement of Inhibition by Additional Negative Charge and/or Hydrophobic Group.* Journal of the American Chemical Society, 1997. **119**(35): p. 8152-8158.

27. von Asmuth, E.J., et al., *Evidence for endocytosis of E-selectin in human endothelial cells.* Eur J Immunol, 1992. **22**(10): p. 2519-26.

28. Gref, R., et al., *'Stealth' corona-core nanoparticles surface modified by polyethylene glycol (PEG): influences of the corona (PEG chain length and surface density) and of the core composition on phagocytic uptake and plasma protein adsorption.* Colloids Surf B Biointerfaces, 2000. **18**(3-4): p. 301-313.

Conclusion générale

Conclusion Générale et perspectives

Le principal objectif de cette thèse a été de développer un vecteur capable de cibler l'endothélium pathologiquement activé, par un moyen de reconnaissance moléculaire entre des molécules portées par le vecteur et des récepteurs spécifiques exprimés sur ces cellules.

Pour réaliser cet objectif, nous avons mis au point un ensemble de techniques de couplage et de polymérisation pour élaborer une famille de copolymères fonctionnels. L'ensemble des méthodes de caractérisation physico-chimique nous a permis de mettre en évidence la structure, la morphologie et la conformation de ces macromolécules.

L'obtention des vecteurs à partir de ces structures macromoléculaires a été réalisée par une méthode très simple et reproductible qui est la nanoprécipitation. La biocompatibilité des différentes formulations des nanoparticules a été démontrée par un test de cytotoxicité sur des cellules en culture.

Avec ce vecteur nanoparticulaire aux propriétés de surface prédéfinies, nous avons montré l'efficacité *in vitro* d'un couple récepteur/ ligand synthétique dans le ciblage moléculaire de sites pathologiques.

L'ensemble des résultats obtenus nous a permis d'atteindre l'objectif fixé au départ de la thèse qui était l'élaboration d'un système vecteur original répondant à plusieurs exigences au niveau de la taille, biocompatibilité, propriétés de surface contrôlées, et une capacité à cibler spécifiquement au niveau moléculaire un récepteur particulier.

En se basant sur ces données encourageantes, les prochaines étapes de ce travail vont se concentrer sur les approches suivantes :

- Améliorer l'encapsulation du méthotrexate à travers la modification de la méthode de préparation des nanoparticules et/ou de la formulation utilisée.
- Optimiser la masse molaire des chaînes PEG utilisées, en fonction de la structure particulière des copolymères que nous proposons pour avoir une meilleure furtivité du vecteur.
- Rechercher d'autres ligands originaux de l'E-sélectine dotés de plus de spécificité vis-à-vis du récepteur.
- Valider la méthode de ciblage *in vivo* par l'accumulation de ces nanoparticules dans les foyers d'inflammation après injection par voie intraveineuse et déterminer la cinétique de cette accumulation.

- Déterminer la quantité optimale de ligand à introduire sur la surface des nanoparticules pour obtenir une reconnaissance maximale.
- Prouver l'efficacité thérapeutique des nanoparticules chargées en MTX dans le traitement de la polyarthrite rhumatoïde via l'analyse de l'expression des cytokines pro-inflammatoires dans le sérum des souris traitées en comparaison avec les souris non traitées. Un examen des articulations par histopathologie pour visualiser l'inflammation, le niveau d'infiltration cellulaire et / ou l'érosion osseuse pourra être pratiqué.

Synthesis and formulation of polymeric nanoparticles targeting E-selectin: *In vitro* evaluation in a model of activated endothelium

Abstract

The objective of this work was to develop a delivery system targeting pathologically activated endothelium within inflamed, infectious, and some tumoral tissues. This system is composed of nanoparticles bearing sugar residues that are able to recognize and interact with E-selectin, a receptor expressed on the activated endothelial cells.

We synthesized an amphiphilic block copolymer with the hydrophilic part terminated by a carbohydrate ligand. The construction was achieved by a combination of click chemisty, ring-opening polymerization and atom transfer radical polymerization. This copolymer was used to prepare nanoparticles of the core/shell type where the central hydrophobic body is surrounded with the hydrophilic shell that can stabilize the particles in aqueous media and limit their opsonisation. Active targeting was achieved by coupling an analogue of sialyl Lewis X, the physiological ligand of E-selectin to the end of the hydrophilic polymer chains on the surface of the particles.

We were able to demonstrate *in vitro* the efficient association of these nanoparticles with defined surface properties with activated endothelial cells. This allowed us to validate our concept of active molecular targeting using this couple receptor/ligand couple. Such a system could be used to improve the therapeutically index and the biodistribution of anti-inflammatory and anti-tumor drugs.

Keywords

Nanoparticles, E-selectin, Activated endothelium, Click chemistry, ROP/ATRP, HUVECs, Amphiphilic polymers, Carbohydrate ligand, Drug targeting, Methotrexate and Molecular imaging.

Résumé

Ce travail de thèse avait pour objectif d'élaborer un système vecteur ciblant l'endothélium pathologiquement activé dans les tissus enflammés, infectés ou tumoraux. Ce vecteur est sous forme de nanoparticules décorées de ligands glycosides capables d'interagir avec l'E-sélectine, un récepteur exprimé sur les cellules endothéliales activées.

Nous avons mis au point une synthèse de copolymère amphiphile avec une architecture à bloc muni sur sa partie hydrophile d'un ligand glucidique. Ce copolymère a été par la suite utilisé pour la préparation de nanoparticules de type cœur/couronne. La partie hydrophobe centrale est entourée d'une couronne hydrophile dont l'encombrement stérique et la mobilité limitent l'opsonisation de la particule. Le ciblage actif a été assuré par la présence d'un ligand du récepteur de l'E-sélectine aux extrémités des chaînes de polymères hydrophiles à la surface du vecteur.

Avec ces nanoparticules dont les propriétés de surface sont prédéfinies, nous avons montré in vitro l'association efficace avec les cellules endothéliales activées, ce qui a permis de validerce concept de ciblage moléculaire actif par l'intermédiaire du couple récepteur/ ligand. Un tel système permettra d'améliorer l'indice thérapeutique et la biodistribution des principes actifs anti-inflammatoire et/ou anticancéreux.

Mots clés

Nanoparticules, E-sélectine, endothélium activé, Click chemistry, ROP/ATRP, polymère amphiphile, ligand glucidique, HUVECs, ciblage des médicaments, Méthotrexate,

Laboratoire de rattachement

Laboratoire de Physicochimie, Pharmacotechnie, et Biopharmacie – UMR CNRS 8612

PÔLE : PHARMACOTECHNIE ET PHYSICO-CHIMIE PHARMACEUTIQUE

UNIVERSITÉ PARIS-SUD 11

UFR «FACULTÉ DE PHARMACIE DE CHATENAY-MALABRY »

5, rue Jean Baptiste Clément

92296 CHÂTENAY-MALABRY Cedex